

Advanced Solid-State Photonics (ASSP)

29 January - 1 February 2012, Rancho Bernardo Inn, San Diego, California, United States

2012 ASSP Best Student Awards are sponsored by Lockheed Martin.

Congratulations to the following ASSP student winners:

Best Student Oral Presentation

Steffen Hädrich, Friedrich-Schiller-University Jena, Germany

Paper: AT1A.6 - "100 W Nonlinear Compression in Hollow Core Fibers at 1 MHz Repetition Rate"

Best Student Poster Presentation

Clara Saraceno, ETH Zurich, Switzerland

Paper AM4A.13 - "SESAMs for high-power femtosecond modelocking: influence of growth temperature on damage and nonsaturable losses"

ASSP – The world's premier meeting for discussing new developments in laser and nonlinear optical materials and devices.

The Advanced Solid-State Photonics Topical meeting specializes in novel solid-state sources of coherent radiation operating in different spectral ranges. Now in its 27th year, this meeting remains the world's premier forum for discussing new developments in solid-state and fiber lasers, ultrashort light sources, amplifier design and power scaling, laser and nonlinear optical materials, and nonlinear frequency conversion devices. These light sources find an increasingly broad range of applications in spectroscopy, metrology, remote sensing, communications, material processing, astronomy, medicine, and life sciences.

Online Access to Technical Digest Now Available! Full Technical Attendees now have an alternate way to access the digest papers at the meeting. Access the papers through [Optics InfoBase](#) using the same login email address and password provided during the meeting registration process. Access is currently limited to Laser Congress Full Technical Attendees only. If you need assistance with your login information, please use the forgot password utility or "Contact Help" link.

General Chair

- Alphan Sennaroglu, Koç Univ., Turkey

Program Chairs

- Gregory Goodno, Northrop Grumman Aerospace Systems, USA
- Andrius Baltuska, Vienna Univ. of Technology, Austria

2012 ASSP Best Student Awards are sponsored by Lockheed Martin.



This event is part of the Lasers, Sources and Related Photonic Devices Congress, allowing attendees to access to all meetings within the Congress for the price of one and to collaborate on topics of mutual interest.

Sponsor:



Lasers, Sources and Related Photonics Devices

29 January - 3 February 2012, Rancho Bernardo Inn, San Diego, California, USA

Advanced Solid- State Lasers Congress, Paris, France, Fall 2013!

OSA's NEW Advanced Solid- State Lasers Congress combines the significant research and distinctive presentations of OSA's Advanced Solid-State Photonics (ASSP), Advances in Optical Materials (AIOM), and Fiber Lasers and Applications (FILAS) meetings into a single track format giving attendees opportunity to focus on their particular area of interest. This new event will be the only international event of its kind covering sources, materials, and applications - all in one meeting.

At the Advanced Solid-State Lasers Congress, you will hear the latest advances in solid-state laser technologies and laser sources while examining important issues and innovations in this technical area. Discussion topics include:

1. How to increase the effectiveness of existing technologies and applications to meet evolving marketplace requirements
2. How to establish the performance requirements for laser sources and associated optics
3. How existing materials limit performance today and what are the needs for new or improved materials in the future
4. How existing performance shortfalls limit increased market penetration and how to overcome those

Exhibit space at this new event is extremely limited (only 50 spaces available). Attendees represent the most prominent figures from the laser industry including key personnel from manufacturers, distributors, government, and academia. The audience for your products will be truly global in scope.

Sponsor:



Advanced Solid-State Photonics (ASSP)

29 January - 1 February 2012, Rancho Bernardo Inn, San Diego, California, United States

Program

The program for Advanced Solid-State Photonics topical meeting will be held 29 January through 1 February 2012. No events are scheduled for Sunday, 1 February 2012; however participants may register and pick up their materials on Sunday afternoon.

[About ASSP and Topic Categories](#)
[Download Pages from the Program book](#)
[Invited Speakers](#)
[Special Events](#)
[Short Courses](#)
[Call for Papers](#)
[Schedule-at-a-Glance](#)
[Online Conference Program](#)

About Advanced Solid-State Photonics (ASSP)

The Advanced Solid-State Photonics Topical meeting specializes in novel solid-state sources of coherent radiation operating in different spectral ranges. Now in its 27th year, this meeting remains the world's premier forum for discussing new developments in solid-state and fiber lasers, ultrashort light sources, amplifier design and power scaling, laser and nonlinear optical materials, and nonlinear frequency conversion devices. These light sources find an increasingly broad range of applications in spectroscopy, metrology, remote sensing, communications, material processing, astronomy, medicine, and life sciences.

A number of distinguished speakers have been invited to present at the meeting. This year's invited presentations focus on ultra-broadband fiber lasers, efficient solid-state waveguide lasers, carbon nanostructures for mode-locking, ultrafast thin disk lasers and amplifiers, multilayer coatings for dispersion control, vertical external cavity surface-emitting lasers for mid-IR emission, high power fiber lasers, and mid-IR frequency conversion using quasi-phase-matched GaAs. In addition, ASSP 2012 features a Summit session devoted to laser beam combining, covering both coherent and incoherent approaches toward increasing spatial brightness beyond the limits of any given source technology.

Papers are being considered in the following topic categories:

- Diode-Pumped Lasers
- Fiber Lasers
- Ceramic Lasers
- High-Power Lasers
- Laser beam combining
- Short-Pulse Lasers
- Frequency-Stable Lasers
- Microchip and Compact Lasers
- Tunable and New Wavelength Solid-State Lasers
- Optically Pumped Semiconductor Lasers
- High-Brightness Diodes
- Optical Sources Based on Nonlinear Frequency Conversion Schemes
- Coherent Sources Based on New Nonlinear Materials
- Coherent Sources Based on New Laser Gain Media
- Applications of Laser Sources in:
 - Science
 - Metrology, including optical frequency combs
 - Astronomy, including gravity wave detection and laser guide star
 - Medicine and Biology
 - Remote Sensing
 - Materials processing
 - Laser display technology

Special Events

Congress Plenary

Wednesday, 1 February

JW1A, 8:00 – 9:30

JW2A, 10:00 – 11:30

San Bernardo Ballroom, Rancho Bernardo

The 2011 Plenary Session will feature world-renowned speakers in the in the fields. See the [invited speaker page](#) for detailed descriptions of the speakers and their presentations.

Featured Plenary Speakers:

Tso Yee Fan, *MIT, USA*

James R. Gord, *Air Force Research Lab., USA*

Philip Russell, *Max Planck Institute, Germany - ADD Speaker*

Jochen Speiser, *Institute of Technical Physics, DLR, Germany*

OSA Corporate Associates Present: Executive Speaker Series

Interview and Reception

Wednesday, 1 February, 18:00 - 19:30

San Bernardo Ballroom, Rancho Bernardo



Interviewer: Robert L. Byer,

Department of Applied Physics, Stanford University



Featured Guest: John Ambroseo,
President and Chief Executive Officer, Coherent

Sit down for an entertaining and intimate conversation with Dr. John Ambroseo, President and Chief Executive Officer, Coherent, as he responds to questions about his career path, corporate observations and personal perspectives. During Dr. Ambroseo's 23-year career with Coherent, he has held positions in sales, marketing, U.S. and international operations and has been involved in multiple mergers and acquisitions. The program begins with a networking reception, followed by a one-on-one interview and concludes with audience questions.

This event is made possible through generous support from IPG Photonics

Conference Banquet

Wednesday, 1 February

19:30 – 21:00

Aragon II & III, Rancho Bernardo

This banquet brings together all of the four meetings, ASSP, AIOM, FILAS and LACSEA, within the congress for a fun evening of networking and dinner. This is open to all technical attendees.



Banquet Speaker: Peter Moulton, *Q-peak, USA*

Life with Solid State Lasers and Nonlinear Optics: Mining for Nuggets

Abstract: I recount nearly 40 years (where did all that time go?) of work in lasers and nonlinear optics, searching for solutions to problems, sometimes finding them, sometimes failing miserably, but managing to have a great time in the process.

Laser Beam Combining Summit

AW3A, 1 February
13:00 – 15:00
Aragon II

This year ASSP is offering this special session, the Summit features a selection of [invited talks](#) from top researchers reviewing progress across a wide variety of source technologies and combining approaches.

ASSP Poster Sessions

AM4A, Monday, 30 January, 15:00 – 16:30
AT4A, Tuesday, 31 January, 15:00 – 16:30
AW4A, Wednesday, 1 February, 15:00- 1630
Aragon I & Foyer, Rancho Bernardo

Poster sessions are an integral part of the technical program and offer a unique networking opportunity, where presenters can discuss their results one-to-one with interested parties. Each author is provided with a 4 ft. x 8 ft. (1.22 m x 2.44 m) board on which to display the summary and results of his or her paper. For poster sessions of the other meetings check the [Schedule at a Glance](#).

Postdeadline Sessions

Time and Location: TBD

The purpose of postdeadline sessions is to give participants the opportunity to hear new and significant material in rapidly advancing areas. Only those papers judged to be truly excellent and compelling in their timeliness were accepted. More information, including the schedule and locations, will be posted in the weeks preceding the conference.

Short Courses

Short courses are a wonderful way to enhance your knowledge of the optical field. ASSP selects experts in their fields to provide you with an in-depth look at intriguing topics. The courses are designed to increase your knowledge of a specific subject while offering you the experience of knowledgeable teachers. An added benefit is the availability of continuing education units (CEUs). CEUs are awarded to each participant who successfully completes the short course. The CEU is a nationally recognized unit of measure for continuing education and training programs that meet established criteria. To earn CEUs, a participant must complete the CEU credit form and course evaluation and return it to the instructor at the end of the course. CEUs will be calculated and certificates will be mailed to participants.

- Tuition for short courses is a separate fee, and advance registration is recommended: the number of seats is limited.
- Short courses will sell out quickly! There will be no waiting list.
- Short course materials are not available for purchase.

Schedule

Sunday 29 January 2011

12:30-15:30

SC380: Laser Noise

Rüdiger Paschotta, *RP Photonics Consulting GmbH, Germany*

Course Level:

Advanced Beginner (basic understanding of topic is necessary)

Course Description:

This course gives an introduction into laser noise with an emphasis on an intuitive understanding and practical application. It begins with an overview on basic mathematics for describing noise. Thereafter, the properties of quantum noise and technical noise sources are discussed. Their effects are then studied for continuous-wave lasers, pulsed lasers and mode-locked lasers. It will also be discussed how lasers can be optimized for low-noise operation.

Benefits and Learning Objectives:

This course should enable you to:

- Understand and use basic mathematical descriptions of noise, particularly for quantifying laser noise/li>
- Explain differences between quantum noise and technical noise sources/li>
- Distinguish different types of noise in the output of lasers/li>
- Understand the effects of quantum noise and technical noise sources on the output of different kinds of lasers

Intended Audience:

This course is designed for researchers and engineers for whom noise in the output of lasers is relevant.



Instructor Biography:

Rüdiger Paschotta started his career in scientific research. In 2002, he achieved the habilitation in applied physics at ETH Zürich and received the Fresnel Prize of the European Physical Society (EPS). In 2004, he started RP Photonics Consulting GmbH. His full-time occupation is now to serve companies in the photonics industry worldwide. Typical tasks are to work out feasibility studies and designs for lasers and other photonic devices, to identify and solve technical problems, to find suitable laser sources for specific applications, and to do tailored staff training courses on specialized subjects.

12:30-15:30

SC381: High-energy Fiber Lasers

Almantas Galvanauskas, CUOS, University of Michigan, Ann Arbor, USA

Course Level:

Advanced Beginner (basic understanding of topic is necessary to follow course material)

Course Description

This course provides with a comprehensive introduction to high energy pulsed fiber laser systems with an emphasis on designing them and understanding achievable performance characteristics, such as pulse energy, duration and average power. It starts by an overview of fundamentals of rare-earth doped fiber gain medium, such as basic spectroscopic properties, rate-equation description of gain dynamics, energy saturation and limits to energy extraction, optical nonlinearity limitations on peak power, and fiber thermal properties at high powers. Then it proceeds to description of key components constituting a fiber laser system, such as large core optical fibers, including advanced designs for single-mode operation with large cores, fiber polarization properties, double-clad fibers and basic pumping considerations to match pump-diode brightness and fiber geometry, monolithic pump combiner designs and operation. After this detailed analysis of basic pulsed laser architecture will follow, starting with a basic layout, seed pulse source choice, different multiple-stage design options, comparison between co- and counter pumping configurations, pulse-shape control, and specific aspects of implementing ultrashort pulse amplification. We will then proceed to survey published state-of-the-art results achieved with different types of pulsed lasers, including long pulse, nanosecond pulse and femtosecond pulse systems, with an objective to explore achievable performance characteristics. After this we will consider advanced high-energy laser designs based on different beam-combining approaches. At the end we will briefly review applications and future outlook for this technology.

Benefits and Learning Objectives

This course should enable participants to

- Design a pulsed fiber laser system
- Specify required components to built such a system
- Identify design trade-offs and challenges
- Define achievable performance characteristics
- Acquire knowledge of state-of-the-art achievements in the field
- Understand applications and direction of further development of this technology

Intended Audience

This course is intended for graduate students, engineers and researchers who need to build or use high energy pulsed or ultrashort pulse fiber lasers, or those who are interested in pulsed laser applications, the current state of the art and future of this technology. Undergraduate training is assumed.

Instructor Biography:



Almantas Galvanauskas is a professor at the Electrical Engineering and Computer Science Department, University of Michigan. He has been working in the field of fiber lasers for approximately twenty years, and has more than 200 publications, including approximately 30 patents and patent applications. He had pioneered ultrashort-pulse fiber CPA and his work had resulted in demonstrating several record-breaking achievements in performance of fiber lasers. Prior to joining University of Michigan he spent eight years in industrial R&D. His current work spans areas from novel fiber designs to advanced fiber laser systems, including beam combining of pulsed and ultrashort pulse lasers, and new fiber laser applications such as high-intensity laser plasma produced EUV and X-ray generation. He is also a co-founder of Arbor Photonics, Inc.

16:00-19:00

SC382: Ultrafast Optical Parametric Amplifiers

Giulio Cerullo, *Politecnico di Milano, Italy*

Course Level:

Advanced Beginner (basic understanding of topic is necessary to follow course material)

Course Description:

This course will present a comprehensive introduction to the topic of ultrafast optical parametric amplifiers (OPAs), starting from the basic principles and progressing to the more advanced applications. OPAs allow not only to generate broadly tunable pulses starting from a fixed frequency source, but also, thanks to their broad gain bandwidths, to dramatically shorten the pulse duration, down to the few-cycle limit.

The course will start by reviewing the nonlinear three-wave interaction equations which describe optical parametric amplification, and deriving from them the main OPA properties, both in the stationary and short-pulse regimes. The design principles of standard OPAs working in the visible, near-infrared and mid-infrared ranges will be presented. We will then describe ultra-broadband OPA architectures, allowing the generation of tunable sub-10-fs light pulses, and review dispersion compensation techniques. We will finally cover more advanced applications, such as passive carrier-envelope-phase stabilization and the generation of ultrahigh peak power pulses by optical parametric chirped pulse amplification.

Benefits and Learning Objectives:

This course will enable you to:

- Understand the nonlinear wave equations describing optical parametric amplification
- Understand how the parameters of the driving laser and of the nonlinear crystal influence the OPA performance
- Design and build an OPA pumped by the fundamental (second harmonic) of Ti:sapphire and generating broadly tunable infrared (visible) pulses
- Design and build a non-collinear OPA for the generation of few-optical-cycle visible pulses
- Explain how OPAs can be used to generate carrier-envelope-phase stable pulses in a passive, all-optical way
- Understand the design principles of optical parametric chirped pulse amplifiers and the limits of energy scaling

Intended Audience:

Students, academics, researchers and engineers in various disciplines who use or build ultrafast optical parametric amplifiers and require a comprehensive introduction to the subject and an overview of future developments. Undergraduate training in engineering or science is assumed.

Instructor Biography:



Giulio Cerullo is a full professor with the Physics Department, Politecnico di Milano. His research activity (240 publications in peer-reviewed journals) has mainly focused on the generation of tunable few-optical-cycle light pulses and on their application to ultrafast spectroscopy, tracking primary photoinduced events in biomolecules and solids. He has pioneered the Non-collinear Optical Parametric Amplifier (NOPA) concept and its extension to the near and mid-IR. He is Topical Editor for the Journal Optics Letters (Optical Society of America) for the area Ultrafast Optical Phenomena. He has been in the Technical Program Committees of the most important international conferences in optics and photonics (CLEO USA, Cleo Europe, EQEC, Ultrafast Phenomena, HILAS, Photonics Europe). Prof Cerullo has delivered numerous invited talks and tutorials at scientific conferences and schools on the topics of few-optical-cycle pulse generation and applications.

16:00-19:00 - CANCELLED

SC383: Average Power Scaling of Ultrafast Solid State Lasers

Dieter Hoffmann, *Fraunhofer Institute of Laser Technology, Aachen, Germany*



Advanced Solid-State Photonics (ASSP)

Advances in Optical Materials (AIOM)

Fiber Lasers and Applications (FILAS)

Laser Applications to Chemical, Security and Environmental Analysis (LACSEA)

29 January–3 February 2012

Rancho Bernardo Inn, San Diego, California, United States

Welcome to the 2012 OSA Optics & Photonics Winter Congress on Lasers, Sources and Related Photonic Devices! This year, we have four topical meetings collocated together to form this Congress. The four meetings are Advanced Solid-State Photonics (ASSP), Advances in Optical Materials (AIOM), Fiber Lasers and Applications (FILAS), and Laser Applications to Chemical, Security and Environmental Analysis (LACSEA). Two joint plenary sessions will be held between these meetings on Wednesday morning, culminating with the joint conference banquet Wednesday evening. We are pleased to have Dr. Peter F. Moulton as the banquet speaker who will deliver a talk titled 'Life with Solid State Lasers and Nonlinear Optics: Mining for Nuggets.' We hope that bringing together leaders and experts among the different communities to share information and discuss topics across disciplines will provide you with a rich experience.

The Advanced Solid-State Photonics Topical meeting (ASSP) specializes in novel solid-state sources of coherent radiation operating in different spectral ranges. Now in its 27th year, this meeting remains the world's premier forum for discussing new developments in solid-state and fiber lasers, ultrashort light sources, amplifier design and power scaling, laser and nonlinear optical materials, and nonlinear frequency conversion devices. These light sources find an increasingly broad range of applications in spectroscopy, metrology, remote sensing, communications, material processing, astronomy, medicine, and life sciences. We have scheduled 1 plenary, 12 invited and 46 contributed oral presentations, together with 86 poster presentations and 3 short courses, for you to attend. The summit on laser beam combining, brought to you through a contribution from DSO National Laboratories in Singapore, will further feature 4 invited presentations. Furthermore, we are grateful to Lockheed Martin for sponsoring the ASSP Best Student Awards for the best oral and poster presentation.

The Advances in Optical Materials (AIOM) Topical Meeting will bring together international experts and researchers to review and discuss the advances in optics, materials science, condensed matter physics, and chemistry relevant to the development of new optical materials. The development of new optical materials has been the key factor in the birth of new technology. We have scheduled 1 plenary, 14 invited, and 29 contributed oral presentations, together with 12 poster presentations, for you to attend.

The Fiber Lasers and Applications (FILAS) meeting brings together researchers from academia, industrial and government laboratories across the world to present and discuss the latest advances in the area of fiber laser technology. In 2011 this conference was held for the first time in Istanbul and it was very successful with a number of world experts in this field in attendance. In 2012 the conference will feature not only high power pulsed and CW fiber lasers and fiber laser amplifiers (both Raman and direct) at wavelengths ranging from UV to IR, but also how they impact numerous application areas, ranging from both classical and novel industrial applications to environmental monitoring and medicine. Specifically applications in high power fiber lasers will include LIDAR, oil and gas exploration, homeland security and perimeter monitoring. FILAS is planned to complement the program of the Advanced Solid State Photonics (ASSP) topical - fundamental scientific aspects are primarily covered by ASSP whereas fiber laser engineering and applications are primarily covered by FILAS. The bridging between fundamental scientific aspects and applications will also be covered by FILAS 2012. We have scheduled 1 banquet keynote, 1 plenary, 13 invited, and 18 contributed oral presentations, together with 18 poster presentations, for you to attend. We would like to thank Multiwave Photonics for sponsoring the FILAS student award and IPG Photonics for generous student travel support; sponsorship of the the Executive Speaker Series and hosting the FILAS Banquet, a private function for FILAS attendees.





The focus of the Laser Applications to Chemical, Security and Environmental Analysis (LACSEA) topical meeting is on the development of new laser-analytical principles, new components, systems and new applications. This year's program is exceptional! It includes 18 well-known invited speakers, 42 contributed speakers, and 13 poster presentations. Our program will cover recent advances in analytical laser spectroscopy including, improved data retrieval techniques in laser spectroscopic analysis and biochemical/biophysical and medical applications of laser techniques. This meeting would like to acknowledge the generous support of Spectral Energies for their outstanding support for speakers and students and their sponsorship of the LACSEA Best Student Awards for best oral and poster presentation.

We all are very pleased to have you join us and we look forward to a great meeting!

Advanced Solid-State Photonics (ASSP)

Alphan Sennaroglu, *Koç Univ., Turkey*, **General Chair**

Gregory Goodno, *Northrop Grumman Aerospace Systems, USA*, **Program Chair**

Andrius Baltuska, *TU Vienna, Austria*, **Program Chair**

Advances in Optical Materials (AIOM)

Shibin Jiang, *AdValue Photonics, USA*, **General Chair**

Richard Moncorge, *Universite de Caen, France*, **General Chair**

Jean-Luc Adam, *Universite de Rennes, France*, **Program Chair**

John M. Zavada, *National Science Foundation, USA*, **Program Chair**

Fiber Lasers and Applications (FILAS)

Valentin Gapontsev, *IPG Photonics Corp., USA*, **General Chair**

Jose Salcedo, *Multiwave Photonics, Portugal*, **General Chair**

Nasser Peyghambarian, *Univ. of Arizona, USA*, **Program Chair**

Francois Salin, *EOLITE, France*, **Program Chair**

Laser Applications to Chemical, Security and Environmental Analysis (LACSEA)

Sukesh Roy, *Spectral Energies, LLC, USA*, **Chair**

Markus W. Sigrist, *ETH Zurich, Switzerland*, **Chair**

Barry McManus, *Aerodyne Research, Inc., USA*, **Chair**



PHAROS

High-power Industrial Femtosecond Lasers



15 W
190 fs
1.5 mJ
1 MHz

- 200 fs-10 ps pulse duration adjustable
- Up to 1.5 mJ pulse energy
- Single pulse to 1 MHz
- Up to 15 W average power
- Industrial, sealed design
- Compact, modular setup
- Yb based with SSLD pumping
- Complete range of harmonic converters and OPA's available

For more information, contact:
Light Conversion
+370.5.2491830
www.lightcon.com



LIGHT
CONVERSION

North American Contact
Altos Photonics Inc
866.658.5404
www.altosphotronics.com



Lasers, Sources and Related Photonic Devices Program Committee

Advances in Optical Materials (AIOM)

General Chairs

Shibin Jiang, *AdValue Photonics, USA*
Richard Moncorge, *Universite de Caen, France*

Program Chairs

Jean-Luc Adam, *Universite de Rennes, France*
John M. Zavada, *National Science Foundation, USA*

Committee Members

Gerard Aka, *Ecole Natl Supérieure de Chimie de Paris, France*
John M. Ballato, *Clemson University The Center for Optical Materials Science and Engineering Technologies, USA*
Tasoltan T. Basiev, *Russian Academy of Sciences, Russia*
Jes Broeng, *NKT Research & Innovation, Denmark*
Mark A. Dubinskii, *US Army Research Laboratory, USA*
Romain M. Gaume, *Stanford University, USA*
Richard Gentilman, *Raytheon - Integrated Defense Systems, USA*
Lili Hu, *Shanghai Institute of Optics and Fine Mechanics, China*
Jonathan C. Knight, *University of Bath, United Kingdom*
Christian Krankel, *University of Hamburg, Germany*
Sergei B. Mirov, *University of Alabama, USA*
Kathleen A. Richardson, *Clemson University, USA*
Jasbinder S. Sanghera, *US Naval Research Laboratory, USA*
Kenneth L. Schepler, *US Air Force, USA*
Peter G. Schunemann, *BAE Systems Inc., USA*
Takunori Taira, *Institute for Molecular Science, Japan*
Xu-Tang Tao, *Shandong University, China*

Advanced Solid-State Photonics (ASSP)

General Chair

Alphan Sennaroglu, *Koç Univ., Turkey*

Program Chair

Gregory Goodno, *Northrop Grumman Aerospace Systems, USA*
Andrius Baltuska, *Vienna Univ. of Technology, Austria*

Program Committee

Liang Dong, *Clemson Univ., USA*
Mark Dubinskii, *US Army Res. Lab, USA*
Majid Ebrahim-Zadeh, *Inst. de Ciències Fotoniques, Spain*
Marc Eichhorn, *French-German Res. Inst. of Saint-Louis (ISL), France*
Katia Gallo, *KTH - Royal Inst. of Technology, Sweden*
Jennifer Hastie, *Univ. of Strathclyde, UK*
F Oemer Ilday, *Bilkent Univ., Turkey*
Yoonchan Jeong, *Seoul Natl. Univ., Republic of Korea*
Jason Jones, *Univ. of Arizona, USA*
James Kafka, *Newport Corp., USA*
Junji Kawanaka, *Osaka Univ., Japan*
Sunao Kurimura, *Natl. Inst. for Materials Science, Japan*
Valentin Petrov, *Max-Born Inst., Germany*
Kathleen Schaffers, *Lawrence Livermore Natl. Lab, USA*
Thomas Schreiber, *Fraunhofer IOF, Germany*
Scott Setzler, *BAE Systems PLC, USA*
Akira Shirakawa, *Univ. of Electro-Communications, Japan*
Thomas Südmeyer, *ETH Zurich, Switzerland*
Brian Walsh, *NASA Langley Res. Ctr., USA*

Fiber Lasers and Applications (FILAS)

General Chairs

Valentin Gapontsev, *IPG Photonics Corp., USA*
Jose Salcedo, *Multiwave Photonics, Portugal*

Program Chairs

Nasser Peyghambarian, *Univ. of Arizona, USA*
Francois Salin, *EOLITE, France*

Committee Members

Farzin Amzajerdian, *NASA Langley Research Center, USA*
Brian Walter Baird, *Summit Photonics, USA*
Arturo Chavez-Pirson, *NP Photonics Inc., USA*
Fabio Di Teodoro, *The Aerospace Corp., USA*
Evgeny M. Dianov, *Russian Academy of Sciences, Russia*
Anatoly B. Grudinin, *Fianium Ltd., United Kingdom*
Yves Hernandez, *MultiTel Inc., Belgium*
Clemens Hoenninger, *Amplitude Systems, France*
Dan Hu, *Lockheed Martin, USA*
Karl W. Koch, *Corning Inc., USA*
Bill O'Neill, *University of Cambridge, United Kingdom*
Sergei Popov, *Kungliga Tekniska Hogskolan, Sweden*
David Pureur, *Quantel, France*
Axel Schulzgen, *University of Central Florida, CREOL, USA*
Irina Sorokina, *Norges Teknisk Naturvitenskapelige Universitet, Norway*
Andrey N. Starodumov, *Coherent Inc., USA*
Andreas Tünnermann, *Friedrich-Schiller-Universität Jena, Germany*

Laser Applications to Chemical, Security and Environmental Analysis (LACSEA)

Chairs

Sukesh Roy, *Spectral Energies, LLC, USA*
Markus W. Sigrist, *ETH Zurich, Switzerland*
Barry McManus, *Aerodyne Research, Inc., USA*

Program Committee

Frank Beyrau, *Imperial College London, United Kingdom*
Joakim Bood, *Lunds Tekniska Hogskola, Sweden*
Timothy Day, *Daylight Solutions Inc., USA*
Thomas Dreier, *Universität Duisburg-Essen, Germany*
Volker Ebert, *Physikalisch Technische Bundesanstalt, Germany*
Wolfgang A. Ertmer, *Leibniz Universität Hannover, Germany*
David W. Hahn, *University of Florida, USA*
Dennis K. Killinger, *University of South Florida, USA*
Waruna Kulatilaka, *Spectral Energies LLC, USA*
Wolfgang Meier, *German Aerospace Center, Germany*
Jerry R. Meyer, *US Naval Research Laboratory, USA*
Terrence R. Meyer, *Iowa State University, USA*
Andrzej W. Miziolek, *Aberdeen Proving Ground, USA*
Thomas A. Reichardt, *Sandia National Labs, USA*
Scott Thomas Sanders, *University of Wisconsin-Madison, USA*
Wolfgang Schade, *Technische Universität Clausthal, Germany*
Thomas B. Settersten, *Sandia National Labs, USA*
David M. Sonnenfroh, *Physical Sciences Inc., USA*
Frank K Tittel, *Rice University, USA*
Petter Weibring, *National Center for Atmospheric Research, USA*

Special Events

Short Courses

Sunday, 29 January 2012, 12:30–19:00
See page 10 for more information.
Separate registration is required.

Sunday Evening Welcome Reception

19:00–20:30
Santiago Room and Courtyard

Please join us for a happy hour on Sunday Evening and share a few drinks with your colleagues to kick off the 2012 Laser Congress.

Joint Plenary Session I

Wednesday, 1 February 2012, 08:00–9:30
San Bernardo Ballroom

Frontiers of Disk Lasers

Fifteen years after first commercialization, the Thin Disk Laser covers a broad spectrum of applications. Nevertheless, a lot of challenges remain, e.g. further scaling of power and pulse energy or the search for different suitable laser materials.

Jochen Speiser; *Institute of Technical Physics, DLR, Germany*



Jochen Speiser is head of the Solid State Lasers and Nonlinear Optics group at the Institute of Technical Physics of DLR, a group working mainly on the development and adaptation of laser sources for application in aerospace as well as security and defence applications. He has been working on the numerical simulation of the thin disk laser since 2001, mainly on thermal modeling and on scaling limits due to amplified spontaneous emission. During the last years his focus was on concepts for power scaling of high brightness thin disk lasers to the 100 kW level. Recent activities also include concepts for high energy, high average power thin disk amplifiers. He is involved in several activities, including European projects, dealing with design analysis for laser systems with several kilojoule energy and 100 kW average power, partially based on thin disk design

Jochen Speiser received his diploma in physics from the University of Kaiserslautern, Germany, in 2001. Before joining DLR, he has been working in the laser development and laser optics department of the Institut fuer Strahlwerkzeuge (IFSW) at the University of Stuttgart, Germany for six years.

Wavelength and Coherent Beam Combining for High Brightness Sources

Beam combining of laser arrays with high efficiency and good beam quality for power and radiance scaling is a long-standing problem in laser technology. Recently, significant progress has been made using wavelength techniques and coherent techniques.

Tso Yee Fan; *MIT Lincoln Laboratory, USA*



Tso Yee (T. Y.) Fan is the Associate Leader of the Laser Technology and Applications Group at MIT Lincoln Laboratory, Lexington, MA. He joined MIT Lincoln Laboratory as a Staff Member in 1987. He is widely recognized for his pioneering work in diode-pumped solid-state lasers particularly the development of Yb:YAG lasers, in advances in cryogenic lasers for improving average-power scalability, in characterization of laser and nonlinear optical materials, and in advances in laser beam combining.

Dr. Fan is a Fellow of the Optical Society of America (OSA) and a Senior Member of the Institute of Electrical and Electronics Engineers (IEEE). He received the 2009 MIT Lincoln Laboratory Technical Excellence Award for his work on Yb lasers, cryogenic lasers and laser beam combining. He served as an Elected Member of the IEEE/LEOS Board of Governors from 1994–1996 and was the Topical Editor, Lasers for *Optics Letters* from 1994–1999. He was Division Editor for the Lasers, Photonics, and Environmental Optics Division of *Applied Optics*. He has been on program committees of numerous conferences, including as Chair of the LEOS Annual Meeting and Chair of the OSA Topical Meeting on Advanced Solid-State Lasers.

Dr. Fan received the S. B. degrees electrical engineering and materials science and engineering from the Massachusetts Institute of Technology (MIT), Cambridge, MA, and the M. S. and Ph. D. degrees in electrical engineering from Stanford University, Stanford, CA.

Special Events continued

Joint Plenary Session II

Wednesday, 1 February 2012, 10:00-11:30
San Bernardo Ballroom

Pumping up the Pressure: Gas-Based Nonlinear Optics in Hollow Core Photonic Crystal Fibre

Single-mode hollow core PCF provides an ideal environment for studying pressure-controlled nonlinear interactions between laser light and gases. An recent success is the efficient generation of tunable deep-UV pulses from ~50fs, ~1uJ pulses at 800nm.

Philip Russell; *Max Planck Institute for the Science of Light, Germany*



Philip Russell is a Director at the Max-Planck Institute for the Science of Light in Erlangen, Germany and holds the Krupp Chair in Experimental Physics at the University of Erlangen-Nuremberg. He obtained his M.A. (1976) and D.Phil. (1979) degrees at the University of Oxford and subsequently worked in research laboratories and universities in France, Germany and the USA. Since 1976 his interests have ranged from the behaviour of light in periodically structured materials to nonlinear optics, waveguides and optical fibres. He is known as the inventor of photonic crystal fibres and the founder of the company BlazePhotonics Ltd. He is a Fellow of the Royal Society and the Optical Society of America (OSA) and has won several international awards for his research including the 2005 Körber Prize for European Science, the 2005 Thomas Young Prize of the Institute for Physics (UK) and the 2000 OSA Joseph Fraunhofer Award/Robert M. Burley Prize. He was a Director-At-Large of the Optical Society of America 2007-2009 and from 2005 to 2006 he was an IEEE-LEOS Distinguished Lecturer and the recipient of a Royal Society/Wolfson Research Merit Award.

Development and Application of Ultrafast Laser Spectroscopy for Combustion Sensing

Optical measurement techniques are powerful tools for detailed study of combustion chemistry and physics. Ultrafast (picosecond- and femtosecond-pulsed) lasers are driving the enhancement of existing diagnostic techniques and enabling the development of new measurement approaches.

James R. Gord; *Propulsion Directorate, Air Force Research Laboratory, USA*



Dr. James R. Gord, Principal Research Chemist with the Air Force Research Laboratory's Propulsion Directorate, leads the development and application of optical measurement techniques for advanced propulsion and fuel systems as Director of the Combustion and Laser Diagnostics Research Complex. His work has produced five patents, four book chapters, more than 130 peer-reviewed journal articles, and more than 675 conference papers and presentations, including more than 160 delivered upon invitation.

Dr. Gord studied at Miami University as a National Merit and Ohio Board of Regents Scholar, receiving a B.S. in chemistry with University and Departmental Honors in 1986. He performed his doctoral research at Purdue University with Prof. Ben S. Freiser through fellowships from the National Science Foundation and the American Chemical Society, receiving a Ph.D. in analytical chemistry with Highest Honors in 1990. Thereafter he pursued postdoctoral studies in chemical physics at the Joint Institute for Laboratory Astrophysics (JILA) with Prof. W. Carl Lineberger.

Dr. Gord joined the Air Force research team in 1991. In 2007 he was named a Fellow of the Optical Society of America. In 2005 he received AFRL's top honor when he was named an AFRL Fellow. Dr. Gord is a two-time winner of AFRL's Award for Outstanding Scientific and Technical Achievement (2004, 2001) and was named one of Dayton's 40 Superachievers Under 40 in 2004. He is also a three-time winner of the Propulsion Directorate's S. D. Heron Award (2010, 2005, 1999) for outstanding technical achievement. In 2001 he was named the Propulsion Directorate's Scientist of the Year. Dr. Gord has been named a Distinguished Alumnus of Purdue University, Miami University, and Miami East High School. He is a member of the American Chemical Society, the American Institute of Aeronautics and Astronautics (Associate Fellow), the American Institute of Physics, the American Society of Mechanical Engineers, the Combustion Institute, the Optical Society of America (Fellow), Phi Beta Kappa, Sigma Xi, and the Society for Applied Spectroscopy.

Special Events continued

Laser Beam Combining Summit

AW3A, Wednesday, 1 February, 13:00–15:00

Aragon II

This year ASSP is offering this special session, the Summit features a selection of invited talks from top researchers reviewing progress across a wide variety of source technologies and combining approaches.

- **Coherent Combination of Fiber Amplified Femtosecond Pulses**, Jens Limpert, *U. Jena, Germany*
- **Coherent Beam Combination of High Repetition Rate, Energetic Lasers using Stimulated Brillouin Scattering Phase Conjugate Mirrors**, Hong-Jin Kong, *KAIST, Korea*
- **Spectral Beam Combining of Fiber Lasers for Power Scaling**, Eric Honea, *Lockheed Martin Aculight, USA*
- **kW-class Direct Diode Lasers with Comparable Brightness to Fiber, Disk, and Carbon Dioxide Lasers**, Robin Huang, *TeraDiode Inc, USA*

OSA Corporate Associates Present: Executive Speaker Series

Interview and Reception

Wednesday, 1 February, 18:00–19:30

San Bernardo Ballroom, Rancho Bernardo Inn, San Diego, California

Interviewer: **Robert L. Byer**, *Department of Applied Physics, Stanford University*



Featured Guest: **John Ambroseo**, *President and Chief Executive Officer, Coherent*



Sit down for an entertaining and intimate conversation with Dr. John Ambroseo, President and Chief Executive Officer, Coherent, as he responds to questions about his career path, corporate observations and personal perspectives. During Dr. Ambroseo's 23-year career with Coherent, he has held positions in sales, marketing, U.S. and international operations and has been involved in multiple mergers and acquisitions. The program

begins with a networking reception, followed by a one-on-one interview and concludes with audience questions.

This event is made possible through generous support from IPG Photonics.

Banquet

Wednesday, 1 February 2012, 19:30-21:00

Aragon II & III

Life with Solid State Lasers and Nonlinear Optics: Mining for Nuggets

I recount nearly 40 years (where did all that time go?) of work in lasers and nonlinear optics, searching for solutions to problems, sometimes finding them, sometimes failing miserably, but managing to have a great time in the process.

Peter F. Moulton; *Q-Peak, USA*



Peter Moulton was born in Springfield, MA in 1946. He received an A.B. in Physics from Harvard College in 1968 and M.S. and Ph.D. degrees in Electrical Engineering from M.I.T. in 1972 and 1975 respectively. After finishing graduate school he was employed in the Quantum Electronics Group at M.I.T. Lincoln Laboratory, Lexington, MA. In 1985 he joined a start-up company, Schwartz Electro-Optics, as Vice-President and managed the founding of the company's Research Division in Concord, Massachusetts. He became Senior Vice-President of SEO in 1997 and was involved in spinning out the Research Division as a separate company, Q-Peak, in 1998, and in the sale of Q-Peak to its current parent company, Physical Sciences Inc. (Andover, MA) in 2001. At present he is the Vice-President and Chief Technology Officer of Q-Peak.

Moulton's technical work began in the field of bulk solid state lasers, and in recent years has extended to include nonlinear optics and fiber lasers. Some of his work has been motivated by defense applications, including infrared countermeasures, detection of chemical and biological weapons, advanced lidar and targeting systems, laser communications and directed-energy systems. He has also been involved in scientific applications, including global monitoring of atmospheric water vapor, ozone, aerosols and wind, in commercial applications in the semiconductor industry, in laser systems for medical treatment and diagnostics, and in the development of lasers for large-screen color displays. The latter has led to the formation of a VC-funded company, Laser Light Engines (Salem, NH), where Moulton has a non-executive role as Chief Scientist.

Moulton has had a long association with the OSA, starting in 1981. He served on the Program Committee for the first CLEO



Special Events continued

meeting and functioned as Program Co-Chair, 1988 Conference Co-Chair, and, for three terms, Member of the Steering Committee, including Chair positions in 1996 and 2007. He established the first OSA-managed Topical Meeting on Tunable Solid State Lasers in 1985, which has continued to this date, renamed as the Advanced Solid State Photonics meeting and, recently was a founding Chair for the PhAST Meeting. In 1998, Moulton was elected to a three-year term as Director at Large, OSA Board of Directors, where he was involved in the Awards and Finance Committees and later, as a member of the Audit Committee. In 2005 he returned to the OSA Board as Co-Chair of the Science and Engineering Council.

In addition to a 2011 IEEE Fellow election, Dr. Moulton is a Fellow of the Optical Society of America (OSA). He was awarded the R.W. Wood Prize from the OSA and the William Streifer Scientific Achievement Award from IEEE/LEOS, both in 1997, and in 2000 he was elected to the National Academy of Engineering.

Postdeadline Papers Presentations

Please see the update sheet for information concerning the Postdeadline Sessions. The purpose of the postdeadline session is to give participants the opportunity to hear new and significant materials in rapidly advancing areas. Only those papers judged to be truly excellent and compelling in their timeliness were accepted.





ADVANCED LASER TECHNOLOGIES

- Solid state lasers for basic research
- Spectroscopy systems
- Industrial lasers
- Laser optoelectronics

Lasers | Laser systems | Optoelectronics

www.ekspla.com

Short Courses

Short courses are a wonderful way to enhance your knowledge of the optical field. ASSP selects experts in their fields to provide you with an in-depth look at intriguing topics. The courses are designed to increase your knowledge of a specific subject while offering you the experience of knowledgeable teachers. An added benefit is the availability of continuing education units (CEUs). CEUs are awarded to each participant who successfully completes the short course. The CEU is a nationally recognized unit of measure for continuing education and training programs that meet established criteria. To earn CEUs, a participant must complete the CEU credit form and course evaluation and return it to the instructor at the end of the course. CEUs will be calculated and certificates will be mailed to participants.

- Tuition for short courses is a separate fee, and advance registration is recommended: the number of seats is limited.
- Short course materials are not available for purchase.

Schedule

Sunday 29 January 2012

SC380: Laser Noise

12:30-15:30

Rüdiger Paschotta, *RP Photonics Consulting GmbH, Germany*



Rüdiger Paschotta started his career in scientific research. In 2002, he achieved the habilitation in applied physics at ETH Zürich and received the Fresnel Prize of the European Physical Society (EPS). In 2004, he started RP Photonics Consulting GmbH. His full-time occupation is now to serve companies in the photonics industry worldwide. Typical tasks are to work out feasibility studies and designs for lasers and

other photonic devices, to identify and solve technical problems, to find suitable laser sources for specific applications, and to do tailored staff training courses on specialized subjects.

Course Level:

Advanced Beginner (basic understanding of topic is necessary)

Course Description:

This course gives an introduction into laser noise with an emphasis on an intuitive understanding and practical application. It begins with an overview on basic mathematics for describing noise. Thereafter, the properties of quantum noise and technical noise sources are discussed. Their effects are then studied for continuous-wave lasers, pulsed lasers and mode-locked lasers. It will also be discussed how lasers can be optimized for low-noise operation.

Benefits and Learning Objectives:

This course should enable you to:

- Understand and use basic mathematical descriptions of noise, particularly for quantifying laser noise
- Explain differences between quantum noise and technical noise sources

- Distinguish different types of noise in the output of lasers
- Understand the effects of quantum noise and technical noise sources on the output of different kinds of lasers

Intended Audience:

This course is designed for researchers and engineers for whom noise in the output of lasers is relevant.

SC381: High-energy Fiber Lasers

12:30-15:30

Almantas Galvanauskas, *CUOS, University of Michigan, Ann Arbor, USA*



Almantas Galvanauskas is a professor at the Electrical Engineering and Computer Science Department, University of Michigan. He has been working in the field of fiber lasers for approximately twenty years, and has more than 200 publications, including approximately 30 patents and patent applications. He had pioneered ultrashort-pulse fiber CPA and his work had resulted in demonstrating several

record-breaking achievements in performance of fiber lasers. Prior to joining University of Michigan he spent eight years in industrial R&D. His current work spans areas from novel fiber designs to advanced fiber laser systems, including beam combining of pulsed and ultrashort pulse lasers, and new fiber laser applications such as high-intensity laser plasma produced EUV and X-ray generation. He is also a co-founder of Arbor Photonics, Inc.

Course Level:

Advanced Beginner (basic understanding of topic is necessary to follow course material)

Course Description

This course provides with a comprehensive introduction to high energy pulsed fiber laser systems with an emphasis on designing them and understanding achievable performance characteristics, such as pulse energy, duration and average power. It starts by an overview of fundamentals of rare-earth doped fiber gain medium, such as basic spectroscopic properties, rate-equation description of gain dynamics, energy saturation and limits to energy extraction, optical nonlinearity limitations on peak power, and fiber thermal properties at high powers. Then it proceeds to description of key components constituting a fiber laser system, such as large core optical fibers, including advanced designs for single-mode operation with large cores, fiber polarization properties, double-clad fibers and basic pumping considerations to match pump-diode brightness and fiber geometry, monolithic pump combiner designs and operation. After this detailed analysis of basic pulsed laser architecture will follow, starting with a basic layout, seed pulse source choice, different multiple-stage design options, comparison between co- and counter pumping configurations, pulse-shape control, and specific aspects of implementing ultrashort pulse amplification. We will then proceed to survey published state-of-the-art results achieved with different types of pulsed lasers, including long

Short Courses continued

pulse, nanosecond pulse and femtosecond pulse systems, with an objective to explore achievable performance characteristics. After this we will consider advanced high-energy laser designs based on different beam-combining approaches. At the end we will briefly review applications and future outlook for this technology.

Benefits and Learning Objectives

This course should enable participants to

- Design a pulsed fiber laser system
- Specify required components to build such a system
- Identify design trade-offs and challenges
- Define achievable performance characteristics
- Acquire knowledge of state-of-the-art achievements in the field
- Understand applications and direction of further development of this technology

Intended Audience

This course is intended for graduate students, engineers and researchers who need to build or use high energy pulsed or ultrashort pulse fiber lasers, or those who are interested in pulsed laser applications, the current state of the art and future of this technology. Undergraduate training is assumed.

SC382: Ultrafast Optical Parametric Amplifiers

16:00-19:00

Giulio Cerullo, *Politecnico di Milano, Italy*



Giulio Cerullo is a full professor with the Physics Department, Politecnico di Milano. His research activity (240 publications in peer-reviewed journals) has mainly focused on the generation of tunable few-optical-cycle light pulses and on their application to ultrafast spectroscopy, tracking primary photoinduced events in biomolecules and solids. He has pioneered the Non-collinear Optical Parametric Amplifier (NOPA)

concept and its extension to the near and mid-IR. He is Topical Editor for the Journal Optics Letters (Optical Society of America) for the area Ultrafast Optical Phenomena. He has been in the Technical Program Committees of the most important international conferences in optics and photonics (CLEO USA, Cleo Europe, EQEC, Ultrafast Phenomena, HILAS, Photonics Europe). Prof Cerullo has delivered numerous invited talks and tutorials at scientific conferences and schools on the topics of few-optical-cycle pulse generation and applications

Course Level:

Advanced Beginner (basic understanding of topic is necessary to follow course material)

Course Description:

This course will present a comprehensive introduction to the topic of ultrafast optical parametric amplifiers (OPAs), starting from the basic principles and progressing to the more advanced applications. OPAs allow not only to generate broadly tunable pulses starting from a fixed frequency source, but also, thanks to their broad gain bandwidths, to dramatically shorten the pulse duration, down to the few-cycle limit.

The course will start by reviewing the nonlinear three-wave interaction equations which describe optical parametric amplification, and deriving from them the main OPA properties, both in the stationary and short-pulse regimes. The design principles of standard OPAs working in the visible, near-infrared and mid-infrared ranges will be presented. We will then describe ultra-broadband OPA architectures, allowing the generation of tunable sub-10-fs light pulses, and review dispersion compensation techniques. We will finally cover more advanced applications, such as passive carrier-envelope-phase stabilization and the generation of ultrahigh peak power pulses by optical parametric chirped pulse amplification.

Benefits and Learning Objectives:

This course will enable you to:

- Understand the nonlinear wave equations describing optical parametric amplification
- Understand how the parameters of the driving laser and of the nonlinear crystal influence the OPA performance
- Design and build an OPA pumped by the fundamental (second harmonic) of Ti:sapphire and generating broadly tunable infrared (visible) pulses
- Design and build a non-collinear OPA for the generation of few-optical-cycle visible pulses
- Explain how OPAs can be used to generate carrier-envelope-phase stable pulses in a passive, all-optical way
- Understand the design principles of optical parametric chirped pulse amplifiers and the limits of energy scaling

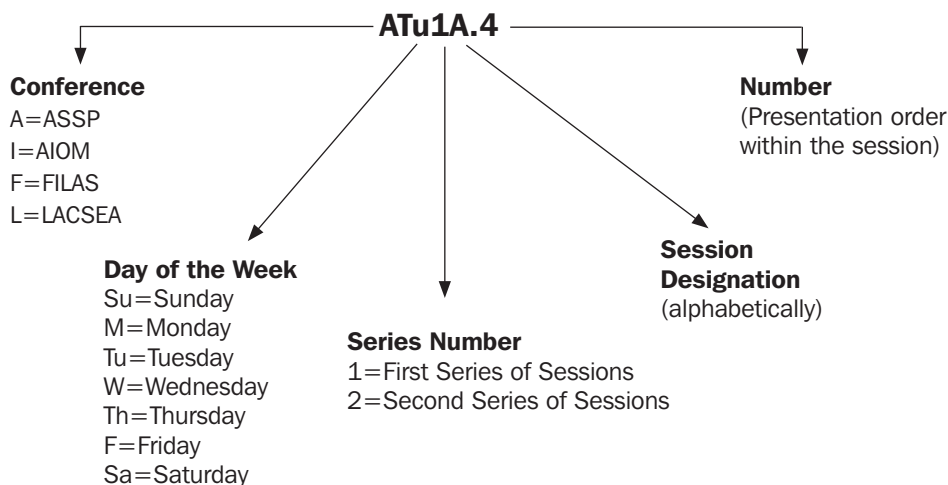
Intended Audience:

Students, academics, researchers and engineers in various disciplines who use or build ultrafast optical parametric amplifiers and require a comprehensive introduction to the subject and an overview of future developments. Undergraduate training in engineering or science is assumed.

Agenda of Sessions — Sunday, 29 January

SHORT COURSES	
Registration Opens, Aragon Foyer 11:30–18:30	
Aragon Ballroom III-A	Aragon Ballroom III-B
SC380: Laser Noise Rüdiger Paschotta, <i>RP Photonics Consulting GmbH, Germany</i> 12:30–15:30	SC381: High-energy Fiber Lasers Almantas Galvanauskas, <i>CUOS, University of Michigan, Ann Arbor, USA</i> 12:30–15:30
SC382: Ultrafast Optical Parametric Amplifiers Giulio Cerullo, <i>Politecnico di Milano, Italy</i> 16:00–19:00	
Welcome Reception, Santiago Room and Courtyard 19:00–20:30	

Explanation of Session Codes



The first letter of the code designates the meeting (For instance, A=Advanced Solid-State Photonics, F=Fiber Lasers and Applications, I=Advances in Optical Materials, L=Laser Applications to Chemical, Security and Environmental Analysis, J=Joint). The second element denotes the day of the week (Monday=M, Tuesday=Tu, Wednesday=W). The third element indicates the session series in that day (for instance, 1 would denote the first parallel sessions in that day). Each day begins with the letter A in the fourth element and continues alphabetically through a series of parallel sessions. The lettering then restarts with each new series. The number on the end of the code (separated from the session code with a period) signals the position of the talk within the session (first, second, third, etc.). For example, a presentation coded ATu1A.4 indicates that this paper is part of Advanced Solid-State Photonics meeting (A) and is being presented on Tuesday (Tu) in the first series of sessions (1), and is the first parallel session (A) in that series and the fourth paper (4) presented in that session.

Key to Conference Abbreviations

ASSP	Advanced Solid-State Photonics
AIOM	Advances in Optical Materials
FILAS	Fiber Lasers and Applications
LACSEA	Laser Applications to Chemical, Security and Environmental Analysis

Agenda of Sessions — Monday, 30 January

	Aragon II	Aragon III-B-C
	ASSP	LACSEA
07:00	Registration, Aragon Foyer 07:00–18:30	
08:00	AM1A • Mid-Infrared Parametric Sources 08:00–10:00	LM1B • Hyperspectral Spectroscopy and Explosive Detection 08:00–10:00
08:30		
09:00		
09:30		
10:00	Coffee Break, Aragon Foyer 10:00–10:30	
10:30	AM2A • Ultrafast Thin Disk Lasers 10:30–12:00	LM2B • Mid-Infrared Sensing I 10:30–12:30
11:00		
11:30		
12:00	Lunch (on your own) 12:00–13:30	
12:30	Lunch (on your own) 12:30–14:00	
13:00	Lunch (on your own) 12:30–14:00	
13:30	AM3A • Beam Combining 13:30–15:00	LM3B • Bio-Sensing 14:00–16:00
14:00		
14:30		
15:00	AM4A • Poster Session, Aragon I & Foyer 15:00–16:30	Exhibits Preview & Coffee Break, Aragon F & Foyer 16:00–16:30
15:30		
16:00	Exhibits Preview & Coffee Break 16:00–16:30	
16:30	AM5A • Semiconductor and Waveguide Lasers 16:30–18:30	LM5B • Laser-Induced Breakdown Spectroscopy and New Spectroscopic Approaches 16:30–18:30
17:00		
17:30		
18:00		
18:30		
20:00	ASSP Postdeadline Papers (tentative)	
20:30	LACSEA Postdeadline Papers (tentative)	
21:00	LACSEA Postdeadline Papers (tentative)	
21:30	LACSEA Postdeadline Papers (tentative)	

Key to Conference Abbreviations

ASSP	Advanced Solid-State Photonics
AIOM	Advances in Optical Materials
FILAS	Fiber Lasers and Applications
LACSEA	Laser Applications to Chemical, Security and Environmental Analysis

Agenda of Sessions — Tuesday, 30 January

	Aragon II	Aragon III-B-C
	ASSP	LACSEA
7:00	Registration, Aragon Foyer 07:00–18:30	
8:00	AT1A • Fiber Devices 08:00–10:00	LT1B • Mid-Infrared Sensing II 08:00–10:00
8:30		
9:00		
9:30		
10:00	Exhibits & Coffee Break, Aragon I & Foyer 10:00–10:30	
10:30	AT2A • Nonlinear Sources 10:30–12:00	LT2B • Laser-Based Sensing for Stand-off Detection 10:30–12:30
11:00		
11:30		
12:00	Lunch (on your own) 12:00–13:30	
12:30	Lunch, (on your own) 12:30–14:00	
13:00		
13:30	AT3A • Near-infrared Sources 13:30–15:00	LT3B • LIF and Polarization Spectroscopy Based Sensing 14:00–16:00
14:00		
14:30		
15:00	AT4A • Poster Session, Aragon I & Foyer 15:00–16:30	Exhibits & Coffee Break, Aragon F & Foyer 16:00–16:30
15:30		
16:00		
16:30	AT5A • Ultrafast Optics 16:30–18:30	LT5B • Mid-Infrared Sensing III 16:30–18:30
17:00		
17:30		
18:00		
18:30		
20:00	LT6B • Poster Session & Exhibits, Aragon I & Foyer 20:00–21:30	

Key to Conference Abbreviations

ASSP	Advanced Solid-State Photonics
AIOM	Advances in Optical Materials
FILAS	Fiber Lasers and Applications
LACSEA	Laser Applications to Chemical, Security and Environmental Analysis

Agenda of Sessions — Wednesday, 1 February

	Aragon II	Aragon III-C	Aragon III-B	Aragon III-A
	ASSP	LACSEA	FILAS	AIOM
7:00	Registration, Aragon Foyer 07:00–18:30			
8:00	JW1A • Joint Plenary Session I, San Bernardo Ballroom 08:00–09:30			
8:30				
9:00				
9:30	Exhibits & Coffee Break, Aragon I & Foyer 09:30–10:00			
10:00	JW2A • Joint Plenary Session II, San Bernardo Ballroom 10:00–11:30			
10:30				
11:00				
11:30	Lunch (on your own) 11:30–13:00	Lunch (on your own) 11:30–13:30		
12:00				
12:30				
13:00	AW3A • Beam Combining Summit 13:00–15:00	LW3B • CARS Spectroscopy for Sensing in Reacting Flows 13:30–15:30	FW3C • Defense and Space Applications of Fiber Lasers 13:30–15:30	IW3D • Laser Materials 1 13:30–15:30
13:30				
14:00				
14:30	<i>Aragon I & Foyer</i> AW4A • Poster Session 15:00–16:30 Exhibits & Coffee Break 15:30–16:00	Exhibits & Coffee Break, Aragon I & Foyer 15:30–16:00		
15:00				
15:30				
16:00	AW5A • Mid-Infrared Sources 16:30–18:00	LW5B • New Spectroscopic Approaches 16:00–18:00	FW5C • Fiber Lasers for Industrial Applications and Material Processing 16:00–18:00	IW5D • Laser Materials II 16:00–18:00
16:30				
17:00				
17:30				
18:00	<i>San Bernardo Ballroom</i> OSA Corporate Associates Present: Executive Speaker Series 18:00–19:30			
19:30	Banquet, Aragon II & III 19:30–21:00			

Key to Conference Abbreviations

ASSP	Advanced Solid-State Photonics
AIOM	Advances in Optical Materials
FILAS	Fiber Lasers and Applications
LACSEA	Laser Applications to Chemical, Security and Environmental Analysis



Agenda of Sessions — Thursday, 2 February

	Aragon III-B	Aragon III-A
	FILAS	AIOM
7:00	Registration, Aragon Foyer 07:00–18:00	
8:00	FTh1A • Short Pulse Fiber Lasers 08:00–09:30	ITh1B • Optical Fibers, Glasses and Ceramics I 08:00–09:30
8:30		
9:00		
9:30	JTh2A • FILAS/AIOM Joint Poster Session, Aragon I & Foyer 09:30–11:00 Exhibits & Coffee Break 09:30–10:00	
11:00	FTh3A • High Power Fiber Lasers and their Applications 11:00–12:30	ITh3B • Optical Fibers, Glasses and Ceramics II 11:00–12:30
11:30		
12:00		
12:30	Lunch (on your own) 12:30–14:00	
13:00		
13:30		
14:00	FTh4A • 2 Micron Fiber Lasers 14:00–16:00	ITh4B • Optical Fibers, Glasses and Ceramics III 14:00–16:00
14:30		
15:00		
15:30		
16:00	Exhibits & Coffee Break, Aragon Foyer 16:00–16:30	
16:30	FTh5A • Tunable Fiber Lasers including UV, Green and IR 16:30–18:30	ITh5B • Semiconductor-based Optical materials 16:30–18:30
17:00		
17:30		
18:00		
18:30		

— Friday, 3 February

	Aragon III-A
	AIOM
7:00	Registration, Aragon Foyer, 07:00–12:00
8:00	IF1A • Waveguides and Thin Films 1, 08:00–10:00
10:00	Coffee Break, Aragon Foyer, 10:00–10:30
10:30	IF2A • Waveguides and Thin Films II, 10:30–12:00

Key to Conference Abbreviations

- ASSP Advanced Solid-State Photonics
 AIOM Advances in Optical Materials
 FILAS Fiber Lasers and Applications
 LACSEA Laser Applications to Chemical, Security and Environmental Analysis





**Advanced Solid-State Photonics (ASSP) would like to
thank the following Corporate Contributors for their
outstanding support:**



Grant Support:

**Lawrence Livermore
National Laboratory**

Student Award Sponsor:





Aragon II

Advanced Solid-State Photonics

Aragon III-B-C

Laser Applications to Chemical, Security and Environmental Analysis

07:00–18:30 Registration, Aragon Foyer

08:00–10:00

AM1A • Mid-Infrared Parametric SourcesScott Setzler; *BAE Systems PLC, USA, Presider***AM1A.1 • 08:00** **Invited**

Quasi-Phase-Matched Gallium Arsenide for Mid Infrared Frequency Conversion, Eric Lallier¹, Arnaud Grisard¹, Bruno Gerard², Anne Hildenbrand³, Christelle Kieleck³, Marc Eichhorn³; ¹*Thales Research & Technology, France*; ²*Alcatel-Thales 3-5 Lab, France*; ³*French-German Research Institute of Saint-Louis, France*. Progress in processing low-loss quasi-phase-matched gallium arsenide crystals allows their excellent nonlinear properties to be employed in practical mid infrared devices. This presentation will address both crystal growth aspects and the most recent devices demonstrations.

AM1A.2 • 08:30

GaAs-based Subharmonic OPO with an Instantaneous Bandwidth of 3.1-5.8 μm Pumped by a Femtosecond Tm-fiber Laser, Nick Leindecker¹, Alireza Marandi¹, Konstantin L. Vodopyanov¹, Jie Jiang², Ingmar Hartl³, Martin Fermann³, Peter G. Schunemann³; *E.L. Ginzton Lab, Stanford University, USA*; ¹*IMRA America, Inc., USA*; ²*BAE Systems, USA*. We extend broadband degenerate OPO operation further into the mid-infrared using a thulium fiber laser to pump orientation-patterned GaAs. Pump threshold is less than 20mW and output exceeds 30mW over a bandwidth of 3.1-5.8 μm .

AM1A.3 • 08:45

Mid-Infrared Optical Parametric Generation in CdSiP₂ Crystal Pumped by 8-ns Long Pulses at 1064 nm, Valentin Petrov¹, Georgi Marchev¹, Aleksey Tyazhev¹, Peter G. Schunemann², Kevin Zawilski², Georg Stoeppler³, Marc Eichhorn³; ¹*Max-Born Inst., Germany*; ²*BAE Systems, USA*; ³*French-German Research Institute of Saint-Louis, France*. A 21.4-mm-long non-critically cut CdSiP₂ crystal, pumped by 8-ns pulses at 1064 nm in a double-pass configuration for pump, signal and idler generated 523 μJ , 5.8-ns idler pulses at 6.125 μm and 100 Hz.

AM1A.4 • 09:00

Compact, High-Energy, Picosecond Optical Parametric Oscillator at 450 MHz near 6 micron, Suddapalli Chaitanya Kumar¹, A. Agnesi², Paolo Dallochio², F. Pirzio², G. Reali², K. Zawilski³, Peter G. Schunemann³, Majid Ebrahim-Zadeh^{1,4}; ¹*NLO, ICFO-The Institute of Photonic Sciences, Spain*; ²*Laser Source Laboratory, University of Pavia, Italy*; ³*BAE Systems, Inc., USA*; ⁴*Institucio Catalana de Recerca i Estudis Avancats (ICREA), Spain*. We report a compact, efficient, 1.5 mJ, 450 MHz, mid-IR picosecond OPO based on CdSiP₂, synchronously-pumped at 1064 nm and tunable across 6091-6577 nm, covering the technologically important wavelength range for surgical applications.

AM1A.5 • 09:15

ZGP RISTRA OPO Operating at 6.45 μm and Application in Surgery, Georg Stoeppler¹, Marc Eichhorn¹, Martin Schellhorn¹, Stefan Been², Rudolf Verdaasdonk³; ¹*French-German Research Institute of Saint Louis ISL, France*; ²*University Medical Center, Netherlands*; ³*Vrije University Medical Center, Netherlands*. We report a Ho:LLF MOPA pumped ZGP OPO based on Rotated Image Singly-Resonant Twisted RectAngle (RISTRA) cavity producing a pulse energy of 5 mJ at 100 Hz at 6.45 μm . Application in surgery is discussed.

AM1A.6 • 09:30

Micro-Joule Octave Spanning Pulses at 6 μm from a Hybrid Femtosecond OPA, Skirmantas Alisaukas¹, Giedrius Andriukaitis¹, Audrius Pugzlys¹, Andrius Baltuska¹, Andrejus Michailovas¹, Poh Boon^{2,3}, Karolis Baskus⁴, Hua-Wei Jonathan Lim², Lihao Tan²; ¹*Photonics Institute, Vienna University of Technology, Austria*; ²*DSO National Laboratories, Singapore*; ³*Nanyang Technological University, Singapore*; ⁴*EKSPLA Ltd, Lithuania*. We demonstrate a few-cycle mid-IR, Yb:CaF₂ driven OPA for verifying the predictions on λ -scaling of strong-field photoelectron wavepacket dynamics and atmospheric sensing. 6- μJ 6- μm pulses compressible to 1.5 optical cycles at 500 Hz were generated.

AM1A.7 • 09:45

High Repetition Rate, 93-MW Mid-infrared Optical Parametric-chirped Pulse Amplifier Based on Apodized Aperiodically Poled Mg:LiNbO₃, Clemens Heese¹, Christopher R. Phillips², Nick Hartmann¹, Lukas Gallmann¹, M. M. Fejer², Ursula Keller¹; ¹*Department of Physics, Institute of Quantum Electronics, ETH Zurich, Switzerland*; ²*Edward L. Ginzton Laboratory, Stanford University, USA*. We present an ultra-broadband optical parametric amplification system based on apodized, aperiodically poled Mg:LiNbO₃ delivering clean 75-fs pulse with energies of 7 μJ at 3.4 μm and a repetition rate of 100 kHz.

08:00–10:00

LM1B • Hyperspectral Spectroscopy and Explosive DetectionSukesh Roy; *Spectral Energies, LLC., USA, Presider***LM1B.1 • 08:00**

Welcome and Announcements

LM1B.2 • 08:15

Real-time Explosive Detection and Imaging using CARS, Arthur Dogariu¹, Alex Pidwerbetsky²; ¹*Princeton University, USA*; ²*LGS Innovations LLC, USA*. We demonstrate fast and efficient detection of trace explosives using backscattered collinear CARS. Vibrational fingerprints of sub-microgram targets are analyzed in real-time. Hyperspectral imaging is demonstrated using Line-CARS.

LM1B.3 • 08:30 **Invited**

Single-Beam CARS for Standoff Detection of Explosives and Development of Fiber Lasers Required for Practical Implementation, Marcos Dantus¹; ¹*Chemistry, Michigan State University, USA*. Sensitivity and selectivity of CARS signal from a single-beam laser setup are evaluated under real-time imaging conditions. Practical implementation would require ultrafast fiber laser oscillators, as will be shown, capable of producing intense ultrashort pulses.

LM1B.4 • 09:00 **Invited**

Development and Application of Optical Frequency Combs, Scott Diddams¹; ¹*National Institute of Standards and Technology, USA*. Various implementations of optical frequency combs will be presented. Recent applications of frequency combs to spectroscopic problems in scientific and technological fields, including precision metrology, trace gas detection, and astronomy will be described.

LM1B.5 • 09:30 **Invited**

Demonstration of High Speed Imaging in Practical Propulsion Systems Using Hyperspectral Tomography, Lin Ma¹, Xuesong Li¹, Sukesh Roy², Andrew Caswell³, James R. Gord³, David Plemmons⁴, Xinliang An⁵, Scott T. Sanders⁶; ¹*Department of Aerospace and Ocean Engineering, Virginia Tech, USA*; ²*Spectral Energies LLC, USA*; ³*Air Force Research Laboratory, Propulsion Directorate, USA*; ⁴*Aerospace Testing Alliance, USA*; ⁵*Department of Mechanical Engineering, University of Wisconsin-Madison, USA*. This paper reports the demonstration of a 30-laser-beam tomography system in a J85 turbojet engine for the imaging of temperature and water vapor concentration at an overall repetition rate of 50 kHz.

10:00–10:30 Coffee Break





Aragon II

Advanced Solid-State Photonics

10:30–12:00

AM2A • Ultrafast Thin Disk Lasers

Thomas Südmeyer; *ETH Zurich, Switzerland, President*

AM2A.1 • 10:30 **Invited**

Invited-Ultrafast Disk Lasers and Amplifiers, Dirk H. Sutter¹, Dominik Bauer¹, Jochen Kleinbauer¹, Alexander Budnicki¹, Martin Wolf¹, Chuong Tan¹, Raphael Gebbs¹, Philipp Wagenblast¹, Sascha Weiler²; ¹Development + Research, TRUMPF Laser GmbH + Co. KG, Germany; ²TRUMPF Inc., USA. Ultrafast laser sources based on disk technology are industry proven tools for precision machining at high throughput. We review the state of the art of fs and ps disk laser oscillators and amplifiers, providing average powers on the order of 150W.

AM2A.2 • 11:00

200 fs Pulses from Kerr Lens Mode Locked Yb: YAG Thin Disk Oscillator, Oleg Pronin¹, Jonathan Brons², Christian Grasse³, Volodymyr Pervak², Gerhard Boehm³, Markus-Christian Amann³, Alexander Apolonskiy^{2,3}, Vladimir Kalashnikov⁴, Ferenc Krausz^{1,2}; ¹Max Planck Institute of Quantum Optics, Germany; ²Ludwig-Maximilians-Universität München, Germany; ³Walter Schottky Institut, Germany; ⁴Institut für Photonik, Austria. We achieved 200fs with 17W average power and 270fs with 45W. We demonstrate shortest pulses from a thin disk Yb:YAG oscillator and a first Kerr lens mode locked thin disk laser.

AM2A.3 • 11:15

Self-referenceable High-power Frequency Comb from a 7-W, 142-fs Yb:Lu2O3 Thin Disk Laser Oscillator-Clara Saraceno¹, Selina Pekarek¹, Oliver Heckl¹, Cyrill Baer¹, Cinia Schriber¹, Matthias Golling¹, Thomas Südmeyer¹, Kolja Beil², Christian Krankel^{2,1}, Günter Huber², Ursula Keller¹; ¹Department of Physics, ETH Zurich, Switzerland; ²Institute of Laser Physics, University of Hamburg, Germany. We present an Yb:Lu2O3 modelocked thin disk laser (TDL) with 7W and record short pulse duration of 142fs. Using 65mW we generated an octave spanning supercontinuum and measured for the first time the carrier envelope offset (CEO) frequency of a TDL.

AM2A.4 • 11:30

Continuous Wave and Mode-locked Yb3+:Y2O3 Ceramic Thin-disk Laser-Masaki Tokurakawa¹, Akira Shirakawa¹, Ken-ichi Ueda¹, Hideki Yagi², Takagami Yanagitani³, Kolja Beil¹, Christian Krankel¹, Klaus Petermann³, Günter Huber³; ¹Institute for Laser Science, University of Electro-Communications, Japan; ²Takuma Works, Konoshima Chemical Co. Ltd., Japan; ³Institute of Laser-Physics, University of Hamburg, Germany. CW and mode-locked laser operation based on an Yb3+:Y2O3 ceramic thin-disk are reported. 70-W output power with 50% optical-to-optical efficiency was achieved in CW operation. 547-fs pulses were obtained in SESAM mode-locked operation.

AM2A.5 • 11:45

Femtosecond Mode-Locked Thulium-Doped Lu2O3 Laser around 2 µm, Andreas Schmidt¹, Valentin Petrov¹, Uwe Griebner¹, Sun Young Choi², Dong-Il Yeom², Fabian Rotermund³, Philipp Koopmann³, Klaus Petermann³, Günter Huber³, Peter Fuhrberg⁴; ¹Max Born Institute, Germany; ²Department of Physics & Division of Energy Systems Research, Ajou University, Republic of Korea; ³Institut für Laser-Physik, Universität Hamburg, Germany; ⁴LISA laser products, Germany. A mode-locked Tm:Lu2O3 laser delivering pulses as short as 175 fs at 2070 nm is demonstrated. The self-starting oscillator is mode-locked by a single-walled carbon nanotube-based saturable absorber and operates at 88 MHz.

12:00–13:30 **Lunch (on your own)**

Aragon III-B-C

Laser Applications to Chemical, Security and Environmental Analysis

10:30–12:30

LM2B • Mid-Infrared Sensing I

Markus Sgrist; *ETH Zurich, Switzerland, President*

LM2B.1 • 10:30

Mid-infrared Sulfur Dioxide Measurements at Elevated Temperatures for Emission Control, Peter Geiser¹, Dung D. Dang¹, Axel F. Bohman¹, Peter L. Kaspersen¹; ¹Norsk Elektro Optikk A/S, Norway. Mid-infrared measurements of sulfur dioxide at gas-temperatures up to 400 °C have been performed using a continuous-wave room-temperature quantum cascade laser and second harmonic detection.

LM2B.2 • 10:45 **Invited**

Recent Progress in Mid-Infrared Quantum Cascade Lasers, Claire Gmachl¹; ¹Dept. of Electrical Engineering & MIRTHE, Princeton University, USA. Quantum Cascade laser performance continues to increase rapidly based on new understanding of materials and interfaces, quantum designs, and optical cavities/waveguides. We review novel approaches to high power-efficiency, single-mode emission in coupled cavities, and applications.

LM2B.3 • 11:15

Mode-Hop Free Tunable Mid-Infrared VECSEL, Matthias Fill^{1,2}, Ferdinand Felder^{1,2}, Mohamed Rahim¹, Amir Khair¹, Hans Zogg¹; ¹ETH Zurich, Switzerland; ²Phocone AG, Switzerland. Continuously tunable Vertical External Cavity Surface Emitting Lasers (VECSEL) have been realized, emitting in the 3-5 µm range. Pulsed output power at room temperature operation is > 10 mWp, in the single Gaussian TEM00 emission mode.

LM2B.4 • 11:30

High-Precision Instrumentation for CO2 Isotope Ratio Measurements, Anthony Gomez¹, Joel A. Silver¹; ¹Southwest Sciences, Inc., USA. A high-precision isotopic CO2 measurement system is being developed that removes effects from pressure, temperature and moisture, and that has characteristics suitable for field deployable instrumentation. Early work exhibits a precision of 0.4%.

LM2B.5 • 11:45

Interband Cascade Lasers for Spectroscopy with Very Low Input Power, Jerry R. Meyer¹, Chales D. Merritt¹, William W. Bewley¹, Chadwick L. Canedy¹, Chul Soo Kim¹, Joshua Abell¹, Igor Vurgafman¹, Mijin Kim²; ¹Code 5613, Naval Research Laboratory, USA; ²Sotera Defense Solutions, USA. We report cw interband cascade lasers operating to 109 C, which at room temperature emit at wavelengths > 5.5 microns with output powers > 150 mW, wallplug efficiencies > 13%, and input powers < 30 mW.

LM2B.6 • 12:00 **Invited**

Standoff Detection of Explosives and High Sensitive Detection of Chemicals in Drinking Water with Quantum Cascade Lasers, Frank Fuchs¹, Stefan Hugger¹, Quankui Yang¹, Michel Kinzer¹, Wolfgang Bronner¹, Rainer Lösch¹, Rolf Aidam¹, Kai Degreif², Werner Konz², Sven Rademacher², Frank Schnürer¹, Wenka Schweikert¹; ¹Fraunhofer IAF, Germany; ²Fraunhofer IPM, Germany; ³Fraunhofer ICT, Germany. Based on broadly tunable external cavity quantum lasers (EC-QCL) an imaging system has been developed for stand-off detection of traces of explosives. A similar EC-QCL serves for detection of hazardous chemicals in drinking water.

12:30–14:00 **Lunch (on your own)**

Monday, 30 January





Aragon II

Advanced Solid-State Photonics

13:30–15:00

AM3A • Beam Combining

Thomas Schreiber; *Fraunhofer IOF Jena, Germany, President*

AM3A.1 • 13:30

Diffraction Beam Combining of a 2.5-kW Fiber Laser Array, Shawn M. Redmond¹, Tso Yee Fan¹, Dan Ripin¹, Peter Thielen², Joshua Rothenberg², Gregory Goodno²; ¹MIT Lincoln Laboratory, USA; ²Northrop Grumman Aerospace Systems, USA. Five 500-W fiber amplifiers were coherently combined with 79% efficiency using a diffractive optical element (DOE) combiner, generating a single beam whose M2 = 1.1 beam quality exceeded that of the inputs.

AM3A.2 • 13:45

Two-Dimensional Diffractive Coherent Beam Combining, Peter Thielen¹, James Ho¹, David Burchman¹, Gregory Goodno¹, Joshua Rothenberg¹, Michael Wickham¹, A. Flores², C. Lu², B. Pulford², C. Robin², A. Sanchez², D. Hult³, K. Rowland⁴; ¹Laser and Optical Products Department, Northrop Grumman Aerospace Systems, USA; ²Directed Energy Directorate, Air Force Research Laboratory, USA; ³TREX Enterprises Corporation, USA; ⁴Boeing LTS Inc, USA. A two-dimensionally patterned diffractive optical element (DOE) was used to coherently combine a 3x5 array of fifteen Yb-doped fiber amplifier beams into a 0.6-kW, M2=1.1 output beam.

AM3A.3 • 14:00

3mJ Coherently Combined Two Channel Femtosecond Fiber CPA Laser System, Arno Klenke^{1,3}, Enrico Seise^{1,3}, Sven Breikopf¹, Stefan Demmler¹, Jan Rothhardt^{1,3}, Jens Limpert^{1,2}, Andreas Tünnermann^{1,2}; ¹Institute of Applied Physics, Friedrich Schiller University Jena, Germany; ²Fraunhofer Institute for Applied Optics and Precision Engineering, Germany; ³Helmholtz-Institute Jena, Germany. We report on the coherent addition of two femtosecond fiber amplifiers. Combined and compressed pulse energies of up to 3mJ and average powers of up to 88W are achieved with high combining efficiencies.

AM3A.4 • 14:15

Coherent Combining of Pulsed Fiber Amplifiers in the Nonlinear Chirp Regime, Stephen P. Palese¹, Eric C. Cheung¹, Gregory Goodno¹, Chun-Ching Shih¹, Mark Weber¹; ¹Northrop Grumman Aerospace Systems, USA. Two tapered fiber amplifier chains were coherently combined to generate 0.42-mJ, 1-ns pulses with 79% efficiency despite 38 radians of intra-pulse phase chirp. Adaptive chirp control significantly reduced intra-pulse chirp errors.

AM3A.5 • 14:30

Group Delay Locking of Broadband Phased Lasers, Stanley B. Weiss¹, Mark Weber¹, Gregory Goodno¹; ¹Northrop Grumman Aerospace Systems, USA. We demonstrate a method for single-detector coherent sensing and co-alignment of group delays in a phased fiber array, enabling robust coherent combining of broadband sources despite initial path mismatches exceeding the laser coherence length.

AM3A.6 • 14:45

Chirp Re-compensated Spectral Beam Combination, Eric C. Cheung¹, James Ho¹, Timothy S. McComb¹, Stephen P. Palese¹; ¹Northrop Grumman Aerospace Systems, USA. Spectral combination of fiber amplifiers at high spectral density is demonstrated with greater than 80% spectral utilization without degradation in beam quality. Amplifiers at 0.5-MW peak power and 0.15-nm wavelength spacing has been combined.

15:00–16:30 AM4A • ASSP Poster Session 1, See page 21

Aragon III-B-C

Laser Applications to Chemical, Security and Environmental Analysis

14:00–16:00

LM3B • Bio-Sensing

J. Barry McManus; *Aerodyne Research Inc., USA, President*

LM3B.1 • 14:00

High-precision Analysis of N2O Isotopomers by QCLAS and its Application to Microbial Processes in Soil and Waste Water, Lukas Emmenegger¹, Albert Manninen¹, Bela Tuzson¹, Jan-Reent Köster², Pascal Wunderlin³, Joachim Mohn¹; ¹Laboratory for Air Pollution & Environmental Technology, Empa, Saint Barthelemy; ²Institute of Plant Nutrition and Soil Science, Christian Albrechts University, Göttingen; ³Process Engineering, Eawag, Switzerland. We report the first continuous measurements of 15N in N2O ($\delta^{15}N\alpha$ and $\delta^{15}N\beta$) by QCL absorption spectroscopy at elevated and ambient mixing ratios with a 0.1% precision, enabling process studies in many new application fields.

LM3B.2 • 14:15 **Invited**

Application of LASER in Detection and Manipulation of Biomolecules in Lab-on-a-Chip Devices, Prashanta Dutta¹; ¹Washington State University, USA. "Lab-on-a-chip" microfluidic devices can be used for various bioanalytical experiments such as sensing single molecules, separation of cells, and purification of proteins.

LM3B.3 • 14:45 **Invited**

Plasmon-Enhanced Sensing and Photodetection, Naomi Halas¹; ¹Rice University, USA. Surface plasmons supported by metallic nanostructures, provide new opportunities for enhanced sensing and photodetection. Two mechanisms- hot electron generation resulting from plasmon decay, and high-intensity, nanoscale local fields- will be discussed in this context.

LM3B.4 • 15:15

Elemental Mercury Detection by Multi-mode Diode Lasers Employing Correlation Spectroscopy, Gabriel Somesfalean^{1,2}, Xiutao Lou^{2,1}, Sune Svanberg^{1,2}, Zhiguo Zhang²; ¹Department of Physics, Lund University, Sweden; ²Department of Physics, Harbin Institute of Technology, China; ³Joint Research Center of Photonics, Zhejiang University-Royal Institute of Technology-Lund University, China. A method for elemental mercury detection was demonstrated by employing multimode laser radiation at 254 nm in combination with correlation spectroscopy. The UV light was generated by sum-frequency mixing of two visible multimode diode lasers.

LM3B.5 • 15:30

Real Time Monitoring of Exhaled Breath Using Intracavity Absorption Spectroscopy with an Er-Doped Fiber Laser, Peter Fjodorow¹, Luis Leal¹, Benjamin Loehden¹, Svetlana Kuznetsova¹, Klaus Sengstock¹, Valery M. Baev¹; ¹Physics, Universität Hamburg, Germany. Intracavity absorption spectroscopy with a broadband Er-doped fiber laser is applied for real time monitoring of the CO2 concentration in human breath. Simultaneous sensitive time-resolved measurements of several molecular species are possible.

LM3B.6 • 15:45

Quantum Cascade Laser for Breath Analysis: Application to Nitric Oxide Monitoring, Julien Mandon¹, Marieann Högman², Peter, J.F.M. Merkus³, Jan van Amsterdam⁴, Frans, J.M. Harren¹, Simona, M. Cristescu¹; ¹Life Science Trace Gas Facility, Institute for Molecules and Materials, Netherlands; ²Department of Medical Sciences, Uppsala University and Centre for Research and Development, Sweden; ³Department of Pediatric Pulmonology, Radboud University Nijmegen Medical Centre, Netherlands; ⁴Laboratory for Health Protection Research, RIVM, Netherlands. Exhaled Nitric Oxide is considered as an indicator of asthma diagnostic. We present a QCL-based sensor for sub-ppbv detection and compare its sensitivity and selectivity with commercial sensors based on chemiluminescence and electrochemistry.

16:00–16:30 Exhibits Preview & Coffee Break





Aragon I & Foyer

Advanced Solid-State Photonics

15:00–16:30 AM4A • ASSP Poster Session 1

AM4A.01

Lens-less Edge-pumping Design for High Power Single Mode Yb:YAG Microchip Laser, Kong Weipeng¹, Takunori Taira^{1,2}, ¹Department of Functional Molecular Science, School of Physical Sciences, The Graduate University for Advanced Studies, Japan; ²Laser Research Center for Molecular Science, Institute for Molecular Science (IMS), Japan. The preliminary result of 3-direction pump and 3.6 W CW power is successfully obtained. In our design, by upgrading of 27-direction pump, up to 100W single-mode output power is expectable within 60-mm-diameter planer laser head including pump diodes.

AM4A.02

Analytical and Experimental Analysis of the Stability of Coherently Combined Femtosecond Laser Systems, Arno Klenke^{1,3}, Enrico Seise^{1,3}, Sven Breitkopf¹, Jens Limpert^{1,2}, Andreas Tünnermann^{1,2}; ¹Institute of Applied Physics, Friedrich Schiller University Jena, Germany; ²Fraunhofer Institute for Applied Optics and Precision Engineering, Germany; ³Helmholtz-Institute Jena, Germany. The process of coherent combining of femtosecond pulses is influenced by different effects like dispersion, self-phase modulation or OPD fluctuations. Their impact on the combining process is investigated theoretically and experimentally.

AM4A.03

Stable MHz-Repetition-Rate Passively Q-Switched Microchip Laser Frequency Doubled by MgO:PPLN, Eva Mehner^{1,2}, Andy Steinmann³, Robin Hegenbarth³, Bernd Braun¹, Harald Giessen²; ¹Georg Simon Ohm University of Applied Sciences Nuremberg, Germany; ²4th Physics Institute and Research Center SCoPE, University Stuttgart, Germany. We present a passively Q-switched microchip laser generating 460 ps pulses at 1064 nm with up to 1.1 MHz repetition rate and a jitter < 1%. The IR-light was frequency doubled in an MgO:PPLN crystal with up to 75% conversion efficiency.

AM4A.04

All-fiber Coherent Beam Combining of Two Ytterbium Doped Single Frequency Fiber Amplifiers, Henrik Tünnermann^{1,2}, Thomas Theeg^{1,2}, Katharina Hausmann^{1,2}, Jörg Neumann^{1,2}, Dietmar Kracht^{1,2}, Peter Wessels^{1,2}; ¹Laser Zentrum Hannover e.V., Germany; ²Centre for Quantum Engineering and Space-Time Research - QUEST, Germany. We demonstrate all-fiber coherent beam combining of two ytterbium doped amplifiers with a total output power up to 25 W, stable operation for more than 6 hours and power noise dominated by the single amplifier.

AM4A.05

Experimental Study of Mode Instabilities in High Power Fiber Amplifiers, Hans-Jürgen Otto¹, Fabian Stutzki¹, Florian Jansen¹, Tino Eidam^{1,2}, Cesar Jauregui¹, Jens Limpert^{1,2}, Andreas Tünnermann^{1,3}; ¹Fiber and Waveguide Lasers, Institute of Applied Physics, Germany; ²Helmholtz-Institute, Germany; ³Fraunhofer Institute for Applied Optics and Precision Engineering, Germany. Mode instabilities in high power fiber laser systems are experimentally studied with a high-speed high-resolution camera proving that energy transfer between modes takes place. These measurements suggest the thermal origin of these instabilities.

AM4A.06

Sub-5ps High Energy Pulses from a Fiber-Amplified and Compressed Passively Q-Switched Microchip Laser, Alexander Steinmetz¹, Florian Jansen¹, Fabian Stutzki¹, Reinhold Lehneis¹, Jens Limpert¹, Andreas Tünnermann^{1,2}; ¹Friedrich-Schiller-Universität Jena, Institute of Applied Physics, Germany; ²Fraunhofer Institute for Applied Optics and Precision Engineering, Germany. Nonlinear compression of Q-switched pulses with high energy at high repetition rate (>500kHz) is obtained from fiber-amplified microchip laser. 70ps pulses are SPM-broadened in fiber-amplifier extracting energies over 10 μ J and compressed to 2.7ps.

AM4A.07

Withdrawn

AM4A.08

Two Colour Pumped OPCPA System Delivering a 1.5 Octave Spanning Coherent Spectrum in the Visible, Anne Harth^{1,2}, Marcel Schultze¹, Tino Lang^{1,2}, Thomas Binhammer³, Uwe Morgner^{1,2}; ¹Institut für Quantenoptik, Leibniz Universität Hannover, Germany; ²Centre for Quantum Engineering and Space-Time Research (QUEST), Germany; ³VENTEON Laser Technologies GmbH, Germany. We present a two-stage OPCPA system using two different pump frequencies which delivers a 450 THz broad coherent spectrum (Fourier limit: 3.5 fs) with 1 μ J pulse energy at a repetition rate of 200 kHz.

AM4A.09

Kerr Lens Mode-locking of Yb:CaF₂, Guillaume Machinet¹, Florent Guichard¹, Romain Dubrasquet^{1,2}, Johan Bouillet², Patrice Camy³, Jean-Louis Doualan³, Richard Moncorge³, Sandrine Ricaud^{4,5}, Frederic Druon⁴, Patrick Georges⁴, Dominique Descamps¹, Eric Cormier¹; ¹Laboratoire CELIA, France; ²Azur light Systems, France; ³Centre de recherche sur les Ions, les Matériaux et la Photonique (CIMAP), France; ⁴Laboratoire Charles Fabry, Institut d'Optique, France; ⁵Amplitude Systèmes, France. Through high-brightness optical pumping with a fiber laser, we demonstrate a soft-aperture Kerr lens modelocked (KLM) operation in a Yb:CaF₂ crystal. Stable 117 fs pulses are producing at an average power of 560 mW.

AM4A.10

Spectral Beam Combining of Diode Lasers with High Efficiency, André Müller¹, Deepak Vijayakumar¹, Ole Jensen¹, Karl-Heinz Hasler², Bernd Sumpf², Götz Erbert², Peter E. Andersen¹, Paul Petersen¹; ¹Department of Photonics Engineering, Technical University of Denmark, Denmark; ²Ferdinand-Braun-Institut, Leibniz-Institut für Höchstfrequenztechnik, Germany. Based on spectral beam combining we obtain 16 W of output power, combining two 1063 nm DBR-tapered diode lasers. The spectral separation within the combined beam can be used for subsequent sum-frequency generation.

AM4A.11

High Gain Single Stage and Single Pass Nd:YVO₄ Passive Amplifier for Picosecond Pulses, Xavier Delen¹, Francois Balembois¹, Patrick Georges¹; ¹Laboratoire Charles Fabry, France. We present a picosecond NdYVO₄ master oscillator power amplifier reaching 10 W output power for only 50 mW of seed at 200 kHz for a single pass single stage high gain passive amplifier.

AM4A.12

Power Scaling Limitations for Cavity-Assisted High-Harmonic Generation, Simon Holzberger^{1,2}, Joachim Puppeza¹, Jan Kaster¹, Tino Eidam³, Birgitta Bernhardt¹, Andreas Vernaleken¹, Oleg Pronin¹, Volodymyr Pervak¹, Ronald Holzwarth¹, Thomas Udem², Jens Limpert³, Alexander Apolonskiy², Ernst E. Fill¹, Theodor W. Hänsch^{1,2}, Andreas Tünnermann³, Ferenc Krausz^{2,3}; ¹Max-Planck-Institut für Quantenoptik, Germany; ²Fakultät für Physik, Ludwig-Maximilians-Universität, Germany; ³Institut für Angewandte Physik, Friedrich-Schiller-Universität, Germany. Harmonics up to order 21 generated in Xe are coupled out of a 78-MHz enhancement cavity with a fused silica Brewster plate. An irreversible degradation of the plate, accelerated by the generated harmonics, is observed.

AM4A.13

SESAMs for High-power Femtosecond Modelocking: Influence of Growth Temperature on Damage and Nonsaturable Losses, Clara Saraceno¹, Martin Hoffmann¹, Cinia Schriber¹, Oliver Heckl¹, Cyrill Baer¹, Matthias Golling¹, Thomas Südmeyer¹, Ursula Keller¹; ¹ETH Zurich, Switzerland. We investigate the influence of growth temperature of high-power oscillator SESAMs on nonlinear reflectivity, response time and damage threshold. Optimized designs combine fast recovery and low nonsaturable losses (0.2% for 4.4% modulation depth).

AM4A.14

Yb-doped Bismuthate Glass Waveguide Laser Fabricated by Ultrafast Laser Inscription, Rose Mary¹, Stephen Beecher¹, Graeme Brown¹, Robert R. Thomson¹, Ajoy Kar¹; ¹EPS-Physics, Heriot-Watt University, United Kingdom. We demonstrate laser action from an ultrafast laser inscribed Yb doped bismuthate glass waveguide. When pumped using a 975 nm diode laser, efficient lasing was observed at 1059 nm with a maximum output power of 148 mW and a slope efficiency of 64%.

AM4A.15

Pulse Duration and Energy Scaling of Femtosecond All-normal Dispersion Fiber Oscillators, Nikolai Chichkov¹, Christian Hapke¹, Jörg Neumann¹, Dietmar Kracht¹, Dieter Wandt¹, Uwe Morgner^{1,2}; ¹Laser Zentrum Hannover e.V., Germany; ²Institut für Quantenoptik, Leibniz Universität Hannover, Germany. The pulse parameters of mode-locked fiber oscillators are scaled by variation of the fiber length and the spectral filter bandwidth. 31-fs pulses with energies of 84 nJ are demonstrated from a step-index fiber oscillator setup.

AM4A.16

High Energy CPA-free Picosecond Yb:YAG amplifier, Markus Loeser¹, Mathias Siebold¹, Fabian Roeser¹, Ulrich Schramm¹; ¹Helmholtz-Center Dresden Rossendorf, Germany. We report on a CPA free picosecond MOPA system with a fs Yb:KGW oscillator and 2 subsequent amplifiers using Yb:YAG active mirrors. A maximum pulse energy of 35mJ at 10Hz repetition rate was achieved.

AM4A.17

High Power Photonic Crystal Fiber Lasers and their Intracavity Coherent Combining, Boris Shulga¹, Amiel A. Ishaaya¹; ¹Electrical and Computer Engineering, Ben-Gurion University of the Negev, Israel. We experimentally demonstrate high power CW and ns pulsed operation of a rod-type photonic crystal fiber laser with single and double pass pump configurations. We further investigate intracavity coherent beam combining of two PCF channels.

AM4A.18

Q-switched Operation of a Novel Ultra-large Mode Area Tm³⁺ doped Photonic Crystal Fiber, Pankaj K. Kadwani¹, Norbert Modshing², Robert A. Sims³, Lasse Leick², Jes Broeng², Lawrence Shah¹, Martin C. Richardson¹; ¹CREOL, College of Optics and Photonics, University of Central Florida, USA; ²West Saxon University of Applied Sciences, Germany; ³NKT Photonics A/S, Denmark. Q-switched laser operation are shown for the first time using a thulium doped polarizing photonic crystal fiber producing 6.5 kW peak-power pulses with diffraction-limited beam quality, high polarization purity, and >1000 μ m² mode field area.

AM4A.19

Single Frequency Multi Milijoule Sub-nanosecond Nd:YAG Laser at kHz Repetition Rate, Danail Chuchumishev¹, Alexander Gaydardzhiev¹, Trifonov Anton¹, Torsten Fiebig², Ivan Bucharov¹; ¹Department of Physics, Sofia University, Bulgaria; ²Argonne-Northwestern Solar Energy Research (ANSER) Center, Northwestern University, USA. We report up to 13 mJ at 0.5 kHz, linearly polarized output with 830 ps pulse duration from a single frequency amplified Nd:YAG microchip laser at 1064 nm.

Monday, 30 January





Monday, 30 January

Aragon I and Foyer

Advanced Solid-State Photonics

AM4A • ASSP Poster Session 1—Continued

AM4A.20

Generation of Tunable Infrared Femtosecond Pulses via Parametric Visible-to-Infrared Frequency Conversion, Julius Darginavičius¹, Gintaras Tamosauskas¹, Gintaras Valiulis¹, Algis Piskarskas¹, Audrius Dubietis¹; ¹Department of Quantum Electronics, Vilnius University, Lithuania. We propose a method for ultrashort pulse parametric visible-to-infrared frequency conversion. Our experiment demonstrate generation of sub-30-fs, sub-100 μJ pulses, broadly tunable across the infrared (1.1–3 μm) spectral range.

AM4A.21

Passively Q-switched GdVO4/Nd:GdVO4 and YVO4/Nd:YVO4 Lasers Using Continuous-grown Composite Crystals Using 879 nm Direct Pumping, Xin Yu¹, Yufei Ma^{1,2}, Frank Tittel², Xudong Li¹; ¹Harbin Institute of Technology, China; ²Rice University, USA. Passively Q-switched GdVO4/Nd:GdVO4 and YVO4/Nd:YVO4 laser performance using 879 nm pumping was demonstrated for the first time. YVO4/Nd:YVO4 compared with GdVO4/Nd:GdVO4 is a more favorable gain medium if higher repetition rates are required.

AM4A.22

Inband-pumped Er3+:LiLuF4 Laser Emitting in the 1.6 μm Spectral Range, Francesca Moglia¹, Christian Brandt¹, Günter Huber¹; ¹ILP - Uni Hamburg, Germany. We present resonantly inband-pumped laser operation at 1.62 μm of an Er3+:LiLuF4 crystal, pumped by a fiber laser emitting at 1536 nm with a maximum power of 1.24W and a slope efficiency of 19%.

AM4A.23

Optical Amplification of Pr3+-doped ZBLA Channel Waveguides for Visible Laser Emission, Méline Olivier¹, Jean-Louis Doualan², Patrice Camy², Hervé Lhermite³, Jean-Luc Adam¹, Virginie Nazabal¹; ¹Equipe Verres et Céramiques, Université Rennes1, France; ²CIMAP, ENI Caen, France; ³IETR Microelectronique, Université Rennes 1, France. Visible laser emission of praseodymium in fluorozirconate glasses is studied to generate compact solid-state laser sources. Gain and losses measurement were performed on channeled waveguides obtained by photolithography followed by ionic exchange.

AM4A.24

Positively Chirped Pulse Evolution in a Passively Mode-locked Thulium-doped Fiber Laser, Frithjof Haxsen^{1,2}, Dieter Wandt^{1,2}, Uwe Morgner³, Jörg Neumann^{1,2}, Dietmar Kracht^{1,2}; ¹Laser Development Department, Laser Zentrum Hannover e.V., Germany; ²Centre for Quantum Engineering and Space-Time Research - QUEST, Germany; ³Institut für Quantenoptik, Leibniz Universität Hannover, Germany. We report on a passively mode-locked thulium fiber laser with fiber based dispersion management. The laser delivers positively chirped pulses with 0.7 nJ of pulse energy, which can be compressed to sub-500 fs duration.

AM4A.25

Femtosecond Pulse Coherent Combining and Spectral Synthesis using Four Parallel Chirped Pulse Fiber Amplifiers, Wei-Zung Chang¹, Tong Zhou¹, Leo Siiman¹, Almantas Galvanauskas¹; ¹Center for Ultrafast Optical Science, University of Michigan, USA. We demonstrate spectral synthesis of femtosecond pulses in a coherently combined four-channel fiber chirped pulse amplifier array. This approach offers a path to overcome gain narrowing limitations of individual fiber amplifier channels.

AM4A.26

Generation of High Contrast Ultrashort Intense 1053nm Laser based on Non-collinear Optical Parametric Amplification, Zhongwei Shen¹, Zhaohua Wang¹, Cheng Liu¹, Haitao Fan¹, Zhiyi Wei¹; ¹Lab of Optical Physics, Institute of Physics, China. We report the experimental research on high contrast ultrashort intense laser with 3 stage OPAs pumped by 400nm laser, 30 uJ laser pulse at 1053nm was obtained by exchanging the signal and idler in each amplifier.

AM4A.27

Tunable Deep UV Narrow Linewidth Laser by Frequency Converted Ti:Sapphire Laser at 5kHz Repetition Rate, Nan Wang¹, Rui Wang¹, Hao Teng¹, Dehua Li¹, Zhiyi Wei¹; ¹Laboratory of Optical Physics, Institute of Physics, Chinese Academy of Sciences, China. A tunable Ti:sapphire laser with line width of 0.05 nm was realized at repetition rate of 5 kHz. By using the BIBO and KBBF as the nonlinear crystals, laser power of 8mW at 195nm was obtained.

AM4A.28

Spatial Chirp and Angular Dispersion Dynamics in Femtosecond Noncollinear OPCPA, Audrius Zaukevičius¹, Vytautas Jukna¹, Roman Antipenkov¹, Vilija Martineaitė¹, Arunas Varanavičius¹, Algis Piskarskas¹, Gintaras Valiulis¹; ¹Quantum electronics, Vilnius University, Lithuania. Theoretical, numerical and experimental results on transformation of chirped pulse spatio-temporal characteristics, when pump and signal pulse fronts are not matched during the amplification in noncollinear optical parametric chirped-pulse amplifier.

NOTES

Horizontal lines for taking notes.





Aragon II

Advanced Solid-State Photonics

16:30–18:30

AM5A • Semiconductor and Waveguide Lasers

Jennifer Hastie; *University of Strathclyde, Glasgow - Institute of Photonics, UK*

AM5A.1 • 16:30 **Invited**

Invited-Highly Efficient Solid-state Waveguide Lasers, Markus Pollnau¹, Dimitri Geskus¹, Edward H. Bernhardt¹, Koop van Dalen¹, Kerstin Worhoff¹, Rene M. de Ridder¹; ¹MESA+ Institute for Nanotechnology, University of Twente, Netherlands. This paper reviews our recent results on highly efficient rare-earth-ion-doped planar and channel waveguide lasers in crystalline potassium double tungstates and amorphous aluminum oxide on silicon chips.

AM5A.2 • 17:00

Recent Advances in Ultrafast VECSELS, Valentin J. Wittwer¹, Oliver D. Sieber¹, Mario Mangold¹, Martin Hoffmann¹, Matthias Golling¹, Thomas Südmeyer¹, Ursula Keller¹; ¹ETH Zurich, Switzerland. We present a femtosecond VECSEL that is continuously tunable from 6.5 to 11.3 GHz. Furthermore, we demonstrate a stabilized VECSEL with a timing jitter <80 fs as well as new gain characterization techniques.

AM5A.3 • 17:15

Thulium Channel Waveguide Laser with 69.7% efficiency, Koop van Dalen¹, Shanmugam Aravazhi¹, Christos Grivas², Sonia Garcia-Blanco¹, Markus Pollnau¹; ¹University of Twente, Netherlands; ²University of Southampton, United Kingdom. Laser experiments on thulium-gadolinium-lutetium-yttrium-codoped, buried, ridge-type channel waveguides in a monoclinic potassium double tungstate demonstrate a maximum slope efficiency of 69.7% and output powers up to ~300 mW at ~1.9 μm.

AM5A.4 • 17:30 **Invited**

GaSb-based 2-3 μm Semiconductor Disk Lasers: Versatile Lasers for High-Power and Narrow-Linewidth Emission, Marcel Rattunde¹, Sebastian Kaspar¹, Tino Töpfer¹, Christian Manz¹, Klaus Köhler¹, Joachim Wagner¹; ¹Fraunhofer IAF, Germany. We will present an overview of long-wavelength GaSb-based semiconductor-disk-lasers emitting in the 2 - 3μm wavelength range. Special emphasis will be on power scaling and single frequency operation.

AM5A.5 • 18:00

Tunable Diamond Raman Laser Intracavity-pumped by an InGaAs Semiconductor Disk Laser, Daniele C. Parrotta¹, Alan J. Kemp¹, Martin D. Dawson¹, Jennifer Hastie¹; ¹Institute of Photonics, University of Strathclyde, Glasgow, United Kingdom. A tunable diamond Raman laser intracavity-pumped within an InGaAs semiconductor disk laser is described. Output power up to 1.3W, conversion efficiency of 14.4%, with M2 ~ 1.1, and tuning from 1209-1245nm are reported.

AM5A.6 • 18:15

Stable Microwave Generation in a Dual-Phase-Shifted Al₂O₃:Yb³⁺ Distributed-Feedback Waveguide Laser, Edward H. Bernhardt¹, Henk van Wolferen², Kerstin Worhoff¹, Rene M. de Ridder¹, Markus Pollnau¹; ¹Integrated Optical MicroSystems Group, University of Twente, Netherlands; ²Transducers Science and Technology Group, University of Twente, Netherlands. A dual-wavelength distributed-feedback channel waveguide laser in ytterbium-doped aluminum oxide was used to create a microwave beat signal at ~15 GHz, with a frequency stability of ±2.5 MHz and a power stability of ±0.35 dB.

Aragon III-B-C

Laser Applications to Chemical, Security and Environmental Analysis

16:30–18:30

LM5B • Laser-Induced Breakdown Spectroscopy and New Spectroscopic Approaches

Waruna Kulatilaka; *Spectral Energies, LLC., USA, President*

LM5B.1 • 16:30 **Invited**

New Developments in Forensic Applications of LIBS and LA-ICP-MS, Jose Almirall¹, Eric Cahoon¹, Sarah Jantzi¹, Emily Schenk¹, Tatiana Trejos¹; ¹International Forensic Institute, Florida International University, USA. The method development for the use of LIBS in the analysis of glass, paint, plant matter, paper and ink will be described along with the observed figures of merit and compared to the more mature Laser Ablation Inductively Coupled Plasma Mass Spectrometry (LA-ICP-MS).

LM5B.2 • 17:00 **Invited**

Laser-induced Breakdown Spectroscopy: A Simple but Versatile Tool for Combustion Diagnostics, Johannes Kiefer¹, Johannes W. Tröger³, Zhongshan Li⁴, Thomas Seeger², Alfred Leipertz², Marcus Alden¹; ¹University of Aberdeen, United Kingdom; ²University Erlangen-Nuremberg, Germany; ³University of Siegen, Germany; ⁴Lund University, Sweden. Laser-induced breakdown spectroscopy (LIBS) is an experimentally simple method capable of measuring elemental composition in a flame. Moreover, the breakdown threshold energy is temperature dependent. Hence, LIBS allows multiple parameter determination in combustion environments.

LM5B.3 • 17:30 **Invited**

Chemometrics and Machine Learning for Spectral Analysis, Peter Torrione¹, Kenneth D. Morton¹, Leslie Collins¹; ¹ECE, Duke University, USA. In this talk, we will review the current state of the art chemometric data processing techniques for LIBS and will highlight techniques we believe hold promise for improving detection and identification using LIBS spectra.

LM5B.4 • 18:00

Fluorescence Lifetime Imaging Through Scattering Media using Dual Imaging Modeling Evaluation in combination with Structured Laser Illumination Planar Imaging, Andreas Ehn¹, Elias Kristensson¹, Olof Johansson¹, Marcus Alden¹; ¹Combustion Physics, Physics, Sweden. Fluorescence lifetime imaging in combination with structured laser illumination planar imaging has been performed in wide field imaging. Measurements were conducted by imaging laminar gaseous flows seeded with toluene through scattering media.

LM5B.5 • 18:15

Photothermal Diffuse Reflectance: A New Tool for Spectroscopic Investigations of Scattering Samples, Julien M. Rey¹, Jonas Kottmann¹, Markus W. Sigrist¹; ¹Physics, ETH Zurich, Switzerland. A new photothermal method which combines mid-infrared high spectral selectivity and strong absorption with large scattering and high detector sensitivity in the near-infrared is presented. It enables spectroscopic studies of turbid media.

Monday, 30 January

NOTES

Blank lined area for notes.





Laser Applications to Chemical, Security and Environmental Analysis (LACSEA) would like to thank the following Corporate Contributors for their outstanding support:



**Silicon
Lightwave
Technology, Inc.**



COHERENT®

HAMAMATSU





Aragon II

Advanced Solid-State Photonics

Aragon III-B-C

Laser Applications to Chemical, Security and Environmental Analysis

07:00–18:30 Registration, Aragon Foyer

08:00–10:00

AT1A • Fiber Devices

F. Oemer Ilday; *Bilkent Univ., Turkey, President*

AT1A.1 • 08:00 **Invited**

High Power Fiber Lasers: Fundamentals and Frontiers, Johan Nilsson¹; ¹Univ. Southampton, United Kingdom. The dramatic advances in high-power fiber lasers have largely been based on evolutionary improvements of telecom technology and cladding-pumping. We consider limiting factors as well as emerging challenges and new developments that aim to address them.

AT1A.2 • 08:30

Fiber Oscillator Producing 91fs Pulses with 0.8μJ at 60W of Average Power, Martin Baumgartl^{1,2}, Caroline Lecaplain³, Ammar Hideur³, Jens Limpert^{1,2}, Andreas Tünnermann^{1,4}; ¹Institute of Applied Physics, Friedrich-Schiller-Universität, Germany; ²Helmholtz Institute Jena, Germany; ³CORIA, Université de Rouen, France; ⁴Fraunhofer Institute for Applied Optics and Precision Engineering, Germany. A mode-locked rod-type fiber oscillator emitting 66W of average power is demonstrated. The pulses are dechirped to 91fs with high efficiency, hence a peak power of 7MW is reached.

AT1A.3 • 08:45

Experimental Demonstration of SRS Suppression in Chirally-Coupled-Core Fibers, I-Ning Hu¹, Xiuquan Ma¹, Cheng Zhu¹, Chi-Hung Liu², Thomas Sosnowski², Almantas Galvanauskas¹; ¹Center for Ultrafast Optical Science, University of Michigan at Ann Arbor, USA; ²Arbor Photonics, Inc., USA. We experimentally demonstrate suppression of Stimulated Raman Scattering using a spectrally tailored transmission of a large-core effectively-single-mode Chirally-Coupled-Core fiber with a large loss at Stokes wavelengths.

AT1A.4 • 09:00

High power Q-switched Fiber Laser System delivering 22mJ Pulse Energy with Excellent Beam Quality, Florian Jansen¹, Fabian Stutzki¹, Andreas Liem², Cesar Jauregui¹, Jens Limpert^{1,2}, Andreas Tünnermann^{1,2}; ¹Institute of Applied Physics Jena, Friedrich-Schiller-Universität Jena, Germany; ²Helmholtz-Institute Jena, Germany. We demonstrate a Q-switched fiber laser system delivering 20ns pulses with 22mJ pulse energy at 110W average power combined with near-diffraction limited beam quality out of a Large-Pitch fiber with 101μm mode field diameter.

AT1A.5 • 09:15

Single-frequency Photonic Bandgap Fiber Amplifier at 1178 nm, Akira Shirakawa¹, Meishin Chen¹, Xinyan Fan¹, Ken-ichi Ueda¹, Christina B. Olausson², Jens K. Lyngso², Jes Broeng²; ¹University of Electro-Communications, Japan; ²NKT Photonics A/S, Denmark. Single-frequency ytterbium-doped photonic bandgap fiber amplifier at 1178 nm is reported. 24.6 W power and 320 kHz linewidth radiation, free from amplified spontaneous emission, linewidth broadening, and stimulated Brillouin scattering, was obtained.

AT1A.6 • 09:30

100 W Nonlinear Compression in Hollow Core Fibers at 1 MHz Repetition Rate, Steffen Hädrich^{1,2}, Jan Rothhardt^{2,4}, Henning Carstens¹, Stefan Demmler¹, Nicholas Herrick¹, Jens Limpert¹, Andreas Tünnermann^{1,2}; ¹Institute of Applied Physics, Germany; ²Helmholtz-Institut Jena, Germany; ³Fraunhofer Institute for Applied Optics and Precision Engineering, Germany. Nonlinear compression of a 200 W, 700 fs, 1 MHz fiber CPA in a xenon filled hollow core fiber results in 93 μJ, 81 fs pulses with 0.75 GW peak and 93 W average power.

AT1A.7 • 09:45

All-Fiber Parametric Generation of Sub-100ps Pulses at 650nm with 9Watt Average Power, Cesar Jauregui¹, Alexander Steinmetz¹, Dirk Nodop¹, Jens Limpert^{1,2}, Andreas Tünnermann^{1,3}; ¹Institute of Applied Physics, Friedrich-Schiller University, Germany; ²Helmholtz-Institute Jena, Germany; ³Fraunhofer Institute for Applied Optics and Precision Engineering, Germany. We present the generation of 9Watt of coherent pulsed radiation at 650nm with excellent beam quality by exploiting degenerate Four-Wave-Mixing in an endlessly single-mode photonic crystal fiber. The pulses had a maximum duration of ~90ps.

08:00–10:00

LT1B • Mid-Infrared Sensing II

Lin Ma; *Virginia Tech, USA, President*

LT1B.1 • 08:00

Diode Laser-Based Measurements for Hypersonic Engine Research, Michael Brown¹; ¹AFRL, USA. Diode laser-based absorption and non-resonant transmission measurements provide a means to gather in-stream data of hypersonic flow paths. Our recent efforts at addressing mass capture and dynamics associated with shock train movement are presented.

LT1B.2 • 08:15

Measurement of Isotopologues of CO2 with a Quantum Cascade Laser based Instrument using a Single Absorption Cell, J. Barry McManus¹, Mark Zahniser¹, David Nelson¹, Bin Xiang²; ¹Aerodyne Research Inc., USA; ²Earth and Planetary Science, Harvard University, USA. We present measurements of isotopologues of CO2 using a quantum cascade laser (2310 cm⁻¹) based spectroscopic instrument with a single absorption cell. This instrument is distinct from our earlier design with dual absorption cells.

LT1B.3 • 08:30 **Invited**

Applications of QCLs in Studies of Chemical Dynamics, Grant Ritchie¹; ¹Oxford University, United Kingdom. This paper reports on cw QCL based pump and probe studies of coherent transient effects in a low pressure gas.

LT1B.4 • 09:00

Frequency Characterization of an External-Cavity Quantum Cascade Laser at 4.5 μm using a Frequency Comb, Kevin Knabe¹, Paul A. Williams¹, Fabrizio R. Giorgetta¹, Chris M. Armacost², Michael B. Radunsky², Nathan R. Newbury¹; ¹NIST, USA; ²Daylight Solutions, USA. We measure the frequency noise spectrum of a free-running external-cavity quantum cascade laser at 4.5 μm through sum frequency generation with a fiber frequency comb.

LT1B.5 • 09:15

Simultaneous Measurements of NO2 and its Dimer N2O4 at Room Temperature with a Multiplexed Intra-pulse Quantum Cascade Laser Spectrometer, Geoffrey Duxbury¹, David Wilson¹, Nigel Langford¹; ¹Physics, University of Strathclyde, United Kingdom. Quantitative measurements of the dimerisation of nitrogen dioxide, in an NO2 and N2O4 mixture, have been made using long duration pulses from 7.84 and 7.46 μm Quantum Cascade (QC) lasers in an intra-pulse QC laser spectrometer.

LT1B.6 • 09:30

Sensitive Detection of Ethane using Tunable Laser Diode Absorption Spectroscopy Near 3.3 μm, Rafal Lewicki¹, Karol Krzempek², Lars Nähle³, Johannes Koeth³, James Gupta⁴, Frank Tittel¹; ¹Electrical and Computer Engineering, Rice University, USA; ²Laser & Fiber Electronics Group, Wrocław University of Technology, Poland; ³nanoplus GmbH, Germany; ⁴Institute for Microstructural Sciences, National Research Council of Canada, Canada. A spectroscopic trace-gas sensor employing a continuous wave, thermoelectrically cooled distributed feedback laser diode and a 100 m optical pathlength astigmatic Herriott cell for sensitive and selective detection of ethane near 3.3 μm is reported.

LT1B.7 • 09:45

Signal Processing for Estimation of Gas Species Using Supercontinuum Absorption Spectroscopy, Alexandre Dobroc¹, Nicolas Cézard¹; ¹DOTA, ONERA, France. In the context of supercontinuum absorption spectroscopy, we present a general algorithm to estimate the concentration of multiple species in a gas mixture. This method yields unbiased estimates and reaches an accuracy close to the Cramer-Rao Bounds.

10:00–10:30 Exhibits & Coffee Break



Aragon II

Advanced Solid-State Photonics

10:30–12:00

AT2A • Nonlinear Sources

Sunao Kurimura; *Nat'l Inst. for Mat. Sci, Japan, Presider*

AT2A.1 • 10:30

> 3 MW Peak Power at 266 nm Using Nd:YAG/Cr4+:YAG Microchip Laser and Fluxless-Grown BBO, Rakesh Bhandari¹, Takunori Taira¹, A. Miyamoto², Y. Furukawa², T. Tago²; ¹Laser Research Center, Institute for Molecular Science, Japan; ²Oxide Corporation, Japan. We use fluxless-grown BBO to obtain fourth harmonic conversion of a linearly polarized Nd:YAG microchip laser, passively Q-switched with [110] cut Cr4+:YAG, achieving 3.4 MW peak power, 250 ps, 100 Hz pulses at 266 nm.

AT2A.2 • 10:45

Rapidly Spectral Ramping of an Ultra-wide Tuneable Femtosecond Non-collinear Optical Parametric Oscillator (NOPO) with High Average Output Power, Tino Lang^{1,2}, Thomas Binhammer³, Stefan Rausch^{1,2}, Guido Palmer¹, Moritz Emons¹, Marcel Schultze¹, Anne Harth^{1,2}, Uwe Morgner^{1,4}; ¹Institute of Quantum Optics, Leibniz Universität Hannover, Germany; ²Center for Quantum Engineering and Space-Time Research (QUEST), Germany; ³VENTEON Laser Technologies GmbH, Germany; ⁴Laser Zentrum Hannover (LZH), Germany. The 3 W NOPO pumped by a frequency doubled thin-disk laser is rapidly tunable from 650 to 950 nm by varying the resonator length. First measurements prove the concept up to 500 Hz ramping frequencies.

AT2A.3 • 11:00

Quadratic Cascading Effects in Broadband Optical Parametric Generation, Martin Levenius¹, Matteo Conforti², Fabio Baronio², Valdas Pasiskevicius¹, Fredrik Laurell¹, Katia Gallo¹; ¹Applied Physics, KTH-Royal Institute of Technology, Sweden; ²Information Engineering, University of Brescia, Italy. We investigate theoretically and experimentally multistep processes in broadband optical parametric generation (OPG) and demonstrate the possibility to control fine features in the gain spectra via the OPG pump.

AT2A.4 • 11:15

Octave Spanning Optical Parametric Amplification of CEP Stable Sub-two Cycle Pulses at High Average Power, Stefan Demmler¹, Jan Rothhardt^{1,2}, Steffen Hädrich^{1,2}, Jens Limpert^{1,2}, Andreas Tünnermann^{1,2}; ¹Institute of Applied Physics, Friedrich-Schiller-University Jena, Germany; ²Helmholtz Institute Jena, Germany. Fiber laser pumped octave spanning optical parametric amplification of CEP-stable sub-two cycle pulses is demonstrated. The system delivers 14 W of average output power at 500 kHz, corresponding to 25 µJ of compressed pulse energy.

AT2A.5 • 11:30

Coherent Synthesis of Ultra-broadband Optical Parametric Amplifiers, Cristian Manzoni¹, Shu-Wei Huang², Giovanni Cirimi², Jeffrey Moses², Franz Kärtner^{3,2}, Giulio Cerullo¹; ¹Politecnico di Milano, Italy; ²Department of Electrical Engineering and Computer Science, Massachusetts Institute of Technology, USA; ³DESY-Center for Free-Electron Laser Science and Hamburg University, Germany. We demonstrate coherent synthesis of two ultra-broadband optical parametric amplifiers, resulting in octave-spanning (500-1000 nm) spectra supporting nearly single-cycle sub-4-fs duration. Synthesized pulse timing is locked to sub-300-as.

AT2A.6 • 11:45

Cross-polarized Wave Generation for Temporal Compression and Cleaning of a High Energy Fiber Chirped Pulse Amplifier, Yoann Zaouter¹, Lourdes Patricia Ramirez², Dimitrios Papadopoulos¹, Clemens Hoenninger¹, Franck Morin¹, Marc Hanna², Frederic Druon², Eric Mottay¹, Patrick Georges²; ¹Amplitude Systemes, France; ²Laboratoire Charles Fabry de l'Institut d'Optique, CNRS - Université Paris Sud, France; ³Institut de la Lumière Extrême, CNRS - Ecole Polytechnique - Institut d'Optique - Université Paris Sud, France. Cross-polarized wave generation is used to perform both pulse shortening and temporal cleaning of a high-energy ytterbium-doped fiber-based femtosecond laser system. This results in the generation of high temporal quality 37 µJ, 115 fs pulses.

12:00–13:30 Lunch (on your own)

Aragon III-B-C

Laser Applications to Chemical, Security and Environmental Analysis

10:30–12:30

LT2B • Laser-Based Sensing for Stand-off Detection

Joakim Bood; *Lund Univ., Sweden, Presider*

LT2B.1 • 10:30 **Invited**

Coherent Control Methods for Detection of Explosives, David Moore¹; ¹Los Alamos National Laboratory (505-665-6089), USA. We are exploring optimal dynamic detection of explosives (ODD-Ex) to exploit recent advances in optimal shaping of laser pulses for control of molecular processes to significantly enhance the standoff detection of explosives.

LT2B.2 • 11:00

Remote Backwards Emission in Air Via Stimulated Emission in Atomic Oxygen, Arthur Dogariu¹, James Michael¹, Richard Miles¹; ¹Princeton University, USA. We demonstrate and investigate coherent stimulated emission in the forward and backward direction from a remotely induced gain region created by an ultraviolet laser which dissociates molecular oxygen and excites atomic oxygen

LT2B.3 • 11:15

Broadband Mid-IR Standoff Spectroscopy of Explosives with a Femtosecond Optical Parametric Oscillator, Tyler W. Neely¹, Lora Nugent-Glandorf¹, Scott Diddams¹; ¹NIST Boulder, USA. We describe a 2.6 - 4.0 µm broadband tunable MIR source based on optical parametric oscillation (OPO). Utilizing this source, we investigate the signatures of solid trace explosives at a standoff distance of 3 m.

LT2B.4 • 11:30 **Invited**

Spatial Offset Stand Off Raman Scattering, Bernhard Lendi¹, Bernhard Zachhuber¹, Christoph Gasser¹, Engeline Chrysostom¹; ¹Institute for Chemical Technologies and Analytics, Vienna University of Technology, Austria, Austria. Identification and quantification of potentially harmful substances concealed in fluorescent containers were achieved at a distance of 12 metres using stand off spatial offset Raman scattering.

LT2B.5 • 12:00

Airborne LIDAR Measurements of Atmospheric Pressure Made Using the Oxygen A-band, Haris Riris¹, Mike Rodriguez², Graham Allan², William E. Hasselbrack², Mark A. Stephen¹, James B. Abshire¹; ¹Laser Remote Sensing Laboratory, NASA Goddard Space Flight Center, USA; ²Sigma Space, USA. We report on airborne measurements of atmospheric pressure using a fiber-laser based lidar operating in the oxygen A-band near 765 nm and the integrated path differential absorption measurement technique.

LT2B.6 • 12:15

A Laser Sounder for Global Measurements of CO2 from Space, Haris Riris¹, James B. Abshire¹, Graham Allan², William E. Hasselbrack², Clark Weaver³, Jianping Mao³; ¹Laser Remote Sensing Laboratory, NASA Goddard Space Flight Center, USA; ²Sigma Space, USA; ³University Space Research Association, USA. We have developed a laser technique for the remote measurement of the tropospheric CO2 concentrations from space. Our goal is to develop a space instrument and mission approach for active CO2 measurements.

12:30–14:00 Lunch (on your own)

Tuesday, 31 January



Aragon II

Advanced Solid-State Photonics

13:30–15:00

AT3A • Near-infrared Sources

Brian Walsh; *NASA Langley Res. Ctr, USA, Presider*

AT3A.1 • 13:30 **Invited**

Ultrabroadband Fiber Lasers, Daniele Brida^{1,2}, Alfred Leitenstorfer¹; ¹*University of Konstanz, Germany*; ²*Politecnico di Milano, Italy*. We demonstrate a passively phase-locked seed source based on fs-Er-fiber technology with CEO-frequency set to zero. Such technology allows the synthesis of pulses with a duration of 4.3 fs. This value corresponds to a single cycle of the carrier wavelength at 1300 nm.

AT3A.2 • 14:00

High Power Nd:YAG Single Crystal Fiber Emitting at 946 nm and 938 nm, Xavier Dèlen¹, Igor Martial^{1,2}, Julien Didierjean², Nicolas Aubry², Francois Balembois¹, Patrick Georges¹; ¹*Laboratoire Charles Fabry, France*; ²*FiberCryst SAS, France*. We demonstrated a 34 W output power cw Nd:YAG laser emitting at 946 nm with a 53% slope efficiency using single crystal fiber. 20 W were also obtained at 938 nm.

AT3A.3 • 14:15

A Hybrid Yb Fiber/Solid State Amplifier: Management of Amplification Dynamics by High-Energy Seeding, Giedrius Andriukaitis¹, Tadas Balciunas¹, Lingxiao Zhu¹, Aart J. Verhoeff¹, Tobias Floery¹, Alma Fernandez¹, Audrius Pugzlys¹, Andrius Baltuska¹, Mikhail Grishin², Andrejus Michailovas²; ¹*Photonics Institute, TU Wien, Austria*; ²*Ekspla LTD, Lithuania*. A broadband μ J-level seed from a monolithic Yb-fiber MOPA efficiently suppresses output pulse bistability and ensures simultaneous energy and average power saturation in a 6-mJ Yb:CaF₂ amplifier at 1 kHz, twice over the cutoff repetition frequency.

AT3A.4 • 14:30

Yb-doped-based High Energy and Broadband Multipass Amplifiers at 100 Hz, Dimitrios Papadopoulos^{1,2}, Sandrine Ricaud^{2,3}, Alain Pellegrina¹, Lourdes P. Ramirez², Marc Hanna², Patrick Georges², Frederic Druon²; ¹*Institut de la Lumiere Extreme, France*; ²*Institut d'Optique, France*; ³*Amplitude Systems, France*. A 27mJ diode pumped multipass Yb:KYW amplifier at 100Hz with 5.5nm bandwidth at 1030nm is presented. First results on the subsequent Yb:CaF₂ power amplifier stage are also presented resulting 51mJ at 20Hz.

AT3A.5 • 14:45

Amplification of Femtosecond Pulses from an Yb:KYW Oscillator in a High-power Yb:YAG Planar Waveguide Amplifier, Cristtel Y. Ramirez-Corral^{1,2}, Ian J. Thomson², Christopher G. Leburn¹, Denis R. Hall², Derryck T. Reid¹, Howard J. Baker¹; ¹*Scottish Universities Physics Alliance, Department of Physics, Heriot-Watt University, United Kingdom*; ²*James Watt Institute for High Value Manufacturing, Department of Physics, Heriot-Watt University, United Kingdom*. The first demonstration of coupling an Yb:KYW femtosecond laser into a high-power single-side pumped Yb:YAG planar waveguide amplifier is described. Five passes of the amplifier yielded 700 fs pulses with average powers of 50 W.

15:00–16:30 AT4A • ASSP Poster Session 1, See page 28

Aragon III-B-C

Laser Applications to Chemical, Security and Environmental Analysis

14:00–16:00

LT3B • LIF and Polarization Spectroscopy Based Sensing

Thomas Seeger; *Univ. of Siegen, Germany, Presider*

LT3B.1 • 14:00

Interference-Free, High-Repetition-Rate Imaging of Atomic-Hydrogen in Flames Using Femtosecond, Femtosecond, Two-Photon- Excited, Laser-Induced Fluorescence (fs-TPLIF), Waruna D. Kulatilaka¹, Sukesh Roy¹, James R. Gord²; ¹*Spectral Energies, LLC, USA*; ²*Air Force Research Laboratory, USA*. We demonstrate femtosecond, two-photon-excited, laser-induced-fluorescence (TPLIF) imaging of atomic hydrogen in reacting flows at 1kHz. Unlike traditional ns or ps laser-based approaches, fs-TPLIF images are nearly free of photolytic interference.

LT3B.2 • 14:15

Thickness Imaging of Evaporating Liquid Water Films by Simultaneous Tracer-LIF, Raman Imaging and Diode Laser Absorption Spectroscopy, Thomas Dreier¹, Daniel Greszik¹, Huinan Yang¹, Christof Schulz¹; ¹*IVG, University Duisburg-Essen, Germany*. The thickness of liquid water films was imaged by a combination of Raman scattering and tracer-based laser-induced fluorescence in combination with local film thickness and temperature measurements by near-infrared diode laser absorption.

LT3B.3 • 14:30 **Invited**

Simultaneous Time-Resolved Detection of Trace Species Using High Repetition Rate LIF and cw-CRDS, Christa Fittschen¹; ¹*CNRS, France*. OH and HO₂ radicals play a major role in atmospheric and combustion chemistry, their time-resolved, simultaneous detection is highly desirable. We present a new experimental set-up combining cw-CRDS and high repetition-rate LIF to Laser Photolysis.

LT3B.4 • 15:00

Imaging of Hydrogen Peroxide in an HCCI Engine using Photofragmentation Laser-induced Fluorescence, Malin Jonsson¹, Bo Li¹, Martin Algotsson², Joakim Bood¹, Zhongshan. S. Li¹, Olof Johansson¹, Martin Tunér², Bengt Johansson² and Marcus Aldén¹; ¹*Div. of Combustion Physics, Lund University, Sweden*; ²*Div. of Combustion Engines, Lund University, Sweden*. Hydrogen peroxide (H₂O₂) is for the first time measured and imaged in two-dimensions in an HCCI engine using photofragmentation laser-induced fluorescence (PF-LIF). Qualitatively, the experimental data agree with simulations.

LT3B.5 • 15:15 **Invited**

UV Fiber-Laser-Based Fluorescence and Blue Diode-Laser-Based Phosphorescence-Lifetime Methods, Frank Keutsch¹, Joshua Paul², Joshua DiGangi¹, Samuel B. Henry¹; ¹*Chemistry, University of Wisconsin, Madison, USA*; ²*Thermo Fischer, USA*. Combination of a novel, tunable pulsed UV-fiber laser with a fluorescence-detection design using carbon nanofiber coatings and blue diode lasers with a novel lifetime-phosphorescence method has provided new turn-key instrumentation for monitoring applications.

LT3B.6 • 15:45

In-cylinder Temperature Measurements via Fiber-based Toluene-LIF Time-correlated Single-photon Counting, Eugen Friesen¹, Christopher Gessenhardt¹, Sebastian Kaiser¹, Thomas Dreier¹, Christof Schulz¹; ¹*IVG, University Duisburg-Essen, Germany*. Time-correlated single photon counting combined with a minimal-invasive fiber-optic spark-plug sensor was used to provide an “on-the-fly” temperature measurement via laser-induced fluorescence lifetime measurements of toluene fuel tracer.

Tuesday, 31 January

16:00–16:30 Exhibits & Coffee Break



Aragon I and Foyer

Advanced Solid-State Photonics

15:00–16:30
AT4A • ASSP Poster Session 2

AT4A.01

Diode-pumped 1617 nm Er:YAG laser with micro-pulling down single-crystal fibers, Igor Martial^{1,2}, Adrien Aubourg^{1,2}, Julien Didierjean³, Nicolas Aubry², Francois Balembois¹, Patrick Georges¹; ¹Institut d'Optique, France; ²FiberCryst, France. We demonstrated diode-pumped laser operation at 1617 nm with Er:YAG 60 mm long and 600 μm diameter single-crystal fibers. We obtained 5.5 W in cw and 0.5 mJ 30 ns pulses at 100 Hz in Q-switched operation.

AT4A.02

Regenerative Amplifier with Pulse-on-Demand Operation, Christian Holtz¹, Joachim Meier¹, Juerg aus der Au¹, Max Lederer²; ¹High Q Laser, Austria; ²European XFEL, Germany. A picosecond regenerative amplifier with repetition rate insensitive output energy is demonstrated. Constant output energy for repetition rates between 0 and 100kHz with a rate change of 2MHz/s is achieved.

AT4A.03

Cr:ZnSe Bulk and Cr:ZnSe Thin Disk cw Lasers, Guenther Renz¹, Jochen Speiser¹, Adolf Giesen¹, Irina Sorokina², Evgeni Sorokin³; ¹German Aerospace Center, Germany; ²University of Trondheim, Norway; ³University of Vienna, Austria. A Thulium-fiber-laser pumped Cr:ZnSe bulk cw laser with an output power of 6.5W as well as a Thulium-fiber-laser or diode-laser-stack pumped Cr:ZnSe thin disk cw laser with almost 2W of output powers will be presented.

AT4A.04

Maximising Performance of Compact, CW, Visible Self-Raman Lasers by Balancing Non-linear SRS and SFG Effects, Xiaoli Li^{1,2}, Helen Pask¹, Andrew Lee¹, Yujing Huo², Jim Piper¹, David Spence¹; ¹Physics and Astronomy, Macquarie University, Australia; ²Electronic Engineering, Tsinghua University, China. We detail evidence of competition between non-linear SRS and SFG within a compact, self-Raman laser. Using experiment and theory, we demonstrate that efficient visible generation can be obtained through careful management of these processes.

AT4A.05

Measurement and Influence of Spectral Phase Mismatch in Femtosecond Coherent Beam Combining Systems, Louis Daniault¹, Marc Hanna¹, Laurent Lombard², Yoann Zaouter³, Eric Mottay², Dider Goulaer², Pierre Bourdon², Frederic Druon¹, Patrick Georges¹; ¹Laboratoire Charles Fabry - CNRS - Institut d'Optique - Univ Paris Sud, France; ²Office National d'Etudes et de Recherches Aérospatiales, France; ³Amplitude Systemes, France. We experimentally investigate the impact of spectral phase mismatch on coherent beam combining in femtosecond regime. This also allows us to quantify the spatial and temporal contributions to the non perfect combining efficiency.

AT4A.06

Single Mode All-Fiber Pulse-Pumped Raman Amplifier for Picosecond Pulses, Veronika Katzy¹, Martin Giesberts¹, Oliver Fitzau¹, Hans-Dieter Hoffmann¹; ¹Fraunhofer Institute for Lasertechnology, Germany. A Raman amplifier for 1064 nm and picosecond pulses pumped by a pulsed fiber amplifier at 1020 nm is demonstrated. An amplification of 32 dB and high peak power conversion of 99 % are achieved.

AT4A.07

A Sub-Watt, Line-narrowing, 193-nm Solid State Laser Operating at 6 kHz with KBBF for Injection-locking ArF Excimer Laser Systems, Shinji Ito¹, Takashi Onose¹, Shuntaro Watanabe², Teruo Kanai¹, Kouji Kakizaki¹, Takashi Matsunaga¹, Chuangting Chen¹, Yohei Kobayashi¹, Chun Zhou², Junichi Fujimoto¹, Hakaru Mizoguchi¹, X.Y. Wang¹; ¹GIGAPHOTON INC., Japan; ²Research Institute for Science and Technology, Tokyo University of Science, Japan; ³Institute for Solid State Physics, University of Tokyo, Japan; ⁴Chinese Academy of Sciences, China. We present a line-narrowing 193-nm solid state laser with a KBBF prism-coupled device. This laser delivers an output power of 0.2 W at a repetition rate of 6 kHz.

AT4A.08

Large Size Yb3+:YAG Crystal and Ceramic Experimental Cross Evaluation in a High Average-power Diode-pumped Laser Amplifier, Daniel Albach¹, Thierry Novo¹, Jean-Christophe Chanteloup¹; ¹LULI, France. We report on the performance of ceramic gain media used in the Lucia main amplifier. Performance regarding small signal gain, wave front deformation and depolarization are compared to their single crystal counterparts.

AT4A.09

Microwatt Average Power High Harmonic Generation with High Repetition Rate Ultrafast Fiber Lasers, Jan Rothhardt^{1,2}, Steffen Hädrich^{1,2}, Manuel Krebs¹, Henning Carstens¹, Stefan Demmler¹, Jens Limpert^{1,2}, Andreas Tünnermann^{1,2}; ¹Institute of Applied Physics, Germany; ²Helmholtz Institut Jena, Germany. We present high harmonic generation with a fiber laser system and subsequent non-linear compression. Calibrated measurements reveal an average power as high as 3.2 μW in a single harmonic at 49 nm.

AT4A.10

Thermally Induced Index Gratings in Few-Mode High-Power Fiber Laser Systems, Cesar Jauregui¹, Tino Eidam¹, Hans-Jürgen Otto¹, Fabian Stutzki¹, Florian Jansen¹, Jens Limpert^{1,2}, Andreas Tünnermann^{2,3}; ¹Institute of Applied Physics, Friedrich-Schiller University, Germany; ²Helmholtz-Institute Jena, Germany; ³Fraunhofer Institute for Applied Optics and Precision Engineering, Germany. Mode-interference in few-mode fiber laser systems induces an oscillating temperature profile which gives rise to an index grating via the thermo-optic effect. Such gratings most likely cause the observed mode instabilities.

AT4A.11

Efficient Tunable Continuous Wave Laser Operation of Tm:LuYSiO5 at Room Temperature, Kejian Yang^{1,2}, Thomas Dekorsy¹, Lihe Zheng³, Jun Xu³, Guangjun Zhao⁴; ¹Physics, AG-Dekorsy, University Konstanz, Germany; ²School of Information Science and Engineering, Shandong University, China; ³Key Laboratory of Transparent and Opto-functional Inorganic Materials, Shanghai Institute of Ceramics, Chinese Academy of Sciences, China; ⁴Key Laboratory of Materials for High Power Laser, Shanghai Institute of Optics and Fine Mechanics, China. We demonstrated an efficient continuous wave and tunable laser actions of a new thulium-doped oxyorthosilicate Tm:LuYSiO5 crystal. A maximum slope efficiency of 50.2% and a discontinuous tunable operation ranging from 1922 to 2061 nm were obtained.

AT4A.12

Single-frequency Yb:YAG Microchip Laser with Ultra-low Timing Jitter, Carlos Sotelo¹, Robert D. Stultz¹; ¹Raytheon Space and Airborne Systems, USA. A diode-pumped, Q-switched, single-mode Yb:YAG microchip laser has been demonstrated. The 55 microjoule, 830 picosecond pulses were synchronized to a command signal within 18 nanoseconds using a diode that bleached the Cr:YAG in the microchip.

AT4A.13

Systematic Study on Shortest Pulse Duration in Mode-locked Yb Lasers, Masaki Tokurakawa¹, Akira Shirakawa¹, Ken-ichi Ueda¹; ¹Institute for Laser Science, University of Electro-Communications, Japan. Systematic study on shortest pulse duration in mode-locked Yb lasers is reported. The relationships between the available shortest pulse duration and modulation depth for both of the bulk and the thin-disk laser geometries are shown.

AT4A.14

Mode Fluctuations in End-pumped Passively Q-switched Solid-state Lasers, Thomas Hülsenbusch¹, Alexander Büttner¹, Mathias Ernst¹, Tino Lang¹, Christian Kollek^{1,2}, Dietmar Kracht^{1,2}, Jörg Neumann^{1,2}; ¹Development, Laser Zentrum Hannover, Germany; ²Centre for Quantum-Engineering and Space-Time Research - Quest, Germany. Axial mode fluctuations in high-energy, passively Q-switched lasers lead to instabilities in pulse energy and beam pointing. Effects of subresonators formed by residual reflection at optical surfaces on axial modes and pulse energy are investigated.

AT4A.15

Gain Measurements of Composite Nd:YAG Ceramic Slab Laser Active Element With Collinear Zigzag Pumping, Aidas Aleknavičius^{1,2}, Martynas Gabalis¹, Andrejus Michailovas^{1,2}, Mikhail Grishin^{1,2}, Kirilas Michailovas¹, Valdas Girdukas³; ¹Institute of physics, Center for Physical Sciences and Technology, Lithuania; ²Ekspla, Lithuania; ³Faculty of Natural Sciences, Vytautas Magnus University, Lithuania. Measurements of gain and beam propagation factor after amplification in suggested composite active element with collinear zig-zag pumping are presented.

AT4A.16

Withdrawn

AT4A.17

High-repetition-rate, Picosecond THz Output from a DAST-DFG Pumped by 1.55 μm Dual-frequency Picosecond Laser, Katsuhiko Miyamoto¹, Andrew Lee², Shuto Ujita¹, Takafumi Saito¹, Takashige Omatsu^{1,3}; ¹Chiba Univ., Japan; ²Macquarie University, Sydney, Australia; ³JST CREST, Tokyo, Japan. We demonstrated MHz-repetition-rate, picosecond THz output from DAST crystal pumped by 1.55 μm dual-frequency laser system based on picosecond Nd-doped vanadate bounce laser. THz output was observed in the frequency range of 2.1-7.1 THz.

AT4A.18

Luminescence Quenching in rare-earth-ion-doped Al2O3 Lasers and its Influence on Relaxation Oscillation Frequency, Laura Agazzi¹, Edward H. Bernhardt¹, Kerstin Worhoff¹, Markus Pollnau¹; ¹University of Twente, Netherlands. The impact of luminescence quenching on rare-earth-ion doped lasers is investigated, and we show that the expression for the relaxation oscillation frequency needs to be modified to take the quenching properly into account

AT4A.19

Chirping Regenerative Amplifier with Dispersive Optics, Junji Kawanaka¹, Hiroaki Furuse¹, Toshiyuki Kawashima², Hirofumi Kan²; ¹Osaka University, Japan; ²Hamamatsu Photonics K. K., Japan. A regenerative amplifier with a chirped volume Bragg grating has been developed. A seed pulse is temporally stretched to 424ps with 1.2mJ at 100Hz. The obtained chirping ratio is as high as 2.1ns/nm.

AT4A.20

Study of Wave-front Distortion in Cryogenic Yb:YAG TRAM Laser and a Novel Coherent Beam Combining (CBC) Technique for Ultra-high Power Laser Systems, Hiroaki Furuse¹, Junji Kawanaka², Haik Chosrowjan¹, Noriaki Miyanaga³, Toshimitsu Sakurai¹, Masayuki Fujita¹, Shinya Ishii³, Kenji Takeshita³, Yasukazu Izawa¹; ¹Institute for Laser Technology, Japan, Japan; ²Institute of Laser Engineering, Osaka University, Japan; ³Mitsubishi Heavy Industries, Japan. We have studied wave-front distortion due to thermal lensing, temperature rise and birefringence of cryogenic Yb:YAG TRAM laser for >100kW ultra-high power laser systems. A novel coherent beam combining technique is also presented.

Tuesday, 31 January





Aragon I & Foyer

Advanced Solid-State Photonics

AT4A • ASSP Poster Session 2—Continued

AT4A.21

Spectroscopic and Oscillation Properties of Pr³⁺ ions in CaF₂-SrF₂-LaF₃ Solid Solutions, Maxim Doroshenko¹, Tasoltan T. Basiev¹, Vasilii Konyushkin¹, Alexander Papashvili¹, Olim Alimov¹, Vyacheslav Osiko¹, Pavel Popov², Günter Huber³, Fabian Reichert³, Matthias Fechner³; ¹General Physics Institute RAS, Russian Federation; ²Bryansk State University, Russian Federation; ³Institute of Laser-Physics, University of Hamburg, Germany. Spectroscopic and oscillation properties of Pr³⁺ doped solid solutions based on fluorides were investigated. Under GaN diode pumping pulsed oscillations in Ca_{0.75}Sr_{0.1}La_{0.14}Pr_{0.07} crystal were obtained at 642 nm with slope efficiency up to 3%.

AT4A.22

Low Noise CW 355 nm Generation by Simple Single Pass Configuration with PPMgSLTs from Fiber Based Laser, Junji Hirohashi¹, Yasuhiro Tomihari¹, Tatsuo Fukui¹, Satoshi Makio¹, Koji Suzuki¹, Koichi Imai¹, Hiroshi Motegi¹, Y. Furukawa¹; ¹OXIDE Corporation, Japan. Low noise CW 355nm with more than 50 mW was generated by frequency conversion of 1064 nm fiber based laser with simple cascaded single pass configuration using two PPMgSLTs.

AT4A.23

Compensation of Thermal Depolarization in CaF₂ with no Additional Phase Elements, Anton G. Vyatkin¹, Ilya Snetkov¹, Efim Khazanov¹, Oleg Palashov¹; ¹Institute of Applied Physics of the Russian Academy of Sciences, Russian Federation. Compensation of depolarization in lasers' active elements at small birefringence without additional phase elements was proposed and experimentally observed. Requirements on the crystals were formulated. A further modification of the scheme was found.

AT4A.24

Diode Pumped 0.61 μm Eu:YAG Laser, Norman Barnes¹, Brian M. Walsh¹, Donald Reichle¹; ¹NASA Langley Research Center, USA. A diode pumped Eu:YAG laser produced continuous wave 0.610 μm output. Blue GaN laser diodes pumped the 5D3 manifold. The laser operates between the 5D0 to 2F2 manifolds. Preliminary experiments produced ~ 2.0 μW.

AT4A.25

Limitations of Narrow-bandwidth Amplification at Different Seed Wavelengths in Ytterbium-doped Fibers, Mirosław Rekas¹, Nicoletta Haarlammert¹, Andrea Kliner², Thomas Schreiber¹, Ramona Eberhardt¹, Andreas Tünnermann^{1,2}; ¹Fraunhofer IOF Jena, Germany; ²Institut of Applied Physics, Germany. We report on our investigations of Ytterbium-doped double-clad fiber amplifiers seeded at 1030nm and 1073nm as well as the combination of both. Limitations are found to be ASE and SRS depending on the seed configuration.

AT4A.26

Fiber Based Dispersion Management in an Ultrafast Thulium-doped Fiber Laser and External Compression with a Normal Dispersive Fiber, Andreas Wienke¹, Frithjof Haxsen^{1,2}, Dieter Wandt^{1,2}, Uwe Morgner^{1,3}, Jörg Neumann^{1,2}, Dietmar Kracht^{1,2}; ¹Laser Zentrum Hannover e.V., Germany; ²Centre for Quantum Engineering and Space-Time Research - QUEST, Germany; ³Institut für Quantenoptik, Leibniz Universität Hannover, Germany. Ultrashort pulses in a thulium-doped fiber laser were generated with a fiber based dispersion management. The laser emitted sub-500 fs pulses which were compressed externally with a normal dispersive fiber below 130 fs.

AT4A.27

Burst-mode Yb Fiber Amplifier Producing 30 μJ Individual Pulse Energy, Hamit Kalaycioglu¹, Y. Burak Eldeniz², F. Oemer Ilday¹, Koray Eken²; ¹Bilkent University, Turkey; ²FiberLAST Ltd., Turkey; ³Electronics Engineering, Ankara University, Turkey. We report 30-μJ individual pulse energy for 150-ns long amplified bursts of 0.4 mJ total energy from a 1-kHz Yb-fiber amplifier. Non-uniformity of pulse energy distribution inside amplified bursts is significantly reduced.

AT4A.28

Octave Spanning Spectrum in Tellurite Fiber using Low Pulse Energy High Repetition Rate Femtosecond Yb: fiber laser, Hongyu Yang¹, Aimin Wang¹, Zhigang Zhang¹; ¹Institute of Quantum Electronics, School of Electronics Engineering and Computer Science, Peking University, China. We present an all-fiber integrated laser system that delivers the octave spanning spectrum in a 20 cm long tellurite photonic crystal fiber at a pulse energy of 30 pJ and fundamental repetition rate of 502MHz.

AT4A.29

Coherent Combining of Two Femtosecond Chirped-pulse Amplifiers in a Passive Architecture, Louis Daniault¹, Marc Hanna¹, Dimitrios Papadopoulos², Yoann Zaouter³, Eric Mottay³, Frederic Druon¹, Patrick Georges¹; ¹Laboratoire Charles Fabry - CNRS - Institut d'Optique - Univ Paris Sud, France; ²Institut de la lumière extrême - CNRS - Polytechnique - ENSTA - Institut d'Optique, France; ³Amplitude Systemes, France. We demonstrate an architecture allowing passive coherent combination of two fiber femtosecond chirped-pulse amplifiers. The experiment shows that temporal, spectral, and spatial qualities of each beam are retained, with a combining efficiency of 96%.

Tuesday, 31 January

NOTES

Blank area for notes with horizontal lines.





Aragon II

Advanced Solid-State Photonics

16:30–18:30

AT5A • Ultrafast Optics

James Kafka; *Newport / Spectra-Physics, USA, President*

AT5A.1 • 16:30 **Invited**

Low-Dimensional Carbon Nanostructures for Ultrafast Bulk Solid-State Lasers, Fabian Rotermund¹; ¹Department of Physics / Division of Energy Systems Research, Ajou University, Republic of Korea. Low-dimensional carbon nanostructures such as carbon nanotubes and graphene have been successfully used as saturable absorbers for laser mode-locking. In this talk, recent progress in carbon nanotube and graphene mode-locked bulk solid-state lasers is presented.

AT5A.2 • 17:00

Compact Gigahertz Frequency Comb Generation: How Short Do The Pulses Need To Be?, Selina Pekarek¹, Max C. Stumpf¹, Steve Lecomte², Stefan Kundermann², Alexander Klenner¹, Thomas Südmeier¹, John M. Dudley³, Ursula Keller¹; ¹ETH Zürich, Switzerland; ²Centre Suisse d'Electronique et de Microtechnique (CSEM) SA, Switzerland; ³Institut FEMTO-ST, Université de Franche-Comté, France. We investigate the required pulse duration for coherent supercontinuum generation for CEO detection in the 1- μ m and 1.5- μ m spectral regime. We demonstrate the first self-referenceable frequency comb from a gigahertz diode-pumped solid state laser.

AT5A.3 • 17:15

Optically Referenced Tm-Fiber-Laser Frequency Comb, Jens Bethge¹, Jie Jiang¹, Christian Mohr¹, Martin Fermann¹, Ingmar Hartl¹; ¹IMRA America, Inc., USA. We report on a fully stabilized optically referenced 100MHz spaced Tm-fiber frequency comb delivering 65fs, 3nJ pulses for mid-infrared conversion.

AT5A.4 • 17:30 **Invited**

Multilayer Dispersive Optics for Ultrafast Lasers, Volodymyr Pervak^{1,2}; ¹Ludwig Maximilian Universität, München, Germany; ²Ultrafast Innovations GmbH, Germany. Since dispersive mirror had been developed, they have been successfully used for the dispersion controlling of femtosecond lasers. The result of the continuous development of dispersive optics allows the pulse to be compressed to a single optical cycle.

AT5A.5 • 18:00

CEP Stabilization of a Cascaded High-energy Yb Amplifier Chain, Tadas Balciunas¹, Giedrius Andriukaitis¹, Audrius Pugzlys¹, Andrius Baltuska¹, Paulius Miseikis², Linas Giniunas³, Romas Danielius², Lucian Hand³, Ronald Holzwarth⁴; ¹Institute of photonics, Vienna University of Technology, Austria; ²Light Conversion Ltd., Lithuania; ³Altos Photonics Inc., USA; ⁴Menlo Systems GmbH, Germany. We implement CEP stabilization of 180-fs 6-mJ pulses from consecutively seeded Yb:KGW and Yb:CaF₂ regenerative amplifiers at a repetition rate of 1 kHz. The system drives a CEP-locked multicolor OPA used for high-order harmonic generation.

AT5A.6 • 18:15

First Experimental Evidence for a Non-instantaneous Lifetime of Nonlinear Optical Chi(3) Effects, Susanta K. Das¹, Martin Bock¹, Rüdiger Grunwald¹, Bastian Borchers¹, Günter Steinmeyer¹, Detlev Ristau^{2,3}, Tobias Vockerodt⁴, Uwe Morgner^{2,3}; ¹Max-Born Institut, Germany; ²Institut für Quantenoptik, Leibniz Universität, Germany; ³Laser Zentrum Hannover, Germany. We present direct experimental evidence for a non-instantaneous nonlinear response in TiO₂. An asymmetry in interferometric FROG measurements indicates a relaxation time constant of about 5 fs.

Aragon III-B-C

Laser Applications to Chemical, Security and Environmental Analysis

16:30–18:30

LT5B • Mid-Infrared Sensing III

J. Barry McManus; *Aerodyne Research Inc., USA, President*

LT5B.1 • 16:30

A Pulsed 2-micron Coherent Differential Absorption Lidar for Atmospheric CO₂ Measurements, Jirong Yu¹, Mulugeta Petros¹, Yingxin Bai², Songsheng Chen¹, Jason Lu³, Upendra N. Singh¹; ¹NASA LaRC, USA; ²SSAI, USA; ³University of Maryland, USA. We report on remote sensing measurements of atmospheric carbon dioxide by a double pulsed 2-micron coherent differential absorption lidar technique.

LT5B.2 • 16:45 **Invited**

Chemical Imaging Using External Cavity Quantum Cascade Lasers, Mark Phillips¹, Jonathan D. Suter¹, Bruce E. Bernacki¹; ¹Pacific Northwest National Laboratory, USA. We describe recent experiments using broadly tunable external cavity quantum cascade lasers to perform hyperspectral chemical imaging of explosives particles and residues in standoff detection and microscopy configurations.

LT5B.3 • 17:15

High Speed In-cylinder Laser Hygrometry for EGR Quantification Using a Wavelength Scanned Vertical Cavity Surface Emitting Laser, Oliver Witzel¹, Alexander Klein¹, Steven Wagner^{1,2}, Christian Meffert³, Christof Schulz³, Volker Ebert^{1,2}; ¹Physikalisch-Technische Bundesanstalt, Germany; ²Center of Smart Interfaces, TU Darmstadt, Germany; ³Institute for Combustion and Gasdynamics, University Duisburg-Essen, Germany. The TDLAS based hygrometer was used for measurements of absolute water vapor concentrations in motored IC engines with time resolutions from 500 μ s up to 100 μ s. Measured concentrations indicate a detection limit of 0.06 vol%.

LT5B.4 • 17:30

Broadband Cavity-enhanced Spectroscopy Using Supercontinuum Radiation, Toni K. Laurila^{1,2}, Ssegawa-Ssekintu Kiwanuka³, Jonathan H. Frank⁴, Clemens F. Kaminski^{3,5}; ¹School of Electrical Engineering, Aalto University, Finland; ²Centre for Metrology and Accreditation, Finland; ³Department of Chemical Engineering, University of Cambridge, United Kingdom; ⁴Combustion Research Facility, Sandia National Laboratories, USA; ⁵School of Advanced Optical Technologies, Friedrich Alexander University Erlangen-Nuremberg, Germany. Spectrometers employing supercontinuum sources and cavity-enhanced absorption spectroscopy will be discussed. Such spectrometers allow simultaneous measurement of multiple trace species both in the gas and liquid phase at high sensitivity and speed.

LT5B.5 • 17:45

High Repetition Rate Hyperspectral Systems for H₂O Vapor Absorption Spectroscopy, Jean Whitney¹, Scott T. Sanders¹, Benjamin Stein¹; ¹ERC, UW Madison, USA. Arbitrary photon generation remains impractical, but in the meantime, use of sources such as those discussed in this paper, either independently or in combination, allows high-performance sensing in gas at almost arbitrary conditions.

LT5B.6 • 18:00

Monitoring Multiple Trace Gas Species during Secondary Organic Aerosol Formation in a Smog Simulation Chamber using Mid-IR Laser and UV Spectroscopic Methods, Boshra Momen Nejad¹, Matthew T. Parsons¹, Ihor Sydoryk¹, Elijah Schnitzler¹, Alan Lim¹, John Tulip¹, Wolfgang Jaeger¹, Karen McDonald²; ¹University of Alberta, Canada; ²Concordia University College of Alberta, Canada. We demonstrate our progress in developing an application of mid-IR External Cavity Quantum Cascade Laser (EC-QCL) for concentration measurements of benzene, toluene, ethylbenzene and o- and p-xylene (BTEX) in a simulation chamber.

LT5B.7 • 18:15

Simultaneous Open-path Detection of Atmospheric N₂O and CO, Lei Tao¹, Kang Sun¹, Mohammad A. Khan¹, David J. Miller¹, Mark A. Zondlo¹; ¹Civil and Environmental Engineering, Princeton University, USA. A novel compact quantum cascade laser (QCL) based open-path gas sensor has been developed for simultaneous detection of atmospheric N₂O and CO. The sensor achieves a sensitivity of 0.26 ppbv of N₂O and 0.24 ppbv of CO with 1 Hz sample rate.

Tuesday, 31 January



Aragon I & Foyer

Laser Applications to Chemical, Security and Environmental Analysis

20:00–21:30 LT6B • LACSEA Poster Session

LT6B.01

Attenuated Total Reflection Mid-IR-spectroscopy for Electrochemical Applications using a QCL, Stefanie Penge¹, Bernd Schönberger¹, Simantini Nayak¹, Andreas Erbe¹; ¹Interface Chemistry and Surface Engineering, Max-Planck-Institut für Eisenforschung, Germany. A setup is presented for ATR-IR spectroscopy based on a pulsed tunable external-cavity QCL. The electronic detection system integrates the detector signal during laser emission. Repeatable measurements of absorption spectra have been achieved.

LT6B.02

Optimizing the Signal-to-Noise Ratio and Dynamic Range of Rhodamine 6G Laser-Induced Fluorescence for Environmental Flow Studies by Improved Spectral Filtering, Claudia Moretto¹, Johannes Kiefer¹; ¹University of Aberdeen, United Kingdom. The sedimentary deposit in rivers influences the water flow. Laser-induced fluorescence employing dye tracers is a suitable tool to study these effects. Herein, we investigate spectral filtering concepts to optimize SNR and dynamic range.

LT6B.03

Hydrogen Sensor Based on Palladium Coated SMS Fiber Structure, Xinwei Lan¹, Jie Huang¹, Tao Wei¹, Qun Han^{1,2}, Zhan Gao¹, Hai Xiao¹; ¹Electrical and Computer Engineering, Missouri University of Science and Technology, USA; ²College of Precision Instrument and Opto-Electronics Engineering, Tianjin University, China. We have developed a new optical fiber hydrogen sensor with palladium thin film coating on SMS fiber structures. The sensor performance is studied in detail.

LT6B.04

Variable Reduction in Partial Least Squares (PLS) through Variation Projection Method, Dahu Qi¹; ¹TSI Inc., USA. A variation projection method is proposed to 1) effectively remove the redundant variables, and 2) improve the measurement accuracy in partial least squares (PLS) prediction.

LT6B.05

Trace NO₂ Detection Using Frequency Modulated Off-Axis Cavity Ring-Down Spectroscopy, Gottipaty N. Rao¹, Andreas Karpf¹; ¹Physics Dept, Adelphi University, USA. Trace detection of NO₂ at ppb-level is demonstrated using a vibration-insensitive variation of cavity ring-down spectroscopy. Modulating the laser frequency and off-axis alignment simplify the detector making it more suitable for in-situ monitoring.

LT6B.06

A Compact, Low Power, Quantum Cascade Laser-based Sensor for CO, David Sonnenfroh¹, Krishnan Parameswaran¹, David Biss¹, John Bradshaw²; ¹Physical Sciences Inc., USA; ²Maxion Technologies, USA. We report on the development of a compact and low power consumption CO sensor for fire detection aboard manned spacecraft. The sensor is a Quantum Cascade laser-based absorption spectrometer.

LT6B.07

Interaction of Multi-Watt CW Laser Beams with a Highly Sooting Atmospheric Pressure Flame, John D. Black¹; ¹School of Electrical and Electronic Engineering, University of Manchester, United Kingdom. Changes induced by collimated laser beams (power 1-30W) passing through a quasi-2-D kerosene diffusion flame are discussed. Soot particle temperature increases by up to 450K, causing changes in flame structure and chemistry.

LT6B.08

Withdrawn

LT6B.09

A Double FFT Procedure to Improve the Sensitivity of a Tunable Diode Laser Open Path Spectrometer for Sensing Local Atmospheric Gas Concentrations on Mars, Youhua Chen¹, Samira Mahdi², Gary Anderson³; ¹Graduate Institute of Technology, University of Arkansas at Little Rock, USA; ²Applied Science, University of Arkansas at Little Rock, USA; ³System Engineering, University of Arkansas at Little Rock, USA. A double FFT procedure is developed to improve the sensitivity of a spectrometer to measure atmospheric gases. Simulations show the DFFT reduces the effects of 1/f noise and increase the sensitivity of the measurement.

LT6B.10

Development of an Open-source Space or Airborne Multi-wavelength LIDAR Modeling Framework and Accompanying Programs with Application to the ASCENDS Mission, Denis Pluotau¹, Narasimha S. Prasad¹; ¹NASA Langley Research Center, USA. Lidar modeling framework to quantitatively evaluate the performance and error contributions in projected space or airborne hard-target lidar measurements is described. Application to the ASCENDS mission CO₂ and O₂ sensing is presented.

LT6B.11

Optimized Wavelength Selection for Molecular Absorption Thermometry, Xinliang An¹, Scott T. Sanders¹; ¹Mechanical Engineering, University of Wisconsin-Madison, USA. A wavelength selection technique is applied to optimize temperature precision of absorption thermometry. The line-of-sight thermometry is analyzed by using an optimization algorithm. This method is also promising for use in 2D absorption tomography.

LT6B.12

Multidimensional Monte Carlo Model for Amplified Spontaneous Emission, Yan Zhao¹, Lin Ma²; ¹Air Products & Chemicals, Inc, USA; ²Virginia Tech, USA. A new model based on the Monte Carlo method has been developed to analyze amplified spontaneous emission in multidimensional. This paper introduces the model, its validation, and implication for diagnostics with high laser irradiance.

LT6B.13

High-precision Trace Gas Measurements Using Quantum Cascade Lasers and Novel Star-like Cell Designs, Lukas Emmenegger¹, Albert Manninen¹, Bela Tuzson¹, Herbert Looser², Yargo Bonetti³; ¹Laboratory for Air Pollution & Environmental Technology, Empa, Switzerland; ²Institute for Aerosol and Sensor Technology, FHNW, Switzerland; ³Institute for Quantum Electronics, ETHZ, Switzerland. We report on the design and characterization of novel star-like multipass cells for high-precision trace gas analysis. Their optical path depends solely on the incident angle and they can be machined as a single piece.

Tuesday, 31 January

NOTES

Blank area for notes with horizontal lines.





Fiber Laser Applications (FILAS) would like to thank the following Corporate Contributor for their outstanding support:



Student Award Sponsor:



Next generation fiber lasers
that you can control™





07:00–18:30 Registration, Aragon Foyer

San Bernardo Ballroom

Joint Advanced Solid-State Photonics / Advances in Optical Materials (AIOM) / Fiber Lasers and Applications (FILAS) / Laser Applications to Chemical, Security and Environmental Analysis (LACSEA)

08:00–09:30

JW1A • Joint Plenary Session I

Alphan Sennaroglu, *Koç Univ., Turkey and Richard Moncorge, Université de Caen, France, Presiders*

JW1A.1 • 08:00

Frontiers of Disk Lasers, Jochen Speiser¹; ¹*Institute of Technical Physics, DLR, Germany*. - Fifteen years after first commercialization, the Thin Disk Laser covers a broad spectrum of applications. Nevertheless, a lot of challenges remain, e.g. further scaling of power and pulse energy or the search for different suitable laser materials.

JW1A.2 • 08:45

Wavelength and Coherent Beam Combining for High Brightness Sources, Tso Yee Fan¹; ¹*MIT Lincoln Laboratory, USA*. Beam combining of laser arrays with high efficiency and good beam quality for power and radiance scaling is a long-standing problem in laser technology. Recently, significant progress has been made using wavelength techniques and coherent techniques.

10:00–11:30

JW2A • Joint Plenary Session II

Sukesh Roy, *Spectral Energies, LLC, USA and Jose Salcedo, Multiwave Photonics, Portugal, Presiders*

JW2A.1 • 10:00

Pumping up the Pressure: Gas-Based Nonlinear Optics in Hollow Core Photonic Crystal Fibre, Philip Russell; *Max Planck Institute for the Science of Light, Germany*. Single-mode hollow core PCF provides an ideal environment for studying pressure-controlled nonlinear interactions between laser light and gases. An recent success is the efficient generation of tunable deep-UV pulses from ~50fs, ~1μJ pulses at 800nm.

JW2A.2 • 10:45

Development and Application of Ultrafast Laser Spectroscopy for Combustion Sensing, James R. Gord¹; ¹*Propulsion Directorate, Air Force Research Laboratory, USA*. Optical measurement techniques are powerful tools for detailed study of combustion chemistry and physics. Ultrafast (picosecond- and femtosecond-pulsed) lasers are driving the enhancement of existing diagnostic techniques and enabling the development of new measurement approaches.

09:30–10:00 Exhibits & Coffee Break

11:30–13:00 Lunch ASSP (on your own)

11:30–13:30 Lunch LACSEA, FILAS, AIOM (on your own)

Aragon II

Advanced Solid-State Photonics

13:00–15:00

AW3A • Beam Combining Summit

Gregory Goodno; *Northrop Grumman Aerospace Systems, Presider*

AW3A.1 • 13:00 **Invited**

Spectral Beam Combining of Fiber Lasers for Power Scaling, Eric Honea¹, Matthias Savage-Leuchs¹, Khushvinder Brar¹, Eric Eisenberg¹, Christian Dille¹, Donald Jander¹, Jeffrey Cao¹, Robert Afzal¹, Richard Humphreys¹; ¹*Lockheed Martin Aculight, USA*. We describe our work on Spectral Beam Combining geometries and design implementations using multilayer dielectric gratings. With appropriate designs, power scaling beyond the single fiber limit can be achieved while maintaining near diffraction limited beam quality.

AW3A.2 • 13:30 **Invited**

kW-class Direct Diode Lasers with Comparable Brightness to Fiber, Disk, and Carbon Dioxide Lasers, Robin Huang¹; ¹*TeraDiode Inc, USA*. TeraDiode has built kW-class direct diode lasers with the same output power and beam quality as existing industrial lasers. Our kW-class direct diode laser has cut gauge-thickness metal with comparable quality as existing industrial lasers.

Aragon III-C

Laser Applications to Chemical, Security and Environmental Analysis

13:30–15:30

LW3B • CARS Spectroscopy for Sensing in Reacting Flows

James Gord; *Air Force Research Laboratory, USA, Presider*

LW3B.1 • 13:30

Gas Phase Temperature Measurements in a Flame Spray Pyrolysis Process by O₂ Pure Rotational CARS, Thomas Seeger^{1,2}, Alfred Leipertz^{2,3}, Wolfgang Peukert^{2,4}; ¹*Institute of Engineering Thermodynamics, University of Siegen, Germany*; ²*Erlangen Graduate School in Advanced Optical Technologies, University of Erlangen, Germany*; ³*Institute of Engineering Thermodynamics, University of Erlangen, Germany*; ⁴*Institute of Particle Technology, University of Erlangen, Germany*. An O₂ rotational CARS setup was applied for gas phase thermometry in a flame spray pyrolysis processes. The temperature results indicate the dissipation of energy by radiation in the presence of particles.

Aragon III-B

Fiber Lasers and Applications

13:30–15:30

FW3C • Defense and Space Applications of Fiber Lasers

Jose Salcedo; *Multiwave Photonics, Portugal, Presider*

FW3C.1 • 13:30 **Invited**

High Power Fiber Lasers for Defense Applications, Mike O'Connor¹; ¹*IPG Photonics Corp, USA*. Fiber lasers are ideal for many defense applications, ranging from tactical and long-range directed energy applications to LIDAR to free-space communications. In this talk, we focus on the directed energy applications of fiber lasers, and the types of fiber lasers under development for use in these applications. Broadband single-mode and multimode lasers, as well as narrow-line, high power amplifiers for beam combining are discussed.

Aragon III-A

Advances in Optical Materials

13:30–15:30

IW3D • Laser Materials 1

Mathias Siebold; *Helmholtz-Centre Dresden-Rossendorf, Germany and Richard Moncorge; CIMAP, Université de Caen, France, Presiders*

IW3D.1 • 13:30 **Invited**

Growth and Efficient Tunable Laser Operation of Tm:Sc₂SiO₅ Crystal, Jun Xu¹, Lihe Zheng¹, Kejian Yang^{2,3}, Thomas Dekorsy³, Qingguo Wang¹, Xiaodong Xu¹, Liangbi Su¹; ¹*Shanghai Institute of Ceramics, China*; ²*Shandong University, China*; ³*University of Konstanz, Germany*. The growth and tunable laser operation of Tm:Sc₂SiO₅ crystal were demonstrated. With continuous wave Ti:Sapphire laser as pump source, maximum slope efficiency of 33.7% and wavelength tunable spectral range over 130 nm were achieved.

Wednesday, 1 February





Aragon II

Advanced Solid-State Photonics

AW3A • Beam Combining Summit—Continued

AW3A.3 • 14:00 **Invited**

Coherent Beam Combination of High Repetition Rate, Energetic Lasers using Stimulated Brillouin Scattering Phase Conjugate Mirrors, Hong J. Kong¹, Sangwoo Park¹, Seongwoo Cha¹, Milan Kalal²; ¹physics, KAIST, Korea, Republic of Korea; ²Nuclear engineering, Czech Technical University, Czech Republic. A coherent beam combination system using stimulated Brillouin scattering phase conjugation mirrors is demonstrated. The phase fluctuation between the SBS waves are stabilized within $\lambda/26$. From the result, a laser fusion energy driver is proposed.

AW3A.4 • 14:30 **Invited**

Coherent Combination of Fiber Amplified Femtosecond Pulses, Jens Limpert¹; ¹FSU Jena, Germany. We review basic considerations, current status, challenges and potential performance of coherently combined spatially separated ultrafast amplifiers.

Aragon III-C

Laser Applications to Chemical, Security and Environmental Analysis

LW3B • CARS Spectroscopy for Sensing in Reacting Flows—Continued

LW3B.2 • 13:45 **Invited**

Latest Developments on Hybrid fs/ps CARS for Combustion Sensing, Joseph Miller¹, Terrence R. Meyer¹, Hans U. Stauffer², Sukesh Roy², James R. Gord³; ¹Department of Mechanical Engineering, Iowa State University, USA; ²Spectral Energies, LLC, USA; ³Propulsion Directorate, Air Force Research Laboratory, USA. Recent developments in vibrational and rotational hybrid fs/ps coherent anti-Stokes Raman scattering for temperature and species concentration measurements are presented. Advances include nonresonant suppression using temporally tailored pulses, collision-free detection, and kHz-rate measurements.

LW3B.3 • 14:15

Advances in Fiber-Coupled Laser Diagnostics for Practical Combustion Measurements, Paul S. Hsu¹, Waruna D. Kulatilaka¹, Anil K. Patnaik², Sukesh Roy¹, James R. Gord³; ¹Spectral Energies, LLC, USA; ²Propulsion Directorate, AFRL, USA; ³Innovative Scientific Solutions, Inc., USA. Fiber-coupled ps-CARS and fiber-coupled ns-UV-PLIF detection systems are being developed for practical combustion applications. Single-shot thermometry using fiber-coupled ps-CARS and single-shot OH-PLIF imaging at 10 kHz are demonstrated in flames.

LW3B.4 • 14:30 **Invited**

Development and Application of Rotational CARS Spectroscopy for Reacting Flows, Alexis Bohlin¹, Emil Nordström¹, Per-Erik Bengtsson¹; ¹Lund Institute of Technology, Sweden. Rotational CARS is a useful diagnostic tool for reactive flows. The talk focuses on recent developments regarding temperature accuracy related to Herman-Wallis factors and Raman linewidths, major species concentration measurements, and applications to turbulent combustion.

Aragon III-B

Fiber Lasers and Applications

FW3C • Defense and Space Applications of Fiber Lasers—Continued

FW3C.2 • 14:00 **Invited**

Short Pulse Fiber Laser Research at NRL, Tariq Manzur¹; ¹NAVSEA Naval Undersea Warfare Ctr, USA. No available

FW3C.3 • 14:30

Raman Amplification of a Narrow Linewidth Continuous Wave Signal for Spectroscopic Remote Sensing Applications Using Longitudinally Varying Core Fibers, James A. Nagel¹, Valery Temyanko¹, Robert Norwood¹, Nasser Peyghambarian¹, Jeremy Dobler², Evgeny Dianov², Aleksander Biriukov³, Aleksander Sysoliatin³; ¹College of Optical Sciences, Univ of AZ, USA; ²ITT Geospatial System, USA; ³Fiber Optic Research Center, Russian Academy of Sciences, Russian Federation. We report on the development of a Raman amplifier using fibers with longitudinally varying cores. Approximately 3.0W of a 1.26 μ m narrow linewidth continuous wave signal has been demonstrated for remote sensing of atmospheric oxygen levels.

FW3C.4 • 14:45

Generation of 50W of 1178 nm via Amplification of the Second Stokes, Leanne J. Henry¹, Jacob Grosek¹, Gerry Moore¹, Thomas M. Shay¹; ¹AFRL/RDLAF, Air Force Research Laboratory, USA. A novel 50 W narrow linewidth 1178 nm Raman laser involving amplification of the second Stokes in a 1121 nm resonance cavity is reported. 1121 nm cavity power along with Stimulated Brillouin Scattering are important design considerations.

Aragon III-A

Advances in Optical Materials

IW3D • Laser Materials 1—Continued

IW3D.2 • 14:00

Diode Pumped Laser Oscillation at 750 nm and Excited State Absorption Measurements of Ho³⁺:LiLuF₄, Fabian Reichert¹, Francesca Moglia¹, Matthias Fechner¹, Philipp Koopmann¹, Günter Huber¹; ¹Institute of Laser Physics, University of Hamburg, Germany. We present the first demonstration of laser oscillation of Ho³⁺:LiLuF₄ in the visible spectral range. Furthermore, we investigated the spectroscopic properties with regard to its potential as an active medium for diode pumped solid state lasers.

IW3D.3 • 14:15

Spectra and Laser Cross Sections of Ceramic Er³⁺:AlN, Larry D. Merkle¹, Tigran Sanamyan¹, Lindsay K. Hussey^{1,2}, Mark Dubinskii¹; ¹US Army Research Laboratory, USA; ²Materials Science and Engineering, North Carolina State University, USA. We report what we believe are the first optical spectroscopy and lifetime data on Er³⁺:AlN ceramic. One type of Er³⁺ center dominates its spectra, for which stimulated emission and absorption cross sections are inferred.

IW3D.4 • 14:30

Growth and Optical Studies of Ytterbium Doped (Gd_{1-x}Y_x)₂SiO₅ Crystals, Lihe Zheng¹, Radoslaw Lisiecki², Qingguo Wang¹, Xiaodong Xu¹, Liangbi Su¹, Witold Ryba-Romanowski², Jun Xu¹; ¹Shanghai Institute of Ceramics, Chinese Academy of Sciences, China; ²Institute of Low Temperature and Structure Research, Polish Academy of Sciences (ILTSR), Poland. The strongest absorption in Yb:(Gd_{1-x}Y_x)₂SiO₅ crystals obtained by Czochralski method blue-shifted from 978nm in YSO phase to 920nm in GSO phase. Crystals with YSO phase displayed broader emission bandwidth than that with GSO phase.

IW3D.5 • 14:45

Structurally Disordered Er³⁺-Doped NaY(WO₄)₂ as a Gain Medium for Resonantly-Pumped Eye-Safe Laser at ~1.6 μ m, Viktor Fromzel¹, Nikolay Ter-Gabrielyan¹, Maria D. Serano², David E. Lahera³, Concepcion Cascales³, Carlos Zaldo², Mark Dubinskii¹; ¹US Army Res. Lab, USA; ²Instituto de Ciencia de Materiales de Madrid, CSIC, Spain. We report crystal growth, spectroscopy and eye-safe laser operation of disordered Er:NaY(WO₄)₂ crystal. We show that crystalline disorder facilitates efficient direct resonant pumping around 1500 nm by the wideband InP laser diode sources.

Wednesday, 1 February





Aragon II

Advanced Solid-State Photonics

15:00–16:30
AW4A • ASSP Poster Session 1,
See below

Aragon III-C

Laser Applications to Chemical,
Security and
Environmental Analysis

LW3B • CARS Spectroscopy for
Sensing in Reacting Flows—
Continued

LW3B.5 • 15:00
High Spatial Resolution 1D Pure Rotational
CARS Imaging Over a Large Field, Christo-
pher Kliewer¹; ¹Combustion Research Facility,
Sandia National Laboratories, USA. A counter-
propagating beam geometry is employed for
high spatial resolution 1D picosecond rotational
CARS measurements, allowing for a factor of 10
higher spatial resolution and 102 signal increase
over a standard small-angle BOX-CARS geometry.

LW3B.6 • 15:15
Nonresonant Background Suppression in
Femtosecond Coherent Anti-Stokes Raman
Scattering for Flame Thermometry at 5000 Hz,
Daniel Richardson¹, Devashish Bangar¹, Robert
Lucht¹; ¹School of Mechanical Engineering, Purdue
University, USA. Polarization suppression of the
nonresonant background in femtosecond CARS
measurements is demonstrated. Single-laser-shot
spectra recorded at 5000 Hz are fit to determine
temperature in unsteady flames over the tempera-
ture range 500–1800 K.

Aragon III-B

Fiber Lasers and Applications

FW3C • Defense and Space
Applications of Fiber Lasers—
Continued

FW3C.5 • 15:00 **Invited**
Fiber Lasers for Underwater, Airborne and
Space Lidar Applications, Shantanu Gupta¹; ¹Fi-
bertek, USA. Fiber laser/amplifiers merged with
state-of-the-art electronics, modulation schemes
and algorithms, allow control of the optical wave
in time, frequency, polarization, coherence,
and spatial domain. Such laser sensors enable
advanced remote-sensing capability for military,
aerospace and space application.

Aragon III-A

Advances in Optical Materials

IW3D • Laser Materials 1—
Continued

IW3D.6 • 15:00
Temperature Dependences of Stimulated Emis-
sion Cross Section in Nd:YAG, Nd:YVO₄, and
Nd:GdVO₄, Yoichi Sato¹, Takunori Taira¹; ¹Laser
Research Center for Molecular Science, Institute
for Molecular Science, Japan. We propose the
experimentally proved numerical model for
temperature dependence of stimulated emission
cross section, where Nd:YAG, Nd:YVO₄, and
Nd:GdVO₄ show -0.20%/degC, -0.50%/degC,
and -0.48%/degC at 1.06 μm under room tem-
perature, respectively.

IW3D.7 • 15:15
Growth of Large 90 mm Diameter Yb:YAG
Single Crystals with Bagdasarov Method,
Mikayel Arzakantsyan^{1,2}, Narine Ananyan¹,
Vladimir Gevorgyan², Jean-Christophe Chan-
teloup¹; ¹LULI, Ecole Polytechnique, CNRS, CEA,
UPMC, France; ²Russian-Armenian (Slavonic)
University, Armenia; ³«Laserayin Tekhnika» CSC,
Armenia. For the first time high optical quality
Yb:YAG single crystals with diameter more than
90mm have been grown by Bagdasarov method
also known as Horizontal Direct Crystallization.

15:30–16:00 Exhibits & Coffee Break

Aragon I and Foyer

Advanced Solid-State Photonics

15:00–16:30
AW4A • ASSP Poster Session 3

AW4A.01

Efficient Ultra-broadband XUV Output Coupler, Oleg Pronin¹, Volodymyr Pervak², Ernst E. Fill¹,
Jens Rauschenberger^{1,2}, Ferenc Krausz^{1,2}, Alexander Apolonskiy^{1,2}; ¹Max Planck Institute of Quantum
Optics, Germany; ²Ludwig-Maximilians-Universität München, Germany. We demonstrate an XUV
output coupler (OC) for enhancement cavities. This OC allows for XUV reflectivity of more than 40%
and ultra-low losses <0.05% for the fundamental radiation.

AW4A.02

Tunable mW Narrow Bandwidth Mid-Infrared Light Source, Erik Krenzen¹, Louis M. Kehlet¹, Peter
Tidemand-Lichtenberg¹, Jeppe S. Dam¹, Ole Jensen¹, Christian Pedersen¹; ¹DTU-Fotonik, Technical
University of Denmark, Denmark. A Tunable Mid-IR light source based on Difference Frequency Generation
is experimentally investigated. The system tunes 500 nm, ranging from 2.9 μm to 3.4 μm with mW's
of output power over the entire range.

AW4A.03

Kilohertz Rate Picosecond Pulses Amplifier for Pumping of OPCPA System, Andrejus Michailovas^{1,2};
¹Ekspla, Lithuania; ²Institute of Physics, CPST, Lithuania. We demonstrate simple and efficient amplifier
operating at 1000Hz repetition frequency producing 48ps pulses of 40mJ output energy. Smooth beam
profile and good stability makes this amplifier ideal pump of OPCPA systems.

AW4A.04

High-energy, In-band pumped Ho:LLF MOPA system, Martin Schellhorn¹; ¹ISL, French German
Research Institute, France. A Tm fiber laser pumped Ho:LuLiF₄ (Ho:LLF) MOPA system is demonstrated
delivering 82 mJ at 2053 nm in TEM₀₀ operation at a repetition rate of 100 Hz with an optical-to-
optical efficiency of 9.9 %.

AW4A.05

Er-doped High Aspect Ratio Core (HARC) Rectangular Fiber Producing 5-mJ, 13-nsec Pulses at 1572
nm, Victor Khitrov¹, Vladimir Shkunov¹, David Rockwell¹, Friedrich Strohkendl¹, Yuri Zakharenkov¹;
¹Raytheon, USA. We demonstrated 5-mJ, 13-nsec pulses using a diode-pumped high-aspect ratio core
(HARC) fiber with an active area of 30 x 580 μm², in good agreement with our model, which predicts
scalability to several 10s of mJ.

AW4A.06

Yb_{0.015}:Lu_{0.162}Gd_{0.823}VO₄ CW Laser Performance, Junhai Liu¹, Weijin Kong¹, Wenjuan Han¹,
Huajin Zhang^{1,2}, Xavier Mateos^{1,3}, Valentin Petrov^{1,4}; ¹College of Physics, Qingdao University, China;
²Shandong University, China; ³Universitat Rovira i Virgili, Spain; ⁴Max-Born-Institute for Nonlinear Optics
and Ultrafast Spectroscopy, Germany. Appreciable discontinuous output power increase is observed in a
Yb_{0.015}:Lu_{0.162}Gd_{0.823}VO₄ mixed vanadate laser during polarization switching. A maximum output
power of 4.3 W is achieved with an average slope efficiency of 73%–77%.

AW4A.07

Withdrawn

AW4A.08

Parasitic Processes in Optical Parametric Amplifiers, Jan Rothhardt^{1,2}, Steffen Hädrich^{1,2}, Jake Brom-
age³, Christoph Dorrer³, Stefan Demmler¹, Jens Limpert^{1,2}, John D. Zuegel³, Andreas Tünnermann^{1,2};
¹Institute of Applied Physics, Germany; ²Helmholtz-Institut Jena, Germany; ³Laboratory for Laser Energetics,
University of Rochester, USA. We study parasitic processes in parametric amplifiers. Experimental and
numerical results show strong second harmonic generation of the signal, resulting in power loss and
spectral modulations, which can be reduced by an adequate configuration.

AW4A.09

Withdrawn

AW4A.10

Two Beam Spatial and Temporal Coherent Phasing with a Sub Picosecond Laser, Jonathan Phillips¹,
Cristina Hernandez-Gomez¹, Ian Musgrave¹, Waseem Shaikh¹, Collier John¹; ¹Central Laser Facility,
Science and Technical Facilities Council, United Kingdom. We have developed a test bed for spatial and
temporal phasing of two beams with the use of a sub ps pulse. With this test bed we have successfully
beam combined two 50 mW apertures.



Aragon I and Foyer

Advanced Solid-State Photonics

AW4A • ASSP Poster Session 3—Continued

AW4A.11

Passive Q-switching of the Diode Pumped Tm³⁺:KLu(WO₄)₂ Laser Near 2- μ m with Cr²⁺:ZnS Saturable Absorbers, Xavier Mateos¹, Martha Segura¹, Martin Kadankov^{2,3}, Maria Cinta Pujol¹, Joan Josep Carvajal¹, Magdalena Aguilo¹, Francesc Diaz¹, Uwe Griebner³, Valentin Petrov³, ¹Universitat Rovira i Virgili, Spain; ²Sofia University, Bulgaria; ³Max-Born Institut, Germany. Pulse energies as high as 145 μ J, peak powers of 6 kW and pulse durations in the 25-30 ns range were generated with a passively Q-switched diode-pumped Tm³⁺:KLu(WO₄)₂ laser using polycrystalline Cr²⁺:ZnS as saturable absorber.

AW4A.12

Influence of Cavity Dispersion on Repetition Rate of Passive Harmonic Mode-locking Soliton Fiber Laser, Chang Su Jun¹, Sun Young Choi¹, Fabian Rotermund¹, Byoung Yoon Kim², Dong-Il Yeom¹, ¹Division of Energy Systems Research, Ajou University, Republic of Korea; ²Department of Physics, KAIST, Republic of Korea. The effect of cavity dispersion on the performance of passive harmonic mode-locking of fiber laser is studied. We found that anomalous cavity dispersion near zero could efficiently increase the repetition rate up to several GHz

AW4A.13

Features of Amplification and Stored Energy in Cryogenic Yb:YAG Disk Laser with Sub-Joule Energy Level, Ivan B. Mukhin¹, Oleg Palashov¹, Olga Vadimova¹, Evgeny Perevezentsev¹, Efim Khazanov¹, ¹department of nonlinear and laser optics, Institute of Applied Physics Russian Academy of Science, Russian Federation. Methods of reduction of amplified spontaneous emission were investigated in cryogenically cooled Yb:YAG disks. The disk with undoped cap is more suitable as active element for cryogenic laser with sub-joule energy at high repetition rate.

AW4A.14

A Cryogenic Gas Cooled Multi-slab Yb:YAG Amplifier Producing 5.9 J at 1 Hz, Paul D. Mason¹, Klaus Ertel¹, Saumyabrata Banerjee¹, Jonathan Phillips¹, Cristina Hernandez-Gomez¹, Collier John¹, ¹Central Laser Facility, STFC, United Kingdom. We present preliminary amplification results for the DiPOLE cryogenic gas cooled multi-slab ceramic Yb:YAG amplifier over a range of temperatures from 88 to 175K using a temporary bow-tie multi-pass extraction architecture.

AW4A.15

10-W, 156-MHz All-fiber-integrated Er-Yb-doped Fiber Laser-amplifier System, Ihor Pavlov¹, Emrah Ilbey¹, Ebru Dulgergil¹, F. Oemer Ilday¹, ¹Department of Physics, Bilkent University, Turkey; ²Meteksan Savunma Inc., Turkey. We demonstrate all-fiber, high-power chirped-pulse-amplifier system, operating at 1550 nm. 156-MHz soliton oscillator seeds a two-stage single-mode amplifier with output power of 10 W. After external compression, pulse duration is 0.6 ps.

AW4A.16

Beyond the Current 10J Energy Level for the Lucia Laser System with a Cryogenically Cooled Second Amplifier Head, Daniel Albach¹, Thierry Novo¹, Bernard Vincent¹, Jean-Christophe Chanteloup¹, ¹LULI, France. Amplified Spontaneous Emission and thermal management solutions to reach Lucia 10J/2Hz performances are presented. Development for the second amplifier head with an innovative thermal management solution and laser system improvements are detailed.

AW4A.17

Enhancement of the Second-Harmonic Phase-Matching Bandwidth and Conversion Efficiency by Control of the Temperature Distribution along a Nonlinear Crystal, Julijanas Zeludevicius¹, Kestutis Regelskis¹, Vytautas Vosylius¹, Nikolajus Gavrilinas¹, Gediminas Raciukaitis¹, ¹Laser Technology, Center for Physical Sciences and Technology, Lithuania. We propose a method for the non-critical second harmonic generation of a broadband light based on the temperature gradient along a nonlinear crystal. Using this approach we demonstrate boost of conversion efficiency from 21% to 55%.

AW4A.18

Narrow Linewidth 1120 nm Semiconductor Disk Laser Based on Strain Compensated GaInAs Quantum Wells, Tomi Leinonen¹, Sanna Ranta¹, Miki Tavast¹, Mircea Guina¹, Ryan J. Epstein², ¹Tampere University of Technology, Finland; ²Optical Systems Research, Areté Associates, USA. We demonstrate a semiconductor disk laser emitting ~0.8 W close to 1120 nm with a short-term linewidth <300 kHz without active stabilization. The disk laser gain mirror used strain compensated GaInAs quantum wells.

AW4A.19

High Brightness Yb:YAG Planar Waveguide Laser with an Unstable Resonator Formed with a Novel Laser-machined, Toroidal Mode-selective Mirror, Ian J. Thomson¹, Krystian L. Włodarczyk¹, Denis R. Hall¹, Howard J. Baker¹, ¹School of Engineering and Physical Science, United Kingdom. A novel toroidal micro-stripe mirror, produced by laser machining, provides transverse mode selection in a hybrid waveguide-unstable resonator. The Yb:YAG-sapphire composite planar waveguide laser produces 326 W at high beam quality.

AW4A.20

Volume Bragg Grating Wavelength Selected Tm:YLF Slab Laser Operating at 1890 nm, Hencharl J. Strauss¹, M J Daniel Esser¹, Gary King¹, Loyiso Maweza¹, ¹National Laser Centre, CSIR, South Africa. An 80 W Tm:YLF Volume Bragg Grating laser selected to operate at 1890 nm is demonstrated. It consisted of a single Tm:YLF slab pumped with a 300 W diode stack using a pump reproducing configuration.

AW4A.21

Combining of Pulses in Time Domain by Second Harmonic Generation, Kestutis Regelskis¹, Julijanas Zeludevicius¹, Nikolajus Gavrilinas¹, Gediminas Raciukaitis¹, ¹Department of Laser Technology, Center for Physical Sciences & Technology (CPST), Lithuania. A novel method that allows combining of two pulses in sequence into a single second harmonic pulse was proposed and experimentally tested.

AW4A.22

Broadband Mid-Infrared Frequency Upconversion with an Aperiodically-Poled LiNbO₃ Waveguide, Lora Nugent-Glandorf¹, Tyler W. Neely¹, Florian Adler¹, Scott Diddams¹, ¹NIST, USA. A Mid-IR frequency comb is upconverted to visible wavelengths by mixing with a 1064 nm cw laser in an aperiodically poled LiNbO₃ waveguide. Upconversion efficiency and stability measurements are reported.

AW4A.23

Investigation of Contrast for Astra-Gemini laser, Yunxin Tang¹, Chris J. Hooker¹, Bryn Parry¹, Oleg V. Chekhlov¹, Steve Hawkes¹, Klaus Ertel¹, Rajeev Pattathil¹, Collier John¹, ¹Central Laser Facility, Rutherford Appleton Lab., United Kingdom. We report the recent progress in contrast campaign for Astra-Gemini, showing that the stretcher grating as the main source of the coherent contrast. Improvement was achieved by new gratings, and further enhanced by using double plasma mirrors.

AW4A.24

Kerr-Lens Mode-Locked Yb:YAG Laser Pumped with a Single-Emitter Laser-Diode Chip, Sadao Uemura¹, ¹National Institute of Advanced Industrial Science and Technology, Japan. We have succeeded in Kerr-lens modelocking of a Yb:YAG laser pumped with a single-emitter laser-diode chip, which enables us to obtain an inexpensive femtosecond-pulse laser source.

AW4A.25

0.7 mJ, 0.5 kHz Mid-IR Tunable PPSLT Based OPO Pumped at 1064 nm, Danaïl Chuchumishev¹, Alexander Gaydardzhiev¹, Torsten Fiebig¹, Ivan Buchvarov¹, ¹Physics Department, Sofia University, Bulgaria; ²Argonne-Northwestern Solar Energy Research (ANSER) Center, Northwestern University, USA. We report up to 0.72 mJ at 0.5 kHz, temperature tunable (3-3.5 μ m) radiation from a sub-nanosecond PPSLT based singly resonant OPO, pumped by an amplified microchip laser at 1064 nm.

AW4A.26

Highly efficient Yb:YAG Master Oscillator Power Amplifier Laser Transmitter for Future Space Flight Missions, Anthony W. Yu¹, Alexander Betin², Michael A. Krainak¹, Derek Hendry², Billie Hendry², Carlos Sotelo², ¹Laser & Electro-Optics Branch, NASA Goddard Space Flight Center, USA; ²Raytheon Space & Airborne Systems, USA. In this paper we will discuss our development effort of a highly efficient master oscillator power amplifier (MOPA) laser transmitter for future space flight missions.

AW4A.27

Injection-seeded, Narrow-line Gain-switched Cr:ZnSe laser, Huseyin Cankaya¹, M. Natali Cizmeciyan¹, Ersen Beyatli¹, A. Tolga Gorgulu¹, Adnan Kurt², Alphan Sennaroglu¹, ¹Department of Physics and Electrical-Electronics Engineering, Koc University, Turkey; ²Teknofil, Inc, Turkey. Injection seeding with a continuous-wave Cr:ZnSe seed laser reduced the output spectral width of a second gain-switched Cr:ZnSe laser from 125 nm to 0.65 nm and enabled its tuning from 2255 nm to 2455 nm.

AW4A.28

Waveguide Parametric Amplifier in Quasi-phase-matched Mg:LiNbO₃, Sunao Kurimura^{1,2}, Kaori Sugiura^{1,2}, Yusuke Muranaka^{1,2}, Kiyofumi Kikuchi^{1,2}, Hirochika Nakajima², Junichiro Ichikawa³, ¹Nat'l Inst. for Mat. Sci, Japan; ²Applied Physics, Waseda University, Japan; ³Sumitomo Osaka Cement Co., LTD, Japan. CW parametric amplification is reported with adhered-ridge waveguide (ARW) of Mg-doped lithium niobate. Parametric gain of 13.6 dB is obtained at eye-safe 1.5 μ m wavelength at a pump power as low as 330 mW.

AW4A.29

Subwavelength Scale Indium Tin Oxide Clad Optical Disk Resonators, Ozlem Senlik¹, ¹Electrical and Computer Engineering, Duke University, USA. We optimize the geometry of nano-scale disk optical cavities incorporating planar indium tin oxide (ITO) electrodes. Optimized cavities of sub-wavelength size in all dimensions exhibit enhanced modal properties such as Q-factors exceeding 10⁴.

AW4A.30

Single-end Pumping, Single-frequency Nd:YVO₄ /LBO Laser with the Output Power of 21.5W, Wang Yajun¹, Zheng Yaohui¹, Kunchi Peng¹, ¹Institute of Opto-Electronics, China. With the methods of direct pumping and self-compensation of astigmatism, a single-frequency green laser (M²<1.1) of 21.5W is obtained with an optical-optical conversion efficiency of 31.9%.

Wednesday, 1 February





Aragon II

Advanced Solid-State Photonics

16:30–18:00

AW5A • Mid-Infrared Sources

Alphan Sennaroglu; *Koç Univ., Turkey, Presider*

AW5A.1 • 16:30

High-efficiency Tm³⁺:LiLuF₄ Thin-disk Laser, Georg Stoeppler¹, Daniela Parisi², Mauro Tonelli², Marc Eichhorn¹; ¹*French-German Research Institute of Saint Louis ISL, France*; ²*NEST-Istituto Nanoscienze-CNR and Dipartimento di Fisica, Università di Pisa, Italy*. We report the first diode-pumped Tm³⁺:LiLuF₄ laser operation in thin-disk design. A maximum output power of 21 W at 1.9 μm and a maximum slope efficiency of 49 % were achieved with continuous pumping.

AW5A.2 • 16:45

High-Efficiency Thin-Disk Tm-Laser Based on 5 at. % Tm:KLu(WO₄)₂/KLu(WO₄)₂ Epitaxy, Valentin Petrov¹, Uwe Griebner¹, Sergei Vatinik², Ivan Vedin², Martha Segura³, Xavier Mateos³, Maria Cinta Pujol¹, Joan J. Carvajal¹, Magdalena Aguilo¹, Francesc Diaz²; ¹*Max-Born Inst., Germany*; ²*Institute of Laser Physics, Russian Federation*; ³*Universitat Rovira i Virgili, Spain*. A diode-pumped thin-disk epitaxial laser with 5 at. % Tm:KLu(WO₄)₂/KLu(WO₄)₂ emits in the 1850–1920-nm spectral range with slope efficiency of 47% and maximum output power of ~6 W in continuous-wave operation.

AW5A.3 • 17:00

Phase-stabilized Few-cycle Optical Parametric Amplification at 2.1 μm with 10 μJ at 100 kHz, Julien Nillon¹, Sébastien Montant¹, Guillaume Machinet¹, Eric Cormier¹; ¹*CELIA, France*. We report on a new scheme for ultra-broadband optical parametric amplification at 2.1 μm delivering CEP-stabilized pulses of duration down to 16 fs (2.2 cycles) and energy up to 10 μJ at 100 kHz.

Aragon III-C

Laser Applications to Chemical, Security and Environmental Analysis

16:00–18:00

LW5B • New Spectroscopic Approaches

Joseph Miller; *Iowa State Univ., USA, Presider*

LW5B.1 • 16:00

Faraday Rotation Spectroscopy of O₂ Using Permanent Rare-Earth Magnets, Brian Brumfield¹, Stephen So², Gerard Wyoski¹; ¹*Electrical Engineering, Princeton University, USA*; ²*Sentinel Photonics, Inc., USA*. Sensitive Faraday rotation spectroscopy of oxygen at atmospheric pressure is performed using permanent rare-earth magnets providing a uniform axial magnetic field. Laser wavelength modulation and balanced detection are used to detect the FRS signals.

LW5B.2 • 16:15

Fundamental Limitations of Photoacoustic Spectroscopy: Thermodynamic Approach, Anatoliy A. Kosterev¹; ¹*LAD, Yokogawa, USA*. A thermodynamic analysis of fundamental limitations of the photoacoustic spectroscopy is presented. A photoacoustic sensor is treated as a heat engine. The results are compared to the shot-noise limit of the absorption spectroscopy.

LW5B.3 • 16:30

Compact Photo-acoustic Sensor with Wide (3.8–4.2 μm) Spectrum Coverage, Margaux Barbier¹, Bertrand Hardy¹, Myriam Raybaut¹, Jean-baptiste Dherbecourt¹, Jean-Michel Melkonian¹, Antoine Godard¹, Michel Lefebvre¹, Florent Thibault², Grégoire Souhaité²; ¹*Onera, The french aerospace lab, France*; ²*Teem Photonics, France*. A compact photo-acoustic sensor for multi-species detection is presented. The widely tunable (3.8–4.2 μm) radiation of a micro-laser pumped OPO is coupled to a resonant acoustic cell. Demonstration experiment is performed on atmospheric CO₂.

LW5B.4 • 16:45

Modulation Cancellation Method for Spectroscopic Measurements, Vincenzo Spagnolo^{1,2}, Lei Dong², Anatoliy A. Kosterev², Frank Tittel²; ¹*Physics, Politecnico di Bari, Italy*; ²*Electrical and Computer Engineering, Rice University, USA*. A novel spectroscopic technique based on modulation spectroscopy is described. We demonstrated three applications: measurement of temperature differences in a gas, detection of broadband absorbing species and isotope ratio measurements.

LW5B.5 • 17:00

Differential Optical Dispersion Spectroscopy, Michal Nikodem¹, Gerard Wyoski¹; ¹*Electrical Engineering, Princeton University, USA*. Optical subtraction of dispersion spectra with differential optical dispersion spectroscopy is presented. Applications to direct comparison of gas samples and to optical subtraction of interfering spectral signature are demonstrated experimentally

Aragon III-B

Fiber Lasers and Applications

16:00–18:00

FW5C • Fiber Lasers for Industrial Applications and Material Processing

Francois Salin; *EOLITE Systems, France, Presider*

FW5C.1 • 16:00 **Invited**

Lasers for Industrial Production Processing: Tailored Tools with Increasing Flexibility, Wolfram Rath; *ROFIN-SINAR Laser GmbH, Germany*. The actual technical properties and features of Rofin's high power fiber lasers and CO₂ Slab lasers are presented with regard to production processing.

FW5C.2 • 16:30 **Invited**

High Power Femtosecond Fiber Amplifiers for Industrial Applications, Clemens Honninger¹, Yoann Zaouter¹, Franck Morin¹, Eric Mottay¹; ¹*Amplitude Systemes, France*. Femtosecond lasers gain increasing interest in industrial applications due to their universality and outstanding machining quality. We present ultrafast fiber amplifier architectures and application results obtained with these lasers.

FW5C.3 • 17:00

Fiber Based Modal Filter for Radially and Azimuthally Polarized Beams, Christoph Jocher¹, Cesar Jauregui¹, Christian Voigtländer¹, Fabian Stutzki¹, Stefan Nolte¹, Jens Limpert^{1,2}, Andreas Tünnermann^{1,3}; ¹*Institute of Applied Physics, Friedrich-Schiller-Universität Jena, Germany*; ²*Helmholtz-Institute Jena, Germany*; ³*Fraunhofer Institute for Applied Optics and Precious Engineering, Germany*. We report on a fiber based mode filter for radially and azimuthally polarized modes. The proof of principle is shown for the azimuthally polarized mode filtered with a step-index fiber and an fs-written Fiber-Bragg-Grating.

Aragon III-A

Advances in Optical Materials

16:00–18:00

IW5D • Laser Materials II

Yasufumi Fujiwara; *Osaka Univ., Japan, Presider*

IW5D.1 • 16:00 **Invited**

High-energy Laser Amplifiers using Ultra-broad Emitting Yb-doped Materials, Mathias Siebold¹, Markus Loeser¹, Fabian Roeser¹, Reinhard Uecker², Joerg Koerner³, Joachim Hein¹, Marco Hornung³, Malte Kaluza³, Ulrich Schramm¹; ¹*Radiation Physics, Helmholtz-Centre Dresden-Rossendorf, Germany*; ²*Institute for Crystal Growth, Germany*; ³*Institute of Optics and Quantum Electronics, Germany*. High-energy laser amplifiers using Yb-doped gain media often show reduced efficiencies especially when operating at ultra-short pulses. We summarize techniques to improve storage and extraction efficiencies of Yb-based laser amplifiers.

IW5D.2 • 16:30

Hydrothermal Crystal Growth and Epitaxy in Garnet Systems, Colin McMillen¹, Cheryl Moore¹, Joseph Kolis¹; ¹*Clemson University, USA*. Hydrothermal methods have been developed for the growth of YAG and LuAG single crystals. This technique allows for the growth of single crystals having multiple layers of optical functionality. Several preliminary examples are described.

IW5D.3 • 16:45

Gradient Doped Yb³⁺:YAG Crystals for Laser Applications, Mikayel Arzakantsyan^{1,2}, Xavier Déléon³, Francois Balembois³, Patrick Georges³, Narine Ananyan³, Vladimir Gevorgyan³, Jean-Christophe Chanteloup¹; ¹*LULI, Ecole Polytechnique, CNRS, CEA, UPMC, France*; ²*Russian-Armenian (Slavonic) University, Armenia*; ³*Laboratoire Charles Fabry, Institut d'Optique, CNRS, Université Paris-Sud, France*; ⁴*Laserayin Tekhnika» CSC, Armenia*. We will present growth process and laser experimental studies on Yb³⁺:YAG single crystals exhibiting controlled distribution of the doping ions in the matrix. A 3 at%/cm gradient was obtained with Horizontal Direct Crystallization method.

IW5D.4 • 17:00

Holmium-Doped Lutetia: A Novel Diode Pumped Laser at 2124 nm, Philipp Koopmann^{1,2}, Samir Lamrini², Karsten Scholle², Christian Kränkel¹, Peter Fuhrberg², Günter Huber¹; ¹*Institute of Laser-Physics, University of Hamburg, Germany*; ²*LISA laser products, Germany*. We present the first 1.9 μm diode pumped Ho:Lu₂O₃ laser at room temperature with an output power of 15 W. The optical-to-optical efficiency with respect to the absorbed power is estimated to exceed 50 %.

Wednesday, 1 February





Aragon II

Advanced Solid-State Photonics

AW5A • Mid-Infrared Sources—Continued

AW5A.4 • 17:15

Progress in Ultrafast Cr:ZnSe Lasers, Evgueni Slobodtchikov¹, Peter Moulton¹; ¹*Q-Peak Inc., USA*. We have operated, for the first time to our knowledge, a directly diode-pumped Cr:ZnSe femtosecond oscillator. In addition, we have constructed a CPA Cr:ZnSe-based ultrafast laser system that generates 2475-nm, 1-kHz-rate, 1 GW-peak-power pulses.

AW5A.5 • 17:30

Kerr-Lens Mode-locked Cr:ZnS Laser, Evgeni Sorokin¹, Nikolai Tolstik², Irina Sorokina²; ¹*TU Vienna, Austria*; ²*NTNU, Norway*. The first Kerr-Lens mode-locked Cr:ZnS laser generates the shortest and highest-energy mid-IR near transform-limited pulses of 69 fs duration at 550 mW output power. The 3.7 nJ pulses have 193 nm wide spectrum around 2.39 μm

AW5A.6 • 17:45

Laser Performance of Highly Doped Er:Lu2O3 at 2.8 μm , Tao Li¹, Kolja Beil¹, Christian Krankel¹, Christian Brandt¹, Günter Huber¹; ¹*Institute of Laser-Physics University of Hamburg, Germany*. We report on diode-pumped laser experiments and spectroscopy of Er:Lu2O3. 1.7 W room-temperature continuous-wave output power at 2.84 μm with a slope-efficiency of 11% was obtained. Moreover, ESA and lifetime measurements were carried out.

Aragon III-C

Laser Applications to Chemical, Security and Environmental Analysis

LW5B • New Spectroscopic Approaches—Continued

LW5B.6 • 17:15

High-spectral-resolution Two-photon Pump Polarization Spectroscopy Probe Technique for H-atom Detection, Aizaz Bhuiyan¹, Aman Satija¹, Sameer Naik¹, Robert Lucht¹; ¹*School of Mechanical Engineering, Purdue University, USA*. We report the development of a two-photon pump polarization spectroscopy probe technique for detection of atomic Hydrogen using two single-mode laser sources. Significant effect of laser parameters on atomic transitions has been observed.

LW5B.7 • 17:30

Miniaturized Fiber-coupled Trace Gas Sensors based on Photoacoustic Spectroscopy, Michael Köhring¹, Ulrike Willer², Wolfgang Schade^{1,2}; ¹*Fiber Optical Sensor Systems, Fraunhofer HHI, Germany*; ²*EFZN, Clausthal University of Technology, Germany*. Fiber coupled trace gas sensors are presented, which operate with photoacoustic excitation using silicon micro tuning forks as sensitive elements. A detection limit of $S = (2.13 \pm 0.02)$ ppm is achieved for ozone.

LW5B.8 • 17:45

Trace Detection of Explosives by Microring Resonators, Rozalia Orghici¹, Peter Lützwow¹, Wolfgang Schade^{1,2}; ¹*Fraunhofer Heinrich Hertz Insitute, Germany*; ²*Institute of Energy Research and Physical Technologies, Clausthal University of Technology, Germany*. A silicon microring resonator coated with specifically synthesized receptor molecules that enables the sensitive and selective detection of trinitrotoluene in the gas phase is presented.

Aragon III-B

Fiber Lasers and Applications

FW5C • Fiber Lasers for Industrial Applications and Material Processing—Continued

FW5C.4 • 17:15

Distributed Mode Filtering Rod Fiber Amplifier With Improved Mode Stability, Marko Laurila¹, Thomas T. Alkeskjold², Jes Broeng³, Jesper Laegsgaard¹; ¹*Department of Photonics Engineering, Technical University of Denmark, Denmark*; ²*NKT Photonics, Denmark*. We report 216W of average output power from a photonic crystal rod fiber amplifier. We demonstrate almost 50% power improvement of the mode onset instability by operating the rod fiber in a leaky guiding regime.

FW5C.5 • 17:30 **Invited**

Recent Trends on Industrial Femtosecond Fiber Lasers, Nam Seong Kim¹, Tae Hyun Yoon²; ¹*Laser Application Research Laboratory, EO Technics, Republic of Korea*; ²*Department of Physics, Korea University, Republic of Korea*. Increasing demand on microelectronics industry for personal mobile devices is possible by industrial laser processings. Some critical processes require industrial femtosecond fiber lasers showing lots of developments recently which is overviewed in this presentation.

Aragon III-A

Advances in Optical Materials

IW5D • Laser Materials II—Continued

IW5D.5 • 17:15

Luminescence Properties and Red/Orange Laser Operation of Pr:KYF4, Richard Moncorgé¹, Florent Starecki¹, Bin Xu¹, Gurvan Brasse¹, Patrice Camy¹, Jean-Louis Doualan¹, Alain Braud¹; ¹*CIMAP-Enscicaen, Université de Caen, France*. Detailed absorption and time-resolved emission data resulting from selective laser excitation are presented. True CW laser operation at red and orange laser wavelengths are reported.

IW5D.6 • 17:30

Er3+:LaF3 as Potential Material for Upconversion Lasers, Francesca Moglia¹, Fabian Reichert¹, Günter Huber¹; ¹*ILP - Uni Hamburg, Germany*. We have grown an Er3+:LaF3 crystal and present the spectroscopic analysis in order to confirm the possibility to realize an excited state absorption pumped upconversion laser in the green spectral range via near-infrared pumping.

IW5D.7 • 17:45

Development of Highly-Reflective Coatings based on Sol-Gel Technology for Megajoule-class Lasers, Bertrand Bertussi¹, Xavier Le Borgne¹, Claude Bonnin¹, Christian Vernagallo¹, Christophe Boscher¹, Luc Bianchi¹, Karine Valle¹, Philippe Belleville¹; ¹*CEA, France*. In high power lasers, dielectric mirrors have to fulfill drastic specifications in terms of reflexion and wave-front distortion. We present an optical thin film technology based on sol-gel process and called Laminar Flow Coating process.

Wednesday, 1 February

19:30–21:00 Banquet, Aragon II & III





Quanta System produces **lasers and laser systems** for a wide range of scientific, medical and industrial applications. DNA Laser Technology is not just a marketing promise: it's also a way of thinking, working, and creating values to be shared.

INNOVATIVE PHILOSOPHY

Quanta System

DNA Laser Technology



DNA LASER TECHNOLOGY



Target Markets

- Medical
- Life & Health
- Science
- Microelectronics
- Advanced Materials
- Advanced Manufacturing Processes
- Fine Arts Conservation

Quanta System
DNA Laser Technology



Quanta System S.p.A

Via IV Novembre, 116 - 21058 Solbiate Olona (VA) Italy
Tel. +39-0331.376797 - Fax +39-0331.367815
quanta@quantasystem.com
www.quantasystem.com





Aragon III-B

Fiber Lasers and Applications

Aragon III-A

Advances in Optical Materials

07:00–18:30 Registration, Aragon Foyer

08:00–09:30

FTh1A • Short Pulse Fiber Lasers

Mike O'Conner; *IPG Photonics Corp, USA, Presider*

FTh1A.1 • 08:00 **Invited**

Pulsed Fiber Laser Development at LLNL, Jay Dawon¹, Michael Messerly¹, Matthew Prantil¹, Paul Pax¹, Arun K. Sridharan¹, Graham Allen¹, John Heebner¹, Craig Siders¹, Christopher Barty²; ¹*Lawrence Livermore National Laboratory, USA*. Pulsed fiber laser systems are under development at Lawrence Livermore National Laboratory as photo-cathode drive lasers for linear accelerators and injection seed lasers. The presents status and future potential will be reviewed.

FTh1A.2 • 08:30

Recent Progress in Mode-locked Fiber Lasers with Carbon Nanotube Saturable Absorber, Khanh Kieu¹, Robert Norwood¹, Nasser Peyghambarian¹; ¹*College of Optical Sciences, University of Arizona, USA*. We report our recent results in the development of compact mode-locked fiber lasers with carbon nanotube saturable absorber for various applications.

FTh1A.3 • 08:45

On the Pulse Fidelity in Monolithic Single Mode Femtosecond Ytterbium Fiber Amplifiers, Aart J. Verhoef, Lingxiao Zhu¹, Tobias Flöry¹, Kim Jespersen², Lars Grüner-Nielsen², Almantas Galvanauskas³, Andrius Baltuska¹, Alma Fernandez¹; ¹*Institut für Photonik, TU Wien, Austria*; ²*OFS Denmark, Denmark*; ³*Center for Ultrafast Optical Science, University of Michigan, USA*. We present the first nonlinear phase characterization of a monolithic fs ytterbium single mode fiber amplifier with a dispersion compensating fiber stretcher that matches a 1480 lines/mm grating compressor, yielding high fidelity sub-200 fs pulses.

FTh1A.4 • 09:00

The Role of the Saturable Absorber in a Mode-Locked Fiber Laser, Dmitriy Churin¹, Khanh Kieu¹, Nasser Peyghambarian¹; ¹*University of Arizona, USA*. We systematically investigated the role of the saturable absorber (SA) in a mode-locked fiber laser.

FTh1A.5 • 09:15

High Power Amplification of a Tailored-pulse Fiber Laser, Julien Saby¹, Benoit Reid², Francois Salin¹; ¹*Eolite Systems, France*; ²*ESI - Pyrophotonics Lasers Inc., Canada*. We present the amplification of a 1064nm pulse-programmable fiber laser up to 100W at 100kHz and frequency conversion to UV. Various output pulse shape and duration can be easily obtained enabling improvements in many laser processes.

08:00–09:30

ITh1B • Optical Fibers, Glasses and Ceramics I

Jean-Luc Adam; *Université de Rennes, France, Presiders*

ITh1B.1 • 08:00 **Invited**

Non-Silica Microstructured Optical Fibers, Heike Ebendorff-Heidepriem, T.M. Monro, *The University of Adelaide, Australia*. We review advances in the fabrication of a diverse range of non-silica glass microstructured optical fibers. We also show the benefits these fibers offer for applications including nonlinear optics, sensing and the mid-infrared.

ITh1B.2 • 08:30 **Invited**

Gas Filled Photonic Crystal Fiber Lasers, Wolfgang Rudolph¹, Chenchen Mao¹, Neil Campbell¹, Vasu Nampootheri¹, Bastian Baumgart¹, Andrew M. Jones², Brian R. Washburn², Kristan L. Corwin²; ¹*University of New Mexico, USA*; ²*Kansas State University, USA*. The recent demonstration of lasing based on population inversion in gas filled photonic crystal fibers opens up new wavelength regions for fiber lasers. The gaseous active medium mitigates some of the power limiting factors of lasers based on solid core fibers.

ITh1B.3 • 09:00

Zeolite Thin Film-Coated Fiber Sensor for Measuring Chemical Trace based on Multimode Interference, Jie Huang¹, Xinwei Lan¹, Tao Wei¹, Qun Han², Zhan Gao¹, Hai Xiao¹; ¹*Electrical and Computer Engineering, Missouri University of Science and Technology, USA*; ²*College of Precision Instrument and Opto-Electronics, Tianjin University, China*. This paper reports the development of zeolite thin film-coated optical fiber sensor for directly measuring trace organic vapors. The sensor was based on multimode interference (MMI) effects.

ITh1B.4 • 09:15

New Mid-infrared Extruded Single and Multi Component Metal Halides Crystalline Fibers, Leonid Butvina¹, Alexey Butvina¹, Evgeny Dianov¹, Ninel Lichkova², Vladimir Zagorodnev²; ¹*FORCRAS, Russian Federation*; ²*IPTM RAS, Russian Federation*. Possibility of extrusion low loss mid-infrared (5-15 μm) micro- and nano-structured crystalline fibers, based on metal (Ag, K, Li) halides (F, Cl, Br) crystals with different design will be presented and discussed.

09:30–10:00 Exhibits & Coffee Break

Aragon I and Foyer

Joint Fiber Lasers and Applications (FILAS) / Laser Applications to Chemical, Security and Environmental Analysis (LACSEA)

09:30–11:00

JTh2A • FILAS/AIOM Joint Poster Session

JTh2A.01

Amplitude-Equalized Dual-Wavelength Rational Harmonic Mode-Locked Fiber Ring Laser, Niloy K. Dutta¹; ¹*Physics, University of Connecticut, USA*. A dual-wavelength amplitude-equalized rational harmonic mode-locked fiber laser operating at ~ 40 GHz based on the technique of nonlinear polarization rotation (NPR) in a highly nonlinear fiber is reported. A simulation is also presented.

JTh2A.02

Continuous Laser Generation of Ultrasound in Materials using High Power Fiber Lasers, James N. Caron^{1,2}, Gregory P. DiComo¹, Sergei Nikitin¹; ¹*Research Support Instruments, USA*; ²*Quarktet, USA*. High power cw lasers can be used to generate ultrasonic wavefronts in materials. Upon detection, these wavefronts provide a new and rapid method of determining strength and defects where contact ultrasound transducers cannot be used.

JTh2A.03

Withdrawn

JTh2A.04

Bismuth-doped Mg-Al-silicate Glasses and Optical Fibers on their Base, Sergei Sverchikov¹, Boris I. Denker¹, Boris I. Galagan¹, Sergei V. Firstov², Igor A. Bufetov², Sergei L. Semenov², Vladimir V. Velmiskin², Evgeny Dianov²; ¹*A.M.Prokhorov General physics institute, Russian Federation*; ²*Fiber Optics Research Center, Russian Federation*. Properties of Bi-doped "powder-in-tube" fabricated fibers were compared with the bulk glass samples of the same Mg-Al-silicate glass composition. The losses in the fibers were an order of magnitude less than in Ir crucible melted glasses.

Thursday, 2 February





Aragon I & Foyer

Joint Fiber Lasers and Applications (FILAS) / Laser Applications to Chemical, Security and Environmental Analysis (LACSEA)

JTh2A • FILAS/AIOM Joint Poster Session—Continued

JTh2A.05

Optical Planar Wave Guide Effect in Cadmium Sulfide (CdS) Thin Film Semiconductor, Dane Cachi¹, Anibal Valera¹, Carmen Eyzaguirre¹, *Physics, Universidad Nacional de Ingeniería, Peru*. We present the result of Cadmium Sulfide Thin Film Semiconductor as Planar Wave Guide. The experimental data of Wave Guide transversal transmission are complemented with spectral frontal transmission. We obtained the effective refractive index.

JTh2A.06

Thickness-dependence of Third Harmonic Generation in Transparent Polymer Films Containing Octupolar Molecules, Myoungsik Cha¹, Hee Joo Choi¹, *Pusan National University, Republic of Korea*. In ethyl-violet polymer thick films formed by over-coating, the third-harmonic output increased monotonically with thickness L, instead of $\sin^2(aL)$ -behavior. The enhancement was attributed to the longer coherence lengths for thicker films.

JTh2A.07

Polarization Conversion in Inhomogeneous Anisotropic Multilayer Structures, Volodymyr I. Fesenko¹, Igor A. Sukhoivanov², *Lab "Photonics", Kharkov National University of Radio Electronics, Ukraine*; *University Guanajuato, Mexico*. The effect of the polarization conversion in porous silicon-based multilayer structures is investigated. The conditions for the effective polarization conversion are presented. The maximum amount of polarization conversion that was obtained was 90%

JTh2A.08

1 μm Yb:CaGdAlO₄ Thin Disk Laser Material, Bruno Viana², Sandrine Ricaud¹, *LCFIO, France*; *LCMCP, France*. Yb³⁺:CaGdAlO₄ is a new laser material with very high thermal conductivity (> 6.5 W K⁻¹m⁻¹) allowing large tunability, high-power diode pumping power and thin disk operation.

JTh2A.09

Novel Synthesis Method and NIR Fluorescence Properties of Bi-Al-Si-O Glass Layers on Si-substrates, Islam Hoxha¹, *Physics, CCNY, USA*. Synthesis and spectroscopic measurements have been performed on Bi-doped glass layers on Si-substrates suitable for planar waveguide applications.

JTh2A.10

Intrinsic Nanocrystallization Effects on the Optical Properties of Eu³⁺-doped Lead Borosilicate Glasses, Acácio A. Andrade¹, Sidney Lourenço², Noelio Dantas³, *Universidade Federal de Uberlândia, Brazil*; *Engenharia de Materiais, Universidade Tecnológica Federal do Paraná, Brazil*. Lead borosilicate glass SBP doped with different Eu³⁺ ion concentrations have been synthesized characterized through optical absorption, photoluminescence and time-resolved photoluminescence spectra in the temperature range from 15 to 300 K.

JTh2A.11

Energy Transfer Between CdSe Nanocrystals and Nd³⁺ Ions Embedded in Vitreous System, Noelio Dantas¹, Elias O. Serqueira¹, Maria J. Bell², *Instituto de Física, Universidade Federal de Uberlândia, Brazil*; *Departamento de Física, Universidade Federal de Juiz de Fora, Brazil*. We have observed energy transfer between CdSe nanocrystals and Nd³⁺ ions embedded in vitreous system SNAB, synthesized by the fusion method. These samples doped have been investigated by optical techniques.

JTh2A.12

Detailed Luminescence Properties, Quasi 3-levels Laser Operation and Intracavity Frequency-doubling and Frequency-mixing of Nd:GGG, Richard Moncorgé¹, Bin Xu¹, Patrice Camy¹, Remi Soular¹, Jean-Louis Doualan¹, Alain Brenier², *CIMAP-Ensaen, Université de Caen, France*; *Université de Lyon, France*. Calibrated ESA and stimulated emission cross section spectra of Nd:GGG are registered. Diode-pumped 3-levels laser operation at 933.6 and 937.3 nm and intracavity frequency conversion at 466.8, 468.6 and 467.7 nm are reported

JTh2A.13

Optical Surface Bloch Modes of Complete Photonic Band Gap Materials, Shu-Yu Su¹, Lingling Tang¹, Tomoyuki Yoshie¹, *ECE, Duke University, USA*. Surface Bloch resonance modes are analyzed for (001), (100), and (110) woodpile surface planes. Low-loss, high-sensitivity surface Bloch modes are also analyzed on a flat-top (001) woodpile planar surface for optical resonance sensing.

JTh2A.14

Tunable Absorptions and Emissions of Chromium Ions in Different Glasses and Glass Ceramics, Céline Point¹, Xiang-Hua Zhang¹, *Université de Rennes 1, France*. We have studied different kind of glasses and ceramics doped with transition metals in order to obtain wide and tunable absorption and emission band.

JTh2A.15

Optical Properties of Freestanding Germanium Nanocrystals, Latha Nataraj¹, Fan Xu², Mark Bundy¹, Sylvain Cloutier^{2,3}, *Vehicle technology Directorate, Army Research Laboratory, USA*; *Department of Electrical and Computer Engineering, University of Delaware, USA*; *Delaware Biotechnology Institute, University of Delaware, USA*. Strained Ge has demonstrated improved optical properties. Mechanically milled Ge nanocrystals have shown tensile strain. Here, we discuss the enhanced optical properties and the efficient room temperature luminescence by Ge nanocrystals.

JTh2A.16

Laser Welding for Cu-Al Electrode of Li-Ion Battery, YouHie Han¹, JooYoung Park¹, SangJin Oh¹, BongMan Kim², ByoungOh Kam², *JPG Photonics Korea Ltd., Republic of Korea*; *MDI Technology, Republic of Korea*. Welding Cu and Al electrodes of Li-ion Battery has several difficulties. A novel 'V' shape of two electrodes was devised, which influences positively on metal-lurgical properties and can also minimize inter-metallic compound.

JTh2A.17

Fs Laser Fabricated D-shaped Fiber for Surface Enhanced Raman Scattering Substrate, Xinwei Lan¹, Jie Huang¹, Qun Han^{1,2}, Zhan Gao¹, Tao Wei¹, Hai Xiao¹, *Electrical and Computer Engineering, Missouri University of Science and Technology, USA*; *College of Precision Instrument and Opto-Electronics Engineering, Tianjin University, China*. Femto-second (fs) laser is applied to fabricate D-shaped fiber with sub-micrometer scale surface roughness. After silver thin film deposition, this kind of structure can work as surface enhanced Raman scattering (SERS) substrate.

JTh2A.18

Pulsewidth Dependence of Laser Scribed Molybdenum for Monolithically Integrated Thin Film Photovoltaic Devices, Tim D. Gerke¹, Brian W. Baird², *Fianium, Inc., USA*; *Summit Photonics, USA*. Ultrafast fiber lasers are used to scribe Mo thin film layers for photovoltaic devices. The scribe quality for sub-nanosecond pulses are significantly improved and the pulse energy required is lower than for nanosecond.

JTh2A.19

A Linear Model for Passive Coherent Combining a Large Number of Fiber Lasers, Erik J. Bochove¹, Will Ray^{2,3}, Frederic Durville², Christopher J. Corcoran², *RDLAF, Air Force Research Laboratory, USA*; *Corcoran Engineering, USA*; *School of Physics, Georgia Institute of Technology, USA*. Based on a simple linear model it is shown that coherent phasing of a regenerative fiber amplifier array may be achievable well in excess of the accepted limit of 8-10 elements.

JTh2A.20

BOTDA Measurements in the Presence of Fiber Vibrations-Avi Motil¹, Yair Peled¹, Lior Yaron¹, Moshe Tur¹, *School of Electrical Engineering, Tel Aviv University, Israel*. The ramification of optical fiber vibrations on the calibration phase of slope-assisted fast distributed Brillouin optical time-domain analysis is studied. It is found that under standard vibrations the calibration phase is still feasible

JTh2A.21

Top Hat Fiber Delivered High Power Sources and Thin Films Photovoltaics Scribing, Nicolas Faletto¹, Francois Salin¹, Julien Saby¹, Anthony Meunier¹, *EOLITE Systems, France*. We have developed laser sources with multiple parallel single mode or multi-mode fiber delivery at 1030 nm and 515 nm. Application to very clean scribing of thin films ITO, CdTe, a-Si or CIGS are presented.

JTh2A.22

Towards High Pulse Energy and Short Pulse Duration Fiber Laser Oscillators, Bai Nie¹, Marcos Dantus^{1,2}, *Department of Chemistry, Michigan State University, USA*; *Biophotonic Solutions Inc., USA*. Recent progress in all-normal dispersion fiber laser design indicates these sources will be capable of producing intense ultrashort pulses. Experimental delivery of 10's of nanojoules compressed to sub-45 fs pulse duration will be presented.

JTh2A.23

Yb-Doped Fiber Lasers Operating in the Range of 1147-1200 nm, Vladislav V. Dvoyrin^{1,2}, Oleg I. Medvedkov², Irina Sorokina¹, *Department of Physics, Norwegian University of Science and Technology, Norway*; *Fiber Optics Research Center, RAS, Russian Federation*. Pump source brightness and heat production per unit fiber length were found to be the critical parameters for the realized and investigated Yb-doped fiber lasers operating in the range of 1147-1200 nm.

JTh2A.24

Fiber-Based Ultrafast Laser Fabrication System with Application to Chirped Fiber Bragg Grating Sensors, Quinn McCulloch¹, Andrew M. Dattelbaum¹, George Rodriguez¹, Richard L. Sandberg¹, Kyle W. Staggs¹, *Los Alamos National Laboratory, USA*. An ultrafast, fiber-based laser fabrication system has been developed. This system has been used for many applications including THz metamaterials, waveguides, microfluidic devices, and here we detail work on Chirped Fiber Bragg Grating Sensors.

JTh2A.25

All-fiber Acousto-optic Q-switched Laser, Yuval Berg^{1,2}, Sharon Goldring¹, Shaul Pearl¹, Ady Arie², *Applied physics, Soreq NRC, Israel*; *Physical electrical engineering, Tel Aviv university, Israel*. A novel all-fiber Q-switched laser is presented and discussed. The Q-switch is based on induced acoustic long period grating on a fiber device which becomes an effective tunable output coupler both in terms of reflectivity and spectral selectivity.

Thursday, 2 February





Aragon I and Foyer

Joint Fiber Lasers and Applications (FILAS) / Laser Applications to Chemical, Security and Environmental Analysis (LACSEA)

JTh2A • FILAS/AIOM Joint Poster Session—Continued

JTh2A.26

Broad-band GVD Measurement of Specialty Fibers in Mid-IR, Dmitry Klimentov^{1,2}, Vladislav V. Dvoyrin^{1,3}, Nikolai Tolstik¹, Irina Sorokina¹; ¹Physics, (NTNU) Norges teknisk-naturvitenskapelige universitet, Norway; ²Natural Sciences Center, General Physics Institute of RAS, Russian Federation; ³Fiber Optics Research Center, General Physics Institute of RAS, Russian Federation. We demonstrate a novel interferometric setup for broad-band (>300nm) GVD measurements in short-length optical fibers in the mid-IR wavelength range using a superluminescent fiber source and investigate specialty fibers for infrared applications.

JTh2A.27

High-power Dispersion Managed Soliton Thulium Doped Fiber Laser, Alexander A. Krylov¹, Maria Chernysheva¹, Petr G. Kryukov¹, Evgeny Dianov¹; ¹Fiber Optics Research Center of Russian Academy of Science, Russian Federation. In this Letter we report on dispersion managed soliton thulium fiber laser operating at 1.93-1.97 μm and thulium-ytterbium amplifier. The anomalous dispersion in the laser cavity is compensated by the insertion of germanium-silicate fiber.

JTh2A.28

High Pulse Energy and High Peak Power Pulse Generation in an All-fiber Integrated Amplifier, Hongyu Yang¹, Aimin Wang¹, Tongxiao Jiang¹, Zhigang Zhang¹; ¹Institute of Quantum Electronics, School of Electronics Engineering and Computer Science, Peking University, China. A femtosecond fiber laser with an all-fiber integrated amplifier system together delivering 12 μJ -energy pulses was demonstrated. The peak power was 200kW.

JTh2A.29

An Inherently Synchronized Yb Fiber Laser Extension Unit for Broadly Tunable, Femtosecond Pulse Ti-sapphire Lasers for CARS Microscopy, Robert Szpoc^{2,1}, Peter Gyula Antal², Daniel Csati²; ¹R&D Ultrafast Lasers Ltd, Hungary; ²Research Institute for Solid State Physics and Optics, Hungary. An inherently synchronized Yb-fiber laser based extension unit for femtosecond pulse, broadly tunable Ti-sapphire lasers is introduced, which is well suited for coherent anti-Stokes Raman scattering microscopy.

JTh2A.30

Experimental Comparison of Infrared Surface Texturing Using a Diode-Pumped Laser and Fiber Laser, Whitney P. Davis¹, Radovan Kovacevic¹; ¹Mechanical Engineering, Southern Methodist University, USA. Surface texturing of a micron dimensioned sinusoidal topology is generated on Aluminum 6111 thin film by comparing a diode-pumped solid state laser and a pulsed fiber laser in the 1064 wavelength experimentally.

JTh2A.31

Dynamically Pulsed Fiber Laser for Material Processing, Jose R. Salcedo¹; ¹Jose' A.R. Salcedo, Multiwave Photonics, Portugal. In this report, we discuss various examples of multipulsing and burst control using a MOPA pulsed fiber laser operating at 1064 nm.

Aragon III-B

Fiber Lasers and Applications

11:00–12:30

FTh3A • High Power Fiber Lasers and their Applications

Farzin Amzajerdian; NASA Langley Research Center, President

FTh3A.1 • 11:00 **Invited**

Power Scaling of Narrow Line-width Fiber Amplifiers, John Edgecumbe, Kevin Farley, Chih-Hao Wang, Kanxian Wei, Scott Christensen, Imtiaz Majid, Bryce Samson, Kanishka Tankala; Nujfern, USA. In this presentation we review the progress on amplification of narrow line-width signals to high power levels in fiber amplifiers using Large Mode Area (LMA) fibers.

FTh3A.2 • 11:30

All-fiber Passive Coherent Beam Combining of Fiber Lasers and Challenges, Baishi Wang¹, Anthony Sanchez²; ¹Vytran LLC, USA; ²Air Force Research Lab, USA. We describe all-fiber and all-passive coherent beam combining of high power fiber lasers. In addition, we discuss effect of fiber nonlinearity and challenges in power and laser number scalability of such laser arrays.

FTh3A.3 • 11:45

Thermal Waveguide Changes in High Power Fiber Lasers, Florian Jansen¹, Fabian Stutzki¹, Hans-Jürgen Otto¹, Tino Eidam^{1,2}, Andreas Liem², Cesar Jauregui¹, Jens Limpert^{1,2}, Andreas Tünnermann^{1,2}; ¹Institute of Applied Physics Jena, Friedrich-Schiller-University Jena, Germany; ²Helmholtz-Institute Jena, Germany. Thermal waveguide changes in high power fiber lasers can have a significant effect on the waveguide properties of large mode area fibers. We demonstrate this by overcoming avoided crossings and measuring the fundamental mode shrinking.

FTh3A.4 • 12:00 **Invited**

Microwave Photonic Applications of Dual-Wavelength Fiber Lasers Using Stimulated Brillouin Scattering Gain, Michael Dennis¹; ¹JHU Applied Physics Laboratory, USA.- Dual-wavelength fiber lasers using stimulated Brillouin scattering gain have been shown to offer unique capabilities for a variety of microwave photonic applications, including millimeter-wave frequency synthesis, communications, and generation of low-phase-noise signals.

Aragon III-A

Advances in Optical Materials

11:00–12:30

ITh3B • Optical Fibers, Glasses and Ceramics II

Pierre Lucas; Univ. of Arizona, USA, Presidents

ITh3B.1 • 11:00 **Invited**

Mid-IR Fiber Sources, Brandon Shaw¹, Rafael Gattass¹, Jasbinder Sanghera¹, Ishwar Aggarwal²; ¹Naval Research Lab, USA; ²Sotera Defense Solutions, USA. Chalcogenide glass fibers have broad transmission in the IR and high intrinsic nonlinearities. These nonlinear processes can be exploited to generate mid-IR sources. We report on mid-IR sources based on these fibers.

ITh3B.2 • 11:30 **Invited**

Advances in Chalcogenide Optical Fibers and Related Devices, J.L. Adam¹, J. Troles¹, L. Brilland², B. Bureau¹, M.L. Anne³, H. Taniel³; ¹Equipe Verres et Céramiques, Institut des Sciences Chimiques de Rennes, France; ²PERFOS, Plate-Forme d'Etude et de Recherches sur les Fibres Optiques Spéciales, France; ³DIAFIR, Rennes-Atalante, France. Latest results are reported on chalcogenide microstructured fibers with very high non-linear optical coefficients for wavelength conversion, and on chalcogenide optical fibers implemented in sensors for (bio)-medical diagnosis.

ITh3B.3 • 12:00

Mid Infrared Transmission Properties of ZnSe Microstructured Optical Fibers, John V. Badding¹, Rongrui He¹, Justin Sparks¹, Anna Peacock², Noel Healy², Pier Sazio², Marco Petrovich²; ¹Chemistry, Penn State University, USA; ²Optoelectronics Research Center, University of Southampton, United Kingdom. ZnSe fibers are fabricated using air-silica photonic band-gap optical fiber as high-pressure microfluidic templates for semiconductor growth via chemical deposition. We examine their transmission properties over a wide spectral range.

ITh3B.4 • 12:15

Polarized Raman Mapping Method for Estimation of Refractive Index Differences on Grain-Boundaries and Inline Transmission for Well-Sintered Translucent Alumina Tomokatsu Hayakawa¹, Syohei Hayashi¹, S. Miyazawa², S. Ohashi², K. Watanabe²; ¹Dept. of Frontier Materials, Nagoya Institute of Technology, Japan; ²NGK Insulators, Ltd., Japan. Polarized Raman mapping technique was applied to determine the orientations of c-axis of each grain and averaged refractive index difference Δn_{avg} in translucent polycrystalline alumina. Light transmission spectra were simulated with it.

12:30–14:00 Lunch (on your own)





Aragon III-B

Fiber Lasers and Applications

14:00–16:00

FTh4A • 2 Micron Fiber Lasers

Arturo Chavez-Pirson; *NP Photonics Inc., USA, President*

FTh4A.1 • 14:00 **Invited**

MJ-level 2 μm Transform-limited Nanosecond Pulses Based on Highly Tm-doped Germanate Fibers, Wei Shi¹, Eliot Petersen^{1,2}, Qiang Fang^{1,3}, Khanh Kieu³, Arturo Chavez-Pirson¹, Nasser Peyghambarian^{1,3}, Jirong Yu⁴; ¹*NP Photonics Inc, USA*; ²*Physics Department, University of Arizona, USA*; ³*College of Optical Sciences, University of Arizona, USA*; ⁴*NASA Langley Research Center, USA*. We report a monolithic ~0.95 mJ pulsed fiber laser in 2 μm regime with transform-limited linewidth and 10-100 ns pulse width. This MOPA-based pulsed fiber laser is based on highly Tm-doped germanate fibers.

FTh4A.2 • 14:30

45-dB, Compact, Single-Frequency, 2-μm Amplifier, Alex Dergachev¹; ¹*Q-Peak, Inc., USA*. This is the first demonstration of a compact, fiber-laser pumped, single-stage, bulk Holmium amplifier providing 45-dB gain with single-frequency, CW or high-repetition-rate pulsed, seeds at 2.05 μm and diffraction-limited beam quality.

FTh4A.3 • 14:45

High Energy High Peak Power Monolithic Single Frequency 2 μm Nanosecond Pulsed Fiber Laser System, Qiang Fang¹, Khanh Kieu¹, Wei Shi², Eliot Petersen^{2,3}, Arturo Chavez-Pirson², Nasser Peyghambarian^{1,2}; ¹*College of Optical Science, University of Arizona, USA*; ²*NP Photonics, USA*; ³*Department of Physics, University of Arizona, USA*. We report an all-fiber single frequency ~15 ns pulsed laser source at ~1918.4 nm, whose energy and peak power was boosted to >0.5 mJ and >33 kW in master oscillator-power amplifier configuration.

FTh4A.4 • 15:00

Thulium-doped Germanosilicate Mode-locked Fiber Lasers, Charles Rudy¹, Michel Dignonet¹, Robert Byer¹, Shubin Jiang², Qing Wang²; ¹*Edward L. Ginzton Laboratory, Stanford University, USA*; ²*AdValue Photonics Inc., USA*. We report two mode-locked thulium-doped fiber lasers in different host materials, including a 682-fs, 8.75-nJ, figure-of-eight, doped silica fiber laser and a 900-fs, 34.1-nJ, SESAM mode-locked, linear cavity, doped germanosilicate fiber laser.

FTh4A.5 • 15:15

Modal Analysis of Large-Mode-Area Photonic Crystal Fiber for High Power 2μm Fiber Lasers, Clemence Jollivet Salvin¹, Charles Loussert², Thomas T. Alkeskjold³, Lasse Leick³, Robert A. Sims¹, Pankaj K. Kadwani¹, Lawrence Shah¹, Martin C. Richardson¹, Rodrigo Amezcua Correa¹, Axel Schulzgen¹; ¹*CREOL, College of Optics and Photonics, University of Central Florida, USA*; ²*LOMA, Université Bordeaux1, France*; ³*NKT Photonics, Denmark*. Modal properties of a new-generation polarizing large-mode-area photonic crystal fiber are studied based on the S2 imaging technique. Single mode operation in the 2μm spectral range is demonstrated for coiling diameters smaller than 40cm.

FTh4A.6 • 15:30

QCW All-fiber Laser at 2.94 Microns, Dominic Faucher¹, Nicolas Caron¹, Martin Bernier¹, Réal Val-lee¹; ¹*Laval University, Canada*. We demonstrate a QCW erbium-doped all-fiber laser emitting 16.1 W peak power pulses at 2942.2 nm at a 21.4% slope efficiency. Pump pulses of 8 ms yielded a maximum output pulse energy of 134 mJ.

FTh4A.7 • 15:45

Nonlinear Propagation of Mid-IR Femtosecond Pulses in ZBLAN Fiber, Nikolai Tolstik², Evgeni Sorokin¹, Vladimir Kalashnikov¹, Irina Sorokina²; ¹*TU Vienna, Austria*; ²*NTNU, Norway*. We demonstrate environmentally protected delivery of high-power femtosecond mid-IR pulses in a single-mode ZBLAN fiber by soliton formation. A 70-fs Cr:ZnS laser at 2.4 μm reaches this regime already at ~1.5 nJ launched pulse energy.

Aragon III-A

Advances in Optical Materials

14:00–16:00

ITh4B • Optical Fibers, Glasses and Ceramics III

Brandon Shaw; *Naval Research Lab., USA, President*

ITh4B.1 • 14:00 **Invited**

Telluride Glasses for Infrared Optical Sensing, Pierre Lucas¹, Bruno Bureau², Zhiyong Yang¹, Marie-Laure Anne², Shubin Jiang³; ¹*University of Arizona, USA*; ²*University of Rennes, France*; ³*Advalue Photonics, USA*. Telluride glasses are gaining interest due to their wide transparency to infrared light and their good formability which enables the design of novel optical devices. This presentation reviews the structure and applications of telluride glasses.

ITh4B.2 • 14:30 **Invited**

Electronic and Optical Properties of Ce³⁺ Doped Garnet Ceramics, Setsuhisa Tanabe¹, Jumpei Ueda¹; ¹*Graduate School of Human & Envir Studies, Kyoto University, Japan*. Electronic structures of Ce³⁺ doped garnet ceramics with various compositions were investigated by photoluminescence, excitation spectra, photoconductivity and their temperature dependences. Overlapping behavior of lower 5d-levels with the host conduction band dominates the phosphor properties.

ITh4B.3 • 15:00 **Invited**

Fluoride Transparent Ceramics, Michel Mortier¹, Andreas Lyberis¹, Patrick Gredin¹, Daniel Vivien¹, Sandrine Ricaud², Frederic Druon²; ¹*Ecole Natl Supérieure de Chimie de Paris, France*; ²*IOGS, France*. We prepare CaF₂:Yb ceramics by a conventional ceramic route. The origin of light scattering sources has been studied and laser effect observed. A spectroscopic study allows comparing the Yb³⁺ sites between ceramics and single crystals.

ITh4B.4 • 15:30

Photorefractive Material for Mid-IR Applications Based on LiF Color Center Crystal, Dmitri V. Martyshkin¹, Anton V. Fedorov¹, Anitha Arumugam¹, David J. Hilton¹, Vladimir Fedorov¹, Sergey Mirov¹; ¹*Department of Physics, The University of Alabama at Birmingham, USA*. γ-irradiated LiF:CC crystals proposed as novel material for volumetric Bragg grating (VBG), operating in mid-IR spectral range. Diffraction on a periodic structure at 1.56 μm is a demonstration of these materials for mid-IR VBG applications.

ITh4B.5 • 15:45

Withdrawn

16:00–16:30 Exhibits & Coffee Break

Thursday, 2 February





Aragon III-B

Fiber Lasers and Applications

16:30–18:30

FTh5A • Tunable Fiber Lasers including UV, Green and IR

Irina Sorokina; *Norges Teknisk Naturvitenskapelige Univ., Norway, Presider*

FTh5A.1 • 16:30 **Invited**

High Power UV Sources for Laser Direct Imaging, Damien Sangla¹; ¹*EOLITE Systems, France*. We developed a high power picosecond laser system at 80 MHz for third harmonic generation. We obtained 291 W at 1030 nm under 580 W of pump power at 976 nm from an all fiber master oscillator power amplifier based on Rod-Type fibers. By frequency tripling, we obtained 63 W at 343 nm with excellent beam quality ($M_{x+y} < 2 < + > 1.2$).

FTh5A.2 • 17:00

Frequency Conversion from IR to UV of High Peak Power Ultrafast Fiber Amplifier, Yoann Zaouter¹, Marc Hanna², Franck Morin¹, Mario Tonin¹, Rysvan Maleck¹, Clemens Hoenninger¹, Eric Mottay¹, Patrick Georges²; ¹*Amplitude Systemes, France*; ²*Laboratoire Charles Fabry de l'Institut d'Optique, France*. We report the frequency conversion from IR to UV of a high peak power ultrashort pulse fiber amplifier based on the use of a state of the art rod type fibre.

FTh5A.3 • 17:15

High Power IR, Green and UV Fiber Lasers, Julien Saby¹; ¹*Eolite Systems, France*. We present Q-switched laser products based on very simple MOPA architecture with rod-type fibers delivering 300W at 1030nm, 130W at 515nm and 50W at 343nm with pulse duration down to 10ns and $M^2 < 1.2$.

FTh5A.4 • 17:30 **Invited**

Supercontinuum Mid-IR Sources going beyond the Silica Transmission Window, Peter M. Mose-lund; *NKT Photonics, Denmark*. In this talk, we will present results on Mid-infrared supercontinuum generation using modelocked lasers. We will also discuss the challenges and potential applications of supercontinuum generation beyond the silica transmission window.

FTh5A.5 • 18:00 **Invited**

Frequency-converted Fiber Laser Tunable from 600 to 4600nm, Angus Henderson¹; ¹*Lockheed Martin Aculight Corp, USA*. A continuous wave optical parametric oscillator pumped by a fiber laser has been developed, producing up to 3 Watts tunable visible output around 610nm. The same device emits in the 1400nm to 4600nm infrared range.

Aragon III-A

Advances in Optical Materials

16:30–18:30

ITh5B • Semiconductor-based Optical materials

Setsuhisa Tanabe; *Kyoto Univ., Japan, Presider*

ITh5B.1 • 16:30 **Invited**

Periodically Oriented GaN for Optical Parametric Generation, Jennifer K. Hite¹, Mark E. Twigg¹, Nabil D. Bassim¹, Michael M. Mastro¹, Francis J. Kub¹, Charles R. Eddy¹; ¹*U.S. Naval Research Lab, USA*. Methods for growing periodically alternating polarities of GaN on GaN substrates have been developed. The resulting periodically oriented samples demonstrate feasibility of the method for producing structures of utility in optical parametric generation.

ITh5B.2 • 17:00

Current Injection Emitters at 1.54 μ m Based on Erbium Doped GaN p-i-n Structures, I-Wen Feng¹, Jing Li¹, Jingyu Lin¹, Hongxing Jiang¹, John M. Zavada²; ¹*Electrical and computer engineering, Texas Tech University, USA*; ²*Electrical and Computer Engineering, Polytechnic Institute of New York University, USA*. GaN:Er p-i-n structures were prepared by metal organic chemical vapor deposition with GaN:Er active layers grown at various pressures. The effect of GaN:Er growth pressure on the performance of these p-i-n structures was studied.

ITh5B.3 • 17:15

Iron Doped II-VI Ternary and Quaternary Semiconductors for Mid-IR Laser Applications, Dmitri V. Martyshev¹, Vladimir Fedorov¹, Sergey Mirov¹; ¹*Department of Physics, The University of Alabama at Birmingham, USA*. We report on crystal-field engineering of solid-state laser gain media based on new transition metal Iron doped II-VI Ternary and Quaternary semiconductor materials for mid-IR tunable laser applications

ITh5B.4 • 17:30 **Invited**

Recent Progress in Red LEDs with Eu-doped GaN, Yasufumi Fujiwara¹; ¹*Division of Materials and Manufacturing Science, Graduate School of Engineering, Osaka University, Japan*. A new type of light-emitting diode with Eu-doped GaN can exhibit characteristic red emission due to the intra-4f shell transitions of Eu³⁺ ions at room temperature. The output light power continues to grow steadily up.

ITh5B.5 • 18:00

All-epitaxial Growth of Orientation-patterned Gallium Phosphide (OPGaP), Peter G. Schunemann¹, Lee Mohnkern¹, Alice Vera¹, Xiaoping S. Yang¹, Angie C. Lin², James S. Harris², Vladimir Tassev³, Michael Snure³; ¹*BAE Systems, Inc., USA*; ²*Paul G. Allen Center for Integrated Systems, Stanford University, USA*; ³*Sensors Directorate, Air Force Research Laboratory, USA*. Significant advances have been made in the quality of orientation-patterned gallium phosphide quasi-phases-matched structures grown by MBE through the use of improved phosphorus and silicon cells, and preliminary bulk HVPE growth results are promising.

ITh5B.6 • 18:15

Electrical Lasing in GaAs Quantum Dots Grown by Droplet Epitaxy, Masafumi Jo¹, Takaaki Mano¹, Kazuaki Sakoda¹; ¹*Advanced Photonic Materials Unit, National Institute for Materials Science, Japan*. We have demonstrated electrically injected lasing in GaAs quantum dot grown by droplet epitaxy. High-quality QDs with superior uniformity were produced by employing improved growth procedures.

NOTES

Blank lined area for notes.

Thursday, 2 February





Aragon III-A

Advances in Optical Materials

Friday, 3 February

08:00–10:00

IF1A • Waveguides and Thin Films 1

Setsuhisa Tanabe; *Kyoto Univ., Japan, Presider*

IF1A.1 • 08:00 **Invited**

Fabrication of Active Waveguides Using Femtosecond Lasers, Ajoy Kar¹; ¹*Heriot-Watt University, United Kingdom*. The successful development of femtosecond lasers has enabled the use of ultrafast laser inscription for device fabrication. I will describe how light-matter interactions have been harnessed for waveguide lasers development in a variety of materials.

IF1A.2 • 08:30

Optical Amplification of Pr³⁺-doped ZBLA Channel Waveguides for Visible Laser Emission, Mélinda Olivier¹, Jean-Louis Doualan², Patrice Camy³, Hervé Lhermite², Jean-Luc Adam¹, Virginie Nazabal¹; ¹*Verres et céramiques, Université Rennes1, France*; ²*IETR Microelectronique, Université Rennes1, France*; ³*CIMAP, ENSI, France*. Visible laser emission of praseodymium in fluorozirconate glasses is studied, to generate compact solid state laser sources. Gain and losses measurement were performed on channelled waveguides obtained by photolithography followed by ionic exchange.

IF1A.3 • 08:45

Directly Written Mid-Infrared Waveguides in Zinc Selenide, John R. Macdonald¹, Patrick A. Berry², Kenneth L. Schelper², Ajoy Kar¹; ¹*Physics, Heriot Watt University, United Kingdom*; ²*Air Force Research Laboratory, USA*. Mid-infrared waveguides were fabricated in ZnSe using ultrafast laser inscription to directly write a cladding region in the material. Single-mode guiding at 3.39 μm was achieved with propagation losses of 1.9 dB/cm-1.

IF1A.4 • 09:00 **Invited**

Whispering Gallery Mode Resonators Coated with Active Layers, Gualtiero Nunzi Conti¹, Simone Berneschi^{2,3}, Stefano Pelli¹, Silvia Soria¹, Ilya Razdolskiy³, Tatiana V. Murzina⁴, Davor Ristic², Maurizio Ferrari³; ¹*Istituto di Fisica Applicata N. Carrara - CNR, Italy*; ²*Centro Studi e Ricerche " Enrico Fermi", Italy*; ³*Institute for Molecules and Materials, Radboud University Nijmegen, Netherlands*; ⁴*Department of Physics, Moscow State University, Russian Federation*; ⁵*Istituto di Fotonica e Nanotecnologie - CNR, Italy*. Whispering-gallery-modes spherical microresonators may be coated with non linear or doped materials in order to exploit their specific properties. We present the examples of a Kerr polymeric material and of rare-earth doped glass ceramics.

IF1A.5 • 09:30

Piezoresponse Force Microscopy on Proton Exchanged LiNbO₃ Layers, Michele Manzo¹, Denise Denning², Brian Rodriguez², Katia Gallo¹; ¹*Laser Physics, Applied Physics, KTH, Sweden*; ²*School of Physics, University College Dublin, Ireland*. We use piezoresponse force microscopy for high resolution investigations on proton exchanged LiNbO₃. We also quantify the reduction of the d₃₃ nonlinear coefficient induced by proton exchange in congruent LiNbO₃ substrates with and without Mg-doping.

IF1A.6 • 09:45

Towards Proton Exchanged Photonic Wires in LiNbO₃, Marc P. De Micheli¹, Oleksandr Stepanenko¹, Emmanuel Quillier¹, Hervé Tronche¹, Pascal Baldi¹, Pierre Aschiéri¹, Sarah Benchabane²; ¹*LPMC, University of Nice, France*; ²*FEMTO ST, University of Franche Comté, France*. Using a modified Proton Exchange process we have realized Photonic Wires in X-cut LiNbO₃. They exhibit highly confined mode, low propagation losses, low strain induced polarization coupling and no reduction of the nonlinear properties.

10:30–12:00

IF2A • Waveguides and Thin Films II

Shibin Jiang; *AdValue Photonics, USA, Presider*

IF2A.1 • 10:30 **Invited**

Pure and Rare-earth Doped Fluorite Crystals for Various Applications, Richard Moncorge¹; *Université de Caen, France*. Some pure and rare-earth doped fluorites, in the form of polycrystalline powders, thin-films and bulk crystals have been recently studied and will be described for their very specific linear and nonlinear spectroscopic and luminescence properties and for various applications.

IF2A.2 • 11:00

Low Loss Depressed Cladding Waveguide Inscribed in YAG:Nd Single Crystal by Femtosecond Pulses, Andrey G. Okhrimchuk¹, Vladimir Mezentsev², Ian Bennion³, Alexander Shestakov³; ¹*FORC of RAS, Russian Federation*; ²*Aston University, United Kingdom*; ³*E.L.S. Co, Russian Federation*. A depressed cladding waveguide with record low loss of 0.12 dB/cm is inscribed in YAG:Nd(0.3at.%). It is shown that depressed cladding is a dominating factor in waveguide formation, and mechanical stress has a minor contribution.

IF2A.3 • 11:15

New Materials for Magneto Optic In-fiber and Waveguide Isolators, Palash Gangopadhyay¹, Alejandra Lopez-Santiago¹, Hannah R. Grant¹, N. Peyghambarian¹, Robert Norwood¹; ¹*College of Optical Sciences, University of Arizona, USA*. We report recent advances in new magneto optic materials including novel colorless magnetic ionic liquids and magnetic nanoparticle-core polymer-shell nanocomposites for non-reciprocal in-fiber and waveguide operation for isolation and circulation.

IF2A.4 • 11:30

Q-Switched Operation of a fs-Laser Written Nd:YAG/Cr⁴⁺:YAG Monolithic Waveguide Laser, Thomas Calmano¹, Anna-Greta Paschke¹, Sebastian Mueller¹, Christian Kraenkel¹, Günter Huber¹; ¹*Institute of Laser-Physics, University of Hamburg, Germany*. A Ti:Sapphire-pumped Q-switched waveguide laser was fabricated by fs-laser-writing of two parallel tracks in a bonded Nd:YAG/Cr⁴⁺:YAG-crystal. We achieved 1-ns-pulses with an average output power of 300 mW and 300 kHz repetition rate.

IF2A.5 • 11:45

Neodymium and Ytterbium Doped Sapphire Films Grown by Pulsed Laser Deposition, Sebastian Heinrich¹, Teoman Gün¹, Günter Huber¹; ¹*Institut für Laser-Physik, Germany*. Sapphire films with various dopant concentrations of both neodymium and ytterbium ions were grown by pulsed laser deposition. Reflection high energy electron diffraction and X-ray diffraction measurements indicate epitaxial growth of the films.

10:30–10:30 Coffee Break





Key to Authors and Presiders

(**Bold** denotes Presider or Presenting Author)

A

Abell, Joshua-LM2B.5
 Abshire, James B-LT2B.5, LT2B.6
 Adam, Jean-Luc-AM4A.23, IF1A.2, **ITh1B**
 Adam, J. L.-ITh3B.2
 Adler, Florian-AW4A.22
 Afzal, Robert-AW3A.1
 Agazzi, Laura-AT4A.18
 Aggarwal, Ishwar-ITh3B.1
 Agnesi, A.-AM1A.4
 Aguilo, Magdalena-AW4A.11, AW5A.2
 Aidam, Rolf-LM2B.6
 Albach, Daniel-AT4A.8, **AW4A.16**
 Alden, Marcus-LM5B.2, LM5B.4, LT3B.4
 Aleknavičius, Aidas-AT4A.15
 Algotsson, Martin-LT3B.4
 Alimov, Olim-AT4A.21
 Alisauskas, Skirmantas-AM1A.6
 Alkeskjold, Thomas T-FTh4A.5, FW5C.4
 Allan, Graham-LT2B.5, LT2B.6
 Allen, Graham-FTh1A.1
 Almirall, Jose-LM5B.1
 Amann, Markus-Christian-AM2A.2
 Amezcua Correa, Rodrigo-FTh4A.5
 Amzajerdian, Farzin-FTh3A
 An, Xinliang-LM1B.5, **LT6B.11**
 Ananyan, Narine-IW3D.7, IW5D.3
 Andersen, Peter E-AM4A.10
 Anderson, Gary-LT6B.9
 Andrade, Acácio Aparecido-JTh2A.10
 Andriukaitis, Giedrius-AM1A.6, **AT3A.3**, AT5A.5
 Anne, Marie-Laure-ITh4B.1
 Anne, J.L.-ITh3B.2
 Antal, Peter Gyula-JTh2A.29
 Antipenkov, Roman-AM4A.28
 Anton, Trifonov-AM4A.19
 Apolonskiy, Alexander-AM2A.2, AM4A.12, AW4A.1
 Aravazhi, Shanmugam-AM5A.3
 Arie, Ady-JTh2A.25
 Armacost, Chris M-LT1B.4
 Arumugam, Anitha-ITh4B.4
 Arzakantsyan, Mikayel-IW3D.7, **IW5D.3**
 Aschiéri, Pierre-IF1A.6
 Aubourg, Adrien-AT4A.1
 Aubry, Nicolas-AT3A.2, AT4A.1
 aus der Au, Juerg-AT4A.2

B

Badding, John V.-ITh3B.3
 Baer, Cyrill-AM2A.3, AM4A.13
 Baev, Valery M-LM3B.5
 Bai, Yingxin-LT5B.1
 Baird, Brian Walter-JTh2A.18
 Baker, Howard J-AT3A.5, **AW4A.19**
 Balciunas, Tadas-AT3A.3, **AT5A.5**
 Baldi, Pascal-IF1A.6
 Baldochi, Sonia Licia-ITh4B.5
 Balembois, Francois-AM4A.11, AT3A.2, **AT4A.1**,
 IW5D.3
 Balskus, Karolis-AM1A.6
 Baltuska, Andrius-AM1A.6, AT3A.3, AT5A.5, FTh1A.3
 Banerjee, Saumyabrata-AW4A.14
 Bangar, Devashish-LW3B.6
 Barbier, Margaux-LW5B.3
 Barnes, Norman-AT4A.24
 Baronio, Fabio-AT2A.3
 Barty, Christopher-FTh1A.1
 Basiev, Tasoltan T.-AT4A.21
 Bassim, Nabil D-ITh5B.1
 Bastock, P.-ITh3B.2

Bauer, Dominik-AM2A.1
 Baumgart, Bastian-ITh1B.2
 Baumgartl, Martin-AT1A.2
 Beecher, Stephen-AM4A.14
 Been, Stefan-AM1A.5
 Beil, Kolja-AM2A.3, AM2A.4, AW5A.6
 Bell, Maria J-JTh2A.11
 Belleville, Philippe-IW5D.7
 Benchabane, Sarah-IF1A.6
 Bengtsson, Per-Erik-LW3B.4
 Bennion, Ian-IF2A.2
 Berg, Yuval-JTh2A.25
 Bernacki, Bruce E-LT5B.2
 Berneschi, Simone-IF1A.4
 Bernhardi, Edward H-AM5A.1
 Bernhardt, Edward Harold-AM5A.6, AT4A.18
 Bernhardt, Birgitta-AM4A.12
 Bernier, Martin-FTh4A.6
 Berry, Patrick A-IF1A.3
 Bertussi, Bertrand-IW5D.7
 Bethge, Jens-AT5A.3
 Betin, Alexander-AW4A.26
 Bewley, William W-LM2B.5
 Beyatli, Ersen-AW4A.27
 Bhandari, Rakesh-AT2A.1
 Bhuiyan, Aizaz-LW5B.6
 Bianchi, Luc-IW5D.7
 Binhammer, Thomas-AM4A.8, AT2A.2
 Biriukov, Aleksander-FW3C.3
 Biss, David-LT6B.6
 Black, John D-LT6B.7
 Bochove, Erik J-JTh2A.19
 Bock, Martin-AT5A.6
 Boehm, Gerhard-AM2A.2
 Bohlin, Alexis-LW3B.4
 Bohman, Axel F-LM2B.1
 Bonetti, Yargo-LT6B.13
 Bonnin, Claude-IW5D.7
 Bood, Joakim-LM5B.4, **LT2B**, LT3B.4
 Boon, Poh-AM1A.6
 Borchers, Bastian-AT5A.6
 Boscher, Christophe-IW5D.7
 Bouillet, Johan-AM4A.9
 Bourdon, Pierre-AT4A.5
 Bradshaw, John-LT6B.6
 Brandt, Christian-AM4A.22, AW5A.6
 Brar, Khushvinder-AW3A.1
 Brasse, Gervan-IW5D.5
 Braud, Alain-IW5D.5
 Braun, Bernd-AM4A.3
 Breikopf, Sven-AM3A.3, AM4A.2
 Brenier, Alain-JTh2A.12
 Brida, Daniele-AT3A.1
 Brilland, L.-ITh3B.2
 Broeng, Jes-AM4A.18, AT1A.5, FW5C.4
 Bromage, Jake-AW4A.8
 Bronner, Wolfgang-LM2B.6
 Brons, Jonathan-AM2A.2
 Brown, Graeme-AM4A.14
 Brown, Michael-LT1B.1
 Brumfield, Brian-LW5B.1
 Buchvarov, Ivan-AM4A.19, **AW4A.25**
 Budnicki, Alexander-AM2A.1
 Bufetov, Igor A-JTh2A.4
 Bundy, Mark-JTh2A.15
 Burchman, David-AM3A.2
 Bureau, Bruno-ITh4B.1
 Bureau, B.-ITh3B.2
 Büttner, Alexander-AT4A.14

Butvina, Alexey-ITh1B.4
 Butvina, Leonid-ITh1B.4
 Byer, Robert-FTh4A.4

C

Cachi, Dane-JTh2A.5
 Cahoon, Eric-LM5B.1
 Calmano, Thomas-IF2A.4
 Campbell, Neil-ITh1B.2
 Camy, Patrice-AM4A.23, AM4A.9, IF1A.2, IW5D.5,
 JTh2A.12
 Canedy, Chadwick L-LM2B.5
 Cankaya, Huseyin-AW4A.27
 Cao, Jeffrey-AW3A.1
 Caron, James N-JTh2A.2
 Caron, Nicolas-FTh4A.6
 Carstens, Henning-AT1A.6, AT4A.9
 Carvajal, Joan J-AW5A.2
 Carvajal, Joan Josep-AW4A.11
 Cascales, Concepcion-IW3D.5
 Caswell, Andrew-LM1B.5
 Cerullo, Giulio-AT2A.5
 Cézard, Nicolas-LT1B.7
 Cha, Myoungsik-JTh2A.6
 Cha, Seongwoo-AW3A.3
 Chaitanya Kumar, Suddapalli-AM1A.4
 Chang, Wei-Zung-AM4A.25
 Chanteloup, Jean-Christophe-AT4A.8, AW4A.16,
 IW3D.7, IW5D.3
 Chavez-Pirson, Arturo-FTh4A, FTh4A.1, FTh4A.3
 Chekhlov, Oleg V-AW4A.23
 Chen, Chuangtian-AT4A.7
 Chen, Meishin-AT1A.5
 Chen, Songsheng-LT5B.1
 Chen, Youhua-LT6B.9
 Chernysheva, Maria-JTh2A.27
 Cheung, Eric C-AM3A.4, **AM3A.6**
 Chichkov, Nikolai-AM4A.15
 Choi, Hee Joo-JTh2A.6
 Choi, Sun Young-AM2A.5, AW4A.12
 Chosrowjan, Haik-AT4A.20
 Christensen, Scott-FTh3A.1
 Chrysostom, Engelen-LT2B.4
 Chuchumishev, Danail-AM4A.19, AW4A.25
 Churin, Dmitry-FTh1A.4
 Cirmi, Giovanni-AT2A.5
 Cizmeciyan, M. Natali-AW4A.27
 Cloutier, Sylvain-JTh2A.15
 Collins, Leslie-LM5B.3
 Conforti, Matteo-AT2A.3
 Corcoran, Christopher J-JTh2A.19
 Cormier, Eric-AM4A.9, AW5A.3
 Corwin, Kristan L-ITh1B.2
 Cristescu, Simona, M.-LM3B.6
 Csati, Daniel-JTh2A.29

D

Da Costa, Renata F-LT6B.8
 Dallochio, Paolo-AM1A.4
 Dam, Jeppe S-AW4A.2
 Dang, Dung D-LM2B.1
 Daniault, Louis-AT4A.29, AT4A.5
 Danielius, Romas-AT5A.5
 Dantas, Noelio-JTh2A.10, **JTh2A.11**
 Dantus, Marcos-JTh2A.22, **LM1B.3**
 Darginavičius, Julius-AM4A.20
 Das, Susanta K-AT5A.6
 Dattelbaum, Andrew M-JTh2A.24
 Davis, Whitney P-JTh2A.30
 Dawon, Jay-FTh1A.1



Dawson, Martin D-AM5A.5
 De Micheli, Marc Pierre-**IF1A.6**
 de Ridder, Rene M-AM5A.1, AM5A.6
 Degreif, Kai-LM2B.6
 Dekorsy, Thomas-AT4A.11, IW3D.1
 Délen, Xavier-**AM4A.11**, **AT3A.2**, IW5D.3
 Demmler, Stefan-AM3A.3, AT1A.6, **AT2A.4**, AT4A.9, AW4A.8
 Denker, Boris I-**JTh2A.4**
 Denning, Denise-IF1A.5
 Dennis, Michael-**FTh3A.4**
 Dergachev, Alex-**FTh4A.2**
 Descamps, Dominique-AM4A.9
 Dherbecourt, Jean-baptiste-**LW5B.3**
 DiComo, Gregory P-JTh2A.2
 DiGangi, Joshua-LT3B.5
 Dianov, Evgeny-FW3C.3, ITh1B.4, JTh2A.27, JTh2A.4
 Diaz, Francesc-AW4A.11, AW5A.2
 Diddams, Scott-AW4A.22, **LM1B.4**, LT2B.3
 Didierjean, Julien-AT3A.2, AT4A.1
 Digonnet, Michel-FTh4A.4
 Dilley, Christian-AW3A.1
 Dobler, Jeremy-FW3C.3
 Dobroc, Alexandre-**LT1B.7**
 Dogariu, Arthur-**LM1B.2**, **LT2B.2**
 Dong, Lei-LW5B.4
 Doroshenko, Maxim-**AT4A.21**
 Dorrer, Christoph-AW4A.8
 Doualan, Jean-Louis-AM4A.23, AM4A.9, IF1A.2, IW5D.5, JTh2A.12
 Dreier, Thomas-**LT3B.2**, LT3B.6
 Druon, Frederic-AM4A.9, AT2A.6, AT3A.4, AT4A.29, AT4A.5, ITh4B.3
 Dubietis, Audrius-AM4A.20
 Dubinskii, Mark-IW3D.3, **IW3D.5**
 Dubrasquet, Romain-AM4A.9
 Dudley, John M-AT5A.2
 Dulgergil, Ebru-AW4A.15
 Durville, Frederic-JTh2A.19
 Dutta, Niloy K.-**JTh2A.1**
 Dutta, Prashanta-**LM3B.2**
 Duxbury, Geoffrey-**LT1B.5**
 Dvoryin, Vladislav V.-**JTh2A.23**, JTh2A.26

E

Eberhardt, Ramona-AT4A.25
 Ebert, Volker-LT5B.3
 Ebrahim-Zadeh, Majid-AM1A.4
 Eddy, Charles R-ITh5B.1
 Edgecumbe, John-FTh3A.1
 Ehn, Andreas-**LM5B.4**
 Eichhorn, Marc-AM1A.1, AM1A.3, AM1A.5, **AW5A.1**
 Eidam, Tino-AM4A.12, AM4A.5, AT4A.10, FTh3A.3
 Eisenberg, Eric-AW3A.1
 Eken, Koray-AT4A.27
 Eldeniz, Y. Burak-AT4A.27
 Emmenegger, Lukas-**LM3B.1**, **LT6B.13**
 Emons, Moritz-AT2A.2
 Epstein, Ryan J-AW4A.18
 Erbe, Andreas-LT6B.1
 Erbert, Götz-AM4A.10
 Ernst, Mathias-AT4A.14
 Ertel, Klaus-AW4A.14, AW4A.23
 Esser, M J Daniel-AW4A.20
 Eyzaguirre, Carmen-JTh2A.5

F

Faletto, Nicolas-JTh2A.21
 Fan, Haitao-AM4A.26
 Fan, Tso Yee-AM3A.1, **JW1A.2**
 Fan, Xinyan-AT1A.5
 Fang, Qiang-FTh4A.1, **FTh4A.3**
 Farley, Kevin-FTh3A.1
 Faucher, Dominic-**FTh4A.6**
 Fechner, Matthias-AT4A.21, IW3D.2
 Fedorov, Anton V-ITh4B.4

Fedorov, Vladimir-ITh4B.4, **ITh5B.3**
 Fejer, M. M-AM1A.7
 Felder, Ferdinand-LM2B.3
 Feng, I-Wen-**ITh5B.2**
 Fermann, Martin-AM1A.2, AT5A.3
 Fernandez, Alma-AT3A.3, FTh1A.3
 Ferrari, Maurizio-IF1A.4
 Fesenko, Volodymyr I-**JTh2A.7**
 Fiebig, Torsten-AM4A.19, AW4A.25
 Fill, Ernst E-AM4A.12, AW4A.1
 Fill, Matthias-**LM2B.3**
 Firstov, Sergei V-JTh2A.4
 Fittschen, Christa-**LT3B.3**
 Fitzau, Oliver-AT4A.6
 Fjodorow, Peter-**LM3B.5**
 Floery, Tobias-AT3A.3
 Flores, A.-AM3A.2
 Flöry, Tobias-FTh1A.3
 Frank, Jonathan H-LT5B.4
 Friesen, Eugen-**LT3B.6**
 Fromzel, Viktor-IW3D.5
 Fuchs, Frank-**LM2B.6**
 Fuhrberg, Peter-AM2A.5, IW5D.4
 Fujimoto, Junichi-AT4A.7
 Fujita, Masayuki-AT4A.20
 Fujiwara, Yasufumi-**ITh5B.4**, **IW5D**
 Fukui, Tatsuo-AT4A.22
 Furukawa, Y.-AT2A.1, AT4A.22
 Furuse, Hiroaki-AT4A.19, **AT4A.20**

G

Gabalís, Martynas-AT4A.15
 Galagan, Boris I-JTh2A.4
 Gallmann, Lukas-AM1A.7
 Gallo, Katia-AT2A.3, IF1A.5
 Galvanauskas, Almantas-AM4A.25, AT1A.3, FTh1A.3
 Gangopadhyay, Palash-**1F2A.3**
 Gao, Zhan-ITh1B.3, JTh2A.17, LT6B.3
 Garcia-Blanco, Sonia-AM5A.3
 Gasser, Christoph-LT2B.4
 Gattass, Rafael-ITh3B.1
 Gavrilas, Nikolajus-AW4A.17, AW4A.21
 Gaydardzhiev, Alexander-AM4A.19, AW4A.25
 Gebbs, Raphael-AM2A.1
 Geiser, Peter-**LM2B.1**
 Georges, Patrick-AM4A.11, AM4A.9, AT2A.6, AT3A.2, AT3A.4, AT4A.1, AT4A.29, AT4A.5, FTh5A.2, IW5D.3
 Gerard, Bruno-AM1A.1
 Gerke, Tim D.-**JTh2A.18**
 Geskus, Dimitri-AM5A.1
 Gessenhardt, Christopher-LT3B.6
 Gevorgyan, Vladimir-IW3D.7, IW5D.3
 Giesberts, Martin-AT4A.6
 Giesen, Adolf-AT4A.3
 Giessen, Harald-AM4A.3
 Giniunas, Linas-AT5A.5
 Giorgetta, Fabrizio R-LT1B.4
 Girdauskas, Valdas-AT4A.15
 Gmachel, Claire-**LM2B.2**
 Godard, Antoine-LW5B.3
 Goldring, Sharone-JTh2A.25
 Golling, Matthias-AM2A.3, AM4A.13, AM5A.2
 Gomez, Anthony-**LM2B.4**
 Goodno, Gregory-AM3A.1, AM3A.2, AM3A.4, AM3A.5, **AW3A**
 Gord, James R.-**JW2A.1**, LM1B.5, LT3B.1, **LW3B**, LW3B.2, LW3B.3
 Gorgulu, A. Tolga-AW4A.27
 Goular, Dider-AT4A.5
 Grant, Hannah R-1F2A.3
 Grasse, Christian-AM2A.2
 Gredin, Patrick-ITh4B.3
 Greszik, Daniel-LT3B.2
 Griebner, Uwe-**AM2A.5**, AW4A.11, AW5A.2
 Grisard, Arnaud-AM1A.1

Grishin, Mikhail-AT3A.3, AT4A.15
 Grivas, Christos-AM5A.3
 Grosek, Jacob-FW3C.4
 Grunwald, Rüdiger-AT5A.6
 Grüner-Nielsen, Lars-FTh1A.3
 Guardani, Roberto-LT6B.8
 Guichard, Florent-AM4A.9
 Guina, Mircea-AW4A.18
 Gün, Teoman-1F2A.5
 Gupta, James-LT1B.6
 Gupta, Shantanu-**FW3C.5**

H

Haarlammert, Nicoletta-**AT4A.25**
 Hädrich, Steffen-**AT1A.6**, AT2A.4, AT4A.9, AW4A.8
 Halas, Naomi-**LM3B3**
 Hall, Denis R-AT3A.5, AW4A.19
 Han, Qun-ITh1B.3, JTh2A.17, LT6B.3
 Han, Wenjuan-AW4A.6
 Han, YouHie-**JTh2A.16**
 Hand, Lucian-AT5A.5
 Hanna, Marc-AT2A.6, **AT3A.4**, **AT4A.29**, **AT4A.5**, FTh5A.2
 Hänsch, Theodor W-AM4A.12
 Hapke, Christian-AM4A.15
 Hardy, Bertrand-LW5B.3
 Harren, Frans, J.M.-LM3B.6
 Harris, James S-ITh5B.5
 Harth, Anne-**AM4A.8**, AT2A.2
 Hartl, Ingmar-AM1A.2, AT5A.3
 Hartmann, Nick-AM1A.7
 Hasler, Karl-Heinz-AM4A.10
 Hasselbrack, William E-LT2B.5, LT2B.6
 Hastie, Jennifer-AM5A.5, **AM5A**
 Hausmann, Katharina-AM4A.4
 Hawkes, Steve-AW4A.23
 Haxsen, Frithjof-**AM4A.24**, AT4A.26
 Hayakawa, Tomokatsu-ITh3B.4
 Hayashi, Syohei, Mr.-**ITh3B.4**
 He, Rongrui-ITh3B.3
 Healy, Noel-ITh3B.3
 Heckl, Oliver-AM2A.3, AM4A.13
 Heebner, John-FTh1A.1
 Heese, Clemens-**AM1A.7**
 Hegenbarth, Robin-AM4A.3
 Hein, Joachim-IW5D.1
 Heinrich, Sebastian-**1F2A.5**
 Henderson, Angus-**FTh5A.5**
 Hendry, Billie-AW4A.26
 Hendry, Derek-AW4A.26
 Henry, Leanne Joan-**FW3C.4**
 Henry, Samuel B-LT3B.5
 Hernandez-Gomez, Cristina-AW4A.10, AW4A.14
 Herrick, Nicholas-AT1A.6
 Hewak, Dan-**ITh1B**, **ITh3B.2**
 Hideur, Ammar-AT1A.2
 Hildenbrand, Anne-AM1A.1
 Hilton, David J-ITh4B.4
 Hirohashi, Junji-**AT4A.22**
 Hite, Jennifer K-**ITh5B.1**
 Ho, James-AM3A.2, AM3A.6
 Hoenninger, Clemens-AT2A.6, FTh5A.2
 Hoffmann, Hans-Dieter-AT4A.6
 Hoffmann, Martin-AM4A.13, AM5A.2
 Högman, Marieann-LM3B.6
 Holloway, Laura-**JTh2A**
 Holtz, Christian-AT4A.2
 Holzberger, Simon-**AM4A.12**
 Holzwarth, Ronald-AM4A.12, AT5A.5
 Honea, Eric-**AW3A.1**
 Honninger, Clemens-**FW5C.2**
 Hooker, Chris J-AW4A.23
 Hornung, Marco-IW5D.1
 Hoxha, Islam-**JTh2A.9**
 Hsu, Paul Steve-**LW3B.3**
 Hu, I-Ning-**AT1A.3**

Key to Authors





Huang, C. C-ITh3B.2
 Huang, Jie-IThB.3, JTh2A.17, LT6B.3
 Huang, Robin-AW3A.2
 Huang, Shu-Wei-AT2A.5
 Huber, Günter-1F2A.4, 1F2A.5, AM2A.3, AM2A.4, AM2A.5, AM4A.22, AT4A.21, AW5A.6, IW3D.2, IW5D.4, IW5D.6
 Hugger, Stefan-LM2B.6
 Hülsenbusch, Thomas-AT4A.14
 Hult, D.-AM3A.2
 Humphreys, Richard-AW3A.1
 Huo, Yujing-AT4A.4
 Hussey, Lindsay K-IW3D.3

I

Ichikawa, Junichiro-AW4A.28
 Ilbey, Emrah-AW4A.15
 Ilday, F. Oemer-AT1A, AT4A.27, AW4A.15
 Imai, Koichi-AT4A.22
 Ishaaya, Amiel A-AM4A.17
 Ishii, Shinya-AT4A.20
 Ito, Shinji-AT4A.7
 Izawa, Yasukazu-AT4A.20

J

Jaeger, Wolfgang-LT5B.6
 Jander, Donald-AW3A.1
 Jansen, Florian-AM4A.5, AM4A.6, AT1A.4, AT4A.10, FTh3A.3
 Jantzi, Sarah-LM5B.1
 Jauregui, Cesar-AM4A.5, AT1A.4, AT1A.7, AT4A.10, FTh3A.3, FW5C.3
 Jensen, Ole-AM4A.10, AW4A.2
 Jespersen, Kim-FTh1A.3
 Jiang, Hongxing-ITh5B.2
 Jiang, Jie-AM1A.2, AT5A.3
 Jiang, Shibin-FTh4A.4, IF2A, ITh4B.1
 Jiang, Tongxiao-JTh2A.28
 Jo, Masafumi-ITh5B.6
 Jocher, Christoph-FW5C.3
 Johansson, Bengt-LT3B.4
 Johansson, Olof-LM5B.4, LT3B.4
 John, Collier-AW4A.10, AW4A.14, AW4A.23
 Jollivet Salvin, Clemence-FTh4A.5
 Jones, Andrew M-ITh1B.2
 Jonsson, Malin-LT3B.4
 Jukna, Vytautas-AM4A.28
 Jun, Chang Su-AW4A.12

K

Kadankov, Martin-AW4A.11
 Kadwani, Pankaj K-AM4A.18, FTh4A.5
 Kafka, James D-AT5A
 Kaiser, Sebastian-LT3B.6
 Kakizaki, Kouji-AT4A.7
 Kalal, Milan-AW3A.3
 Kalashnikov, Vladimir-AM2A.2, FTh4A.7
 Kalaycioglu, Hamit-AT4A.27
 Kaluza, Malte-IW5D.1
 Kam, ByoungOh-JTh2A.16
 Kaminski, Clemens F-LT5B.4
 Kan, Hirofumi-AT4A.19
 Kanai, Teruo-AT4A.7
 Kar, Ajoy-AM4A.14, IF1A.1, IF1A.3
 Karow, Malte-AM4A.7
 Karpf, Andreas-LT6B.5
 Kärtner, Franz-AT2A.5
 Kaspar, Sebastian-AM5A.4
 Kaspersen, Peter L-LM2B.1
 Kaster, Jan-AM4A.12
 Katzy, Veronika-AT4A.6
 Kawanaka, Junji-AT4A.19, AT4A.20
 Kawashima, Toshiyuki-AT4A.19
 Kehlet, Louis M-AW4A.2

Keller, Ursula-AM1A.7, AM2A.3, AM4A.13, AM5A.2, AT5A.2
 Kemp, Alan J-AM5A.5
 Keutsch, Frank-LT3B.5
 Khan, K.-ITh3B.2
 Khan, Mohammad A-LT5B.7
 Khazanov, Efim-AT4A.23, AW4A.13
 Khair, Amir-LM2B.3
 Khitrov, Victor-AW4A.5
 Kiefer, Johannes-LM5B.2, LT6B.2
 Kieleck, Christelle-AM1A.1
 Kieu, Khanh-FTh1A.2, FTh1A.4, FTh4A.1, FTh4A.3
 Kikuchi, Kiyofumi-AW4A.28
 Kim, BongMan-JTh2A.16
 Kim, Byoung Yoon-AW4A.12
 Kim, Chul Soo-LM2B.5
 Kim, Mijin-LM2B.5
 Kim, Nam Seong-FW5C.5
 King, Gary-AW4A.20
 Kinzer, Michel-LM2B.6
 Kiwanuka, Ssegawa-Ssekintu-LT5B.4
 Klein, Alexander-LT5B.3
 Kleinbauer, Jochen-AM2A.1
 Klenke, Arno-AM3A.3, AM4A.2
 Klenner, Alexander-AT5A.2
 Kliewer, Christopher-LW3B.5
 Klimentov, Dmitry-JTh2A.26
 Klimm, Detlef-ITh4B.5
 Kliner, Andrea-AT4A.25
 Knabe, Kevin-LT1B.4
 Kobayashi, Yohei-AT4A.7
 Koerner, Joerg-IW5D.1
 Koeth, Johannes-LT1B.6
 Köhler, Klaus-AM5A.4
 Köhring, Michael-LW5B.7
 Kolis, Joseph-IW5D.2
 Kolleck, Christian-AT4A.14
 Kong, Hong Jin-AW3A.3
 Kong, Weijin-AW4A.6
 Konyushkin, Vasilii-AT4A.21
 Konz, Werner-LM2B.6
 Koopmann, Philipp-AM2A.5, IW3D.2, IW5D.4
 Köster, Jan-Reent-LM3B.1
 Kosterev, Anatoliy A.-LW5B.2, LW5B.4
 Kottmann, Jonas-LM5B.5
 Kovacevic, Radovan-JTh2A.30
 Kracht, Dietmar-AM4A.15, AM4A.24, AM4A.4, AM4A.7, AT4A.14, AT4A.26
 Kraenkel, Christian-1F2A.4
 Krainak, Michael A-AW4A.26
 Krankel, Christian-AM2A.3, AM2A.4, AW5A.6, IW5D.4
 Krausz, Ferenc-AM2A.2, AM4A.12, AW4A.1
 Krebs, Manuel-AT4A.9
 Krenzen, Erik-AW4A.2
 Kristensson, Elias-LM5B.4
 Krylov, Alexander A-JTh2A.27
 Kryukov, Petr G-JTh2A.27
 Krzempek, Karol-LT1B.6
 Kub, Francis J-ITh5B.1
 Kulatilaka, Waruna D-LM5B, LT3B.1, LW3B.3
 Kundermann, Stefan-AT5A.2
 Kurimura, Sunao-AT2A, AW4A.28
 Kurt, Adnan-AW4A.27
 Kuznetsova, Svetlana-LM3B.5
 Kwasniewski, Albert-ITh4B.5

L

Laegsgaard, Jesper-FW5C.4
 Lahera, David E-IW3D.5
 Lallier, Eric-AM1A.1
 Lamrini, Samir-IW5D.4
 Lan, Xinwei-ITh1B.3, JTh2A.17, LT6B.3
 Landulfo, Eduardo-LT6B.8
 Lang, Tino-AM4A.8, AT2A.2, AT4A.14
 Langford, Nigel-LT1B.5
 Laurell, Fredrik-AT2A.3

Laurila, Marko-FW5C.4
 Laurila, Toni K-LT5B.4
 Le Borgne, Xavier-IW5D.7
 Leal, Luis-LM3B.5
 Leburn, Christopher Gilmour-AT3A.5
 Lecaplain, Caroline-AT1A.2
 Lecomte, Steve-AT5A.2
 Lederer, Max-AT4A.2
 Lee, Andrew-AT4A.17, AT4A.4
 Lefebvre, Michel-LW5B.3
 Lehneis, Reinhold-AM4A.6
 Leick, Lasse-AM4A.18, FTh4A.5
 Leindecker, Nick-AM1A.2
 Leinonen, Tomi-AW4A.18
 Leipertz, Alfred-LM5B.2, LW3B.1
 Leitenstorfer, Alfred-AT3A.1
 Lendl, Bernhard-LT2B.4
 Levenius, Martin-AT2A.3
 Lewicki, Rafal-LT1B.6
 Lhermite, Hervé-AM4A.23, IF1A.2
 Li, Bo-LT3B.4
 Li, Dehua-AM4A.27
 Li, Jing-ITh5B.2
 Li, Tao-AW5A.6
 Li, Xiaoli-AT4A.4
 Li, Xudong-AM4A.21
 Li, Xuesong-LM1B.5
 Li, Zhongshan-LM5B.2, LT3B.4
 Lichkova, Ninel-ITh1B.4
 Liem, Andreas-AT1A.4, FTh3A.3
 Lim, Alan-LT5B.6
 Lim, Hua-Wei Jonathan-AM1A.6
 Limpert, Jens-AM3A.3, AM4A.12, AM4A.2, AM4A.5, AM4A.6, AT1A.2, AT1A.4, AT1A.6, AT1A.7, AT2A.4, AT4A.10, AT4A.9, AW3A.4, AW4A.8, FTh3A.3, FW5C.3
 Lin, Angie C-ITh5B.5
 Lin, Jingyu-ITh5B.2
 Lisiecki, Radoslaw-IW3D.4
 Liu, Cheng-AM4A.26
 Liu, Chi-Hung-AT1A.3
 Liu, Junhai-AW4A.6
 Loehden, Benjamin-LM3B.5
 Loeser, Markus-AM4A.16, IW5D.1
 Lombard, Laurent-AT4A.5
 Looser, Herbert-LT6B.13
 Lopez-Santiago, Alejandra-1F2A.3
 Lösch, Rainer-LM2B.6
 Lou, Xiutao-LM3B.4
 Lourenço, Sidney-JTh2A.10
 Loussert, Charles-FTh4A.5
 Lu, C.-AM3A.2
 Lu, Jason-LT5B.1
 Lucas, Pierre-ITh3B, ITh4B.1
 Lucht, Robert-LW3B.6, LW5B.6
 Lützw, Peter-LW5B.8
 Lyberis, Andreas-ITh4B.3
 Lyngso, Jens K-AT1A.5

M

Ma, Lin-LM1B.5, LT1B, LT6B.12
 Ma, Xiuquan-AT1A.3
 Ma, Yufei-AM4A.21
 Macdonald, John Robert-IF1A.3
 Machinet, Guillaume-AM4A.9, AW5A.3
 Mahdi, Samira-LT6B.9
 Majid, Imtiaz-FTh3A.1
 Makio, Satoshi-AT4A.22
 Maleck, Rysvan-FTh5A.2
 Mandon, Julien-LM3B.6
 Mangold, Mario-AM5A.2
 Manninen, Albert-LM3B.1, LT6B.13
 Mano, Takaaki-ITh5B.6
 Manz, Christian-AM5A.4
 Manzo, Michele-IF1A.5
 Manzoni, Cristian-AT2A.5





Manzur, Tariq-**FW3C.2**
 Mao, Chenchen-**ITh1B.2**
 Mao, Jianping-**LT2B.6**
 Marandi, Alireza-**AM1A.2**
 Marchev, Georgi-**AM1A.3**
 Martial, Igor-**AT3A.2, AT4A.1**
 Martinenaite, Vilija-**AM4A.28**
 Martyshekin, Dmitri V-**ITh4B.4, ITh5B.3**
 Mary, Rose-**AM4A.14**
 Mason, Paul D.-**AW4A.14**
 Mastro, Michael M-**ITh5B.1**
 Mateos, Xavier-**AW4A.11, AW4A.6, AW5A.2**
 Matsunaga, Takashi-**AT4A.7**
 Maweza, Loyiso-**AW4A.20**
 McComb, Timothy S-**AM3A.6**
 McCulloch, Quinn-**JTh2A.24**
 McDonald, Karen-**LT5B.6**
 McManus, J. Barry-**LM3B, LT1B.2, LT5B**
 McMillen, Colin-**IW5D.2**
 Medvedkov, Oleg I-**JTh2A.23**
 Meffert, Christian-**LT5B.3**
 Mehner, Eva-**AM4A.3**
 Meier, Joachim-**AT4A.2**
 Melkonian, Jean-Michel-**LW5B.3**
 Merkle, Larry D.-**IW3D.3**
 Merkus, Peter, J.E.M.-**LM3B.6**
 Merritt, Charles D.-**LM2B.5**
 Messerly, Michael-**FTh1A.1**
 Meunier, Anthony-**JTh2A.21**
 Meyer, Jerry R.-**LM2B.5**
 Meyer, Terrence R.-**LW3B.2**
 Mezentsev, Vladimir-**IF2A.2**
 Michael, James-**LT2B.2**
 Michailovas, Andrejus-**AM1A.6, AT3A.3, AT4A.15, AW4A.3**
 Michailovas, Kirilas-**AT4A.15**
 Miles, Richard-**LT2B.2**
 Miller, David J-**LT5B.7**
 Miller, Joseph-**LW3B.2, LW5B**
 Mirov, Sergey-**ITh4B.4, ITh5B.3**
 Miseikis, Paulius-**AT5A.5**
 Miyamoto, A.-**AT2A.1**
 Miyamoto, Katsuhiko-**AT4A.17**
 Miyayama, Noriaki-**AT4A.20**
 Miyazawa, S.-**ITh3B.4**
 Mizoguchi, Hakaru-**AT4A.7**
 Modshing, Norbert-**AM4A.18**
 Moglia, Francesca-**AM4A.22, IW3D.2, IW5D.6**
 Mohn, Joachim-**LM3B.1**
 Mohnkern, Lee-**ITh5B.5**
 Mohr, Christian-**AT5A.3**
 Momen Nejad, Boshra-**LT5B.6**
 Moncorge, Richard-**AM4A.9, IW3D, IF2A.1**
 Moncorge, Richard-**IW5D.5, JTh2A.12**
 Monroe, Tanya-**ITh1B.1, ITh3B**
 Montant, Sébastien-**AW5A.3**
 Moore, Cheryl-**IW5D.2**
 Moore, David-**LT2B.1**
 Moore, Gerry-**FW3C.4**
 Moreira, Paulo F-**LT6B.8**
 Moretto, Claudia-**LT6B.2**
 Morgner, Uwe-**AM4A.15, AM4A.24, AM4A.8, AT2A.2, AT4A.26, AT5A.6**
 Morin, Franck-**AT2A.6, FTh5A.2, FW5C.2**
 Mortier, Michel-**ITh4B.3**
 Morton, Kenneth D-**LM5B.3**
 Moselund, Peter M.-**FTh5A.4**
 Moses, Jeffrey-**AT2A.5**
 Motegi, Hiroshi-**AT4A.22**
 Motil, Avi-**JTh2A.20**
 Mottay, Eric-**AT2A.6, AT4A.29, AT4A.5, FTh5A.2, FW5C.2**
 Moulton, Peter-**AW5A.4**
 Mueller, Sebastian-**IF2A.4**
 Mukhin, Ivan Borisovich-**AW4A.13**
 Müller, André-**AM4A.10**
 Muranaka, Yusuke-**AW4A.28**

Murzina, Tatiana V-**IF1A.4**
 Musgrave, Ian-**AW4A.10**

N

Nagel, James A.-**FW3C.3**
 Nähle, Lars-**LT1B.6**
 Naik, Sameer-**LW5B.6**
 Nakajima, Hirochika-**AW4A.28**
 Nakamura, Gerson Hiroshi de Godoy-**ITh4B.5**
 Nampoothiri, Vasu-**ITh1B.2**
 Nataraj, Latha-**JTh2A.15**
 Nayak, Simantini-**LT6B.1**
 Nazabal, Virginie-**AM4A.23, IF1A.2**
 Neely, Tyler W.-**AW4A.22, LT2B.3**
 Nelson, David-**LT1B.2**
 Neumann, Jörg-**AM4A.15, AM4A.24, AM4A.4, AM4A.7, AT4A.14, AT4A.26**
 Newbury, Nathan R-**LT1B.4**
 Nie, Bai-**JTh2A.22**
 Nikitin, Sergei-**JTh2A.2**
 Nikodem, Michal-**LW5B.5**
 Nillon, Julien-**AW5A.3**
 Nilsson, Johan-**AT1A.1**
 Nodop, Dirk-**AT1A.7**
 Nolte, Stefan-**FW5C.3**
 Nordström, Emil-**LW3B.4**
 Norwood, Robert-**IF2A.3, FTh1A.2, FW3C.3**
 Novo, Thierry-**AT4A.8, AW4A.16**
 Nugent-Glandorf, Lora-**AW4A.22, LT2B.3**
 Nunzi Conti, Gualtiero-**IF1A.4**

O

O'Connor, Mike-**FTh1A**
 O'Connor, Mike-**FW3C.1**
 Oh, SangJin-**JTh2A.16**
 Ohashi, S., Dr.-**ITh3B.4**
 Okhrimchuk, Andrey Gordeevich-**IF2A.2**
 Olausson, Christina B-**AT1A.5**
 Olivier, Mélinda-**AM4A.23, IF1A.2**
 Omatsu, Takashige-**AT4A.17**
 Onose, Takashi-**AT4A.7**
 Orghici, Rozalia-**LW5B.8**
 Osiko, Vyacheslav-**AT4A.21**
 Otto, Hans-Jürgen-**AM4A.5, AT4A.10, FTh3A.3**

P

Palashov, Oleg-**AT4A.23, AW4A.13**
 Palese, Stephen P-**AM3A.4, AM3A.6**
 Palmer, Guido-**AT2A.2**
 Papadopoulos, Dimitrios-**AT2A.6, AT3A.4, AT4A.29**
 Papashvili, Alexander-**AT4A.21**
 Parameswaran, Krishnan-**LT6B.6**
 Parisi, Daniela-**AW5A.1**
 Park, JooYoung-**JTh2A.16**
 Park, Sangwoo-**AW3A.3**
 Parrotta, Daniele C.-**AM5A.5**
 Parry, Bryn-**AW4A.23**
 Parsons, Matthew T-**LT5B.6**
 Paschke, Anna-Greta-**IF2A.4**
 Pasiskevicius, Valdas-**AT2A.3**
 Pask, Helen-**AT4A.4**
 Patnaik, Anil K-**LW3B.3**
 Pattathil, Rajeev-**AW4A.23**
 Paul, Joshua-**LT3B.5**
 Pavlov, Ihor-**AW4A.15**
 Pax, Paul-**FTh1A.1**
 Peacock, Anna-**ITh3B.3**
 Pearl, Shaul-**JTh2A.25**
 Pedersen, Christian-**AW4A.2**
 Pekarek, Selina-**AM2A.3, AT5A.2**
 Peled, Yair-**JTh2A.20**
 Pellegrina, Alain-**AT3A.4**
 Pelli, Stefano-**IF1A.4**
 Peng, Kunchi-**AW4A.30**
 Pengel, Stefanie-**LT6B.1**

Perevezentsev, Evgeny-**AW4A.13**
 Pervak, Volodymyr-**AM2A.2, AM4A.12, AT5A.4, AW4A.1**
 Petermann, Klaus-**AM2A.4, AM2A.5**
 Petersen, Eliot-**FTh4A.1, FTh4A.3**
 Petersen, Paul-**AM4A.10**
 Petros, Mulugeta-**LT5B.1**
 Petrov, Valentin-**AM1A.3, AM2A.5, AM5A, AW4A.11, AW4A.6, AW5A.2**
 Petrovich, Marco-**ITh3B.3**
 Peukert, Wolfgang-**LW3B.1**
 Peyghambarian, N.-**IF2A.3**
 Peyghambarian, Nasser-**FTh1A.2, FTh1A.4, FTh4A.1, FTh4A.3, FW3C.3**
 Phillips, Christopher R-**AM1A.7**
 Phillips, Jonathan-**AW4A.10, AW4A.14**
 Phillips, Mark-**LT5B.2**
 Pidwerbetsky, Alex-**LM1B.2**
 Piper, Jim-**AT4A.4**
 Pirzio, F.-**AM1A.4**
 Piskarskas, Algis-**AM4A.20, AM4A.28**
 Plemmons, David-**LM1B.5**
 Pliutau, Denis-**LT6B.10**
 Point, Céline-**JTh2A.14**
 Pollnau, Markus-**AM5A.1, AM5A.3, AM5A.6, AT4A.18**
 Popov, Pavel-**AT4A.21**
 Prantil, Matthew-**FTh1A.1**
 Prasad, Narasimha S-**LT6B.10**
 Pronin, Oleg-**AM2A.2, AM4A.12, AW4A.1**
 Pugzlys, Audrius-**AM1A.6, AT3A.3, AT5A.5**
 Pujol, Maria Cinta-**AW4A.11, AW5A.2**
 Pulford, B.-**AM3A.2**
 Pupeza, Joachim-**AM4A.12**

Q

Qi, Dahu-**LT6B.4**
 Quillier, Emmanuel-**IF1A.6**

R

Raciukaitis, Gediminas-**AW4A.17, AW4A.21**
 Rademacher, Sven-**LM2B.6**
 Radunsky, Michael B-**LT1B.4**
 Rahim, Mohamed-**LM2B.3**
 Ramirez, Lourdes P-**AT3A.4**
 Ramirez, Lourdes Patricia-**AT2A.6**
 Ramirez-Corral, Cristtel Y-**AT3A.5**
 Ranta, Sanna-**AW4A.18**
 Rao, Gottipaty N-**LT6B.5**
 Rath, Wolfram-**FW5C.1**
 Rattunde, Marcel-**AM5A.4**
 Rausch, Stefan-**AT2A.2**
 Rauschenberger, Jens-**AW4A.1**
 Ray, Will-**JTh2A.19**
 Raybaut, Myriam-**LW5B.3**
 Razdolskiy, Ilya-**IF1A.4**
 Reali, G.-**AM1A.4**
 Redmond, Shawn M.-**AM3A.1**
 Regelskis, Kestutis-**AW4A.17, AW4A.21**
 Reichert, Fabian-**AT4A.21, IW3D.2, IW5D.6**
 Reichle, Donald-**AT4A.24**
 Reid, Benoit-**FTh1A.5**
 Reid, Derryck T-**AT3A.5**
 Rekas, Miroslaw-**AT4A.25**
 Renz, Guenther-**AT4A.3**
 Rey, Julien M-**LM5B.5**
 Ricaud, Sandrine-**AM4A.9, AT3A.4, ITh4B.3, JTh2A.8**
 Richardson, Daniel-**LW3B.6**
 Richardson, Martin C-**AM4A.18, FTh4A.5**
 Ripin, Dan-**AM3A.1**
 Riris, Haris-**LT2B.5, LT2B.6**
 Ristau, Detlev-**AT5A.6**
 Ristic, Davor-**IF1A.4**
 Ritchie, Grant-**LT1B.3**
 Robin, C.-**AM3A.2**
 Rockwell, David-**AW4A.5**
 Rodriguez, Brian-**IF1A.5**





Rodriguez, George-JTh2A.24
 Rodriguez, Mike-LT2B.5
 Roeser, Fabian-AM4A.16, IW5D.1
 Rotermund, Fabian-AM2A.5, AT5A.1, AW4A.12
 Rothenberg, Joshua-AM3A.1, AM3A.2
 Rothhardt, Jan-AM3A.3, AT1A.6, AT2A.4, AT4A.9,
AW4A.8
 Rowland, K.-AM3A.2
 Roy, Sukesh-LM1B, LM1B.5, LT3B.1, LW3B.2, LW3B.3
 Rudolph, Wolfgang-ITh1B.2
 Rudy, Charles-FTh4A.4
 Ryba-Romanowski, Witold-IW3D.4

S

Saby, Julien-FTh1A.5, FTh5A.3, JTh2A.21
 Saito, Takafumi-AT4A.17
 Sakoda, Kazuaki-ITh5B.6
 Sakurai, Toshimitsu-AT4A.20
 Salcedo, Jose R-FW3C, JTh2A.31
 Salin, Francois-FTh1A.5, FW5C, JTh2A.21
 Samson, Bryce-FTh3A.1
 Sanamyan, Tigran-IW3D.3
 Sanchez, A.-AM3A.2
 Sandberg, Richard L-JTh2A.24
 Sanders, Scott Thomas-LM1B.5, LT5B.5, LT6B.11
 Sanghera, Jasbinder-ITh3B.1
 Sangla, Damien-FTh5A.1
 Sanzhez, Anthony-FTh3A.2
 Saraceno, Clara-AM2A.3, AM4A.13
 Satija, Aman-LW5B.6
 Sato, Yoichi-IW3D.6
 Savage-Leuchs, Matthias-AW3A.1
 Sazio, Pier-ITh3B.3
 Schade, Wolfgang-LW5B.7, LW5B.8
 Schellhorn, Martin-AM1A.5, AW4A.4
 Schelper, Kenneth L-IF1A.3
 Schenk, Emily-LM5B.1
 Schmidt, Andreas-AM2A.5
 Schnitzler, Elijah-LT5B.6
 Schnürer, Frank-LM2B.6
 Scholle, Karsten-IW5D.4
 Schramm, Ulrich-AM4A.16, IW5D.1
 Schreiber, Thomas-AM3A, AT4A.25
 Schriber, Cinia-AM2A.3, AM4A.13
 Schultze, Marcel-AM4A.8, AT2A.2
 Schulz, Christof-LT3B.2, LT3B.6, LT5B.3
 Schulzgen, Axel-FTh4A.5
 Schunemann, Peter G-AM1A.2, AM1A.3, AM1A.4,
ITh5B.5
 Schweikert, Wenka-LM2B.6
 Schönberger, Bernd-LT6B.1
 Seeger, Thomas-LM5B.2, LT3B, LW3B.1
 Segura, Martha-AW4A.11, AW5A.2
 Seise, Enrico-AM3A.3, AM4A.2
 Semenov, Sergei L-JTh2A.4
 Sengstock, Klaus-LM3B.5
 Senlik, Ozlem-AW4A.29
 Sennaroglu, Alphan-AW4A.27, AW5A
 Serqueira, Elias O-JTh2A.11
 Serrano, Maria D-IW3D.5
 Setzler, Scott-AM1A
 Shah, Lawrence-AM4A.18, FTh4A.5
 Shaikh, Waseem-AW4A.10
 Shaw, Brandon-ITh3B.1, ITh4B
 Shay, Thomas M-FW3C.4
 Shen, Zhongwei-AM4A.26
 Shestakov, Alexander-1F2A.2
 Shi, Wei-FTh4A.1, FTh4A.3
 Shih, Chun-Ching-AM3A.4
 Shirakawa, Akira-AM2A.4, AT1A.5, AT4A.13
 Shkunov, Vladimir-AW4A.5
 Shulga, Boris-AM4A.17
 Siders, Craig-FTh1A.1
 Sieber, Oliver D-AM5A.2
 Siebold, Mathias-AM4A.16, IW3D, IW5D.1
 Sigrist, Markus Werner-LM2B, LM5B.5

Siiman, Leo-AM4A.25
 Silver, Joel A-LM2B.4
 Sims, Robert A-AM4A.18, FTh4A.5
 Singh, Upendra N-LT5B.1
 Slobodchikov, Evgeni-AW5A.4
 Snetkov, Ilya-AT4A.23
 Snure, Michael-ITh5B.5
 So, Stephen-LW5B.1
 Somesfalean, Gabriel-LM3B.4
 Sonnenfroh, David-LT6B.6
 Soria, Silvia-IF1A.4
 Sorokin, Evgeni-AT4A.3, AW5A.5, FTh4A.7
 Sorokina, Irina-AT4A.3, AW5A.5, FTh4A.7, FTh5A,
 JTh2A.23, JTh2A.26
 Sosnowski, Thomas-AT1A.3
 Sotelo, Carlos-AT4A.12, AW4A.26
 Souhaité, Grégoire-LW5B.3
 Soulard, Remi-JTh2A.12
 Spagnolo, Vincenzo-LW5B.4
 Sparks, Justin-ITh3B.3
 Speiser, Jochen-AT4A.3, JW1A.1
 Spence, David-AT4A.4
 Sridharan, Arun Kumar-FTh1A.1
 Staggs, Kyle w-JTh2A.24
 Starecki, Florent-IW5D.5
 Stauffer, Hans U-LW3B.2
 Steffens, Juliana-LT6B.8
 Stein, Benjamin-LT5B.5
 Steinmann, Andy-AM4A.3
 Steinmetz, Alexander-AM4A.6, AT1A.7
 Steinmeyer, Günter-AT5A.6
 Stepanenko, Oleksandr-IF1A.6
 Stephen, Mark A-LT2B.5
 Stoeppler, Georg-AM1A.3, AM1A.5, AW5A.1
 Strauss, Hencharl Johan-AW4A.20
 Strohkendl, Friedrich-AW4A.5
 Stultz, Robert D-AT4A.12
 Stumpf, Max C-AT5A.2
 Stutzki, Fabian-AM4A.5, AM4A.6, AT1A.4, AT4A.10,
 FTh3A.3, FW5C.3
 Su, Liangbi-IW3D.1, IW3D.4
 Su, Shu-Yu-JTh2A.13
 Südmeyer, Thomas-AM2A, AM2A.3, AM4A.13,
 AM5A.2, AT5A.2
 Sugiura, Kaori-AW4A.28
 Sukhoivanov, Igor A-JTh2A.7
 Sumpf, Bernd-AM4A.10
 Sun, Kang-LT5B.7
 Suter, Jonathan D-LT5B.2
 Sutter, Dirk H.-AM2A.1
 Suzuki, Koji-AT4A.22
 Svanberg, Sune-LM3B.4
 Sverchkov, Sergei-JTh2A.4
 Sydoryk, Ihor-LT5B.6
 Sysoliatin, Aleksander-FW3C.3
 Szpocs, Robert-JTh2A.29

T

Tago, T.-AT2A.1
 Taira, Takunori-AM4A.1, AT2A.1, IW3D.6
 Takeshita, Kenji-AT4A.20
 Tamosauskas, Gintaras-AM4A.20
 Tan, Chuong-AM2A.1
 Tan, Lihao-AM1A.6
 Tanabe, Setsuhisa-IF1A, ITh4B.2
 Tang, Lingling-JTh2A.13
 Tang, Yunxin-AW4A.23
 Tankala, Kanishka-FTh3A.1
 Tao, Lei-LT5B.7
 Tariel, H.-ITh3B.2
 Tassev, Vladimir-ITh5B.5
 Tavast, Miki-AW4A.18
 Temyanko, Valery-FW3C.3
 Teng, Hao-AM4A.27
 Ter-Gabrielyan, Nikolay-IW3D.5
 Theeg, Thomas-AM4A.4

Thibault, Florent-LW5B.3
 Thielen, Peter-AM3A.1, AM3A.2
 Thomson, Ian J-AT3A.5
 Thomson, Ian James-AW4A.19
 Thomson, Robert R-AM4A.14
 Tidemand-Lichtenberg, Peter-AW4A.2
 Tittel, Frank-AM4A.21, LT1B.6, LW5B.4
 Tokurakawa, Masaki-AM2A.4, AT4A.13
 Tolstik, Nikolai-AW5A.5, FTh4A.7, JTh2A.26
 Tomihari, Yasuhiro-AT4A.22
 Tonelli, Mauro-AW5A.1
 Tong, Limin-1F2A.1
 Tonin, Mario-FTh5A.2
 Töpfer, Tino-AM5A.4
 Torrione, Peter-LM5B.3
 Trejos, Tatiana-LM5B.1
 Tröger, Johannes W-LM5B.2
 Troles, J.-ITh3B.2
 Tronche, Hervé-IF1A.6
 Tulip, John-LT5B.6
 Tuner, Martin-LT3B.4
 Tünnermann, Andreas-AM3A.3, AM4A.12, AM4A.2,
 AM4A.5, AM4A.6, AT1A.2, AT1A.4, AT1A.6,
 AT1A.7, AT2A.4, AT4A.10, AT4A.25, AT4A.9,
 AW4A.8, FTh3A.3, FW5C.3
 Tünnermann, Henrik-AM4A.4
 Tur, Moshe-JTh2A.20
 Tuzson, Bela-LM3B.1, LT6B.13
 Twigg, Mark E-ITh5B.1
 Tyazhev, Aleksey-AM1A.3

U

Udem, Thomas-AM4A.12
 Uecker, Reinhard-IW5D.1
 Ueda, Jumpei-ITh4B.2
 Ueda, Ken-ichi-AM2A.4, AT1A.5, AT4A.13
 Uemura, Sadao-AW4A.24
 Ujita, Shuto-AT4A.17

V

Vadimova, Olga-AW4A.13
 Valera, Anibal-JTh2A.5
 Valiulis, Gintaras-AM4A.20, AM4A.28
 Valle, Karine-IW5D.7
 Vallée, Réal-FTh4A.6
 van Amsterdam, Jan-LM3B.6
 van Dalsen, Koop-AM5A.1, AM5A.3
 van Wolferen, Henk-AM5A.6
 Varanavičius, Arunas-AM4A.28
 Vatnik, Sergei-AW5A.2
 Vedin, Ivan-AW5A.2
 Velmiskin, Vladimir V-JTh2A.4
 Vera, Alice-ITh5B.5
 Verdaasdonk, Rudolf-AM1A.5
 Verhoef, Aart J-AT3A.3, FTh1A.3
 Vernagallo, Christian-IW5D.7
 Vernaleken, Andreas-AM4A.12
 Viana, Bruno-JTh2A.8
 Vijayakumar, Deepak-AM4A.10
 Vincent, Bernard-AW4A.16
 Vivien, Daniel-ITh4B.3
 Vockerodt, Tobias-AT5A.6
 Vodopyanov, Konstantin L-AM1A.2
 Voigtländer, Christian-FW5C.3
 Vosylius, Vytautas-AW4A.17
 Vurgaftman, Igor-LM2B.5
 Vyatkin, Anton G.-AT4A.23

W

Wagenblast, Philipp-AM2A.1
 Wagner, Joachim-AM5A.4
 Wagner, Steven-LT5B.3
 Walsh, Brian M.-AT3A, AT4A.24
 Wandt, Dieter-AM4A.15, AM4A.24, AT4A.26
 Wang, Aimin-AT4A.28, JTh2A.28



Wang, Baishi-**FTh3A.2**
 Wang, Chih-Hao-**FTh3A.1**
 Wang, Nan-**AM4A.27**
 Wang, Qing-**FTh4A.4**
 Wang, Qingguo-**IW3D.1, IW3D.4**
 Wang, Rui-**AM4A.27**
 Wang, X. Y-**AT4A.7**
 Wang, Zhaohua-**AM4A.26**
 Washburn, Brian R-**ITh1B.2**
 Watanabe, K.-**ITh3B.4**
 Watanabe, Shuntaro-**AT4A.7**
 Weaver, Clark-**LT2B.6**
 Weber, Mark-**AM3A.4, AM3A.5**
 Wei, Kanxian-**FTh3A.1**
 Wei, Tao-**ITh1B.3, JTh2A.17, LT6B.3**
 Wei, Zhiyi-**AM4A.26, AM4A.27**
 Weiler, Sascha-**AM2A.1**
 Weipeng, Kong-**AM4A.1**
 Weiss, Stanley Benjamin-**AM3A.5**
 Wessels, Peter-**AM4A.4, AM4A.7**
 Whitney, Jean-**LT5B.5**
 Wickham, Michael-**AM3A.2**
 Wienke, Andreas-**AT4A.26**
 Willer, Ulrike-**LW5B.7**
 Williams, Paul A-**LT1B.4**
 Wilson, David-**LT1B.5**
 Wittwer, Valentin J-**AM5A.2**
 Witzel, Oliver-**LT5B.3**
 Wlodarczyk, Krystian L-**AW4A.19**
 Wolf, Martin-**AM2A.1**
 Worhoff, Kerstin-**AM5A.1, AM5A.6, AT4A.18**
 Wunderlin, Pascal-**LM3B.1**
 Wyoscki, Gerard-**LW5B.1, LW5B.5**

X

Xiang, Bin-**LT1B.2**
 Xiao, Hai-**ITh1B.3, JTh2A.17, LT6B.3**
 Xu, Bin-**IW5D.5, JTh2A.12**
 Xu, Fan-**JTh2A.15**
 Xu, Jun-**AT4A.11, IW3D.1, IW3D.4**
 Xu, Xiaodong-**IW3D.1, IW3D.4**

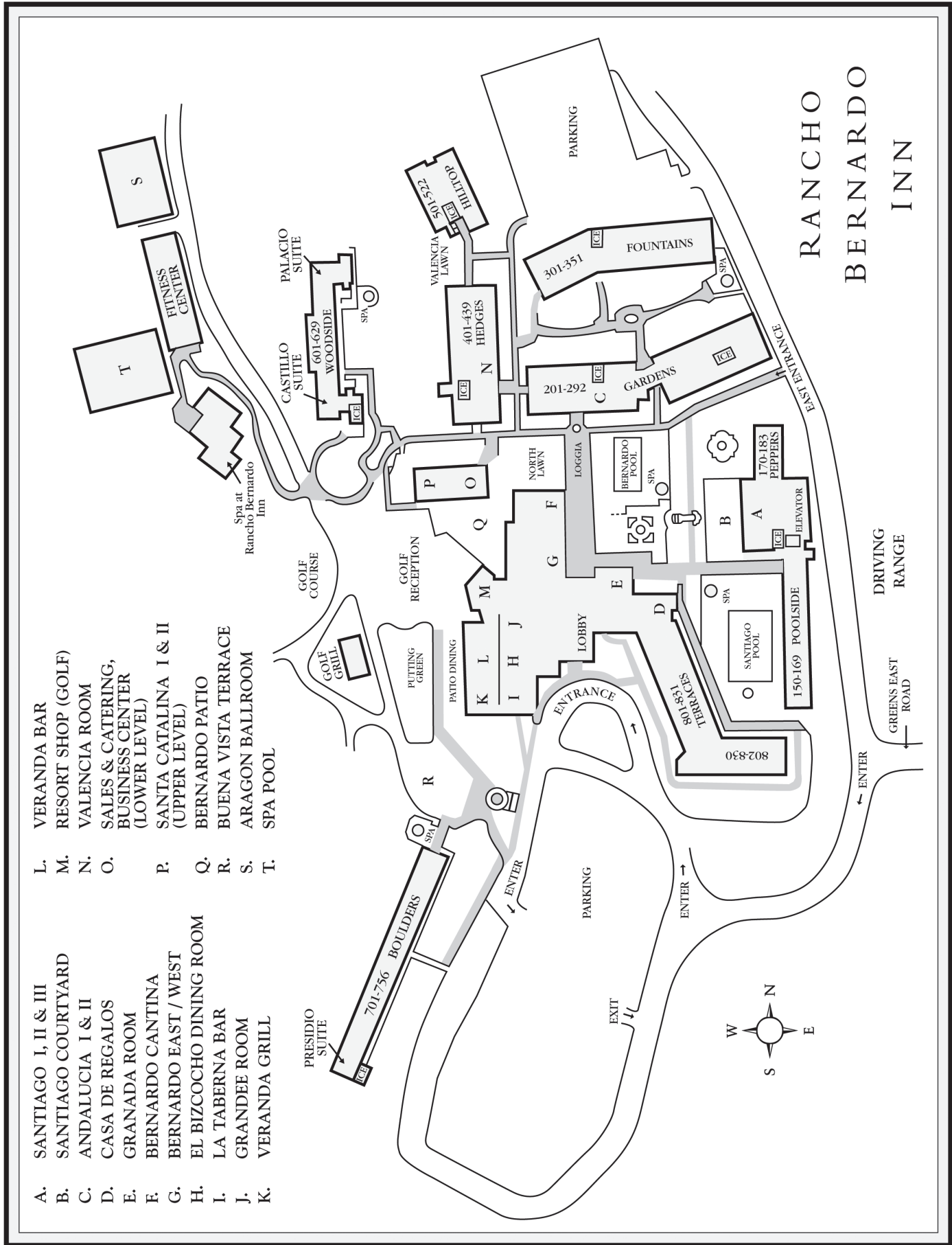
Y

Yagi, Hideki-**AM2A.4**
 Yajun, Wang-**AW4A.30**
 Yanagitani, Takagimi-**AM2A.4**
 Yang, Hongyu-**AT4A.28, JTh2A.28**
 Yang, Huinan-**LT3B.2**
 Yang, Kejian-**AT4A.11, IW3D.1**
 Yang, Quankui-**LM2B.6**
 Yang, Xiaoping S-**ITh5B.5**
 Yang, Zhiyong-**ITh4B.1**
 Yaohui, Zheng-**AW4A.30**
 Yaron, Lior-**JTh2A.20**
 Ye, Ziheng-**JTh2A.3**
 Yeom, Dong-Il-**AM2A.5, AW4A.12**
 Yoon, Tae Hyun-**FW5C.5**
 Yoshie, Tomoyuki-**JTh2A.13**
 Yu, Anthony W-**AW4A.26**
 Yu, Jirong-**FTh4A.1, LT5B.1**
 Yu, Xin-**AM4A.21**

Z

Zachhuber, Bernhard-**LT2B.4**
 Zagorodnev, Vladimir-**ITh1B.4**
 Zahniser, Mark-**LT1B.2**
 Zakharenkov, Yuri-**AW4A.5**
 Zaldo, Carlos-**IW3D.5**
 Zaouter, Yoann-**AT2A.6, AT4A.29, AT4A.5, FTh5A.2, FW5C.2**
 Zaukevičius, Audrius-**AM4A.28**
 Zavada, John Michael-**ITh5B, ITh5B.2**
 Zawilski, K.-**AM1A.4**
 Zawilski, Kevin-**AM1A.3**
 Zeludevicius, Julijanas-**AW4A.17, AW4A.21**
 Zhang, Huaijin-**AW4A.6**
 Zhang, Xiang-Hua-**JTh2A.14**
 Zhang, Zhigang-**AT4A.28, JTh2A.28**
 Zhang, Zhiguo-**LM3B.4**
 Zhao, Guangjun-**AT4A.11**
 Zhao, Yan-**LT6B.12**
 Zheng, Lihe-**AT4A.11, IW3D.1, IW3D.4**
 Zhou, Chun-**AT4A.7**
 Zhou, Tong-**AM4A.25**
 Zhu, Cheng-**AT1A.3**
 Zhu, Lingxiao-**AT3A.3, FTh1A.3**
 Zogg, Hans-**LM2B.3**
 Zondlo, Mark A-**LT5B.7**
 Zuegel, John D-**AW4A.8**





- | | | | |
|----|-------------------------|----|---|
| A. | SANTIAGO I, II & III | L. | VERANDA BAR |
| B. | SANTIAGO COURTYARD | M. | RESORT SHOP (GOLF) |
| C. | ANDALUCIA I & II | N. | VALENCIA ROOM |
| D. | CASA DE REGALOS | O. | SALES & CATERING,
BUSINESS CENTER
(LOWER LEVEL) |
| E. | GRANADA ROOM | P. | SANTA CATALINA I & II
(UPPER LEVEL) |
| F. | BERNARDO CANTINA | Q. | BERNARDO PATIO |
| G. | BERNARDO EAST / WEST | R. | BUENA VISTA TERRACE |
| H. | EL BIZCOCHO DINING ROOM | S. | ARAGON BALLROOM |
| I. | LA TABERNA BAR | T. | SPA POOL |
| J. | GRANDEE ROOM | | |
| K. | VERANDA GRILL | | |

Lasers, Sources, and Related Photonic Devices: OSA Optics and Photonics Congress Update Sheet 2012

Postdeadline Information:

LACSEA Postdeadline Session

Monday, 30 January 2012
18:30-18:45
Aragon III-B-C

ASSP Postdeadline Session

Monday, 30 January 2012
20:00-21:15
Aragon II

FILAS Postdeadline Session

Thursday, 2 February 2012
12:30-13:00
Aragon III-B

Presentation Changes:

IW3D.4 by Lihe Zheng will be presented at 14:00

IW3D.2 by Fabian Reicher will be presented at 14:30

Withdrawn Papers and Poster:

IW3D.1 is withdrawn, February 1, 2012 at 13:30

AM2A.1 is withdrawn January 30th at 10:30

Presenter Changes:

JTh2A.4 will be presented by Masha Chernysheva, *A.M. Prokhorov General Physics Institute, Russian Federation*

JTh2A.22 will be presented by Anton Ryabtsev; *Michigan State University, USA*

AW4A.13 will be presented by Efim Khazanov, *Institute for Applied Physics, Russian Academy of Sciences, Russian Federation*

Presider Changes:



Irina Sorokina of *Norges Teknisk Naturvitenskapelige University in Norway*

will preside over the OSA Speaker Series Wednesday, 1 February 18:00-19:00

Irina T. Sorokina was born in 1963 in Moscow, Russia. She received her Masters Degree in Physics and Mathematics from the Lomonosov State University in Moscow and Ph.D. degree in laser physics from the General Physics Institute of the Russian Academy of Sciences in 1992, and in 2003 a Habilitation degree in Quantum Electronics and Laser Technology from the Technical University of Vienna, where she has been working since 1991 as a PostDoc researcher, and then a University Lecturer and University Docent. Since

2007 she is a full professor of physics at the Norwegian University of Science and Technology in Trondheim, where she is leading a Laser Physics group, concentrating on the development of femtosecond solid-state and fiber lasers based on novel materials.

Irina T. Sorokina has authored and co-authored more than 300 publications and edited several books. In 2004 she was awarded the Snell Premium IEE Award for her contributions to the development of Cr:ZnS/Cr:ZnSe lasers. She is a Fellow of The Optical Society, and an elected member of the Norwegian Academy of Science and Letters.

Title Correction:

JTh2A.9 title was incorrectly printed in the program guide. The title should be *Bi-Al-Si-O Glass on Si-Substrates as a Potential Material for NIR Broad Band Planar Waveguide Applications: Synthesis and Characterization*

OSA Foundation Student Travel Award Winners:

Julius Darginavicius, *Vilnius University, Lithuania*

Hongyu Yang, *Institute of Quantum Electronics, Peking University, China*

Leonor Garcia-Martinez, *Centro de Ciencias Aplicadas y Desarrollo Tecnológico (CCADET), Mexico*

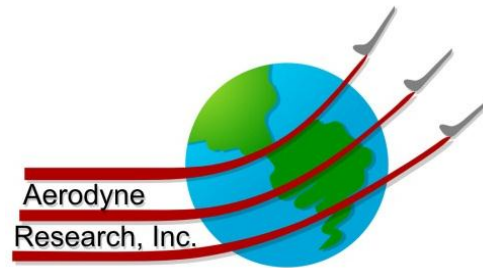
Laser Applications to Chemical, Security and Environmental Analysis (LACSEA) would like to thank the following Corporate Contributors for their outstanding support:



Student Award Sponsor



Silicon
Lightwave
Technology, Inc.



Fiber Lasers and Applications (FILAS) would like to thank the following Corporate Contributors for their outstanding support:



Student Award Sponsor:



Next generation fiber lasers
that you can control™

**Advanced Solid-State Photonics (ASSP) would like to thank
the following Corporate Contributors for their outstanding
support:**



Grant Support:

**Lawrence Livermore
National Laboratory**

Student Award Sponsor:

LOCKHEED MARTIN



2012 OSA
OPTICS &
PHOTONICS
CONGRESS

POSTDEADLINE PAPERS

Lasers, Sources and
Related Photonic Devices

Advanced Solid-State Photonics (ASSP)

Fiber Lasers and Applications (FILAS)

**Laser Applications to Chemical, Security
and Environmental Analysis (LACSEA)**

ISBN 978-1-55752-934-3

29 January – 3 February 2012

Rancho Bernardo Inn
San Diego, California, USA

www.osa.org/congresses

OSA[®]
The Optical Society

Postdeadline Sessions

Laser Application to Chemical Security, and Environmental Analysis (LACSEA)

Aragon III-B-C

Monday, January 30, 2012

18:30-18:45

LM5.1B • LACSEA Postdeadline Session

Waruna Kulatilaka, *Spectral Energies, LLC., USA, Presider*

LM5.1B.1 • 18:30

A New, Nondispersive Raman Analyzer to Measure Molecular Densities with high Sensitivity in Complex Environments, M. Fink¹, ¹Physics, The University of Texas at Austin, USA., ²P. Varghese, ²Center for Aeromechanics Research, The University of Texas at Austin, USA; ³J. Borysow, ³Physics Department, Michigan Technological University, USA. A novel Raman spectral analyzer will be used to measure the concentrations of dilute species in complex systems with high resolutions (0.3 cm⁻¹), and high sensitivity (0.1 Pa) within minutes. Examples of this are aqueous dissolved gases at the water-surface interface in oceans; or Hydrates imbedded in sub-surfaces.

Advanced Solid State Photonics (ASSP)

Aragon II

Monday, January 30, 2012

20:00-21:00

AM6A • ASSP Postdeadline Session

Andrius Baltuska, Vienna Univ. of Technology, Austria, Presider

AM6A.1 • 20:00

2 GW peak power ultrafast fiber system using passive coherent beam combining, Y. Zaouter¹, F. Morin¹, C. Hoenninger, E. Mottay¹, ¹ Amplitude Systems, Pessac, FRANCE; L. Daniault², M. Hanna, F. Druon², P. Georges², ² Laboratoire Charles Fabry, Institut d'Optique, CNRS, Université Paris-Sud, Palaiseau, FRANCE; ³D. Papadopoulos, ³ Institut de la Lumière Extrême, CNRS, Ecole Polytechnique, ENSTA Paristech, Institut d'Optique, Université Paris Sud, Palaiseau, FRANCE. Using passive coherent beam combining of two ultrafast fiber amplifiers, we demonstrate the generation of high temporal quality 300 fs 650 μJ pulses at 92 kHz repetition rate, corresponding to 60 W average power.

AM6A.2 • 20:15

250 W single crystal fiber Yb:YAG laser ; X. Délen¹, F. Balembois¹, P. Georges¹, ¹Laboratoire Charles Fabry, Palaiseau Cedex, FRANCE; ²S. Piehler, ²A. Voss, ²M. Abdou Ahmed, ²T. Graf, ² Institut für Strahlwerkzeuge (IFSW), GERMANY; ³ J. Didierjean, Fibercryst SAS, FRANCE; We demonstrate an Yb:YAG single crystal fiber laser with 251 W output power and 44 % efficiency. Oscillator performance shows potential power amplification from 40 W to 200 W in a double pass configuration.

AM6A.3 • 20:30

High power top-hat pulses from an Yb MOPA for efficient OPA pumping, ¹ T. Balciunas, ¹G. Fan, ¹G. Andriukaitis, ¹A. Pugzlys, ¹A. Baltuska, ¹Institute of photonics, Vienna University of Technology, Austria. We apply a programmable acousto optic dispersion filter for inline phase-only pulse shaping in a 6-mJ kHz DPSS Yb:CaF₂ amplifier resulting in near-rectangular 1030-nm pulses optimized for energy conversion in a white-light seeded parametric amplifier.

Postdeadline Sessions continued...

Advanced Solid State Photonics (ASSP)

AM6A.4 • 20:45

Stabilization of carrier-envelope phase with MHz bandwidth by an intra-cavity graphene electro-optic modulator, ¹C. Lee, S. Suzuki, ¹T.R. Schibli, ¹Physics, University of Colorado at Boulder, USA; ²C. Mohr, J. Bethge, ²M. Fermann, ²I. Hartl, ²IMRA America, USA. An intra-cavity, sub-micrometer thick graphene electro-optic modulator enables orthogonal offset-frequency control far beyond the stimulated lifetime of the gain medium. We demonstrate this new locking scheme in a Tm:fiber comb with record-low residual phase noise.

Fiber Lasers and Applications (FILAS)

Aragon III-B

Thursday, February 02, 2012

12:30-13:00

FTh3.1A • FILAS Postdeadline Papers

Nasser Peyghambarian, *Univ. of Arizona, USA*

FTh3.1A.1 • 12:30

Noise Characterization of a Mode-Locked, All-Fiber, All-Normal-Dispersion Ytterbium Ring Oscillator Using Two-Channel Polarization Control by a Computer, ¹D. Csati, ¹R. Szipocs, ¹Institute for Solid State Physics and Optics, Wigner Research Centre for Physics, Hungarian Academy of Sciences, Hungary; ²R. Szipocs, ²R&D Ultrafast Lasers Ltd., Hungary. Mode-locked operation of an all-fiber, all-normal dispersion Yb-fiber ring laser is actively optimized by a two-channel polarization controller according to the measured, normalised, single-sideband noise power.

FTh3.1A.2 • 12:45

Fiber Doppler Lidar for Precision Navigation of Space Vehicles, ¹F. Amzajerjian, ¹L. Petwat, ¹G. Hines, ¹B. Barnes, ¹NASA Langley Research Center, USA; ²D. Pierrottet, ²G. Lockard, ²Coherent Applications Inc., USA. A fiber-based coherent Doppler lidar capable of providing highly accurate vector velocity and altitude data has been developed for precision navigation of space vehicles landing on the Moon, Mars, or asteroids.

A New, Nondispersive Raman Analyzer to Measure Molecular Densities with high Sensitivity in Complex Environments

Manfred Fink

*The University of Texas at Austin,
Physics Department, RLM Bldg. 10.315, Austin, TX 78712
fink@physics.utexas.edu*

Philip Varghese

*The University of Texas at Austin
Center for Aeromechanics Research, C0604, Austin TX 78712*

Jacek Borysow

*Michigan Technological University
Physics Department, Houghton, MI*

Abstract: A novel Raman spectral analyzer will be used to measure the concentrations of dilute species in complex systems with high resolutions (0.3 cm^{-1}), and high sensitivity (0.1 Pa) within minutes. Examples are: aqueous dissolved gases at the water-surface interface in oceans; or Hydrates imbedded in sub-surfaces.

A new Raman spectral analyzer has been developed which can be lowered into the ocean to any desired depths up to 8000 meters. This instrument is small, rugged and specially designed to record several preselected compounds with high resolution and high sensitivity. The detector unit and the incident laser are physically separated and they communicate by optical fibers. Therefore, data can be recorded in hostile environments such as elevated temperatures and in loosely packed deposits such as sands. We are also investigating applications to trace isotopes distributions to do analysis of breath, and to help to understand the progressing hypoxia in the Gulf of Mexico by isotope dilution.

Usually gas chromatograph mass spectrometer systems are used to do the analysis, however spontaneous Raman spectroscopy is a more suitable technique to achieve these goals [1] because it is portable, much cheaper and needs no skilled operator. The laser light incident on the species of interest will polarize their electron cloud and scatter on the induced dipole moment. This is a non-resonant process and therefore no primary or secondary extinction occurs and absolute target densities can be recorded. Furthermore this process suppresses all higher harmonics and combination lines, which makes the spectrum very lean and free of interferences.

Figure 1 shows a design of a Raman instrument. A single mode diode laser beam enters a multi-pass cell formed by 2 highly reflective, concave mirrors. The molecules present at the focal point scatter the light elastic, producing the Rayleigh light, and inelastic generating the spontaneous Raman spectrum. The deflected photons are collected at right angles to the incident radiation. In one direction (up in fig.1) an optical system collects the light with a large acceptance cone, and the Raman spectrum is recorded with a 0.4 m spectrometer equipped with a CCD-camera [2]. The multi-pass cell is an addition to the common Raman unit. It will increase the scattered light intensity by the number of passes we could reach (up to 85). This gain will also apply to the elastic scattered photons (Rayleigh light) which are often 6 orders of magnitude larger than the Raman intensities. Therefore, the diode laser is tuned to the D1 or D2 transition of

Rubidium or Cesium. The Rayleigh component will be removed very effectively by passing the scattered light through a cell, which contains the alkali vapor [2]. The spectrum can now be recorded free of interferences from background radiation. We demonstrated the effectiveness of this procedure with the rotational Raman spectrum of H_2 at the ppm level [3]

The improved generic Raman instrument, described above, must be modified further when solutes are to be analyzed, such as CO_2 , NO_3 or CH_4 -hydrates. We built a very small multi-pass cell (size: 3x3x5 cm), which is filled with the surrounding frit filtered water at the local hydrostatic pressure determined by the submerged depth. The design is shown in figure 2. Two gold coated, planar /convex lenses form the multi-pass cavity. The planar, uncoated sides are in contact with the saltwater. Attenuations due to refraction are avoided because the index of reflection of BK7-glass and saltwater are very close to each other. The convex backsides of the lenses are coated with protected gold layers (200 nm thick) forming the spherical mirrors needed for the multi pass arrangement. Small stainless steel welded bellows compress the distilled water and generate equilibrium between the pressure in the cell and the surrounding water.

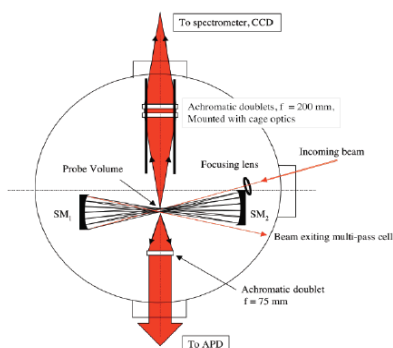


Fig. 1 Generic Raman Spectrometer

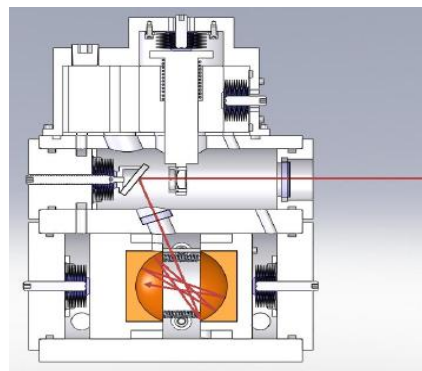


Fig. 2 Raman Analyzer Head with Multi-pass Cell

A diode laser beam, guided by a single mode fiber, is focused into the center of the multi pass cell by an entrance lens. The photons inelastic scattered from the foci generate the Raman spectrum. The photons, leaving at right angles to the incident light, exit the cell through a cylindrical opening with anti-reflection coated windows to be focused into a multi-mode fiber, which is connect with the detector system. The optical fibers separate the Raman head from the analyzer and can thus be employed in hostile environments. The intake manifold is built with a welded bellow which is compressed and expanded by a plunger activated by a rotating housing as seen in Figure 3. The in-port and out- port are covered with ultra fine frits to prevent impurities to enter the multi pass cell and cause undesired fluorescence.

Figure 4 shows the spectral analyzer. The light from the multi mode fiber collected from the Raman cell will pass a narrow band pass filter (about 3 nm). Most light will be reflected except the spectral lines whose frequencies are within the window of the filter. Table 1 shows the species which are currently accessible. The set-up, seen in figure 4, extents the analysis to extremely high resolution (about 0.1 cm^{-1}). This is very helpful when 2 spectral lines are very close to each other as is common for spectra of isotopomers. Note this resolution is achieved without loss of sensitivity.

Currently our non-dispersive Raman technique is applied to the measurements of the NH_4^+ and NO_3^- ion concentrations in the water of the Gulf of Mexico. This study was stimulated by the researchers at the Marine Institute at Port Aransas of the University of Texas. We plan to

determine the nitrification of the Gulf and the development of the hypoxic zones. These measurements are carried out on samples which have been taken from boats and frozen on site to be analyzed in the laboratory later. Our Raman set-up will speed-up this analysis 50-fold and increases the sensitivity by about a factor 10. [4]

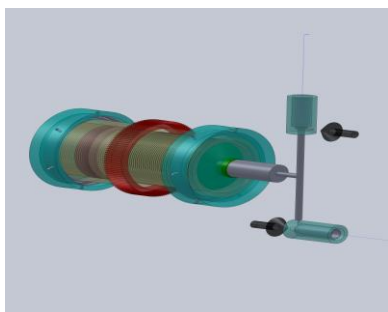


Fig. 3 Sample inlet system

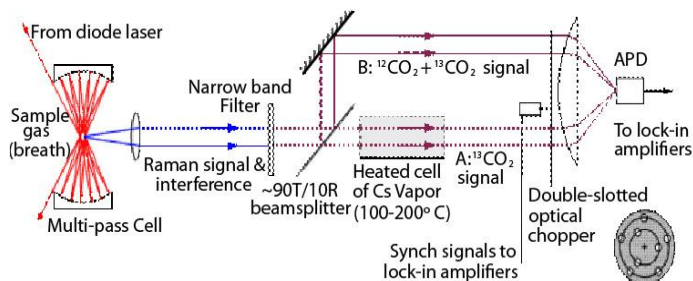


Fig. 4 Detector system of our Raman spectral analyzer

Table 1 Raman frequencies of some small molecules

O ₂	1551 cm ⁻¹	N ₂	2331 cm ⁻¹	H ₂ (J=0)	364 cm ⁻¹	D ₂ (J=0)	179 cm ⁻¹
¹² CO ₂	1388 cm ⁻¹	¹³ CO ₂	1370 cm ⁻¹	CO	2147 cm ⁻¹	H ₂ O(aqua)	1648 cm ⁻¹
NO ₃	1145 cm ⁻¹	NO ₂	1325 cm ⁻¹	N ₂ O	1281 cm ⁻¹	NO	1904 cm ⁻¹
NH ₄ ⁻	1405 cm ⁻¹	NO ₃ ⁺	1463 cm ⁻¹	H ₂ S	1218 cm ⁻¹	SO ₂	1149 cm ⁻¹

For this work and in order to extend the measurements to complex environments we have to separate the Raman head and the analyzer and reconnected them with optical fibers. Their individual performance remains the same. Many experiments can be carried out either at GEO-MAR at Kiel, Germany [5] or at ARL and the Physics Department at The University of Texas at Austin in high pressure tanks which can be filled with sand, water and gases to prepare a data base, as a function of concentrations, pressure and temperature, for comparisons with data taken in the ocean[6], [7]. The most important progress we can achieve is to focus on the hydrates; they have been studied in detail at GEO-MAR with X-ray diffraction and standard Raman spectroscopy. Our instrument will reproduce the previous measurements in the same containers but with nearly 100-fold higher sensitivity.

[1] H. Amann, "Laser Spectroscopy for Monitoring and Research in the Ocean," Physics Scripta, T78, 68 (1998)

[2] J. Sabbaghzadeh, W. Buell, J. Holder and M. Fink, "A Very Narrow, High-Throughput Rayleigh Filter For Raman-Spectroscopy," Applied Physics B-Lasers and Optics 60, S261 (1995)

[3] J. Borysow and M. Fink, "NIR Raman spectrometer for monitoring protonation reactions in gaseous hydrogen," J. Nuclear Materials 341, 224 (2005)

[4] Wayne Gardner, University of Texas at Austin, Marine Institute, Port Aransas

[5] GEO-MAR[6] Xin Zhang, P. M. Walz, W. J. Kirkwood, K. C. Hester, W Ussler, E.T. Peltzer and P. G. Brewer, Deep Sea Research I, <57>, 297, 2010

[7] Xin Zhang, K. C. Hester, W. Ussler, P. M. Walz, E. T. Petzler and P. G. Brewer, "In situ, Geophysical Research Letters, <38>, L08605, 2011

2 GW peak power ultrafast fiber system using passive coherent beam combining

Yoann Zaouter,^{1,*} Louis Daniault,² Marc Hanna², Dimitris N. Papadopoulos³, Franck Morin¹, Clemens Hönninger¹, Frédéric Druon², Eric Mottay¹, and Patrick Georges²

1 Amplitude Systèmes, 6 allée du Doyen Georges Brus, 33600 Pessac, France

2 Laboratoire Charles Fabry de l'Institut d'Optique, CNRS, Université Paris Sud, RD 128, 91127 Palaiseau Cedex, France

3 Institut de la Lumière Extrême, CNRS, Ecole Polytechnique, ENSTA Paristech, Institut d'Optique, Université Paris Sud, Palaiseau Cedex, France

Author e-mail address: yzaouter@amplitude-systemes.fr

Abstract: Using passive coherent beam combining of two ultrafast fiber amplifiers, we demonstrate the generation of high temporal quality 300 fs 650 μ J pulses at 92 kHz repetition rate, corresponding to 60 W average power.

OCIS codes: (320.7110) Ultrafast nonlinear optics; (190.4360) Nonlinear optics, devices; (140.3510) Lasers, fiber

1. Introduction

The peak power obtained from high repetition rate ytterbium-doped ultrafast fiber amplifiers has grown extremely rapidly during the last decade to reach the multi-GW level owing to the development of very large mode area fiber designs [1]. To further scale this peak power and obtain compact and efficient high repetition rate high energy sources, the coherent combination of several such femtosecond fiber lasers has recently been demonstrated. Early demonstrations have involved an active control of the relative phase between two fiber chirped-pulse amplifiers (FCPA). A first experiment used the measurement of the polarization state of the combined beam, and a feedback on a piezo-mounted mirror located in one amplifying arm [2]. The same group scaled up the performances to a record energy of 3 mJ [3]. A second demonstration was based on of the frequency tagging technique [4], while the feedback is done through an integrated fiber-coupled LiNbO₃ phase modulator [5]. Both these implementations have demonstrated feedback bandwidths in the 1-10 kHz range. They require complex opto-electronic feedback schemes, and the stability of such sources in noisy environments will depend on the sophistication of the feedback loop. Recently, we proposed an alternative technique to achieve coherent combining of two amplifiers in a passive architecture involving a Sagnac interferometer [6]. The phase stability of this simple scheme is inherently guaranteed by the fact that both combined beams travel along the exact same optical path in a counter propagating geometry. Our proof-of-principle experiment showed that the passive technique is compatible with high nonlinearity levels, and that the limiting factor is the ability to maintain the symmetry of both paths. In this contribution, we use the passive combining architecture and rod-type fiber amplifiers to generate high temporal quality 300 fs pulses with 650 μ J of energy per pulse at a repetition rate of 92 kHz. This corresponds to an average power of 60 W, and a peak power in excess of 2 GW. Furthermore, at 2 MHz of repetition rate, combining average powers of 135 W before and 105 W after compression have been measured. These results clearly demonstrate the potential of the technique in a high performance fiber system.

2. Experimental setup and results

Figure 1 shows the experimental setup used in our work. To maintain a good temporal pulse quality simultaneously with a high energy level, we implement a moderately nonlinear FCPA in which the impact of nonlinearities is partially compensated by the dispersion mismatch of the stretcher and compressor units [7]. Furthermore, the two amplifiers that we intend to coherently combine are built within a Sagnac interferometer that is seeded, through an optical isolator, by a frontend. This frontend is composed of a passively mode-locked ultrafast oscillator, a pulse picker, a pulse stretcher, and a single-mode fiber pre-amplifier. The oscillator generates pulses at the central wavelength of 1030 nm. The full width at half maximum of the spectrum is 9 nm and sustains pulse durations below 200 fs. The repetition rate of the oscillator of \sim 25 MHz is divided by an acousto-optic modulator pulse picker and can be varied from 92 kHz to 25 MHz. Sufficient pulse stretching is then applied to the pulses in order to mitigate the impact of nonlinearities in the power amplifiers. The stretching ratio is designed to preserve a pulse duration of \sim 600 ps after the power amplifiers when operated at maximum gain. A single mode fiber amplifier is used to boost the average power to about 100 mW, which is sufficient to seed both power amplifiers. An optical isolator is placed after the frontend to prevent any optical feedbacks coming from the power amplifiers. It is also used to separate the combined and the uncombined outputs of our passively coherently combined amplification

scheme. Then, the beam is split by a polarizer and each secondary beams seed a power amplifier (denoted as Amp #1 and Amp #2, *see* Figure 1) made of state-of-the art ytterbium-doped rod-type photonic crystal fibers. These rigid fibers are kept straight in un-cooled V-groove holders and are optically pumped by 976 nm fiber coupled pump diodes. The mode field diameter of the fibers is 85 μm , the pump cladding diameter is 285 μm and their length of 1 m ensures sufficient pump absorption and optical efficiency [8]. The outputs of each amplifier are connected to each other to close the Sagnac interferometer. Therefore, after the polarizer, the light propagating clockwise is first pre-amplified in Amp #1 and then amplified in Amp #2 while the light travelling counterclockwise is first pre-amplified in Amp #2 before reaching its maximum power / energy at the output of Amp #1. Both beams are then recombined on the polarizer, with linear polarizations orthogonal to each other. If both beams are in-phase, they form a combined output beam propagating back to the isolator with a linear polarization state at an angle of 45°. This beam is therefore transmitted back through the rotator and ejected by the polarizer located at the input of the isolator. The uncombined part of the beam is removed by the polarizer located at the output of the isolator. Measurement of the average power at both outputs allows us to compute the combination efficiency defined as the ratio between the combined power and the total power.

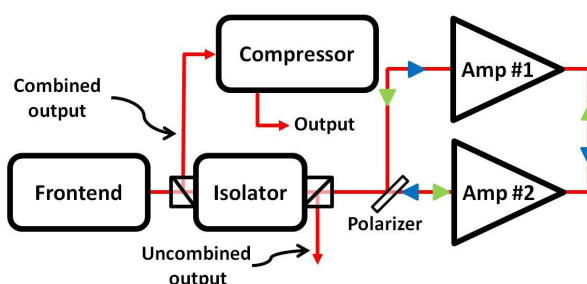


Figure 1 : Experimental setup

The path length for one round trip in the Sagnac interferometer is 5.5 m, making this setup immune to all phase noises with frequency contents below 27 MHz. This large bandwidth essentially removes all environmental sources of noise such as acoustic and thermal fluctuations of the relative phase. To highlight the robustness of this architecture with respect to phase noise, we compare the pulse-to-pulse relative power fluctuation of the frontend to the one measured at the output at maximum energy. This pulse-to-pulse stability is 1.1% for the frontend, and reaches 2% at the maximum compressed energy. This very small decrease of the pulse-to-pulse stability for a nonlinear FCPA, built on an uncovered breadboard, clearly indicates that phase noise has very little impact, if any, on the global coherent combination stability. This is of particular importance if lasers using our passive coherent combination architecture are to be used in harsh environments or if the pulse-to-pulse stability is of particular importance for the targeted scientific or industrial applications. Finally, the coherently combined beam is sent through a compressor optimized to get the highest possible peak power. The high efficiency gratings used allow for only 21 % loss in the compressor. The passive coherent combination setup described above is first aligned at low power and low energy in order to obtain the best possible degree of combination related to spatial aspects such as beam profile and wavefront mismatch. We found out that slight differences in the rod type fibers end-facet preparation is currently the main limitation to the combination efficiency, with a maximum value of ~95%. The pulse picker is then set to down-counter the repetition rate of the frontend to 92 kHz. Figure 2 shows the amplifier characteristics at this repetition rate with the combined and uncombined average powers measured at the output ports of the isolator. At the maximum total pump power of 160 W, we reach 75 W of passively coherently combined power, i.e. 815 μJ , with a slope efficiency close to 60 %. It is noticeable that despite the accumulation of a large quantity of nonlinear phase shifts in the amplifiers (estimated to be ~7 rad per roundtrip), the combining efficiency decreases by less than 3.5 %. We investigated the origin of this loss and found out that nonlinearity mismatch between the two circulating directions is the main source of drop in combining efficiency. Indeed, at 75 W and 2 MHz of repetition rate the rejected uncombined power is only 5W, resulting in a combining efficiency close to 94 %. At even higher average power we see another roll off in efficiency that originates from a worst spatial overlap of the two beams. Nevertheless, for 270 W of total pump power at 2 MHz of repetition rate, we reached 135 W of coherently combined power with a passive coherent combining efficiency of 91.5 %. The compressed average power of 105 W (pulse duration < 300 fs) is to our knowledge the highest average power ever generated by any active or passive coherently combined ultrashort amplifiers.

We now investigate the compressibility of the amplified pulses at maximum energy. At 92 kHz, the maximum average power measured after the compressor is 60 W (76 W before) i.e. 650 μJ of energy per pulse. Figure 3 shows the autocorrelation traces acquired with an intensity autocorrelator and independently measured with a second-harmonic generation frequency-resolved optical gating apparatus (FROG). These autocorrelations

can hardly be differentiated and exhibit a FWHM duration of 400 fs. Figure 3 also shows the retrieved temporal profile of the pulse from the FROG measurement. Its duration is 300 fs, corresponding to a time-bandwidth product (TBP) of 0.75. The very good temporal quality obtained allows us to measure a peak power in excess of 2 GW.

Finally, we analyze the beam quality after compression. M^2 measurements are systematically carried out and show no degradation of the beam quality with increasing combined average power with constant values of $M_x^2 = 1.25$ and $M_y^2 = 1.15$.

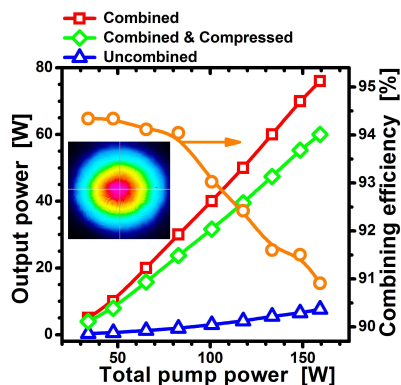


Figure 2: Left scale: output powers of the amplifier as a function of pump power at a repetition rate of 92 kHz. Right scale: combining efficiency as a function of pump power. Inset: beam profile taken at maximum energy at the output of the system.

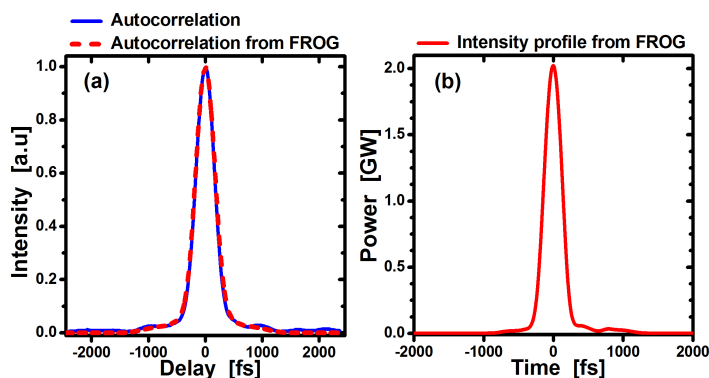


Figure 3: (Color online) (a) Autocorrelation traces measured at 650 μ J (blue) with an independent autocorrelator and (red dash) from a FROG measurement. (b) Retrieved temporal profile of the pulse from the FROG measurement (Error $27 \cdot 10^{-4}$ on a 256×256 grid).

3. Conclusion

In conclusion, we demonstrate a significant performance scaling of the passive coherent combining concept introduced in Ref. [5] in a moderately nonlinear FCPA. The use of state-of-the-art ytterbium-doped rod-type photonic crystal fibers permits to generate ultrashort pulses with 650 μ J of energy per pulse together with a measured duration of 300 fs at a repetition rate of 92 kHz. The very good temporal quality of the recompressed pulses allows obtaining more than 2 GW of peak power. At the higher repetition rate of 2 MHz, 135 W of passively coherently combined average power resulting in 105 W of compressed average power has been measured which is to our knowledge the highest average power ever reported from an ultrafast coherent combining system. All the performances reported in this Letter have been obtained with combination efficiencies over 90 %. Moreover, a careful preparation of the end-facets of the fibers together with a better thermo-mechanical management could help increasing this value. The authors strongly believe that this concept of amplification has the potential to generate more than 10 GW of peak power. This could be directly obtained with an additional post compression module based on a hollow core fiber or by increasing the stretching ratio to the level of Ref. [1]. The average power of these fiber systems could also be scaled to 1.5 kW by using adequate fiber designs such as those demonstrated in Ref. [9], with pulse duration well below 500 fs in all cases.

4. References

- [1] Tino Eidam, Jan Rothhardt, Fabian Stutzki, Florian Jansen, Steffen Hädrich, Henning Carstens, Cesar Jauregui, Jens Limpert, and Andreas Tünnermann, *Opt. Express* 19, 255-260 (2011)
- [2] Enrico Seise, Arno Klenke, Jens Limpert, and Andreas Tünnermann, *Opt. Express* 18, 27827-27835 (2010)
- [3] Arno Klenke, Enrico Seise, Stefan Demmler, Jan Rothhardt, Sven Breitkopf, Jens Limpert, and Andreas Tünnermann, *Opt. Express* 19, 24280-24285 (2011)
- [4] T. Shay, V. Benham, J. T. Baker, A. D. Sanchez, D. Pilkington, and C. A. Lu, *IEEE J. Sel. Top. Quantum Electron.* 13, 480 (2007).
- [5] L. Daniault, M. Hanna, L. Lombard, Y. Zaouter, E. Mottay, D. Goular, P. Bourdon, F. Druon, and P. Georges, *Opt. Lett.* 36, 621-623 (2011)
- [6] Louis Daniault, Marc Hanna, Dimitris N. Papadopoulos, Yoann Zaouter, Eric Mottay, Frédéric Druon, and Patrick Georges, *Opt. Lett.* 36, 4023-4025 (2011)
- [7] Y. Zaouter, J. Boulet, E. Mottay, and E. Cormier, *Opt. Lett.* 33, 1527-1529 (2008)
- [8] F. Röser, D. Schimpf, J. Rothhardt, T. Eidam, J. Limpert, A. Tünnermann, and F. Salin, *Advanced Solid-State Photonics*, OSA 2008, paper WB22.
- [9] Tino Eidam, Stefan Hanf, Enrico Seise, Thomas V. Andersen, Thomas Gabler, Christian Wirth, Thomas Schreiber, Jens Limpert, and Andreas Tünnermann, *Opt. Lett.* 35, 94-96 (2010)

250 W single crystal fiber Yb:YAG laser

Xavier Délen^{1,*}, Stefan Piehler², Julien Didierjean³, Andreas Voss², Marwan Abdou Ahmed², Thomas Graf², Francois Balembos¹, and Patrick Georges¹.

¹Laboratoire Charles Fabry, Institut d'Optique, CNRS, Univ Paris-Sud, 2 Av A. Fresnel, Palaiseau, France

²Institut für Strahlwerkzeuge (IFSW), Universität Stuttgart, Pfaffenwaldring 43, 70569 Stuttgart, Germany

³Fiberocryst SAS, La Doua-Bâtiment l'Atrium, Boulevard Latarjet, F- 69616 Villeurbanne Cedex, France

*Corresponding author: xavier.delen@institutoptique.fr

Abstract: We demonstrate an Yb:YAG single crystal fiber laser with 251 W output power and 44 % efficiency. Oscillator performance shows potential power amplification from 40 W to 200 W in a double pass configuration.

OCIS codes: (140.3615) Lasers, ytterbium; (140.3480) Lasers, diode-pumped

1. Introduction

High average-power pulsed lasers are widely used in materials processing. Above 100 W of average power, Yb-doped diode-pumped solid-state lasers implemented in master oscillator power amplifier configuration clearly dominate this field of application with pulse durations ranging from ns to fs. However, closer investigations showed that different technologies can be used, each having individual advantages and drawbacks. Optical fiber lasers have proven to be very efficient and to enable high output powers in the continuous wave regime with up to several kW output power in multimode operation. However, due to the strong signal confinement, their use is limited by the damage threshold of the facets and non linear effects such as self focusing in pulsed regime [1]. The thin disk technology does not exhibit this limitation in pulsed regime but suffers from a weak small signal gain due to the tiny disk thickness usually used [2] leading to limited energy per pulse and to complex amplifier setups. Finally, the slab technology has recently shown clear competitive advantages with over 1kW of output power obtained in femtosecond regime [3]. Its drawback is the complexity of the signal beam propagation through the gain medium. Therefore, simple and versatile high power amplifiers for pulsed operation are still a subject to research.

In this paper, we show that single crystal fibers might be an alternative to these technologies. A single crystal fiber consists of a crystal rod of a few centimeters length and a typical diameter of 1 mm in which a pump beam provided by a fiber coupled laser diode is guided by total internal reflection while the signal beam is not guided. This concept provides a good thermal management thanks to the high thermal conductivity of Yb:YAG and the high surface-to-volume ratio offered by the relatively thin and long rod geometry. Moreover, it enables the use of low brightness diode lasers in combination with a long crystal thanks to pump guiding.

Up to now, a maximum of 65W of output power in continuous-wave has been demonstrated using an Yb:YAG single crystal fiber at a pump power of 200W at 940 nm [4]. It has started to reveal its potential as femtosecond amplifier with a combination of high gain (30) and significant output power (12W) in a very simple two-pass configuration [5]. In this paper, we propose an exploration of the step further in terms of power scaling and report on the performances of Yb:YAG single crystal fiber oscillator pumped at 600 W with a fiber coupled laser diode. Furthermore, we discuss the potential of this technology for its use as a power amplifier.

2. Concept

The idea of the single crystal fiber technology is to use a thin and long crystal rod in which the pump is guided by total internal reflection and the signal is in free propagation, permitting a better control of the signal mode. The crystal used in our experiments has a length of 40 mm and a diameter of 1 mm. With a low doping concentration of 1%, the distribution of the thermal load over the relatively long length of the rod reduces the temperature increase in the gain medium. Additionally, the small transverse dimension of the rod provides an efficient radial cooling and hence a limited temperature increase in the crystal. Finite element analysis indicates that the small distance between the edge of the crystal and the center results in maximum temperature increases as small as 46 degrees for 600 W of incident pump power when using a 1 mm diameter 40 mm long fiber with 90% overall absorption and a 600µm pump spot diameter. The same temperature difference for a more conventional 3 mm diameter rod would be over two times higher with 117 degrees.

Low doping concentration and small transverse dimensions are not the only parameters to limit the temperature increase: the thermal contact between the gain medium and its cooled mount may be a key issue as well. This might even become critical when the reduced diameter limits the exchange surface with the mount. As shown in [4], the thermal contact was responsible of 80% of the temperature increase in a single crystal fiber surrounded by thermal

grease in a non-optimized mount. In collaboration with Fibercryst we have performed an excellent metallic contact in single crystal fiber TARANIS modules [6] as shown in [7] : a temperature difference between the crystal edge and the module of below 5°C has been measured for 86W of incident pump power at 808 nm on a 0.2% doped Nd:YAG.

The pump guiding in the single crystal fiber allows increasing the overlap between the pumped beam and the signal beam in free propagation when compared to standard bulk technology. Using ray tracing analysis with Apilux software, we obtained the pump intensity distribution in the fiber, clearly showing a higher intensity in the central area of the fiber (fig 1.a). This pump intensity was calculated for a 0.22 NA and 600 μm diameter pump on a single crystal fiber of 1mm diameter assuming no absorption. The geometrical overlap between a flat-top signal beam and the pump beam is given as a function of the signal beam radius in figure 1-b. It shows that up to 69% of overlap can be obtained for a signal beam radius of 350 μm which covers 70% of the total rod radius.

Fig 1-c shows the overlap between a 700 μm diameter pump and a flat-top signal in each plane along the propagation axis. The overlap first increases until the focal point is reached (see fig 1-a) and starts decreasing afterwards until it reaches a minimum of 56% at a distance of about 9 mm from the entrance face of the fiber, corresponding to a position where major part of the pump beam is reflected on the fiber surface. For the last 2 cm of fiber length, the overlap remains almost constant with a value of 67%. Considering a 90% overall absorption, we have calculated the overlap increase to be 2.3 times higher than what would be obtained in the same configuration without pump guiding.

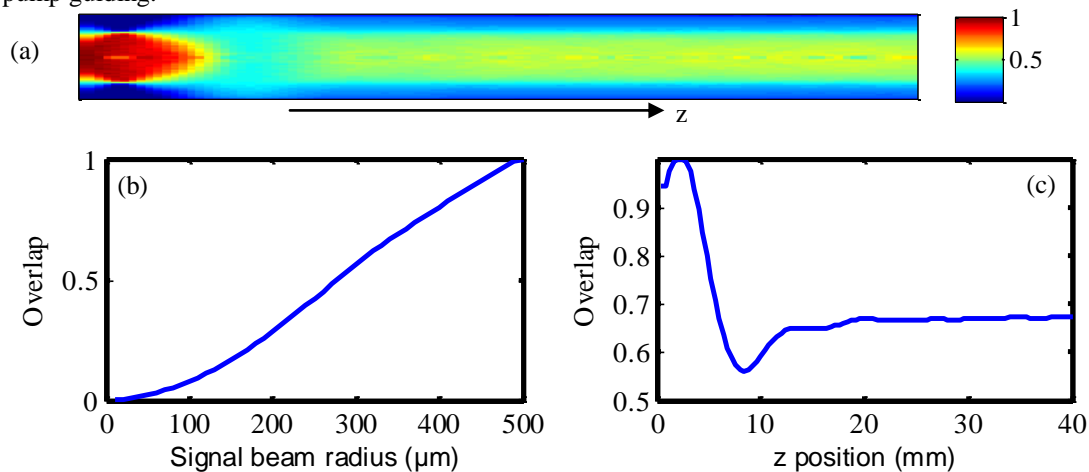


Figure 1 – (a) Pump intensity distribution for a 1 mm diameter 40 mm long single crystal fiber. (b) Total geometrical overlap between the pump beam and a flat-top signal beam as a function of the signal beam radius. (c) Geometrical overlap between the pump beam and a 700 μm diameter flat-top beam as a function of the axial position.

3. Experimental results

In order to explore the potential of the single crystal fiber in terms of power scalability, a simple two mirrors cavity design has been used. As shown in figure 2, the single crystal fiber was placed in between a meniscus of 50 mm radius of curvature and an output coupler of 100 mm radius of curvature. A fiber coupled diode laser emitting at 940 nm with 600 μm core diameter, 0.22 NA and 600 W of maximum output power was used for optical pumping. The fiber output was imaged onto the crystal with a 1:1 magnification ratio using 2 aspheric lenses of 50 mm focal length. The TARANIS module provided by Fibercryst contained a 40 mm long 1 mm diameter 1% doped Yb:YAG single crystal fiber placed in a 3x40x70 mm³ copper block. Two copper microchannel plates were used to cool the module. The mounts of the aspheric lenses and the mirrors were water cooled in order to limit the temperature increase of the optics due to residual absorption. A dichroic mirror was used to filter out the residual pump power for the output power measurement.

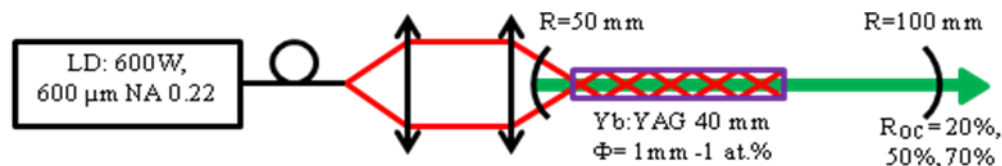


Figure 2 – Experimental setup

The output power as a function of the incident pump power was measured for three different output couplers having reflectivities of 20%, 50% and 70%. A maximum output power of 251 W was measured for an output mirror reflecting 70% and an incident pump power of 570 W. The optical efficiency is 44% and the slope efficiency reaches 53%. To the best of our knowledge, this is the highest efficiency ever measured in a single crystal fiber laser. As shown in figure 3, no rollover is visible on the efficiency curve showing that further power scaling should be possible. Finite Element Analysis indicates, that the pump power limit before fracture should be at 1kW for one pumped face.

The beam profile at full pump power is shown on figure 4. We measured a beam quality factor M^2 of about 15. This is presumably due to the cavity design and to the low brightness of the pump which does not provide a soft aperture mode filtering as observed previously [4].

The lowest reflecting mirror ($R_{oc}=20\%$) can give an idea of the potential of the gain medium as power amplifier. Neglecting passive losses, laser oscillation with this mirror means that the active medium provides a saturated gain of 5. This gain might supposedly be even higher, if passive losses are taken into account. At maximum pump power, the output power of 200W (fig 3) means that the gain medium amplifies the intracavity beam from 40W (the fraction of power reflected by the 20% output coupler) to 200 W in one roundtrip. This reveals the high potential of single crystal fiber technology providing both high gain and high extraction efficiency for power amplifier design.

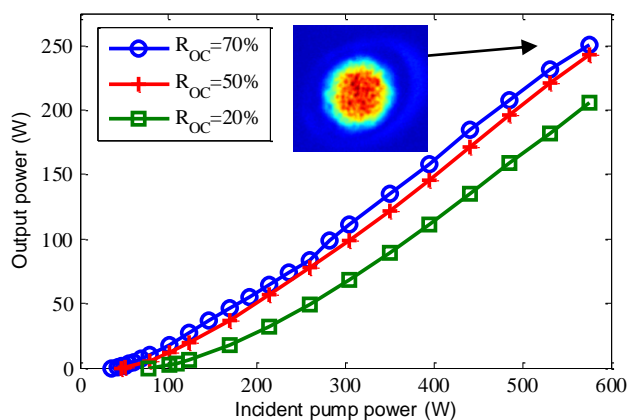


Figure 3 – Efficiency curves

4. Conclusion

We have demonstrated the potential of the single crystal fiber technology for the high power regime with over 250 W of output power obtained out of an Yb:YAG continuous wave laser. To our knowledge, this is a record, exceeding previous results reported on single crystal fibers by a factor of 4. This corresponds to an optical efficiency of 44 % and a slope efficiency of 53 % representing the highest efficiency ever achieved with a single crystal fiber laser. The analysis of the performances obtained with a low reflecting output coupler indicates that a power amplifier boosting power from 40W to 200 W in a two pass configuration should be feasible with this Yb:YAG single crystal fiber. This proves that the route towards simple and efficient power amplifiers in the "100W class" is widely opened for Yb:YAG single crystal fibers.

Xavier Délen acknowledges the French DGA for the funding of his PhD.

5. References

- [1] D. J. Richardson, J. Nilsson, and W. A. Clarkson, "High power fiber lasers: current status and future perspectives," *J. Opt. Soc. Am. B* 27, B63-B92 (2010).
- [2] D. Blázquez-Sánchez, B. Weichelt, A. Austerschulte, A. Voss, Th. Graf, A. Killi, H. C. Eckstein, M. Stumpf, A. L. Matthes, and U. D. Zeitner, "Improving the brightness of a multi-kilowatt single thin-disk laser by an aspherical phase front correction," *Opt. Lett.* 36, 799-801 (2011).
- [3] P. Russbuedt, T. Mans, J. Weitenberg, H. D. Hoffmann, and R. Poprawe, "Compact diode-pumped 1.1 kW Yb:YAG Innoslab femtosecond amplifier," *Opt. Lett.* 35, 4169-4171 (2011).
- [4] D. Sangla, I. Martial, N. Aubry, J. Didierjean, D. Perrodin, F. Balembois, K. Lebbou, A. Brenier, P. Georges, O. Tillement, and J. M. Fournigie, "High power laser operation with crystal fibers," *Appl. Phys. B* 97, 263-273 (2009).
- [5] Y. Zaouter, I. Martial, N. Aubry, J. Didierjean, C. Hönninger, E. Mottay, F. Druon, P. Georges, and F. Balembois "Direct amplification of ultrashort pulses in μ -pulling-down Yb:YAG single crystal fibers," *Opt. Lett.* 36, 748-750 (2011).
- [6] www.fiberocryst.com
- [7] X. Délen, I. Martial, J. Didierjean, N. Aubry, D. Sangla, F. Balembois, P. Georges, "34W continuous wave Nd:YAG single crystal fiber laser emitting at 946 nm," *Appl. Phys. B* 104, 1-4 (2011).

High power top-hat pulses from an Yb MOPA for efficient OPA pumping

T. Balčiūnas,¹ G. Y. Fan,¹ G. Andriukaitis,¹ A. Pugžlys¹ and A. Baltuška¹

¹ Photonics Institute, Gußhausstraße 27-387, A-1040, Vienna, Austria

E-mail address: tadas.balciunas@tuwien.ac.at

Abstract: We demonstrate shaping of a high energy broadband Yb amplifier pulses for the generation of a top-hat temporal profile that provides efficient pumping of an optical parametric amplifier. For the shaping an acousto-optic programmable dispersion filter (AOPDF) is used as a phase-only filter. The scheme is scalable to a high average power and simple due to a rather broad bandwidth of the Yb:CaF₂ gain medium used in the amplifier that supports sub-150 fs transform limited pulse duration.

OCIS codes: (320.7090) Ultrafast lasers; (320.5540) Pulse shaping

1. Introduction

Optical parametric chirped pulse amplification (OPCPA) is rapidly gaining ground as an approach to generate intense few-cycle pulses [1] and reach IR wavelength ranges [2] where there are no suitable laser gain media for high-energy amplification. Parametric amplification permits extraordinarily broad phase-matching bandwidths and a huge single-pass gain, thus dismissing the concern for spectral gain narrowing which is a perennial problem in laser amplifiers. However, the high OPA gain has its negative side: for a bell-shaped intensity profile of the pump pulse/beam the unsaturated gain varies exponentially with intensity, resulting in an effective temporal/spatial filter. The obvious remedy would be a top-hat pump pulse and a top-hat pump beam.

Here, we demonstrate the advantage of a relatively large bandwidth of a DPSS Yb:CaF₂ amplifier which allows us to implement a straightforward inline shaping technique and obtain a pulse profile optimized for OPA pumping. Whereas the described technique requires minimal changes of the pump laser source, it pays off by significant advantages, which include: 1) a substantial increase in the OPA conversion efficiency, 2) avoidance of OPCPA gain roll-off in the pump pulse wings, i.e. the temporal equivalent of spectral gain narrowing, 3) increase of the OPA signal and idler pulse contrast as compared to the standard use of bell-shaped pump pulses whereby the chirped seed pulse is purposely overlapped only with a narrow temporal section of the pump around the pulse peak and the temporal wings of the pump pulse are responsible for raising the ASE (superfluorescence) background outside the temporal overlap with the seed pulse.

Our method of choice relies on phase-only shaping, or chirping, of the pump pulse. Notably, the resultant carrier frequency variation in time is comparatively small and allows us to safely disregard any resultant temporal modulation of the phase mismatch in the OPA process. Crucially, the chirped pump pulses emitted by the femtosecond Yb amplifier can still be used for seeding the OPA/OPCPA system. This is achieved by splitting-off a micro-Joule-level 1030-nm pulse and passing it through a block of glass in order to recompress the pulse to a level sufficient for the generation of supercontinuum (OPA seed) radiation in a bulk crystal.

Previously, temporal gain flattening and energy extraction optimization in OPA [3] was demonstrated with electro-optically sliced nanosecond pump pulses and multiple staggered picosecond pulses shifted with respect to each other by controlled time delays [4]. Broadband Yb media, especially Yb:CaF₂ [5] which is suitable for high-energy operation with ~200-fs pulses and >10 nm FWHM of bandwidth, are suitable for a simple phase shaping that can be implemented in a CPA scheme before the amplifier.

In this contribution, we generate top-hat pulses using an acousto-optic programmable dispersion filter (AOPDF, DAZZLER) included in an Yb:CaF₂ MOPA chain, and demonstrate the corresponding improvement in the performance of an OPCPA pumped by this Yb system.

2. Setup

The general scheme of the laser system is shown in Fig. 1. The laser system is a cascaded regenerative amplifier with a Yb:KGW MOPA as a front-end and Yb:CaF₂ regenerative amplifier (RA) as a power amplifier. The Yb:KGW RA is seeded by a Kerr-lens mode-locked oscillator based on the same gain medium and delivers ≈100 μJ pulses at a tunable repetition rate. The pre-amplified pulses are then sent into another stretcher that additionally stretches the pulses so that the pulse duration in the final amplification stage is >500 ps in order to reduce self-phase modulation in the amplifier. Low third order susceptibility and intensity-dependent refractive index allows reducing the B-integral while still maintaining high energy density and tight beam on the crystal. A

very low quantum defect ($\approx 5\%$) allows reducing the thermal load on the crystal. The laser crystal is cryogenically cooled, which increases gain cross-section as well as improves thermal properties of the crystal leading to reduced thermal effects, such as thermal lensing and depolarization losses.

The stretched pulses from the front-end are then sent to an AOPDF (Dazzler, FastLite Ltd.) before amplification in the second amplifier. The length of the dazzler crystal is 25 mm, which allows applying approximately 3 ps time delay and supports pulse rep. rates up to several 10 kHz. Pulses are compressed in a reflection grating compressor in order to avoid self-phase modulation. The stretcher and compressor are matched so that when the AOPDF is removed, the pulses are compressed nearly to the Fourier limit. The bandwidth of the final pulses supports 150 fs pulse duration. The output energy of the amplified pulses is over 6 mJ. Noteworthy, the AOPDF phase-only shaping of the CPA seed pulses has virtually no effect on the amplification in Yb:CaF₂ because the seed introduced additional pulse chirping is negligible in comparison with the overall > 200 ps pulse stretch imposed by the CPA system.

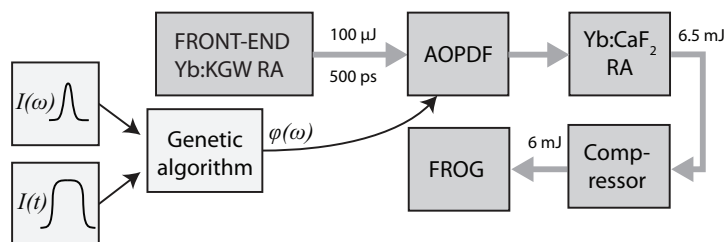


Fig. 1. A general layout of the laser amplifier for the generation of top-hat temporal profile pulses.

3. Results

The top-hat pulse is obtained by imprinting a calculated spectral phase by an AOPDF. The spectral phase that transforms the initial pulse with given spectral intensity $I(\omega)$ into top-hat temporal profile $I(t)$ pulse is calculated using a genetic algorithm. The algorithm optimizes the spectral phase $\phi(\omega)$ using provided measured spectral intensity $I(\omega)$ and target pulse shape $I(t)$ so that the r.m.s. difference between the calculated temporal profile $F\{I(\omega)\exp(\phi(\omega))\}$ and the target pulse shape $I(t)$ is minimal, here $F\{\}$ denotes Fourier transformation. The target top-hat pulse shape $I(t)$ is approximated using a 6th-order super-Gaussian function $I(t) = \exp(-(t/\tau)^6)$. If the spectrum of the amplified laser pulse is symmetric, the optimal spectral phase is also symmetric and can be expressed as a polynomial which contains only even orders. However, for an arbitrary spectral shape, the spectral phase is asymmetric.

In order to check the concept and understand the optimal spectral phase shape better, a pulse splitting concept can be adopted similar to the one that was used with picoseconds pulses [4]. The transform limited pulse can be split into two replicas by setting different group delays for different spectral portions. A linear variation of spectral phase causes a group delay $\tau = d\phi/d\omega$. By splitting the spectrum into two parts with approximately equal total energy and setting the linear phase variation of the two parts with opposite signs of the slopes so that the pulse is split into two replicas separated by 2τ . If the delay is chosen appropriately, the two pulses overlap and produce approximately top-hat pulse shape. The idea was previously demonstrated using ultrabroadband pulses and a deformable mirror pulse shaper [6]. Here we show that even for much less broadband pulses from Yb:CaF₂ amplifier the similar method can be used with a compact AOPDF shaper.

The temporal profiles of the shaped and initial pulses were measured using SHG FROG (Fig. 2 c) and d)). First a residual phase had to be measured and compensated with the AOPDF. Due to non-perfect matching of the stretcher and compressor gratings (the groove densities were 1700 and 1750 lp/mm respectively) and a rather large cumulative optical path in the RA amplifiers, there is some uncompensated high order spectral phase left after the compressor which distorts the temporal pulse profile. The measured residual phase was later taken into account for the optimal pulse shape calculation simply by subtracting the residual phase from the target phase profile. The measurement results are summarized in Fig. 2. The applied spectral phase and the retrieved from FROG matches rather well as shown in panel a). The spectrum at the time of the measurement was rather modulated which causes modulation of the temporal profile of the shaped pulse as shown in Fig. 2 b). The reconstructed saw-tooth temporal phase exhibits two linear phase ramps with opposite sign. The slope of the temporal phase corresponds to instantaneous frequency $\omega(t) = d\phi/dt$, meaning that there is an abrupt jump of instantaneous frequency approximately in the center of the pulse.

Another aspect is seeding of an OPA via a supercontinuum generation. The most attractive property of an OPA pumped by a femtosecond laser is the possibility to directly seed it with a spectrally broadened pulse obtained by supercontinuum generation. In order to achieve efficient supercontinuum generation, a steep temporal intensity

gradient $dl(t)/dt$ is needed. The top-hat pulses are not efficient for such spectral broadening, because the intensity is constant during the pulse therefore the frequency change is zero due to constant nonlinear phase $\phi_{nl} = n_2 I(t)$. We show that the shaped rectangular pulses can be transformed to a shorter pulse that is more efficient for the supercontinuum generation using just a simple block of material provided that the sign of the spectral phase is chosen correctly. The shaped top-hat pulses have the property that the pulses are chirped. If the spectral phase is chosen such that the spectral part with higher frequency precedes the part with the lower frequency, as is the case shown in Fig. 2, the negative chirp can be partially compensated by a positive dispersion material block.

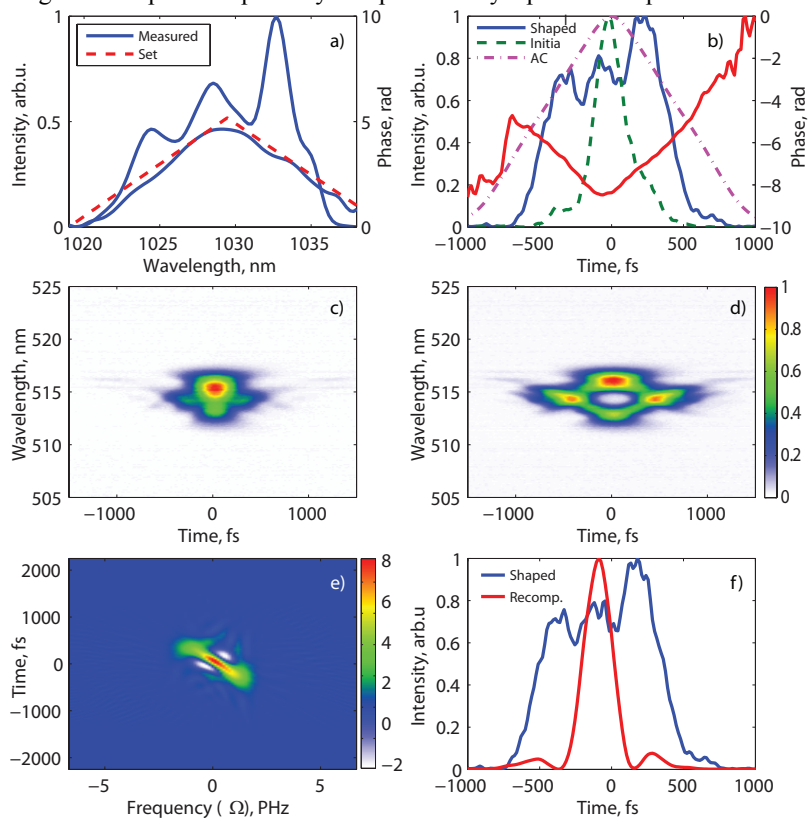


Fig. 2. Temporal characterization of shaped pulses: a) spectral intensity and reconstructed phase. Dashed line shows the phase setting for the AOPDF shaper, b) reconstructed temporal profile of the pulse and temporal phase. For reference a second-order autocorrelation function of the rectangular pulse and temporal profile of the initial pulse without phase mask are shown c) and d) FROG traces of the initial and shaped pulses respectively, e) calculated Wigner distribution of the measured rectangular pulse, f) calculation of the recompression of the rectangular pulse in a bulk dispersive material. For the calculation a 30 cm long SF57 block of glass was used.

4. Conclusions

We demonstrated generation of top-hat pulses from Yb:CaF₂ MOPA amplifier. The system delivers up to 6.5 mJ pulses at 1 kHz and is scalable to a high average power due to the availability of high power laser diodes at 976 nm for direct diode pumping. The system is especially attractive for efficient amplification of an ultrabroadband pulses in OPCPA. The idler can also be used; however, in that case additional phase compensation should be used.

5. References

1. G. Cerullo, A. Baltuska, O. D. Mücke, and C. Vozzi, *Laser Photonics Reviews* **5**, 323-351 (2011).
2. G. Andriukaitis, T. Balčiūnas, S. Ališauskas, A. Pugžlys, A. Baltuska, T. Popmintchev, M.-C. Chen, M. M. Murnane, and H. C. Kapteyn, *Optics Letters* **36**, 2755-2757 (2011).
3. L. J. Waxer, V. Bagnoud, I. A. Begishev, M. J. Guardalben, J. Puth, and J. D. Zuegel, *Optics Letters* **28**, 1245-1247 (2003).
4. J. A. Fülöp, Z. Major, B. Horváth, F. Tavella, A. Baltuska, and F. Krausz, *Applied Physics B* **87**, 79-84 (2006).
5. M. Siebold, M. Hornung, R. Boedefeld, S. Podleska, S. Klingebiel, C. Wandt, F. Krausz, S. Karsch, R. Uecker, A. Jochmann, J. Hein, and M. C. Kaluza, *Optics Letters* **33**, 2770-2772 (2008).
6. S. Bonora, D. Brida, P. Villoresi, and G. Cerullo, *Optics Express* **18**, 23147-23152 (2010).

Stabilization of carrier-envelope phase with MHz bandwidth by an intra-cavity graphene electro-optic modulator

C.-C. Lee¹, C. Mohr², J. Bethge², S. Suzuki¹, M.E. Fermann², I. Hartl² and T. R. Schibli^{1,3,4}

¹Department of Physics, University of Colorado at Boulder, 2000 Colorado Avenue, Boulder, CO 80309, USA

²IMRA America, Inc., 1044 Woodridge Ave., Ann Arbor, MI 48105, ihartl@imra.com

³Department of Electrical, Computer and Energy Engineering, University of Colorado, Boulder, CO 80309-0425, USA

⁴JILA, National Institute of Standards and Technology and University of Colorado, Boulder, CO 80309-0440, USA

Abstract: An intra-cavity, sub-micrometer thick graphene electro-optic modulator enables orthogonal offset-frequency control far beyond the stimulated lifetime of the gain medium. We demonstrate this new locking scheme in a Tm: fiber comb with record-low residual phase noise.

OCIS codes: (140.3425) Laser stabilization; (140.7090) Ultrafast lasers; (140.3510) Lasers, fiber

1. Introduction

Optical frequency combs based on fiber lasers have proven to be a reliable tool for metrology and spectroscopy. To achieve a fully phase-stabilized frequency comb, a fast feedback control of the carrier-envelope offset frequency (f_{CEO}) is required. Typically, the f_{CEO} is stabilized by an electronic feedback loop acting on the pump power of the laser. This method, however, suffers from a limited bandwidth (typically less than 100 kHz) due to the long stimulated lifetime of the gain medium, which results from the coupled dynamics of gain and pulse energy in the laser [1]. To overcome this bandwidth limitation set by the intra-cavity dynamics, an extra-cavity feed-forward method using an acoustic-optic modulator (AOM) was proposed [2,3]. Although this feed-forward scheme can provide fast corrections to f_{CEO} , it still requires a slow feedback loop to the laser to ensure long-term stability. It further cuts the available output power in half, could add to beam-pointing fluctuations or mode-distortions, and increases the overall complexity of the original feedback scheme notably. Here we demonstrate for the first time, that an intra-cavity loss modulation can overcome those issues and MHz bandwidth f_{CEO} control can be achieved.

2. Methods

The experimental setup is shown in Fig. 1, the details of the Fabry-Perot type Tm-fiber similariton oscillator used in the experiment are described in [5]. The oscillator was pumped by an Er-fiber amplified single frequency diode laser centered at 1564 nm with a pump power of up to 1.3 W. Additionally up to 10 mW of pump power was provided by a second single-frequency diode laser which allowed fast pump-modulation. The intra-cavity dispersion was set to net positive close to zero, allowing mode-locking in the similariton regime. Stable mode-locked operation was achieved by a saturable-absorber mirror which was used as a cavity end-mirror. An output-coupling ratio of 20% provided 20 mW of average output power centered at 1950 nm with 60 nm bandwidth and 100 MHz repetition rate. A graphene electro-optic modulator with <5% insertion loss and ~2% modulation depth served as the second end mirror, as shown in Fig. 1. The modulator consists of single-layer graphene as the absorbing layer and a field-effect structure that changes the electronic Fermi level in graphene and therefore the transparency (see Fig. 1 right) [4]. The mode-field diameter on the graphene modulator was set by a single lens to approximately 150 μm , the

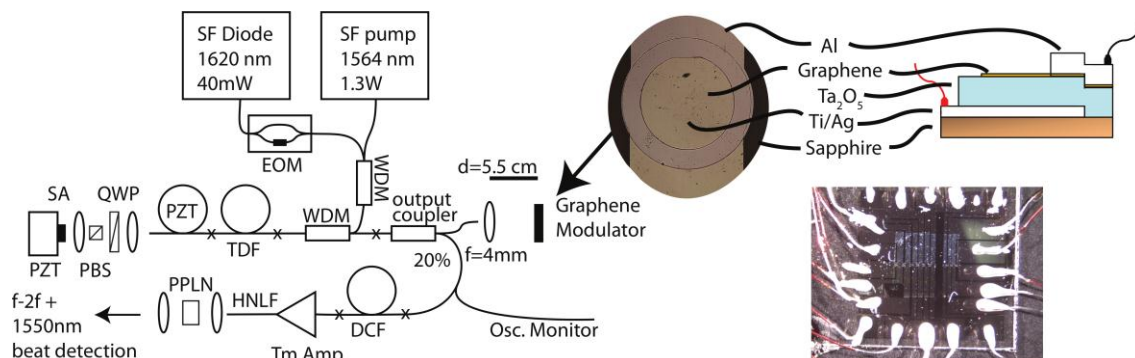


Fig. 1. (Left) Experimental setup. WDM: wavelength-division multiplexer; TDF: thulium-doped fiber; PZT: piezo tube for repetition rate stabilization; QWP: quarter-wave plate; PBS: polarization beam-splitter; SA: saturable absorber mirror; HNLF: highly nonlinear fiber; PPLN: Periodically poled lithium niobate. (Right) A microscope image of the graphene electro-optic modulator. The diameter of the inner ring is 280 μm . (Right, bottom) A picture of the device, which contains a series of independent modulators.

modulator size was 280 μm in diameter. The modulator did not have an adverse effect on mode-locked operation and it increased the pump threshold only minimally ($<1\%$).

A pure cavity loss modulation, unlike pump power modulation, leads to a direct change in pulse energy without coupling to the gain, and thus the bandwidth of this loss modulation is not limited by the stimulated lifetime of the gain medium but rather by the roundtrip time of the cavity, as has been pointed out theoretically in [1]. This difference in pump power and loss modulation can be seen from the following equations, which describe the small deviations of roundtrip gain (Δg) and pulse energy (ΔE_p) from their steady-state values in a laser mode-locked by a saturable absorber:

$$T_R \frac{\partial \Delta E_p}{\partial t} = \underbrace{-\frac{\partial q}{\partial E_p} E_p \Delta E_p}_{\text{Self amplitude modulation}} + \underbrace{E_p \Delta g}_{\text{Gain}} - \underbrace{E_p \Delta l}_{\text{Loss}} \quad (1)$$

$$T_R \frac{\partial \Delta g}{\partial t} = \underbrace{-\frac{g}{E_{sat,L}} \Delta E_p}_{\text{Gain saturation}} + \underbrace{\left[-\frac{T_R}{\tau_L} - \frac{E_p}{E_{sat,L}} \right] \Delta g}_{\text{Gain relaxation}} + \underbrace{\frac{\eta T_R}{E_{sat,L}} \Delta P_{pump}}_{\text{Pumping}} \quad (2)$$

where T_R is the roundtrip time, g and l are the roundtrip power gain and loss, q is the nonlinear loss as a function of pulse energy, $E_{sat,L}$ is the saturation energy of the gain medium, τ_L is the upper-state spontaneous gain relaxation time, η is the conversion efficiency from pump power to signal power, and P_{pump} is the pump power. Pump power modulations (ΔP_{pump}) lead to variations in the gain (Δg), which subsequently lead to changes in the pulse energy. The characteristic time scale of this process is the well-known stimulated gain lifetime, which is given to the first order by the gain relaxation in Eq. 2. Any modulation in the pump power faster than this time scale is low-pass filtered by the gain dynamics. On the other hand, the loss term in Eq. (1) modulates the pulse energy at the time scale of one cavity roundtrip (T_R), and the pulse energy relaxes in a damped fashion determined by the saturation of self-amplitude modulation. The bandwidth of loss modulation is given approximately by $(2\pi T_R)^{-1} E_p (\partial q / \partial E_p)$, which is ~ 1 MHz for typical fiber lasers with 100 MHz repetition rate (see Fig. 2). Higher repetition rates result in even high modulation bandwidth. A bulk Ti:sapphire laser with 10 GHz repetition rates, for example, can have modulation bandwidths as high as 100 MHz, which would be two orders of magnitude higher than that of pump modulation.

Despite its advantages over pump power modulation, there has so far not been any realization of this loss modulation scheme for stabilizing f_{CEO} due to the lack of high-speed electro-optic modulators that are suitable for intracavity, pure-amplitude modulation. Here we demonstrate the effectiveness of an ultrathin, graphene-based electro-optic amplitude modulator [4] that enables record high f_{CEO} locking bandwidths without adverse impact on the laser performance. Due to the low insertion-loss and sub-micrometer thickness, these novel devices might open up a pathway to fully phase-stabilized, monolithic lasers with multi-GHz repetition rates.

The frequency responses of output power to pump power modulation and loss modulation from the graphene modulator were measured with an HP89441A vector signal analyzer (see Fig. 2). f_{CEO} was detected with an in-line f - $2f$ interferometer at $\sim 1100\text{nm}$ after amplifying the power from the oscillator to $\sim 200\text{mW}$. Phase error detection was performed using an analog phase detector (Minicircuits ZRPD-1), followed by a 10MHz low-pass filter. We phase-

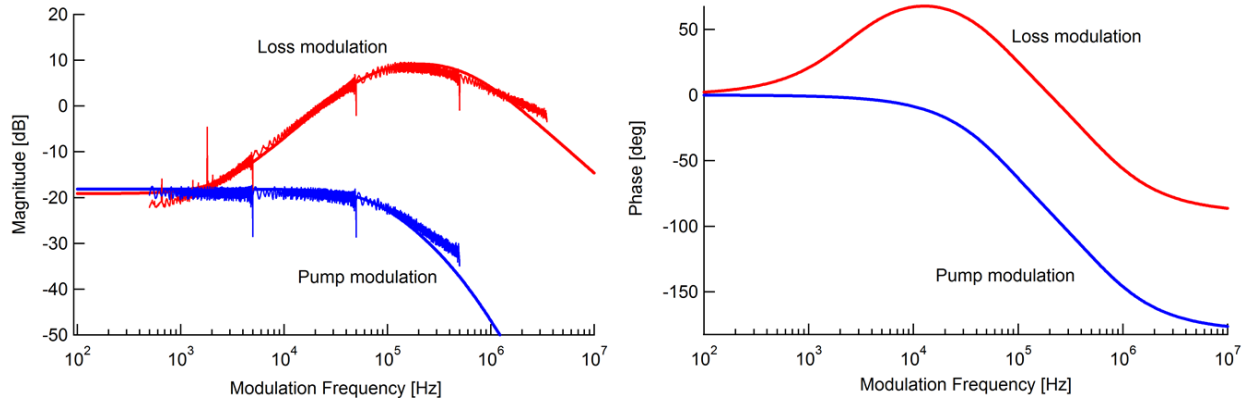


Fig. 2. (Left) Frequency responses of the output power to pump power (blue) and loss (red) modulation. Thin lines are measured traces and thick lines are fitted transfer functions calculated from Eq. (1) and (2). The following laser parameters are used in fitting the Tm: fiber data: $E_p = 1.1$ nJ; $T_R = 10$ ns; $P_{pump} = 1$ W; $\eta = 15\%$; $E_{sat,L} = 8.5$ μJ ; $\tau_L = 535$ μs ; $E_p (\partial q / \partial E_p) = 0.04$. (Right) Calculated phase response of the same fitted model shown in the left figure. Negative phase values represent phase lag. The phase response of pump modulation has a phase lag of 180 degrees at low frequencies and is shifted up to zero here.

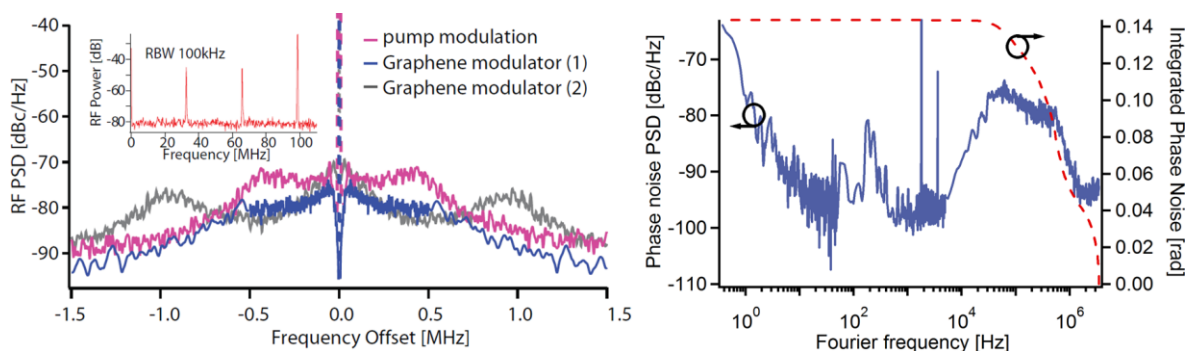


Fig. 3. (Left) In-loop RF spectra of phase-locked f_{CEO} beats recorded with only pump current modulation and two tries with the graphene modulator. RBW: 10 kHz. Inset: free-running f_{CEO} and repetition rate at 100MHz. (Right) Phase noise density from 0.3Hz to 3.5MHz. The integrated phase noise is 144 mrad over the full span.

locked the f_{CEO} beat to a stable RF synthesizer with a low time-delay loop filter. The stabilization was performed both with and without a division-by-4 pre-scaler.

3. Results

The frequency responses of output of the laser to pump power and cavity loss modulation are shown in Fig. 2. Pump power modulation has a -3dB corner at 89 kHz, whereas the loss modulation from the graphene modulator has a higher corner at 600 kHz and slower roll-over. By fitting the frequency responses derived from the model described by Eq. (1) and (2) to the data, a set of laser parameters were found (see Fig. 2 caption) and are close to the experimental values. It should be noted that a flat low frequency response can be achieved with lasers having high-Q cavities or higher gain saturation.

The results of the f_{CEO} stabilization are shown in Fig. 3. The free-running linewidth of the f_{CEO} beat (Fig 3, inset) was estimated to be around 50 kHz. With the traditional pump power modulation alone (compare purple trace in Fig3, left), we achieved stable phase-locking of the f_{CEO} . After optimization of the feedback-loop we were able to concentrate 95.1% of the RF power of the beat-signal in the coherent carrier. Due to the aforementioned limitation in the pump-modulation scheme, even with a good loop-filter design the servo bump could not be pushed much beyond 400 kHz. By feeding back to the graphene modulator we achieved much larger modulation bandwidths (see Fig. 3, left). Initially, we observed a servo bump at ~ 1 MHz (curve “Graphene modulator (2)”), with optimized loop filter settings (curve “Graphene modulator (1)”), we found $\sim 98\%$ of the RF power in the coherent carrier and the complete absence of any servo bumps. In this optimized setting we measured a record low integrated residual phase noise of 144 mrad (integration from 0.3 Hz to 3.5 MHz). Due to a limited DC response of the current modulator we still required a slow feedback to the pump power of the laser for long-term operation. Alternatively, the long-term stability could be guaranteed by a thermal feedback to an intra-cavity fiber grating. Currently the performance is limited by the locking electronics and the frequency response of the modulator in the cavity. With an improved design of the laser parameters, better phase noise performance may be achieved.

4. Conclusion

To the best of our knowledge, this work presents the first successful f_{CEO} stabilization of an optical frequency comb by means of a pure intra-cavity loss modulator. The phase noise of the stabilized f_{CEO} -beat frequency was 144 mrad, a record low value for a fiber-laser frequency comb. This was enabled by a novel low-insertion loss graphene electro-optic modulator, allowing feedback bandwidths far beyond the current limit imposed by the stimulated gain-lifetime. The non-existent cross-talk to the repetition rate allowed further much tighter control of the offset frequency without affecting the repetition rate lock. Due to their low insertion loss and their ultra-compact design, these modulators could soon empower a new breed of monolithic, rare-earth-based phase-locked combs with multi-GHz fundamental pulse repetition rates.

Acknowledgement

We gratefully acknowledge partial funding from NSF under Grant No. ECS-0335765 and by the Defense Advanced Research Projects Agency (DARPA), Contract No. YFA N66001-11-1-4156.

References

- [1] N. R. Newbury et al., IEEE Journal of Quantum Electronics **41**, 1388-1402 (2005).
- [2] R. J. Jones et al., Physical Review Letters, **86**, 3288-3291 (2001).
- [3] S. Koke et al., Nature Photonics, **4**, 462-465 (2010).
- [4] C.-C. Lee et al., submitted to Optics Express.
- [5] J. Bethge et al., Advanced Solid State Photonics, presentation AT5A.3, San Diego, (2012).

Noise Characterization of a Mode-Locked, All-Fiber, All-Normal-Dispersion Ytterbium Ring Oscillator Using Two-Channel Polarization Control by a Computer

D. Csáti¹, R. Szipócs^{1,2,*}

¹ Institute for Solid State Physics and Optics, Wigner Research Centre for Physics of HAS, P.O. Box 49, H-1525 Budapest, Hungary

² R&D Ultrafast Lasers Ltd, P.O. Box 622, H-1539 Budapest, Hungary

* r.szipocs@szipocs.com

Abstract: Mode-locked operation of an all-fiber, all-normal dispersion Yb-fiber ring laser is actively optimized by a two-channel polarization controller according to the measured, normalised, single-sideband noise power.

OCIS codes: (140.3510) Lasers, fiber, (140.3615) Lasers, ytterbium, (140.7090) Lasers, ultrafast

1. Introduction

Passively mode-locked fiber lasers have gained scientific interest because of their potentially compact, environmentally stable and alignment-free design. Mode-locked operation of an Yb-fiber laser operating at around 1 micron can be obtained either in the net positive or negative dispersion regime. The former solution typically results in a more compact cavity design, since there is no need for intra-cavity dispersion compensating elements such as a grating pair, prism pair, a hollow-core photonic crystal fiber, a higher-order mode fiber or a chirped fiber grating. Stable, cw mode-locked operation of an all-fiber, all-normal-dispersion ring laser, however, requires spectral filtering of the pulses. In [1], it was obtained by a fiber-integrated spectral filter having a spectral bandwidth of ~15 nm. Recently, we also reported on an all-fiber, all-normal dispersion ring oscillator where pulse-shaping was based on nonlinear polarization rotation in the fiber together with spectral and temporal filtering by a fiber integrated polarizing element [2]. In the experiment, fiber-polarization controllers were used, in which the different paddles were manually set for optimum cw mode-locked operation of the laser.

In this paper, we report on a similar all-fiber, all-normal-dispersion Yb ring oscillator, in which the polarization controller element is replaced by an electronically controllable device. This simple upgrade in the laser setup, together with some improvement in the laser control electronics and data analysis hardware and software, allowed us to perform a detailed analysis on the mode-locked laser performance as the function of different polarization states of the optical pulses reaching the fiber integrated polarization element. Based on such an analysis, one can precisely control the mode-locked operation of an all-fiber, all-normal dispersion Yb-fiber ring laser, or any other laser of a similar kind.

2. Experimental setup

The laser setup is shown in Fig. 1. A highly doped ytterbium fiber (Yb) is used as the gain media, which is pumped by a 980 nm laser diode (LD) via a 980/1030 nm wavelength-division multiplexer (WDM). The Yb-doped fiber is followed by an isolator (ISO) realizing the unidirectional cavity. The initiation and stabilization of mode-locking is obtained by application of a semiconductor saturable absorber (SA). Between the SA and the polarizing beam splitter (PBS), we placed the new, electronically adjustable polarization controller (PC, Type: PolarRITE III - Mini dynamic polarization controller, product of General Photonics). The rest of the components are the same that were reported in [2].

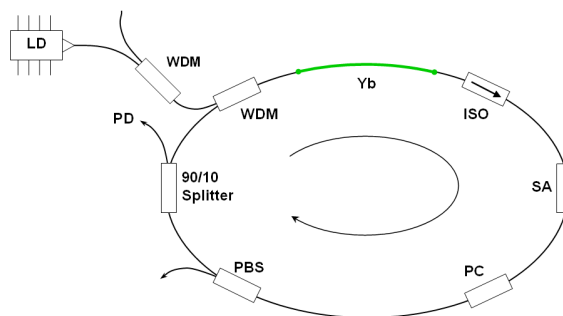


Fig. 1 Laser setup

The nonlinear polarization evolution of the optical pulses results in a variation of the polarization state along the pulse spectrum, leading to a strong spectral filtering effect by the PBS [2]. The PBS is followed by a 90%-10% splitter, where the 10% output port is directed to a fast photodiode (PD, Type: DET10C/M, product of Thorlabs).

3. Results

The laser output detected by the fast photodiode (PD) is analysed by a radio-frequency spectrum analyser (FSV3, product of Rohde&Schwarz). Depending on the control voltage values of the polarization controller (PC), we can obtain cw mode-locked, Q-switched or noise-like pulse, as shown in Fig. 2. The laser repetition rate is 26.267 MHz, the radio-frequency spectrum is measured over a 2 MHz bandwidth around the laser central frequency.

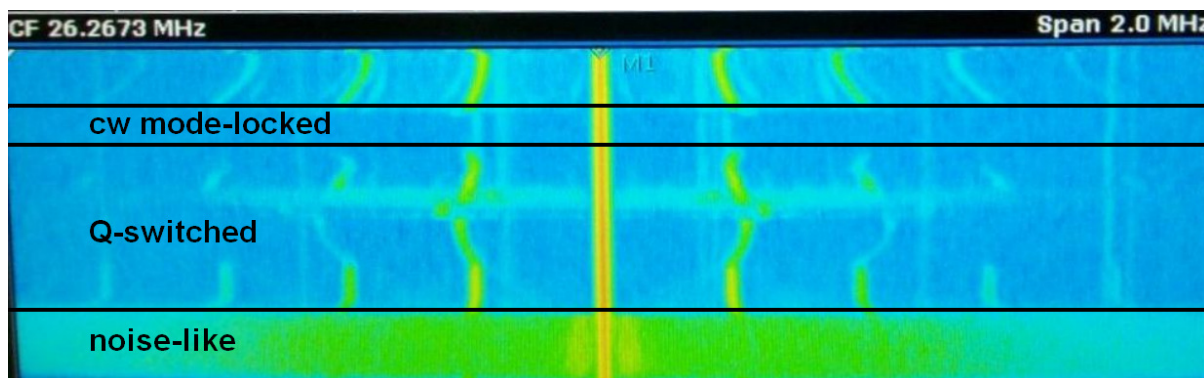


Fig. 2 Measured radio-frequency power spectrum at around the central frequency of the all-fiber, all-normal-dispersion Yb-fiber ring laser

Unfortunately, the radio-frequency spectra measured by the spectrum analyser can not be directly used for optimization of the cw mode-locked performance of the laser by setting the control voltages of the polarization controller by a computer or a microcontroller. In order to solve this problem, we have developed high sensitivity, radio-frequency amplifiers and filters providing electronic signals proportional to the measured signal power (P_{signal}) and the measured single sideband noise power (P_{noise}). Taking the advantage of this new electronics, we could easily measure P_{signal} and P_{noise} as the function of the control voltages applied on the polarization controller device, as shown in Fig. 3. Please note that this function is periodic for both the Quarter-Wave Plate Control Voltage (horizontal axis) and the Half-Wave Plate Control Voltage (vertical axis), and only one period is displayed in Fig. 3.

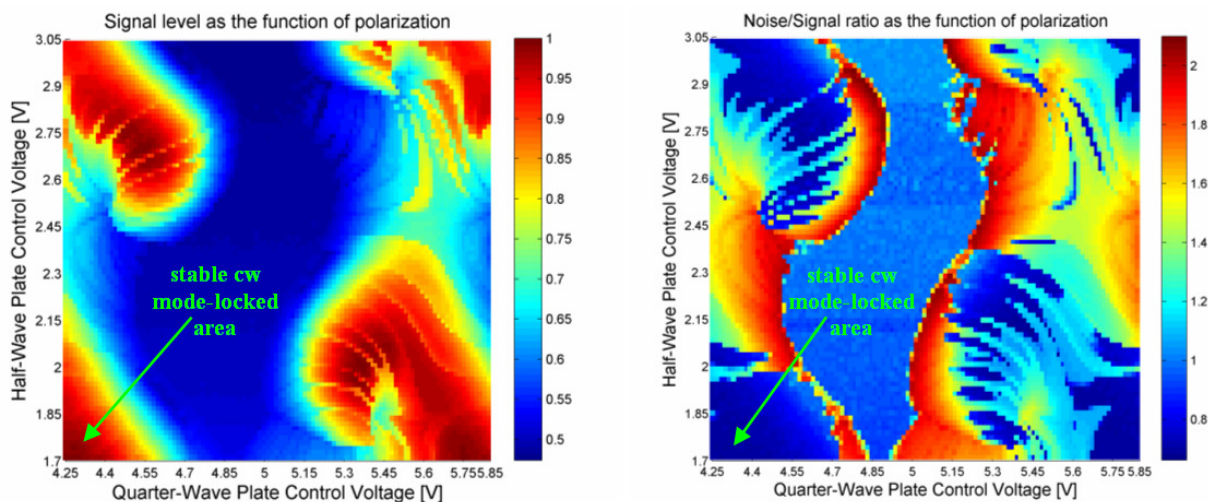


Fig. 3 Measured signal power (left) and normalized noise power (right) as the function of control voltage on the polarization controllers.

For stable cw mode-locked operation of the Yb-fiber laser, we require high signal levels (high P_{signal} values) and low rms noise (low P_{noise}) values. This requirement can be easily visualized if we plot the normalized noise power (P_{noise}/P_{signal}) as the function of control voltage values (see Fig. 3, right). The stable cw mode-locked operation area is indicated by a dark blue color in this Figure. During the experiments with our new laser setup and electronics, we had several interesting findings, which are summarized as follows: first of all, the shape of the “stability maps” that are shown in Fig. 3 were significantly different depending on the pump power, length of the SM fiber in front of the PBS, the round-trip time of the laser and other parameters, such as the method of rolling up of the fiber onto the holder mechanics. Without going into details, it is important to note that large stable cw-mode locked areas could be obtained only if we rolled up the optical fiber in a figure-8 configuration and provided sufficiently high pump power for the Yb-oscillator. In order to come to a stable laser configuration, such as demonstrated in Fig. 3, we preferred to take several “stability maps” during the different stages of the mechanical fixing of the optical fibers and components, and correct the configuration accordingly. Having the laser configuration fixed and the final “stability maps” recorded, we could easily find the optimum control voltage values of the polarization controller, for which the laser operated in the cw mode-locked regime at the highest average signal and the lowest noise power levels (shown in Fig. 3 by arrows).

There are two additional issues that should be mentioned before using the method introduced for computer or microcontroller control of an all-fiber, all-normal dispersion Yb-fiber ring oscillator for everyday use. Firstly, the Yb-fiber laser tested (and the corresponding stability map) had some thermal drift according to the temperature change in the laboratory, even if all of the optical components and fibers were fixed in the housing. This fact requires a continuous, fine re-adjustment of the polarization control voltages during the operation of the laser in order to keep the highest signal to noise ratios. Secondly, the all-fiber, all-normal dispersion Yb-fiber ring oscillator reported here had some inherent nonlinearity, which resulted in an optically bistable behaviour [3], as demonstrated in Fig. 4. For recording the „stability maps” shown in Fig. 4, the quarter-wave plate control voltage values (horizontal axis) were increased and reduced for the even and odd rows, respectively. It is clearly seen that the cw mode-locked status of the laser had a feedback to the stability maps (the stable/unstable borders were slightly shifted), which fact arises additional challenges when writing a computer code for laser control.

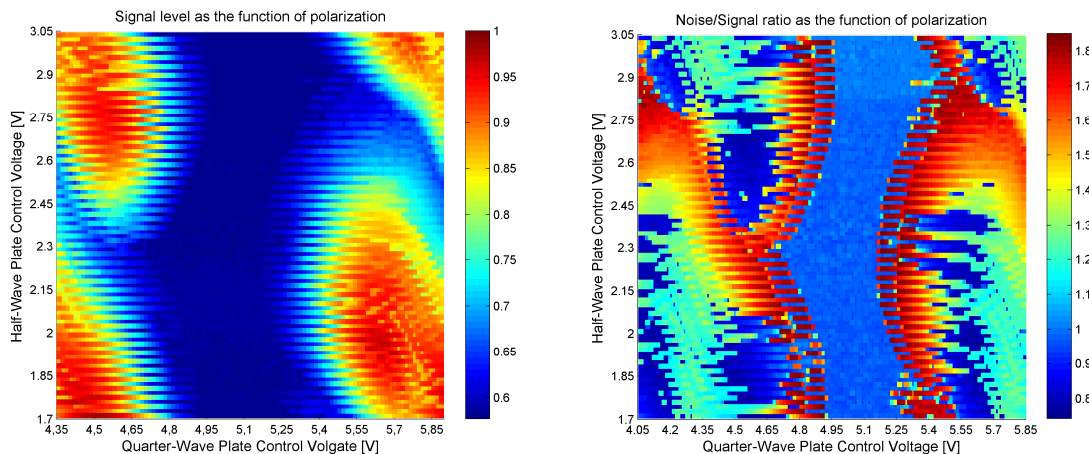


Fig. 4 Demonstration of optical bistability of the all-fiber, all-normal dispersion Yb-fiber ring oscillator. Parameters are the same than in Fig. 3, but the data plotted were recorded for increasing and reducing quarter-wave plate control voltages for even and odd rows, respectively.

In spite of the difficulties mentioned above, we are convinced that the information obtained by the application of our newly developed electro-optic and electronic devices can be well suited for active polarization control of Yb-fiber oscillators to assure drop-out-free, stable, cw mode-locked operation at low RMS noise levels, which might be a critical issue in different applications such as nonlinear microscopy.

4. References

- [1] K. Kieu and F.W. Wise, “All-fiber normal-dispersion femtosecond laser,” *Opt. Express* **16**, 11453–11458, (2008).
- [2] J. Fekete, A. Cserteg, R. Szipócs, “All-fiber, all-normal dispersion ytterbium ring oscillator,” *Laser Physics Letters* **6**, 49-53 (2009).
- [3] Komarov A, Leblond H, Sanchez F, “Theoretical analysis of the operating regime of a passively-mode-locked fiber laser through nonlinear polarization rotation,” *Phys. Rev. A* **72**, 063811 (2005).

Fiber Doppler Lidar for Precision Navigation of Space Vehicles

Farzin Amzajerdian, Larry Petway, Glenn Hines and Bruce Barnes

NASA Langley Research Center, Hampton, VA 23681

f.amzajerdian@nasa.gov

Diego Pierrottet and George Lockard

Coherent Applications Inc., Hampton, VA 23666

ABSTRACT: A fiber-based coherent Doppler lidar capable of providing highly accurate vector velocity and altitude data has been developed for precision navigation of space vehicles landing on the Moon, Mars, or asteroids.

OCIS codes: (010.0280) Remote sensing and sensors, (280.3340) Laser Doppler velocimetry, (280.3640) Lidar, (060.2320) Fiber optics amplifiers and oscillators.

1. Introduction

Precision navigation to the designated landing site on the surface of the Moon or Mars, formation flying or landing on asteroids, and rendezvous and docking with orbiting spacecraft or space station, all require accurate knowledge of the vehicle relative velocity and altitude [1-4]. For example, future landing missions may require landing within a few meters of pre-deployed assets or landing in a small area surrounded by rocks, craters, or steep slopes [5-7]. To meet this requirement, a Doppler lidar is being developed by NASA under the Autonomous Landing and Hazard Avoidance Technology (ALHAT) project [8,9]. The range and velocity measurements provided by this lidar sensor will be used by an autonomous Guidance, Navigation, and Control (GN&C) system to accurately navigate the vehicle to the designated landing location.

As a landing sensor, the Doppler lidar will begin its operation during the powered descent phase from an altitude of a few kilometers above the ground. The GN&C system processes the lidar data to improve position and attitude data from the Inertial Measurement Unit (IMU). The improved position and attitude knowledge along with the lidar precision vector velocity data enable the GN&C system to continuously update the vehicle trajectory toward the landing site. In addition to the precision trajectory determination, the lidar data will play important role in performing the soft landing maneuver. For example, large robotic or manned vehicles must control their horizontal and vertical velocities to better than 0.5 m/s in order to avoid the risk of tipping over and ensure a gentle touchdown. To control to these limits will require measurement accuracies to better than 10 cm/s. The coherent Doppler lidar, being described in this paper, exceeds these requirements by over an order of magnitude.

2. System Description

The Doppler lidar obtains high-resolution range and velocity information from a frequency modulated continuous wave (FMCW) waveform for which the laser frequency is modulated linearly with time. Figure 1 shows the transmitted laser waveform and the retuned waveform from the target delayed by t_a , the light round trip time. When mixing the two waveforms at the detector, an interference signal will be generated whose frequency is equal to the difference between the transmitted and received frequencies. This intermediate frequency (IF) is directly proportional to the target range. When the target or the Lidar platform is not stationary during the beam round trip time, the signal frequency will be also shifted due to the Doppler effect. Therefore by measuring the frequency during “up chirp” and “down chirp” periods of the laser waveform, both the target range and velocity can be determined. The difference in up-ramp and down-ramp frequency provides the vehicle velocity and their mean value provides the range to the target.

Figure 2 illustrates the system design concept utilizing an optical homodyne configuration. A relatively low power, single frequency laser operating at eye safe wavelength of 1.55 micron, is used as the master oscillator. The output of this laser is modulated per the waveform of Figure 1. Part of the laser output is amplified to be transmitted and the remaining is used as the local oscillator (LO) for optical homodyne detection. The lidar transmits three laser beams which are separated 120 degrees from each other in azimuth and are pointed 22.5 degrees from nadir. The signal from each beam provides the platform velocity and range to the ground along the laser line-of-sight (LOS). The three LOS measurements are then combined in order to determine the three components of the vehicle velocity vector, and to accurately measure altitude and attitude relative to the local ground. The 45 degrees separation between the transmitted beams was chosen as a compromise between horizontal velocity accuracy that favors large angles, and higher operational altitude that is inversely proportional to the beam nadir pointing angle.

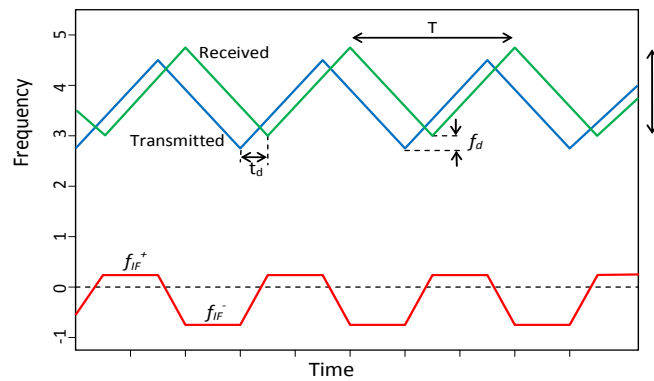


Fig. 1. Laser frequency is linearly modulated to create a sawtooth waveform. Returned waveform from the target is delayed in time. In presence of platform or target velocity, the returned waveform will be Doppler shifted. The difference frequency (lower trace) obtained by homodyning the laser and returned beams contains both range and velocity information.

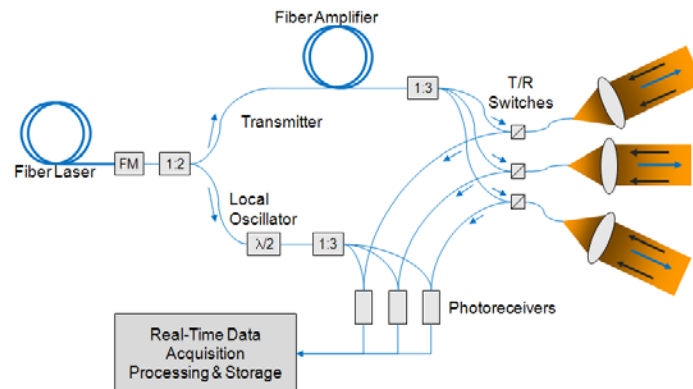


Fig. 2. Doppler lidar system configuration illustrating three transmitted beams and their corresponding receivers providing line-of-sight velocity and range measurements in three different directions.

The main factors determining the precision of the Doppler lidar measurement are the spectral linewidth of laser, the linearity of the modulation waveform, the signal-to-noise ratio, and the signal processor frequency resolution [8,9]. Fortunately, the advances in single-frequency fiber laser, high quantum efficiency detector, high-speed analog electronics, and powerful processor technologies have enabled the development a system with sufficient precision and operational range for a number of applications including planetary landing.

3. System Development and Tests

The capabilities of the Doppler lidar were evaluated and its performance characterized through two helicopter flight test campaigns. These campaigns were facilitated by NASA Jet Propulsion Laboratory (JPL), and were held at NASA Dryden Flight Research Center in California in 2008 and 2010 over vegetation-free terrain [10,11]. A prototype version of the Doppler lidar has recently been completed for a series of demonstration flight tests. As shown in Figure 4, the system consists of an electronics chassis and an optical head. The optical head will be mounted rigidly on the vehicle with a clear field-of-view to the ground, and connected by an armored fiber cable to the Doppler lidar electronics chassis. It is planned to demonstrate the viability of this lidar sensor system for future landing missions through a series of flight tests onboard a rocket-powered terrestrial free-flyer vehicle in 2012. The test vehicle, referred to as Morpheus, is being developed by NASA-JSC to demonstrate advanced propulsion and GN&C technologies for future landing missions. The lidar will be operating in a closed-loop with a GN&C system controlling the vehicle flight trajectory and soft landing at the selected safe site.

4. References

- [1] Aron A. Wolf, Jeff Tooley, Scott Ploen, Mark Ivanov, Behcet Acikmese, and Konstantin Gromov, "Performance Trades for Mars Pinpoint Landing," Proc. of IEEE Aerospace Conference, paper no.1661 (2006).
- [2] Brian D. Pollard and Gregory Sadowy, "Next Generation Millimeter-wave Radar for Safe Planetary Landing," Proc. of IEEE Aerospace Conference, paper no. 1188 (2004).
- [3] David C. Woffinden and David K. Geller, " Navigating the Road to Autonomous Orbital Rendezvous," Journal of Spacecraft And Rockets, Vol. 44, No. 4, July–August 2007
- [4] Andrew E. Johnson, Allan R. Klumpp, James B. Collier, and Aron A. Wolf, "Lidar-Based Hazard Avoidance for Safe Landing on Mars," Journal of Guidance, Control, and Dynamics, Vol. 25, No. 6 (2002).

- [5] Edward C. Wong and James P. Masciarelli, "Autonomous Guidance and Control Design For Hazard Avoidance and Safe Landing on Mars," AIAA Atmospheric Flight Mechanics Conference, Paper no. 4619 (2002).
- [6] C. D. Epp, E. A. Robinson, and T. Brady, "Autonomous Landing and Hazard Avoidance Technology (ALHAT)", Proc. of IEEE Aerospace Conference, pp.1-7 (2008).
- [7] Farzin Amzajerjian, Diego Pierrottet, Larry Petway, Glenn Hines, and Vincent Roback, "Lidar systems for precision navigation and safe landing on Planetary Bodies," Proc. of SPIE, Vol. 8192, (2011).
- [8] O. Uttam, and B. Culshaw "Precision time domain reflectometry in optical fiber systems using a frequency modulated continuous wave ranging technique", IEEE J. Lightwave Technol., LT-3, pp. 971-977 (1985).
- [9] C.J. Karlsson, and F.A. Olsson "Linearization of the frequency sweep of a frequency-modulated continuous-wave semiconductor laser and the resulting ranging performance" App. Opt. Vol. 38, No. 15, pp 3376-3386 (1999).
- [10] D. Pierrottet, F. Amzajerjian, L. Petway, B. Barnes, and G. Lockard, "Flight test performance of a high precision navigation Doppler lidar," Proc. SPIE, Vol. 7323 (2009).
- [11] Diego Pierrottet, Farzin Amzajerjian, Larry Petway, Bruce Barnes, George Lockard, and Glenn Hines, "Navigation Doppler Lidar Sensor for Precision Altitude and Vector Velocity Measurements Flight Test Results." Proceeding SPIE Vol. 8044, May (2011).

Key to Authors and Presiders

A

M. Abdou Ahmed, AM6A.2
F. Amzajerian, FTh3.1A.2
G. Andriukaitis, AM6A.3

B

T. Balciunas, AM6A.3
F. Balembois, AM6A.2
A. Baltuska, **AM6A**, AM6A.3
B. Barnes, FTh3.1A.2
J. Bethge, AM6A.4
J. Borysow, LM5.1B.1

C

D. Csati, FTh3.1A.1

D

X. Délen, AM6A.2
F. Druon, AM6A.1

F

G. Fan, AM6A.3
M. Fermann, AM6A.4

G

P. Georges, AM6A.2
P. Georges, AM6A.1
T. Graf, AM6A.2

H

M. Hanna, AM6A.1
I. Hartl, AM6A.4
G. Hines, FTh3.1A.2
C. Hoenninger, AM6A.1

K

W. Kulatilaka, **LM5.1B**

L

C. Lee, AM6A.4
G. Lockard, FTh3.1A.2

M

F. Morin, AM6A.1
E. Mottay, AM6A.1

N. Peyghambarian, **FTh3.1A**

L. Petwat, FTh3.1A.2
D. Pierrottet, FTh3.1A.2
A. Pugzlys, AM6A.3

S

T.R. Schibli, AM6A.4
S. Suzuki, AM6A.4
R. Szipocs, FTh3.1A.1

V

P. Varghese, LM5.1B.1
A. Voss, AM6A.2

Z

Y. Zaouter, AM6A.1

